Cellular phenotypes associated with autism an iPSC study

Kathuria, Annie

Awarding institution:
King's College London

CELLULAR PHENOTYPES ASSOCIATED WITH AUTISM: An iPSC study

Annie Kathuria/1150983

Thesis submitted for the degree of Doctor of Philosophy

The Institute of Psychiatry, Psychology & Neuroscience (IoPPN)
King's College London

Abstract

Autism is a neurodevelopmental disorder that affects around 700,000 in the UK (Baird G. et al., 2006; Burgha et al., 2011) and these numbers are constantly increasing. Nonetheless, our understanding of the cellular and molecular processes underlying autism is limited. This has hindered the development of effective treatments and created a need for human specific models. The potential of modeling autism through the use of human induced pluripotent stem cells (iPSCs) is an exciting advancement towards uncovering the mechanisms underlying a disorder that affects the lives of so many people. Recent studies report that mutations in the *SHANK3* gene are a major cause of autism (Nemirovsky et al., 2015; Bentancur et al., 2013; Buccoto et.al, 2013). This project aimed to track and compare the development of neurons generated from iPSCs lines derived from *SHANK3* patients and healthy individuals. These lines were produced from hair root biopsies from three categories of individuals: three healthy control individuals, two autistic patients with a heterozygous deletion in the *SHANK3* gene and one sporadic ASD individual. iPSCs were differentiated into hypothalamic neurons and their structural and functional development was tracked during the various stages of neuralisation. These studies revealed that during early neuronal development, *SHANK3* iPSC derived neurons have a smaller cell soma, but more and longer primary neurites than control cells. These morphogenetic deficits were rescued by overexpressing *SHANK3*. Further, embryonic stem cell lines, with homozygous and heterozygous deletion of the *SHANK3* gene, gave rise to neurons with similar morphogenetic deficits to those seen in the *SHANK3* patient neurons. Both studies validate that the reduced expression of *SHANK3* is the cause for these morphogenetic deficits.

The discovery of these early morphological defects in human *SHANK3* mutant neurons has provided new insight into the mechanisms underpinning autism. This research has also developed a robust cell-based platform that can, not only be used to test these potential mechanisms, but also as a screen for potential therapies.

Acknowledgements

First and foremost, I would like to express my deepest gratitude for my first supervisor Prof. Jack Price for helping me throughout my PhD years. I thank him for giving me the opportunity to work in his amazing lab, his continual confidence in me and his encouragement. Second, I am really very grateful to Dr. Brenda P Williams, who has been my pillar of support in both scientific and non-scientific matters. Lastly, I would like to extend my appreciation to my second supervisor Dr. Deepak P Srivastava, whose passion in science is an inspiration. Thank you all!

None of this work would have been possible without the organizations that funded it. I am grateful to EU-AIMs (European Autism Interventions - A Multicentre Study for Developing New Medications) and MRC (Medical Research council) funded IOPPN scholarship for creating this studentship. Also, indebted to Dr. Sarah Curran for providing us with SHANK3 patient samples.

I must thank the Price lab members for creating such a friendly and amazing environment to work. I am thankful to Dr. Graham Cocks for generating the iPSCs lines that were used in the study. I am appreciative for all the help the lab technicians Victoria Wood, Paulina Nowosiad and Rosemary D'Oyly-Watkins provided. I thank Jacqueline Robbins and Dr. Katherine Warre Cornish for their wonderful company and friendship.

Special thanks to Dr. Wajeeha Aziz for being a great listener, friend and I will always appreciate our lovely walks and chats. Also, I would like to thank my parents and sister for believing in me. My PhD years would not have been possible without their support and love. Thank you so much for being there.

Table of Contents

Abstract 2

Acknowledgements 3

Table of contents 4

List of Tables 8

List of Figures 9

Abbreviations 11

Introduction 14

- **1.1 Autism Spectrum disorder** 14
- **1.2 Genetics of ASD** 14
- **1.3 Current Hypothesis for ASD** 16
- **1.3.1 First hypothesis for the underlying mechanism of autism-"Synaptic dysfunction"** 16
- **1.3.1 (a) Examples for the first hypothesis "Synaptic dysfunction"- Cell adhesion molecules** 17
- **1.3.1 (b) Examples for the first hypothesis "Synaptic dysfunction"- Scaffolding proteins** 18
- **1.3.2 Second Hypothesis for the underlying mechanism of autism-"Abnormal Neuronal growth** 19
- **1.3.2 (a) Examples for the second hypothesis "Abnormal Neuronal growth** 19
- **1.3.3 Third hypothesis for the underlying mechanism of autism-"Protein translation"** 21
- **1.4 *SHANK3* and autism** 24
- **1.5 The structure and function of *SHANK3* gene** 25
- **1.5 (a) Isoforms of *SHANK3*** 27
- **1.5 (b) *SHANK3* at the postsynaptic density** 28
- **1.5 (c) *SHANK3* associations with the cytoskeleton** 28
- **1.6 Rodent studies of *Shank3*** 30
- **1.6 (a) Synaptic Proteins altered in *Shank3* mutant mice** 31

- **1.6 (b) Morphological deficits in *Shank3* mutant mice** **32**
- **1.6 (c) Synaptic dysfunction in *Shank3* mutant mice** **33**
- **1.6 (d) Behavioral phenotypes associated with *Shank3* mutant mice** **35**
- **1.7 Can we link *Shank3* mutant mice studies to Human ASD?** **36**
- **1.8 The need for human cellular models** **37**
- **1.9 Modeling ASD in a dish using iPSC** **38**
- **1.9 (a) Rett Syndrome (RTT)** **39**
- **1.9 (b) Fragile X syndrome (FXS)** **39**
- **1.9 (c) Phelan McDermid Syndrome (PMDS)** **41**
- **1.10 Limitations of the iPS model and future** **42**
- **1.11 Hypothalamus and ASD** **43**
- **1.12 Neuralisation** **46**
- **1.13 Project Rationale** **47**
- **1.14 Aims of our study** **52**

Chapter 2 Methods **54**

- **2.1 iPSC generation and characterization** **54**
- **2.2: iPSC Cell Culture** **56**
- **2.3 Neuralisation** **57**
- **2.4 Plating and Quality check for Neurons** **59**
- **2.5 Cryopreservation and Thawing of neural progenitors** **59**
- **2.6 Immunocytochemistry for Confocal Microscopy** **61**
- **2.7 Immunocytochemistry for High Content Imaging** **62**
- **2.8 Actin staining** **63**
- **2.9 Neuronal morphological assessment via GFP transfections** **64**
- **2.10 Global Morphological analysis of control and *SHANK3* neurons (High content screening)** **65**
- **2.11 Manual counting and Error Rate** **68**
- **2.12 Neurite Outgrowth** **70**
- **2.13 Puromycin Assay** **72**

- **2.14 Preparation of Cell Lysates** **72**
- **2.15 Electrophoresis and Dry transfer of proteins** **73**
- **2.16 Analysis of the western blot** **73**
- **2.17 Synaptic Assay** **74**
- **2.19 Shank3 overexpression vector generation** **75**
- **2.20 Shank3 lentiviral particle generation** **77**
- **2.21 Verification of SHANK3 overexpression constructs** **79**
- **2.22 Rescue cells via IGF1 and BDNF** **81**
- **2.23 ES culture** **81**
- **2.24 Data analysis and statistics** **83**

Chapter 3 Results: Morphogenetic deficits reported in *SHANK3* patient neurons **84**

- **3.1 Verification of hypothalamic neurons** **90**
- **3.2 Morphological analysis of *SHANK3* patient neurons** **94**
- **3.2.1 Morphological analysis of single cell via eGFP** **94**
- **3.2.2 Tracking morphological changes through neuronal development** **96**
- **3.2.3 Neurite Outgrowth** **99**
- **3.3 Discussion** **103**
- **3.3 (a) ASD and Hypothalamus** **103**
- **3.3 (b) *SHANK3* haplo-insufficiency effects morphology of the neuron** **104**

Chapter 4: Rescue of morphogenetic deficits in *SHANK3* patient neurons **107**

- **4.1 Enhancing the expression of SHANK3 rescues the morphogenetic phenotype seen in SHANK3 patient neurons.** **108**
- **4.2 Morphogenetic deficits reported in genetically modified human embryonic stem cells (es)** **115**
- **4.3 Growth factors are unable to rescue *SHANK3* morphogenetic deficits** **120**

- **4.4 Discussion** 123

Chapter 5: The effects of *SHANK3* haplo-insufficiency on neuronal development 126

- **5.1 Do the levels of F and G actin change in *SHANK3* patient neurons?** 130
- **5.2 Does global protein synthesis vary in *SHANK3* patient neurons?** 132
- **5.3: Are there changes in the number synaptic puncta in SHANK3 patient neurons?** 134
- **5.4 Cell soma changes in sporadic ASD patients** 137
- **5.5 Discussion** 139
- **5.5 (a) Association of actin to *SHANK3*** 139
- **5.5 (b) Global protein synthesis is not altered in *SHANK3* patient neurons** 142
- **5.5 (c) Synaptic changes associated with *SHANK3* patient neurons** 142
- **5.5 (d) Decrease in cell soma area a global ASD phenotype** 144

Chapter 6 Discussion 148

- **6.1 How can *SHANK3* influence neurite outgrowth?** 148
- **6.2 How is neuronal migration linked to *SHANK3*?** 152
- **6.3 Cell soma size and Autism** 158
- **6.4 Possible mechanism on how *SHANK3* contributes to cell soma size** 160
- **6.5: Possible drug targets for ASD** 163
- **6.5 (a) Glutamate receptor agonists** 164
- **6.5 (b) Cofilin inhibitors** 165
- **6.5 (c) Oxytocin** 166

Bibliography 168

Supplementary information 201

Live Imaging Video (control and *SHANK3*) CD

List of Tables

Table 1.0: Summary of genes involved in ASD that affect the synapse.	**18**
Table 1.1: Common Cellular and Behavioral phenotypes	**21**
Table 1.2: *SHANK3* domains and its function.	**25**
Table 1.3: Cellular and molecular phenotypes associated with *Shank3* mutant mice.	**35**
Table 1.4: Function of hypothalamus	**45**
Table 2.1: Cell Lines	**55**
Table 2.2: Volumes	**56**
Table 2.3: Culture media and reagents	**58**
Table 2.4: Antibody list	**62**
Table 2.5: Secondary antibody list	**62**
Table 2.6: The average error rate percentage for the false positive cell shown by the cell insight.	**70**
Table 2.7: ES cell lines	**82**
Table 3.1: Percentage of each neuronal type	**91**
Table 3.2.1: Morphological analysis using High Content imaging.	**96**
Table 3.2.2: Neurite Outgrowth	**100**
Table 4.0: Neurons positive for Myc and transduction percentage	**109**
Table 4.1: Enhanced expression of *SHANK3* rescues morphogenetic phenotypes	**110**
Table 4.2: Morphological phenotypes of es derived neurons.	**116**
Table 5.1: Protein translational changes.	**132**

List of Figures

Figure 1.0: Pathogenic pathway of autism **23**

Figure 1.1: *SHANK3* structure and function at the synapse **26**

Figure 1.2: *SHANK3* expression pattern during early stages of neuralisation **49**

Figure 1.3: Project Rationale **50**

Figure 2.1: Neuralisation protocol **58**

Figure 2.2: eGFP plasmid vector **64**

Figure 2.3: Cellomics scan **68**

Figure 2.4: False reading done by the cell insight **69**

Figure 2.5: The *SHANK3* rescue vectors **76**

Figure 2.6: Format of *SHANK3* rescue experiment. **78**

Figure 2.7: Verification of *SHANK3* overexpression virus via immunocytochemistry **80**

Figure 3.1: Neuralisation **88**

Figure 3.1.2: Characterization of the neurons generated from iPSCs **93**

Figure 3.2: *SHANK3* patient neurons exhibit morphogenetic deficits **95**

Figure 3.2.2: Morphological deficits found in immature *SHANK3* patient neurons **98**

Figure 3.2.3: *SHANK3* patient neurons exhibit abnormal neurite outgrowth **101**

Figure 3.2.4: Cell soma movement **102**

Figure 4.0: Overexpression of *SHANK3* rescues morphogenetic phenotype **111**

Figure 4.1: *SHANK3* rescue versus control **113**

Figure 4.2: Morphogenetic deficits reported in genetically modified human embryonic stem cells (es). **117**

Figure 4.2.1: Neurite deficits reported in genetically modified human embryonic stem cells (es). **118**

Figure 4.3: Effect of IGF1 and BDNF on the morphology of SHANK **122**

3 patient neurons
Figure 5: Polymerisation of G actin to form F actin 127
Figure 5.1: Levels of F and G actin in control and *SHANK3* neurons 131
Figure 5.2: Protein translational changes in day 30 neurons 133
Figure 5.3: Changes in the number of synaptic puncta in day 70 neurons 136
Figure 5.4: Change in cell soma area in sporadic ASD patient neurons 138
Figure 6.1: Proposed mechanism of *SHANK3* in actin regulation 150
Figure 6.2: Priming of Arp2/3 complex leading to elongation 153
Figure 6.3: Possible mechanisms of GnRH neuron migration 156
Figure 6.4: SHANK3-Abi complex triggers activation of Arp2/3 complex for cellular migration 157
Figure 6.5: Possible mechanisms linking *SHANK3* to cell growth 162

Abbreviations

Abi-1-Abelson interactor 1

Abp1-Auxin binding protein 1

ACR-Acrosin

AMPA-α-amino-3-hydroxy-5-methyl-4-isoxazolepropionic acid

Arp2/3-Actin-Related Protein 2 and 3

ASD- Autism spectrum disorder

BDNF-Brain-derived neurotrophic factor

CACNAC1C- Calcium Channel, Voltage-Dependent, L Type, Alpha 1C Subunit

Cdc42- Cell division control protein 42 -

CNTNAP2- Contactin associated protein-like 2

CNVs- Copy Number Variants

Cortactin- Cortical actin binding protein

CRH- Corticotropin-releasing hormone

DA-Dopamine

DAPI- 4',6-diamidino-2-phenylindole

DAPT- N-[N-(3,5-Difluorophenacetyl)-L-alanyl]-S-phenylglycine t-butyl ester

DMSO- Dimethyl sulfoxide

DNase1- Deoxyribonulease

DCX-Doublecortin

EF1- Elongation factor-1 alpha promoter

ERK pathway- Extracellular signal-regulated kinases pathway

ES-Embryonic stem cells (human)

F actin- Filamentous

FMPR- fragile X mental retardation protein

FMR1 -fragile X mental retardation 1

FSH- Follicle stimulating hormone

FXS-Fragile X Syndrome

G actin-Globular actin

GEF- Guanine exchange factor

GFP-Green Fluorescent protein

GHRH- Growth-hormone-releasing hormone

GKAP- Guanylate kinase-associated protein

GnRH- Gonadotropin-releasing hormone

HBSS- Hanks' Balanced Salt solution

HEK293- Human embryonic kidney cells 293FT line

Homer- Homer protein homolog 1

HPA-Hypothalamus pituitary axis

IGF1-Insulin Growth Factor

iPSCs- Induced pluripotent stem cells

Klf4- Kruppel-like factor 4 KO-knockout

LH- Luteinizing hormone

LIMK- LIM Domain Kinase 1

FGF8-Fibroblast growth factor8

LTD-Long term depression

LTP- Long-term potentiation

MECP2- Methyl CpG binding protein 2

mEPSCs- Miniature excitatory postsynaptic currents

mGLuR- Metabotropic glutamate receptors

mTORC1- Mammalian target of rapamycin complex 1

Myc- Myc proto-oncogene

NDS-Normal Donkey Serum

NGLN-Neuroligin

NMDA- N-methyl-D-aspartate receptor

NOS2- Nitric Oxide Synthase 2

NRXN- Neurexin

N-WASP- Neuronal Wiskott–Aldrich Syndrome protein

OXTR-Oxytocin receptors

PAK1- neuronal Wiskott–Aldrich Syndrome protein

PBS- Phosphate-buffered saline

PFA-Para Formaldehyde

PGK-Phosphoglycerate Kinase 1 Promoter

PMDS- Phelan-McDermid Syndrome

PP2-Kinase inhibitor

PSD95-Post synaptic density95

PSD-post synaptic density

RABL2-Rab-like protein 2A

Rac1- Ras-Related C3 Botulinum Toxin Substrate 1

ROCKi- Rho-associated protein kinase (ROCK) inhibitor

RTT-Rett's Syndrome

SHANK1- SH3 And Multiple Ankyrin Repeat Domains 1

SHANK2- SH3 And Multiple Ankyrin Repeat Domains 2

SHANK3/ PROSAP2 -SH3 and multiple ankyrin repeat domains 3/Proline-rich synapse-associated protein 2

Sirt1-Sirtuin1

SMADi-SMAD inhibition

SOX2- SRY (sex determining region Y)-box 2

SPIN90- SH3 protein interacting with Nck, 90 kDa

SST- Somatostatin

SUnSET-Surface sensing of translation

TBR1- T-box, brain, 1

TRH- Thyrotropin-releasing hormone

TSC1/2- TSC1 tuberous sclerosis 1

TSH- thyroid - stimulating hormone-

Tuj1- Neuron-specific class III beta-tubulin

UBEA3A-Ubiquitin Protein Ligase E3A

Chapter 1
Introduction

1.1 Autism Spectrum disorder

Kanner first characterized autism in 1943 “As a group of children with an unusual pattern of behavior present from birth or before 30 months” (Kanner 1943). Autism is now considered as a spectrum of neural developmental disorders defined by the following behavior- (1) restricted repetitive behavior, interests and activities, (2) deficits in social interaction and communication and (3) decreased cognitive abilities (Carbonetto 2014). The worldwide prevalence of ASD is about 1-2.6 percent and is about four times more common in males than in females (Lord 2011; Baird et al., 2006).

There are no individual tests to confirm a diagnosis of ASD. Instead a diagnosis is usually based on the characteristics that the child displays. A series of interviews takes place and a detailed family history is taken, to track any genetic link that might exist. Assessments are mostly based on language and social behavior skills (Baird 2003).

In this introduction, I will present an overview of ASD, with special emphasis on the gene *SHANK3* as its cause.

1.2 Genetics of ASD

The etiology of autism is not fully understood; though recent data shows that 10-20 percent of ASD patients reported have an underlying genetic alteration (Betancur, 2011). There is a strong genetic basis to ASDs, as emphasized by studies with monozygotic twins where the concordance rate is up to 90 percent, while in dizygotic twins it is up to 20 percent (Hallmayer et al., 2011).

A fundamental challenge with the genetics of ASD is the large heterogeneity in the types of genetic mutations that contribute to ASD. These mutations include a large number of rare mutations including monogenic disorders, large chromosomal aberrations and multiplicative effects of common gene variants (Carbonetto 2014; VanderWeele et al., 2004). Approximately 5 to 7 percent of chromosomal abnormalities reported are 15q11-q13 duplications or 2q37, 22q11.2 and 22q13.3 deletions (Betancur 2011; Fishawy et al., 2014). Monogenetic causes of ASD are reported in approximately 2 percent of cases. Some examples of these are Fragile X syndrome caused due to mutation in the *FMR1* gene (Fragile X Mental Retardation 1), Rett's syndrome caused due to the mutation in *MECP2* gene (Methyl CpG binding protein 2), Angelman syndrome caused due to the mutation in *UBE3A* (Ubiquitin Protein Ligase E3A) and Timothy syndrome caused due the mutation in *CACNA1C* gene (Calcium channel, voltage-dependent, L type, alpha 1C subunit) (Kleijer et al., 2014).

Entire exome and genome analyses have converged on a particular chromosomal abnormality in autism. These are submicroscopic structural changes in the chromosomes called copy number variants (CNVs) (LaFlamme 2015). Recent evidence suggests that ASD can arise from *de novo* CNVs that result from deletions or duplications of relatively large regions of chromosome (Huguet et al., 2013). Thus, there is a huge emphasis on studying rare, highly penetrant CNVs in order to understand the underpinnings of brain connectivity in ASD.

One such example is the current research on the gene *SHANK3*. More than 1000 cases of *SHANK3* 22q.13 deletion have been reported. 75 percent of these have ASD and 95 percent display severe mental developmental delay (Jiang et al., 2013). Moreover, 2 percent of people who have autism carry a harmful deletion in the *SHANK3* gene (Leblond CS et al., 2014; Durand et al., 2007). Another example is of a cohort study carried out on 133 patients from USA and 83

patients from Italy that revealed five detrimental mutations in the SHANK3 gene with an occurrence rate of 2.3 percent (Buccoto et.al, 2013; Bayés À et.al 2010).

Additionally, two recent studies have shown that *SHANK3* is the most under diagnosed highly penetrant monogenic cause of ASD. The first study used whole genome sequencing to reveal a de *novo SHANK3* mutation in familial autism spectrum disorder (Nemirovsky et al., 2015). The second evaluated 32 patients and 0.5 percent of these cases revealed *SHANK3* haplo-insufficiency as the monogenic cause of ASD (Bentancur et al., 2013). Therefore, mutations in *SHANK3* can be considered as one of the causes of ASD.

Although, the main aim of this project is to describe the role of SHANK3 gene in ASD. I will first describe the current ideas on mechanism that underpin autism and how these relate back to the *SHANK3* gene.

1.3 Current Hypothesis for ASD

A number of interesting hypotheses have been proposed for autism. In this section I describe the three major ones that pertain mainly to cellular and molecular mechanism underlying autism.

1.3.1 First hypothesis for the underlying mechanism of autism-"Synaptic dysfunction"

The first hypothesis is the "**synaptic dysfunction**" that is primarily based on data from various genomic studies. The exome-sequencing analysis of 3871 autism cases implicated many genes that encode proteins for voltage-gates ion channels or proteins that are involved in synapse formation, synaptic scaffolding, and synaptic cell adhesion proteins (Rubeis SD et al., 2014; Bourgeon 2009; Zoghbi 2003). This data strongly indicates that synaptic dysfunction contributes to the cellular cause of autism.

Mutations in synaptic cell adhesion molecules, scaffold proteins and receptors and transporters have been linked to autism (Table 1.0). I give examples of some of the genes that are linked to first hypothesis below-

1.3.1 (a) Examples for the first hypothesis "Synaptic dysfunction"- Cell adhesion molecules

Several synaptic cell adhesion molecules have been linked to autism. These include Neurexins (*NRXNs*) and Neuroligins (NGLNs), *NRXNs* and *NGLNs* play an important role in the formation, maturation and maintenance of synapses (Kleijer et al., 2014) by acting as the glue between scaffolding protein and synaptic receptors. The loss of these protein results in synaptic transmission deficits. For example, Nlgn3 knockout (KO) studies in mice have shown a loss of mGLUR-dependent LTD in the cerebellum. Furthermore, knock in studies of the same gene showed increased mEPSCs, (miniature excitatory postsynaptic current) and enhanced LTP (Long term potentiation) in the hippocampus. Also, nrxn1 knockout in mice showed electrophysiological phenotypes such as reduced mEPSC frequency in the hippocampus (Baudouin et al., 2012; Etherton et al., 2011; 2009).

Another synaptic cell adhesion protein that has been associated with autism is Contactin-associated protein like 2 (*CNTNAP2*). The *CNTNAP2* is known to bind with *PSD95* (Post synaptic protein 95). PSD95 is a postsynaptic density protein and helps recruit various postsynaptic channels. *CNTNAP2* connects with *PSD95* and participates in the clustering of potassium channels at the postsynaptic density (Horresh et al., 2008). A RNAi-mediated knockdown of *Cntnap2* in rodent hippocampal neurons resulted in reduction of both excitatory and inhibitory synapses. This lead to asynchronous firing in cortical neurons (Geschwind et al., 2012).

1.3.1 (b) Examples for the first hypothesis "Synaptic dysfunction"- Scaffolding proteins

The proline rich synapse associated SH3 domain and ankryrin repeat family of postsynaptic scaffold proteins comprises of three members: *SHANK1, SHANK2 and SHANK3*. All three have been implicated as a cause of autism (Kleijer et al., 2013).

Various studies on autism, report that *SHANK1* mutations were detected more in males than in females (Sato et al., 2012). Studies by Hung et al., 2008 on *Shank1* knockout mice show decreased levels of Homer 1 b/c and mGLURs (metabotropic glutamate receptors). These authors also reported that these mice have a deficiency in basal synaptic transmission.

In mice hippocampal culture *Shank2* was knocked down which resulted in a loss synaptic clustering, mainly AMPA receptors (Berkel et al., 2012). Moreover, *Shank2* mutant mice with deletion in exon 6 and 7 of *Shank2*, displayed increase in NMDA (*N*-methyl-D-aspartate receptor) regulation (Schmeisser et al., 2012; Won et al., 2012).

Function	Process	ASD genes
Synaptic Structure	Cell adhesion	*NRXN1, NLGN3, NGLN4X, CNTNAP2, CNTN3, CNTN4, CNTN5, CNTN6, NRCAM, CDH9*
Synaptic Structure	Scaffolding	*PSD95, SHANK2, SHANK1, SHANK3*
Synaptic Signaling	Receptors and transporters	*VIPR, SSTR5, MET, GRIN2A, SCN1A, CACNA1C, FMR1, MECP2*

Table 1.0: Summary of genes involved in ASD that affect the synapse (Adapted from Kleijer et al., 2014).

As mentioned above, multiple studies have identified deleterious *SHANK3* mutations in patients with ASD (Moessner et al., 2007; Hamdan et al., 2011;

Denayer et al., 2012). Compared to *SHANK1* and *SHANK2*, mutations in *SHANK3* are highly penetrant and the vast majority of patients carrying a mutation in this gene develop severe cognitive deficits. There have been five *Shank3* mutant mice reported and one iPSCs (induced pluripotent stem cells) study of Phelan Mcdermid Syndrome. I will discuss these in detail in sections 1.6 and 1.9, as the emphasis of this thesis is to study the effects of *SHANK3* in autism.

Hence, in the section above we have described some of the synaptic genes that form the basis of autism. Nevertheless, there are many more genes that support the synaptic hypothesis of ASD; we have summarized some of these representative genes in Table 1.0.

1.3.2 Second Hypothesis for the underlying mechanism of autism- "Abnormal Neuronal growth"

The second hypothesis of ASD proposes that autism is caused by neuronal miscommunication, which arises from "**abnormal neuronal growth**". (Shepard 2013; Bourgeon 2009). Specifically, abnormal neuronal growth leads to irregular neuronal connections, which results in miscommunication between neurons. This hypothesis stems from the observation that 30 percent of ASD patients present with macrocephaly (Amaral David G et al., 2008). Moreover, a number of ASD studies account for abnormal neuronal structure.

1.3.2 (a) Examples for the second hypothesis "Abnormal Neuronal growth"

The first example for the second hypothesis is Fragile X syndrome (FXS) that is caused by a mutation in the *FMR1* gene. This gene encodes for a protein called fragile X mental retardation protein (FMRP) (Doers et al., 2014). This protein plays a role in *mRNA* transport from the nucleus to the cytoplasm in the neuronal cell soma. It is also involved in dendritic localization of *mRNA* and has a

suggested role in synaptic plasticity via stimulation of mGluRs (metabotropic glutamate receptors) (Lozano et al., 2014; Antar LN et al., 2005). Also, FMRP acts as a protein translational repressor (Darnell and Klann 2013). Almost 30 percent of FXS patients report symptoms of ASD (Doers et al., 2014).

Rodent models of FXS display an abnormal neuronal morphology such as thin and elongated dendritic spines in pyramidal neurons, increased spine density, fewer and shorter neurites and smaller cell body volume (Comer et al., 1997; Castren et al., 2005). Post mortem studies of FXS patients revealed a similar morphology to that observed in the mouse models - longer slender dendritic spines, smaller cell bodies and neurons with shorter neurites (Irwin et al., 2001; Castren et al., 2005). This suggests that the *FMR1* gene plays a role in structural development of a neuron.

In addition to these morphological changes, electrophysiological changes were also reported in *Fmr1* knockout mice. The most common one was an impaired mGLUR- dependent LTP (long term potentiation) but also a decrease in the frequency of spontaneous mEPSCs was also described (Bassell et al., 2008).
Taken together, this suggests that the loss of *Fmr1* gene leads to abnormal neuronal morphology that could result in synaptic dysfunction.

Another evidence for abnormal neuronal growth that leads to autism is the loss of vertical and horizontal organization of the cortical layers. This occurs due to the loss of neuronal polarity resulting in migration deficits (Wegiel et al., 2010). Impaired migrations of cortical projection neurons have been reported in *Cntnap2* knockout mice, resulting in a great imbalance in electrical activity, leading to epileptic seizures (Penagarikano et al., 2011). An interesting point to note is that this gene is also involved in the first hypothesis of synaptic dysfunction as discussed in section 1.3.1 (a).

Additionally, co-morbid disorder associated with autism is Rett Syndrome. Rett's syndrome is caused by the deletion of MeCP2 (methyl-CpG-binding protein 2). The MeCP2 protein acts as a transcriptional regulator and is associated with maturation of the central nervous system, particularly with the formation of synaptic contacts (Luikenhuis et al., 2004; Lombardi et al., 2015). Various rodent and human post mortem studies have found abnormal neuronal morphology associated with this disorder. For instance, reduced neuronal size, dendritic arborization, spine density and cell size have been reported (Brennand et al., 2012). Thus, providing support to the second hypothesis of abnormal neuronal growth.

Table 1.1: Common Cellular and Behavioral phenotypes: phenotypes found in mice models and postmortem studies of selective synaptic genes that are implicated in ASD (Adapted from Kleijer et al., 2014; Brennand et al., 2012).

Phenotypes	CNTNAP2$^{-/-}$	NLGN3$^{-/-}$	MeCP2$^{-/-}$	SHANK1$^{-/-}$	SHANK2$^{-/-}$	FMR1$^{-/-}$
Spine density	No change	-	Decrease	Decrease	Decrease	Decrease
Dendritic Aborization	Decrease	Increase	Decrease	-	-	Decrease
Cell volume	-	-	Decrease	-	-	Decrease
mGLUR dependent LTP and LTD	Imbalance of synaptic transmission	Decrease		-	Decrease	Decrease
Social interaction	Decrease	Decrease			Decreases	
Communication	Decrease	Decrease		Decrease	Decrease	Decrease
Repetitive behavior	Increase	Increase			Increase	Increase

1.3.3 Third hypothesis for the underlying mechanism of autism-"Protein translation"

The third hypothesis of autism suggests that **excess protein synthesis** at the synapse leads to chemical imbalance in the brain (Kelleher et al., 2008).

Protein synthesis/translation is the process by which *mRNA* produced during transcription is converted into a specific amino acid chain. A number of mouse models of autism have shown an increase in protein production especially at the

synapse (Kelleher et al., 2008). These are *PTEN1* (Phosphatase and tensin homolog), *TSC1*/2 (Tuberous sclerosis complex) and *UBE3A*.

Moreover, mice lacking 4E-BP2 (Eukaryotic translation initiation factor 4E-binding protein 2) show an increase in production of neuroligins. They also exhibit social interaction deficits and abnormal electrical activity, both of which are autism-like behaviors (Gkogkas CG et al., 2013; Kelleher et al., 2008).

From the above examples and Table 1.1, we observe that many of the genes implicated in the synaptic dysfunction hypothesis of ASD are also involved in the abnormal neuronal growth hypothesis. For example, *Cntnap2, Ngln3, Shank1, Shank2 and Fmr1* knockout mice all showed abnormal neuronal growth and synaptic dysfunction (Table 1.1). This leads to impaired communication between neurons, which results in desynchronization in the brain network (Welsh JP et al., 2005; He BJ et al., 2007; Zikopoulos et al., 2010). All together causing behavioral deficits, which is the key symptom of ASD. Therefore, we can imply that both the hypotheses, the synaptic dysfunction and abnormal cellular growth are intertwined. It is highly likely that the electrophysiological deficits that we have shown in the first section could be due to abnormal cell growth.

Therefore, I propose the following underlying mechanism for autism. ASD candidate genes disrupt the morphological structure of the neuron leading to aberrant synapse formation. This in turn causes deficits in synaptic transmission, which results in autistic phenotypes and symptoms (Figure 1.0).

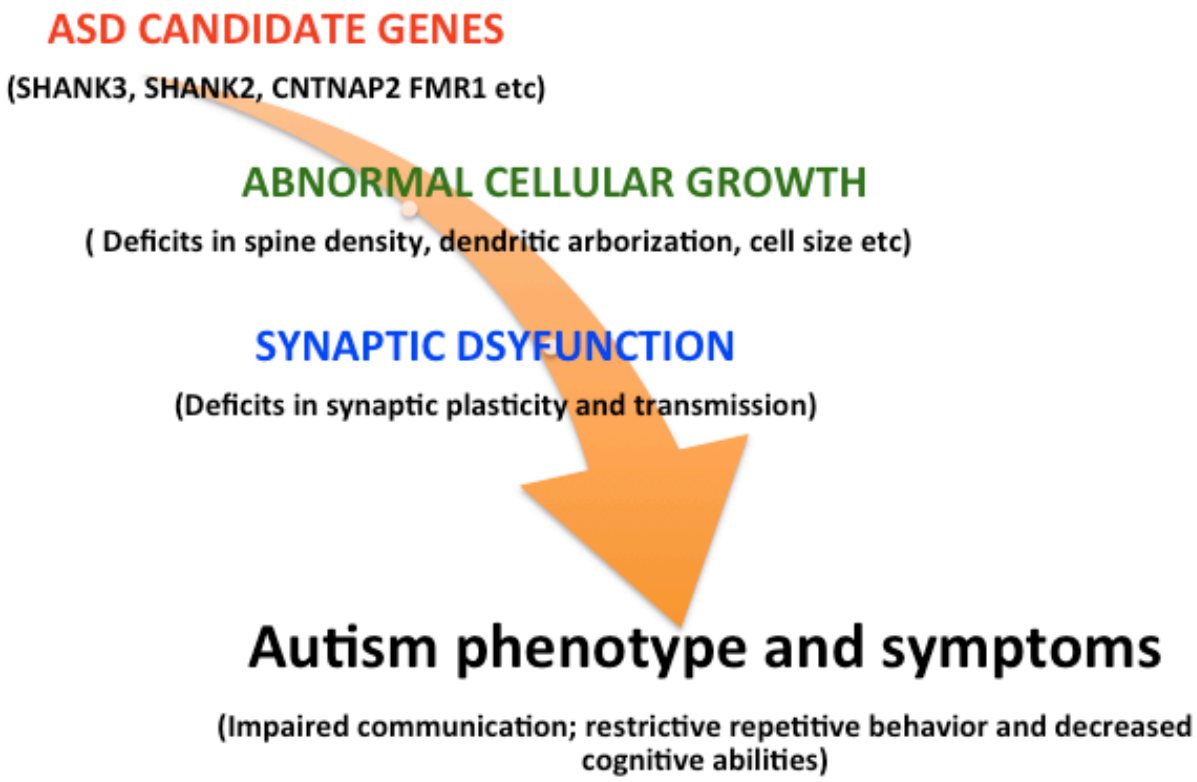

Figure 1.0: Pathogenic pathway of autism: The figure describes the proposed underlying mechanism for ASD. The candidate genes for ASD cause abnormal neuronal growth, which leads synaptic dysfunction resulting autistic phenotypes.

In next section of this thesis, I discuss the role of *SHANK3* in autism, as discussed in section 1.2. More than thousand cases of *SHANK3* 22q.13 deletion have been reported. 75 percent of these have ASD and 95 percent display severe mental developmental delay (Jiang et al., 2013). Several studies have reported that *SHANK3* has the highest pentrance rate in monogenic cause of Autism (Kolevzon A et al., 2011; Nemirovsky et al., 2015; Bentancur et al., 2013).

1.4 *SHANK3* and autism

Durand et al (2007) described three ASD patients with severe language delay carrying *SHANK3* mutation. The first two mutations were inherited missense mutations, termed R12C and R300C, which disrupted the N terminal ankyrin repeats within the gene (Figure 1.1). The third mutation was a de novo truncating stop mutation resulting in the loss of the C terminal of the gene. Subsequently, these human *SHANK3* mutants were overexpressed in vitro in mice hippocampal culture by Durand et al (2012). These resulted in disruption of several morphological and physiological functions of the neuron. In particular, the stop mutation resulted in loss of spine density and impaired synaptic transmission. Thus, suggesting that the mutant SHANK3 protein causes disruption in neuron morphology and synaptic signaling. An interesting point to note in this experiment is that SHANK3 mutant protein supersedes the function of wildtype protein. However, the cause for this is unknown.

Similarly, Moessner et al (2007) screened a cohort of 400 patients with ASD and found two gene deletions and one de novo mutation in *SHANK3* gene. The patients exhibited severe hyperactivity and absence of speech.

Additionally, Buccoto et al (2013) and Gautheir et al (2009) both reported more than 2% of *SHANK3* mutation in their study of ASD patients. All patients with *SHANK3* mutations exhibited signs of extreme speech delay and repetitive behavior. Likewise, a Japanese population study looked at 128 ASD patients with *SHANK3* mutations and all of them displayed a language development delay, hypotonia and mental retardation (Waga et al 2011).

Taken together the above studies demonstrate that *SHANK3* mutation could be considered as a cause of ASD. As it has been reported that *SHANK3* haplo-insufficiency is the highest cause of monogenic autism (Kolevzon A et al., 2011; Nemirovsky et al., 2015; Bentancur et al., 2013). Therefore, it is important to

understand how the loss of *SHANK3* might impact neuronal function and synaptic development, leading to ASD. The next section describes the known function of SHANK3 from various biochemical and mouse studies.

1.5 The structure and function of *SHANK3* gene

The *SHANK3* gene consists of 22 exons and encodes a multidomain protein as in shown figure 1.1. These domains comprise of N terminal ankyrin repeats (ANK), PDZ domain, sterile alpha motif (SAM) domain, SRC Homology (SH3) domain and proline rich domain (pro) (Uchino et al., 2013). The function of each domain is explained in table 1.2.

Binding Domain	**Interacting partner**	**Function found in Rodent studies**	**References**
N terminal ankyrin repeats (ANK)	Alpha fodrin, Sharpin	Development of spines and synapses	C Verpelli et al., 2011; Uchino et al., 2013; Jiang et al., 2013
PDZ	GKAP, PSD95, SPIN90,β-pix, NMDA and AMPA receptors	Formation of the post synaptic structure	Nasbitt et al., 1999; Verpelli et al., 2011; 2012; Uchino et al., 2013; Jiang et al., 2013
SH3 (SRC homology)	Densin 180		Quitsch et al., 2005
Proline rich area (Pro)	Homer1, Cortactin, Abp-1, Abi-1, mGLuRs.	Cytoskeletal remodeling and	Proepper C et al., 2007; Verpelli et al., 2012; Uchino et al., 2013; Jiang et al., 2013
A sterile Alpha domain (SAM)	Zinc	Regulation of Protein structure	Verpelli et al., 2012 and 2011

Table 1.2: SHANK3 domains and its function.

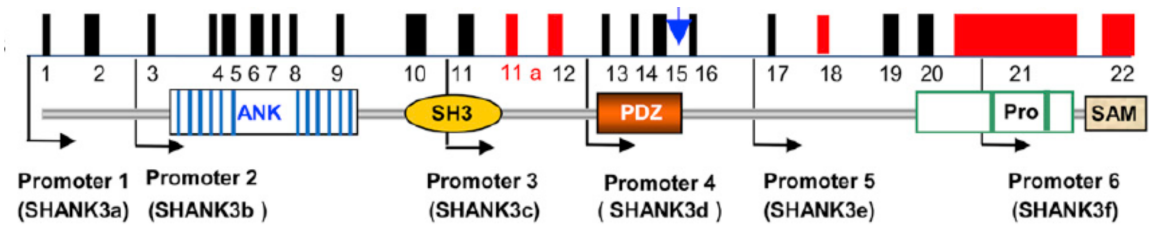

A

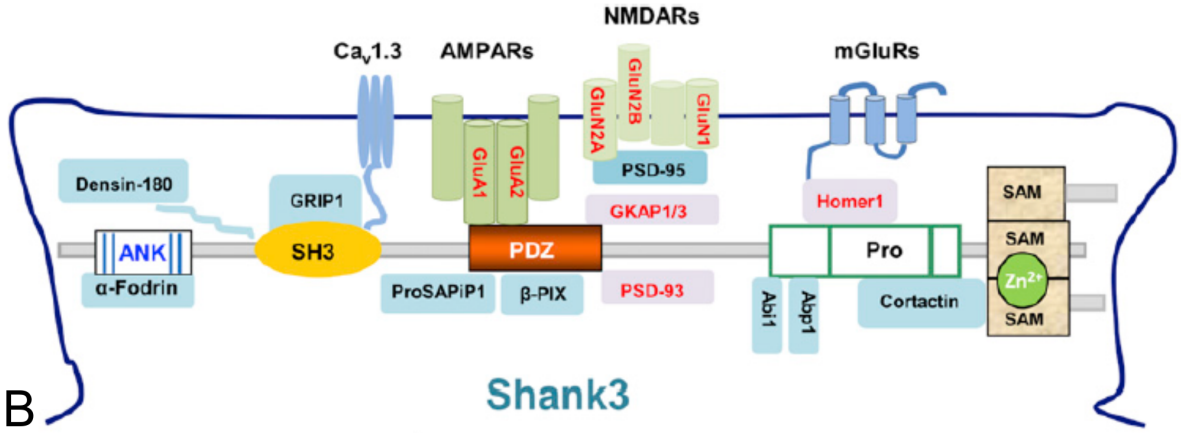

B

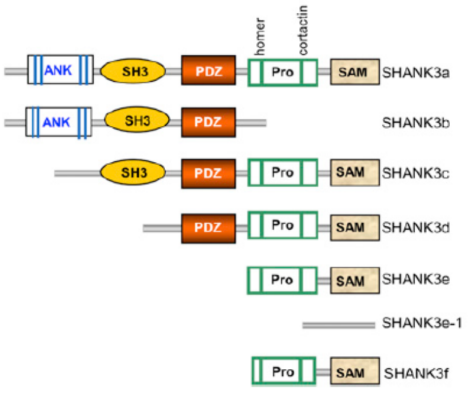

C

Figure 1.1: *SHANK3* structure and function at the synapse. A. The structure of the human *SHANK3* gene. Arrows represent the various intragenic promoters. B. SHANK3 and it various binding partners. C. Protein isoforms of *SHANK3* deduced from *mRNA* expressed in the human and mouse brain (Images are adapted, Jiang et al., 2013).

Various transcriptional studies have deduced the gene structure of *SHANK3*, for both mouse and human (Bonaglia MC et al., 2006; Wang et al., 2011; Boeckers TM et al., 1999). The generic *SHANK3* structure shown in figure1.1 is the same for both. However, the mouse *Shank3* gene structure has been characterized more extensively than the human *SHANK3* (Wang et al., 2011; Mameza et al. 2013; Bonaglia MC et al., 2006; Boeckers TM et al., 1999). Moreover, not the entire *SHANK3* gene has been mapped out, as it is highly GC rich which creates a difficulty in any method of DNA/RNA characterization. Thus, due to general similarity between the mouse and the human *SHANK3*, the functions of the *SHANK3* are thought to be similar in both cases.

1.5 (a) Isoforms of *SHANK3*

As of yet the exact number of protein isoforms encoded by the SHANK3 gene have not been determined. Nonetheless, various *mRNA* studies (Durand et al., 2007; Wang et al., 2011; Maunakea et al., 2010) have deduced the existence of seven isoforms, as shown in figure 1.1C in both human and mouse. As each domain of *SHANK3* has a unique function (Summarized in Table 1.2) and each isoform has a different combination of *SHANK3* domains, it is highly likely that each *SHANK3* isoform has a different function. For example, *SHANK3e* and *SHANK3f* lack the PDZ domain, which binds to the NMDA receptors via PSD95, while *SHANK3b* lacks the proline rich and the SAM domain, which is the Homer binding site. Therefore, this suggests that the different *SHANK3* isoforms may have different functions. As of yet there are no studies that have investigated the function of different *SHANK3* isoforms.

An interesting phenomenon is that different ASD patients have different mutations in SHANK3 gene, these could be isoform specific. For instance, a splicing mutation in intron 5 encoding the N terminal ANK repeats would only affect *SHANK3* isoforms a and b (Figure 1.1C, Jiang et al., 2013). Other deletions, in exons1-9, will affect different isoforms of *SHANK3*. Thus, we could

propose that isoform specific disruption of *SHANK3* could lead to different phenotypic effects. This could also explain clinical heterogeneity seen in *SHANK3* deleted ASD patients. There is also the possibility that some isoforms could be expressed earlier in development while others are expressed later in development. Till date no studies have been performed to observe the differential isoform expression of *SHANK3* during development. To test these hypotheses we would need to generate isoform specific antibodies as qPCR fails to work due to high GC content in *SHANK3* gene.

1.5 (b) *SHANK3* at the postsynaptic density

In humans the SHANK3 protein is abundantly expressed in the brain, heart and spleen (Lim Sangmi et al., 1999). In the brain of both mice and humans, SHANK3 is mainly expressed at the synapse and acts as a scaffolding protein for synaptic proteins (Jiang et al., 2013). Most studies have used mouse cDNA to characterize the binding partners of SHANK3. For example, it interacts with NMDAR via the PSD95 (Post synaptic density 95)/GKAP (guanylate kinase associated protein) complex that binds to its PDZ domain. This complex also binds the GluR1 subunit of the AMPAR (α-amino-3-hydroxy-5-methyl-4-isoxazolepropionic acid receptor). In addition, the proline rich domain of SHANK3 binds to the mGluR (metabotropic glutamate receptor) via Homer1 (Homer Scaffolding Protein 1) (Nasbitt et al., 1999; Lim S et al., 1999; M Sheng et al., 2000; Uchino et al., 2006; Uchino et al., 2013). This suggests that SHANK3 recruits various synaptic receptors to post-synapse. The activation of these receptors causes synaptic transmission and many forms of synaptic plasticity such as LTP and LTD.

1.5 (c) SHANK3 associations with the cytoskeleton

The cytoskeleton is an intracellular matrix that maintains the cell's shape and function. There is a dynamic interplay between SHANK3 and actin via proteins

that attach directly or indirectly to actin. For instance, Densin -180 binds to the SH3 domain and N terminal ANK domain of SHANK3 protein antagonizes dendritic branching. SHANK3 binds to C terminus of Densin-180 making the PDZ domain of Densin-180 inaccessible to δcatenin. δcantenin binds with Densin-180 and is required for the formation of new branches (Quitsch et al., 2005). Thus, suggesting that SHANK3 plays a role in maintenance of dendritic morphology.

Alpha fodrin interacts with the ANK domain of SHANK3 and helps regulate F actin elements in the spines (Bocker et al., 2001). Actin binding protein 1 (Abp1) and cortactin-actin-binding protein (cortactin) both bind to the proline rich domain of SHANK3 and are involved in regulation of spine morphology and actin polymerization at spine heads. Abp1 regulates Apr2/3 complex (Actin-Related Proteins ARP2 and ARP3) via N-WASP (neuronal Wiskott–Aldrich Syndrome protein) interaction to polymerize F actin to regulate spine density. As overexpression of Abp1 increases spine density this increases the number of synapses. (Du et al., 1998; Qualmann et al., 2004; Haeckel et al., 2008; Hering et al., 2003; Verpelli et al., 2012).

SHANK3 also binds with SPIN90 (SH3 protein interacting with Nck90), a known partner of the Arp2/3 complex and N-WASP (Kim et al., 2009). SPIN90 binds with both Arp2/3 complex and G actin leading to actin polymerization, which causes cell membrane ruffling to form lamellipodia. This helps the cell to move, leading to cell motility (Kim et al., 2006). Hence, suggesting that SHANK3 with the help of SPIN90 may play a role in cell migration.

The signal transduction molecule βPIX interacts with the PDZ domain of SHANK3 contributing to cytoskeletal organization within dendritic spines with the help of (guanine exchange factor) GEF. The downstream effectors of GEF are the GTPases Rac1 (Ras-related C3 botulinum toxin substrate 1) and Cdc42 (Cell division control protein 42). Both are involved in a wide variety of cellular

functions such as cell shape, structure, cell polarity, cell cycle and locomotion (Park et al., 2003; Verpelli et al., 2012).

It has also been reported that the Abelson interacting protein (Abi-1) binds to the proline rich area of SHANK3. This protein controls actin assembly via the WAVE1 complex (Wiskott-Aldrich syndrome protein family member 1) (Proepper C et al., 2007; Verpelli et al., 2012). Abi-1 acts as synapse to nuclear messenger. It is localised in the neurites and growth cones during early development. At later stages, the protein is found in post synaptic density in spines. As soon as NMDAR reached the PSD, the Abi-1 shuttles back to the nucleus to enhance E-box regulatated gene transcription (Proepper C et al., 2007).

In conclusion, the multiple binding domains of SHANK3 and its binding partners form the core element of the post synaptic density. Not only does SHANK3 play a role in synaptic recruitment, but it also binds with actin cytoskeletal elements to modulate synapse assembly.

1.6 Rodent studies of *Shank3*

Most of the known function of *SHANK3* has come from studying mice engineered to comprehend the role of *SHANK3* in autism. Five lines of *Shank3* mutant mice carrying different deletions in the *Shank3* gene have been generated (Wang et al., 2011; Yang et al., 2012; Bozdagi et al., 2010; Peca et al., 2011; Schmeisser et al., 2012). Three of these carry deletions in the N terminal ankyrin domain (ANK); the homozygous deletion of exon4-9$^{-/-}$ (Wang et al (2011); the heterzygous deletion of exon4-9$^{+/-}$ (Bozdagi et al., 2010) and a homozygous deletion in exon4-7$^{-/-}$ (Peca et al 2011). Peca et al (2011) also made a SHANK3 mutant line with homozygous deletion in exon13-16$^{-/-}$, which encodes for PDZ domain, while Schmeisser et al (2012) made mutant mice with a homozygous deletion in exon11$^{-/-}$ that encodes for SH3 domain. The cellular and molecular

phenotypes associated with these *Shank3* mutant mice are summarized in Table 1.3.

1.6 (a) Synaptic Proteins altered in *Shank3* mutant mice

Alterations have consistently been reported in the postsynaptic density (PSD) protein in all five mutant mice. Homer1 and GKAP protein levels were reduced in exon4-9$^{-/-}$ mice in the PSD fraction of the both hippocampal culture and tissue (Wang et al., 2011). Similarly, Homer 1, GKAP and PSD93 protein levels were also reduced in the PSD fraction of the striatum tissue in exon13-16$^{-/-}$ mice (Peca et al., 2011). However, no changes were reported in exon11$^{-/-}$ mice in Homer1 or GKAP protein levels in the neocortex tissue of the PSD fraction. However, Peca et al (2011) did not examine PSD fractions from neocortex and hippocampus, while Wang et al (2011) did not examine the striatum or neocortex. Therefore, this suggests that the protein level changes in PSD of mutant *Shank3* are tissue specific and/or could be mutant specific too.

Moreover, *Shank2* was found to be increased in this mutant model (Schmeisser et al., 2012). This could mean that there might be compensatory mechanisms if one SHANK family membrane protein destabilizes the other comes to rescue. It would be of interest to examine if this also occurs in the rest of the *Shank3* mutant mice models.

Mutations in the *Shank3* gene have caused a change in the levels of both AMPA and NMDA receptors (Jiang et al., 2013). For example, the GluA1 subunit of AMPA receptor was reduced in the hippocampus of exon4-9$^{-/-}$ and exon4-9$^{+/-}$ mice, and GluA2 was reduced in the striatum of exon13-16$^{-/-}$ mice (Wang et al., 2011; Bozdagi et al., 2010; Peca et al., 2011). There was a reported decrease in NMDA receptor subunits, namely GluN2A and GluN2B in the striatum of exon13-16$^{-/-}$ (Peca et al., 2011). In contrast, GluN2B was increased in the hippocampus of exon11$^{-/-}$ mutant mice (Schmeisser et al., 2012; Jiang et al., 2013). This

suggests that the loss of *Shank3* in these mutants alters postsynaptic protein. Also, the loss of these receptor molecules would impact synaptic transmission, which is known to affect behavior.

In conclusion, the pattern of synaptic protein alteration is different in each mutant mouse; this could be due to *Shank3* isoform specific effect of each mutation. For example, Peca et al 2011 *Shank3* mutant targets exon13-16$^{-/-}$, the PDZ domain report reduction in GKAP levels while Schmeisser et al., (2012) SHANK3 mutant targets exon11$^{-/-}$ SH3 domain reports no reductions in GKAP. This phenotype could be purely due to the isoform specific loss of *Shank3*, as the PDZ domain binds GKAP and not the SH3 domain. Table 1.3 shows in green some of the similarities and differences between the *Shank3* mutant models that could arise due to different isoforms being analyzed or the different brain tissues being examined by each *Shank3* mutant mice model.

Therefore, to fully understand the effects of *Shank3* mutations on synaptic protein composition, a simultaneous comparison of each mutant line at matching ages and matched brain tissues would need to be carried out.

1.6 (b) Morphological deficits in *Shank3* mutant mice

Since, *Shank3* plays a major role in cytoskeleton modeling of the neuron, the neuronal structure was examined in these *Shank3* mutant mice models.

The neuronal structure of medium spiny neurons in the striatum brain slices was analyzed in exon13-16$^{-/-}$ mice and an increase in dendritic length and arborization was reported (Peca et al., 2011). Furthermore, they examined PSD thickness and length, which were both decreased, suggesting that Shank3 helps in the development of the PSD. Spine length was increased and spine density was decreased in the hippocampus of exon4-9$^{-/-}$ mice (Wang et al., 2011) and similar observations were observed in exon13-16$^{-/-}$ mice, where spine density was

decreased in the striatum (Peca et al., 2011). Neuron morphology has not been examined in any of the other mutant mice (Jiang et al., 2013). From the above studies we can reflect that Shank3 through its various cytoskeleton binding partners regulates neuronal and spine morphology (section 1.5 c).

Another example of morphological changes to neurons was reported by Durand et al (2012), where they introduced two inherited deletion variants of *SHANK3* and two de novo mutations of *SHANK3* were transfected into rat hippocampal neurons. The inherited mutations (R12C and R300C) caused a decrease in spine density, while the two de novo mutations (truncating mutation STOP and ankyrin domain mutation Q321) decreased the development of dendritic spines and inhibited growth cone motility. They proposed that the mechanism by which *SHANK3* regulated spine formation was through F actin polymerization (as discussed above section 1.4). They overexpressed wild type *SHANK3* in rat hippocampal neurons and this lead to an increase in spine density and the same spines showed co-localization of *SHANK3* with F actin. Hence, suggesting that SHANK3 binds to F actin to regulate spine formation.

Thus, the morphological analysis of *SHANK3* in mutant mice revealed that *SHANK3* plays a complex role in synapse development particularly, its shape, size and structure.

1.6 (c) Synaptic dysfunction in *Shank3* mutant mice

Synaptic transmission and plasticity were examined in all the *Shank3* mutant mice. mEPSC frequency and amplitude, paired pulse ratio, input /output curves, synaptic transmission and LTP were reduced in hippocampal of exon4-9$^{+/-}$ mice (Bozdagi et al., 2010). However, exon4-9$^{-/-}$ mice only showed a decrease in LTP (Wang et al., 2011). Also, a decrease in frequency and amplitude of EPSCs were observed in the striatum of exon13-16$^{-/-}$ mice. EPSCs were also mildly affected in exon4-7$^{-/-}$ mutant mice (Peca et al., 2011). These variations between

studies could be due to mice genetic background, animal age and protocols used.

Taken all together the data supports that synaptic transmission is perturbed in *Shank3* mutant mice. However, it is not very clear whether there is a common core synaptic dysfunction in the various mutants, as all *Shank3* mutant mice show variation in synaptic phenotypes. This as mentioned before could be due to genetic heterogeneity between the *Shank3* mutant mice. For instance, one *Shank3* mice targets the PDZ domain (Peca et al., 2011) the other targets the SH3 domain (Schmeisser et al., 2012).

Similarly, *SHANK3* caused ASD patients to report various types of *SHANK3* deletion. For example, Moessner et al (2007) a missense mutation in exon 8 while Bonaglia et al (2001) describes a mutation that disrupts exon 21 of the *SHANK3* gene. The first patient in Messer's study has a verbal repetitive behavior, understands complex instruction and has no motor disorder while Bonaglia's study patient has severe language delay, mental retardation and hypotonia. Even though the patients have deletion in the same gene, there is clinical heterogeneity in symptoms. This could be due to the different *SHANK3* isoforms that are disrupted by each mutation.

Bozdagi et al., 2010 and Yang et al., 2012 *Shank3* exon4-9+/-	Wang et al., 2011 *Shank3* exon4-9-/-	Peca et al., 2011 *Shank3* exon13-16-/-	Schmeisser et al.,2012 *Shank3* exon 11-/-
Frameshift caused by a deletion of exon4-9 (Ankyrin repeats) disrupted only 50% full length *Shank3*	Frameshift caused by a deletion of exon4-9 (Ankyrin repeats) disrupted *Shank3* isoforms shank3 a and b only	Frameshift caused by a deletion of exon13-16 (Ankyrin repeats) disrupted *Shank3* isoforms shank3 a,b,c and d	Frameshift caused by a deletion of exon11 (SH3 domain) disrupted *Shank3* isoforms shank3 a,b,c and d
Reduction of GluA1, decreased spine density, decreased mEPSC frequency and increased amplitude have been reported.	Reduction of GKAP, Homer1b/c, GluA1, GluN2A; longer dendritic spine, decreased spine density and reduced LTP	Reduction of SAPAP3/GKAP3, Homer1, PSD93,GluA2, GluN2A,GluN2B; Increase in striatal volume, dendritic length and dendritic number; Decreased spine density, length and thickness of PSD and reduced mEPSC frequency and amplitude.	Increased GluN2B and Shank2

Table 1.3: Cellular and molecular phenotypes associated with *Shank3* mutant mice (References Wang et al., 2011; Yang et al., 2012; Bozdagi et al., 2010; Peca et al., 2011; Schmeisser et al., 2012).

1.6 (d) Behavioral phenotypes associated with *Shank3* mutant mice

Extensive behavioral analysis has been performed on all five *Shank3* mutant mice. Reduced social interaction was the most consistent behavior noted in all five *Shank3* mutant mice (Jiang et al., 2013). An increase in repetitive behavior such as behavior inflexibility and increased self-grooming were observed in exon4-9$^{-/-}$ and exon4-9$^{+/-}$ mice (Bodazagi et al., 2010; Wang et al., 2011).
Exon13-16$^{-/-}$ mice showed a more marked increase in self-injurious and self-grooming behavior, while no behavioral change was reported in exon4-7$^{-/-}$ mutant mice (Peca et al., 2011). In addition, exon11$^{-/-}$ mutant mice also reported an increase in self-grooming behavior (Schmeisser et al., 2012).

Intellectual disability is commonly reported in patients with a *SHANK3* mutation. In *Shank3* mutant mice they tested this using learning and memory tasks such as the Morris water maze task. Only exon4-9$^{-/-}$ mice showed impairment in this area (Wang et al., 2011).

Thus, we can conclude that most behavioral changes reported in these mice can be somewhat linked to behaviors observed in autistic patients in humans, but a difficulty arises from these studies since none of these *Shank3* mice mutations have been found in human ASD. A better experiment would be to take human *SHANK3* mutants and introduce those into mice, to see if it changes behavior. These have not been modeled in vivo because *SHANK3* gene is very difficult to manipulate, as it is highly GC rich. Durand et al., 2012 has done this in vitro in mice hippocampal culture but not in vivo to study the cellular effects of mutant *SHANK3*.

1.7 Can we link *Shank3* mutant mice studies to Human ASD?

In humans, ASD is diagnosed through behavioral symptoms. Currently, there are no reliable biomarkers or anatomical and functional imaging studies that can be predictive of autism (Kleijer et al., 2014). Moreover, little is known about the etiology of autism although several brain region and circuits have been implicated in autism (Kleijer et al., 2014; Jiang et al., 2013). Mice behavioral studies such as social, communication and intellectual ability studied by a range of learning and memory paradigms are not robustly translatable to humans (Silverman et al., 2010; Jiang et al., 2013). In addition, there is a huge variability in the clinical presentation of these impairments in humans, which cannot be characterized in mice models.

A burning issue is to understand the common pathophysiology that underlies autism, as this will help us develop better diagnostic tools and drugs to treat or prevent the disease. Studies on *Shank3* mutant mice have provided somewhat overlapping but not identical phenotypes indicating, cellular disruption which leads synaptic dysfunction. However, this is still not robust enough because of the variability between mice models probably reflecting the heterogeneity of mutations studied. Thus, there is a need to study specific *Shank3* mutations that correspond to the mutations that occur in humans and are known to cause ASD.

One way of doing this would be to study these *SHANK3* mutations in human cellular models. These studies could help us understand the cellular pathway that forms the basis of autism.

1.8 The need for human cellular models

Much of our current knowledge of the molecular pathways that leads to human developmental disorders such as ASD have come from heterologous systems and genetic animal models, in particular, mouse models. However, there are considerable differences that exist between the human and mouse genomes. Mouse models cannot fully represent the disease pathophysiology because of differences in brain development and signaling pathways. For example, Nitric oxide synthase-2 (NOS2) gene in the brain produces different levels of nitric oxide in humans than mice (Hoos et al., 2014). There is no debate that mouse models of autism have provided some insight into the mechanism of the disease but these have not resulted into any translational benefits for patients. Human cellular models have the potential to address these issues as cellular phenotypes found in these model could be a reflection of the diseased state. Drugs can then be tested on the phenotypes found to cure or prevent the disease from happening.

There are different types of human cellular models that could be considered. The first are immortalized human cell lines. These lines have been used to overexpress mutant proteins to understand disease pathophysiology (Eigenmann et al., 2012). Yet, these lines in prolonged culture acquire genetic abnormalities and massive overexpression of human proteins does not reflect human pathophysiology. Thus, this approach has significant limitations.

Another possibility could be the use of human embryonic stem cells (es). These cells are derived from embryos at the blastocyst stage and are pluripotent in nature and can self renew (Narinh Hazim et al., 2011). Nonetheless, the use of

human embryos for research purposes remains ethically controversial and logistically challenging because of the limited supply of human embryo donors (Narinh Hazim et al., 2011).

The last and most recent approach to generating human cellular models is to reprogram adult somatic cells to generate pluripotent stem cells (Cocks et al., 2014). The advantage of using induced pluripotent stem cells (iPSCs) is that we can generate patient-specific iPS cell lines to model complex disorders like autism. iPSCs retain the capacity to indefinitely renew and differentiate into cells from all three germ layers (Sterneckert et al., 2014). This makes iPSCs valuable for disease modeling, drug discovery and personalized medicine applications (Sterneckert et al., 2014).

1.9 Modeling ASD in a dish using iPSC

Takahashi and Yamanaka et al (2006) first reprogrammed mouse fibroblasts to generate pluripotent cell by overexpressing four transcription factors, Oct4, Klf4, Sox2 and c-Myc). Later, Takahashi et al (2007) used human fibroblasts to reprogram into a pluripotent stage. iPSCs have the capacity to self renew and to differentiate into various types of cells (Yamanaka 2012). Studies have shown that iPSCs retain the genetic memory of the parent cell (Shao et al., 2013;Yamanaka 2012). Hence, the phenotype discovered from iPSC-derived cells would be indication of the parental genotype.

Various human disorders have been successfully modeled using iPSC, including ASD (see section 1.9) and studies using iPSCs have resulted in the development of new drug treatment strategies. For example, Parkinson Disease platelet deficiency, spinal cord injury and macular degeneration (Yamanaka 2012) have all been modeled through iPSCs. Thus, iPSCs have allowed the investigation of the complex mechanisms behind disease pathophysiology and explore potential new treatment.

1.9 (a) Rett Syndrome (RTT)

To date three main iPSC studies have been reported for RTT syndrome. RTT is a neurodevelopmental autism spectrum disorder. It is caused by a mutation in the *MECP2* gene. Marchetto et al (2010) studied three female patients with missense mutations and one female patient with a frameshift mutation in this gene. They generated iPSCs lines from these patients. The neurons differentiated from patient lines reported fewer synapses, altered calcium signaling and a decrease in frequency and amplitude of spontaneous current. Morphological deficits were also evident, with neurons having a reduced cell soma size and reduced spine density. Additionally as mentioned above, post mortem and rodent studies of RTT syndrome have described morphological deficits in neurons such as reduced cell soma. Ananiev et al (2011) and Cheung et al (2011) both generated iPSC lines from RTT syndrome patients and showed that neurons generated from such lines had a decrease in cell soma area. The iPSCs studies of RTT corroborate the morphological phenotype as observed in post mortem studies of RTT. Thus, suggesting that iPSCs can be used as a model for neurodevelopmental disorders.

1.9 (b) Fragile X syndrome FXS

There have been a number of iPSC studies that have modeled FXS (Urbach et al., 2010; Sheridan et al., 2011; Jing Liu et al., 2012; Doers et al., 2014).
FXS is a common form of mental retardation and is closely linked to autism. The genetic basis of FXS is an expansion of CGG repeats in the 5' untranslated region of *FMR1* gene (Fragile X mental retardation protein). The expansion of this nucleotide repeats leads to loss of function of *FMR1* (Doers et al., 2014).

Post morterm studies of FXS have described cortical neurons with smaller cell volume, neurons with shorter and fewer neurites. iPSCs models of FXS have

described similar phenotypes. For instance, Liu et al (2012) used FXS patients to generate iPSCs, which were then converted into cortical neurons. They described neuronal phenotypes associated with FXS, such as reduced neurite length, neurite number and synaptic puncta. Also, these neurons were functionally abnormal, with calcium transients that were increased in amplitude and frequency.

Similarly, Sheridan et al (2011) studied iPSC-derived neurons from FXS patients. These also had fewer, shorter neurites and more compact cell soma. Moreover, this was further confirmed by Doer et al (2014), they also studied neurite outgrowth and reported deficits in neurite initiation and extension.

Taken together the iPSC studies validate the deficits in neurite morphology as they were also observed in post mortem studies. This also suggests that the iPSCs generated neurons can produce disease related phenotype.

Recently, FXS iPS derived patient cells have been used as a high throughput screen to find compounds that could increase the expression of FMRP1 and reverse the phenotypes reported. Out of the 5000 compounds screened they found 6 compounds that modestly increased the expression of *FMR1* (Kumari D et al., 2015), suggesting new compounds for developing therapeutics. These compounds have not been tested to see if they can reverse the disease phenotype as reported above. Hence, this indicates that patient derived iPSCs can be used for drug screening which could be useful in generating future therapeutics for neural developmental disorders.

1.9 (c) Phelan McDermid Syndrome (PMDS)

Phelan McDermid syndrome also known as 22q13 deletion syndrome is a neurodevelopmental disorder characterized by global developmental delay, speech delay, intellectual disability, poor motor coordination and ASD (Costales Jesse et al., 2015). Among the various genes deleted in this syndrome, *SHANK3* is considered the most likely candidate for causing the neurological abnormalities observed in patients (Scheglovitov et al., 2013). The cellular and molecular phenotypes associated with PMDS have been studied in iPSC lines generated from two patients. They found that iPSC-derived PMDS neurons have a reduced expression of SHANK3 and impaired excitatory synaptic transmission. Both amplitude and frequency of mEPSCs were significantly reduced and synaptic puncta staining revealed a decrease in both pre- and post-synaptic puncta, suggesting that there were fewer synapses in these neurons. Interestingly, these phenotypes could be rescued by treating the neurons with *SHANK3* overexpression.

A few points to be noted in this study are first; that the study supports the first hypothesis that “synaptic dysfunction” causes autism (section 1.3). Second that the study focuses on synaptic phenotypes, which occur late in development. They did not look at morphological deficits in neurons. Third, the rescue experiment was performed using a rat *Shank3* overexpression construct, which is similar to humans yet not completely the same. My study also looks at the role of *SHANK3* not in PMDS but in ASD, therefore, the above points are my reflection on what are the potential gaps in the PMDS iPSC study that my study would fill in as described in section 1.12.

1.10 Limitations of the iPS model and future

There are a few issues regarding the modeling of diseases with iPSCs. They exist in the form variability between (1) neuron to neuron (intra-patient) (2) cell line to cell line from the same patient (intra patient) (3) patient to patient (inter patient) (Brennand et al.,2012).

The variability between types of neurons generated exists due to the type of neutralization protocol used, all the iPSCs models described above use a mixed neuronal population. Currently, there are no studies that produce a specific neuronal subtype. There are, however, protocols for different lineages, such as cortical, hypothalamic or motor neurons (Salimi et al., 2014). Also, all the iPSC studies mentioned above looked at cortical lineage. This would be important because there might be a disease those effects only specific subtype of neuron and the phenotype of disease might get diminished in the mixed population. For instance, Parkinson's disease affects dopaminergic neurons. To study specific neuronal subtypes one could separate the cells of interest by FACs (Fluorescence-activated cell sorting) or use immunocytochemistry to identify the neural subtypes present.

It has been well established that there is variability in lines generated from the same patient (Brennand et al., 2012). Genetic variations can occur due to location and number of viral integration during the reprogramming process, iPSC generation and expansion (Brennand et al., 2012). However, these can be checked for by quality control testing for each iPS line generated. For example, our lab performs karyotyping analysis after each line generation and high passaged number lines are discarded (Cocks et al., 2014).

Inter patient variability comes from the clinical heterogeneity of the patients (Brennand et al., 2012). Most studies compare 2-3 patients' iPSC lines and there is always a concern about whether such findings pertain to the whole patient

population. To overcome this we need to develop more robust methods that are less time consuming and permit the examination of thousands of patients simultaneously.

1.11 Hypothalamus and ASD

Most autism studies focus on neuronal defects within cortex, hippocampus and striatum. Nevertheless, there is another part of the brain that we can consider plays an important role in ASD – the hypothalamus**.** Recently, an MRI study was performed where 52 autistic children were compared to 52 matched controls (Kurth et al., 2012). This study looked at various brain regions and found diminished grey matter in the hypothalamus (Kurth et al., 2012). These findings lead to our interest in understanding the role of the hypothalamus in autism.

iPSCs can be converted into various neuronal lineages by using specific protocols (Salimi et al., 2014). A postdoctoral researcher in our lab, Dr. Graham Cocks, has generated a protocol to generate hypothalamic neurons. The hypothalamus controls for social behavior, growth, body temperature, appetite, sleep, energy storage and circadian rhythms (Brodal Per 2004).

The hypothalamus is located above the pituitary gland and occupies about two percent of our brain. In terms of neuroanatomy, it is the most ventral part of the diencephalon (Lechan et al., 2013). The hypothalamus is a highly connected area of the brain forming connections with the limbic system including the amygdala and septum. It receives input from the brain stem, including the nucleus of the solitary tract, ventrolateral medulla and locus coeruleus (Lechan et al., 2013). The hypothalamus can be divided into three regions, the Anterior, Posterior and Tuberal region and these areas are further divided into nuclei, which releases different neurohormones that regulate different functions of the body (Table 1.4; Brodal Per 2004).

For example, the para ventricular nucleus of the anterior hypothalamus produces the hormone cortisol releasing hormone (CRH). This hormone stimulates the adrenocorticotropic hormone (ACTH), which helps regulates stress responses in the body (Brodal Per 2004). GnRH (Gonadotropic releasing hormone) released from the preoptic nucleus of the hypothalamus stimulates follicle stimulating hormone and luteinizing hormone, which play an important role in regulating sex hormones (Lechan et al., 2013).

Children with autism have difficulty adapting to new environments (Spratt EG et al., 2012). When cortisol levels were compared in children with and without autism, higher peaks of cortisol with a prolonged duration were found in autistic children (Spratt EG et al., 2012). Cortisol is a downstream product of CRH, which is often regulated through the hypothalamic –pituitary-axis (HPA). The HPA axis regulates various body function such as stress responses, digestion, immune system and social behavior (Smith et al., 2006). In primates elevated cortisol levels produce social withdrawal symptoms (Kerickson et al., 2005). Since, in autistic children the cortisol levels are higher due to the imbalance of HPA axis, I propose that this could lead to the social withdrawal symptoms often reported in ASD.

A recent study reported that gestational hypothyroxinemia in rodents induced impaired cortical neuronal migration. Neuronal migration deficits have been reported in autistic children (Belmonte et al., 2005). TSH (Thyroid stimulating hormone) is produced by the hypothalamus and regulates thyroid hormone production (Roman GC et al., 2013). Moreover, low levels of TSH during mid pregnancy have been shown to significantly increase the odds of a child being diagnosed with autism (Yau et al., 2015).

Using mass spectrometry and liquid chromatography, the concentrations of four sex steroid hormones, progesterone, testosterone, 17α-hydroxy-progesterone androstenedione, have been studied in autistic children. All of these were found

elevated (Baron-Cohen et al., 2015). GnRH produced by the hypothalamus is a precursor to all of these hormones. All the above studies have clearly established a link between hypothalamus and autism. Therefore, in this study we focus on the role of hypothalamic neurons in autism (section 1.1).

Region	Nucleus	Hormone	Function
Anterior	Medial Preoptic nucleus	GnRH (Gonodatropic releasing hormone)	Stimulate the release of follicle stimulating hormone (FSH) and luteinizing hormone (LH) from anterior pituitary
	Superoptic nucleus	Vasopressin	Oxytocin-Uterine contraction
		Oxytocin	Lactation
			Vasopressin-reabsorption of water in collecting ducts.
	Paraventricular Nucleus	Thyrotrophic releasing hormone (TRH)	TRH- stimulates the release of thyroid stimulating hormone (TSH) from the anterior pituitary
		Corticotrophin releasing hormone (CRH)	CRH- releases adrenocorticotropic hormone from anterior pituitary
		Somatosatin (SST)	SST-Inhibit growth hormone and TSH from anterior pituitary
Tuberal	Arcuate nucleus	Growth hormone releasing hormone (GHRH)	GHRH-stimulate growth (GH) from anterior pituitary
		Dopamine(DA)	DA-Inhibit prolactin release from anterior pituitary
Posterior	Tuber mammillary nucleus	-	Learning
			Memory
			Sleep
			Feeding
			Energy
			Attention
	Lateral nucleus	Orexin	Regulates wakefulness and appetite
	Mammillary	-	Memory
	Posterior nucleus	-	Autonomic regulation of nervous system. Regulates blood pressure, shivering and vasopressin release

Table 1.4: Function of hypothalamus: The table describes the various hypothalamic nuclei and their respective function (Burbach et al., 2001; Ronald Lechan et al., 2013; Brodal Per 2004).

1.13 Neuralisation

Neuralisation can be defined as the process of directing differentiation of stem cells (iPS or ES) into various neural lineages using small synthetic molecules. Over the years various protocols have been devised to make different neuronal types. A few examples are described below:

- **Cortical neurons**: The "dual smad inhibition" methodology has been shown as the most robust protocol to make cortical neurons (Shi, Yichen et al., 2012; Boissart et al., 2013). In this protocol iPS/ES cells are cultured as an adherent monolayer and is exposed to two smad inhibition molecules, SB431542 and Noggin. SB431542 blocks the phosphorylation of the ALK4, ALK5 and ALK7 (Anaplastic lymphoma kinase receptors), which leads to the inhibition of Lefty/Activin/TGFβ pathways (Transforming growth factor beta) . Noggin inactivates BMP4 (bone morphogenetic protein) . Both treatments together are required for the conversion of stem cells into neurons, specifically cortical (Chambers et al.,2009). This protocol is now widely used to study various neurological disorders such as Autism, Schizophrenia, Alzheimer's and Stroke. Recently, a study successfully transplanted hiPSC derived cortical neural progenitors into rats suffering from Stroke. These cortical progenitors not only differentiated into cortical neurons but also improved the neurological symptoms of the rats (Tornero et al., 2013). Now, research is moving towards generating three dimensional models of the cerebral cortex known as cerebral organoids using the same principles as small molecules inhibition (Lancaster et al., 2013).
- **Midbrain Dopaminergic neurons**: Directing the differentiation of iPSC neurons into dopaminergic neurons is fundamental for realizing its potential as a treatment for Parkinson disease. Once the stem cells are exposed to smad inhibitors (Noggin and SB431542), which cause neural induction, additional factors such as SHH and FGF8 are added. The signaling of these molecules causes the neurons to turn into midbrain/hindbrain fate (Perrier et al., 2004, Fasano et al., 2010). In 2011, Jaeger et al. reported a high efficient way of making dopaminergic neurons. They induced neural differentiation using dual smad inhibiton for 3 days and then blocked FGF8 signaling using two small molecules namely PD0325901 and PD173074. This caused early neural induction and directed ventral midbrain neuronal characteristics. This treatment was followed by FGF8 and SHH treatment that promoted the generation of dopaminergic neurons and restricted alternative fates.
- **Striatal Projection neurons**: The primary projection neurons of the striatum are the GABAergic medium-sized spiny neurons. These neurons

specifically degenerated in the early phases of Huntington's disorder. Hence, neural differentiation protocols have been developed to make these striatal neurons. For example, a recent study uses Activin A to induce the formation of lateral ganglionic eminence (LGE) neural progenitors from human iPSCs and ES cells. These LGE neural progenitors differentiate into DARPP32 positive striatal neurons (Charles Arber et al., 2015).

- **Other neuronal differentiation**: There are many other neuralisation protocols that are still under development, such as the differentiation of stem cells into motor, hypothalamic and cerebellar neurons (Boulting et al., 2011; Wang et al.,2015, Erceg et al., 2012).

Hence, through the above examples, we can infer that there are many neuralisation protocols that have not only allowed us to study various aspects of neuronal development but also to model neuron specific disorders such as Parkinson's, Huntington's, Autism and many more.

1.14 Project Rationale

In the above sections we have described various rodent and human cell-based models of autism. Also, *SHANK3* has been reported as the highest monogenic cause of ASD. Hence, the next question that arises is what can we do to understand more about the role of *SHANK3* in autism. This will help us understand the function of *SHANK3* in humans and *also* provide us with tools to develop better therapeutics for ASD caused due to *SHANK3*.

Recently, a postdoctoral researcher Dr. Walter Luchessi in our laboratory was studying *SHANK3* expression at different stages of neuralisation. Neuralisation can be defined as the process of converting iPSCs into neurons. There are five main stages of neuralisation- the iPSC (day 0), the neural progenitor (day 12/13), the rosette (day18/19), the immature neurons (day 24 to 36) and mature neuron (day 70) stage (Figure 2.3A). He looked at the gene expression pattern of *SHANK3* over the first four stages and compared four control lines taken from two healthy patients (Control P1 C1; Control P1 C2 and Control P2 C1; Control

P2 C2) to two *SHANK3* patient lines taken from one *SHANK3* ASD patient (SHANK3 P1 C1; SHANK3 P1 C2)

He found that there is an early expression of *SHANK3* from day 13 of neuralisation (Figure1.2A). This qPCR expression analysis was carried out using eight primer sets encompassing the various regions of the *SHANK3* gene. For the purpose of this discussion, Walter provided me with the results of two primer sets namely exon3-5 and exon16-18 (Figure 1.2 A and B). The position of these exons is shown in Figure1.2C, with a black line indicating exons 3-5 and a red line indicating exons16-18. Both graphs show *SHANK3* expression starting from day 19 of neuralisation. To support this, the western blot in figure 1.2 D shows the SHANK3 protein expression starting from day 19 of neuralisation in a control line. It also depicts that SHANK3 protein is being expressed throughout neuralisation day 24 and 36.

This data is also indicative of various SHANK3 isoform being expressed at different stages. For example, in SHANK3 exons3-5 are being expressed from day 13 onwards while *SHANK3* exon16-18 expression only starts from day19 (Figure 1.2 A). This suggests that as cells go through the rosette stage (day19) and enter the immature neuronal stage (day24), expression of the *SHANK3* exon16-18 isoform goes up. Thus, taken together these results suggest that *SHANK3* is being expressed early during neuralisation and there might be an isoform switch.

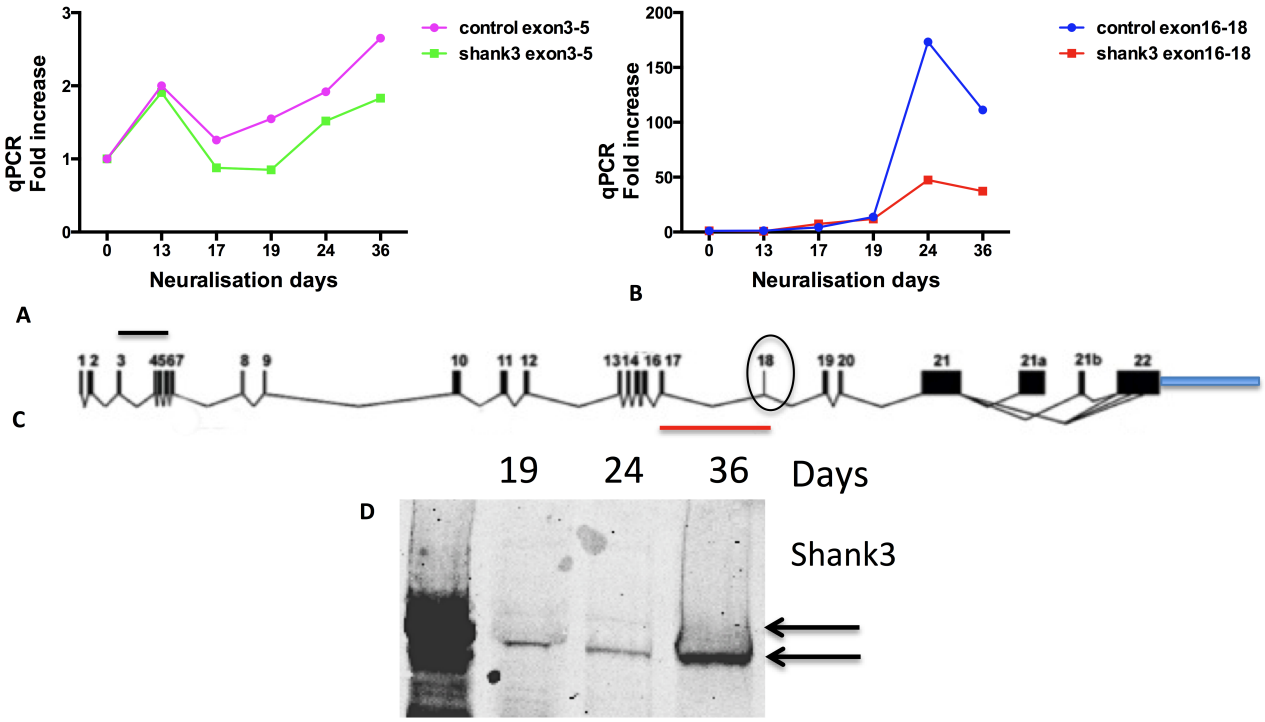

Figure 1.2: *SHANK3* expression pattern during early stages of neuralisation. Dr Walter Lucchesi performed these experiments. A. qPCR fold increase of control versus shank3 of exon3-5. B. qPCR fold increase of control versus shank3 of exon16-18. C. Black line highlights the exon3-5 primer and red line highlights exon16-18 primer in the *SHANK3* gene. D. Western blot showing the SHANK3 protein expression from day19 to day 36 from a control line. This study was performed in two controls versus one shank3 patient, with one clonal replicate of each (4 control vs. 2 *SHANK3* lines, n=3). The antibody used in these experiments has an epitope against SHANK3 exon 21. The gene expression (Fold increase) of *SHANK3* is compared to day 0, the iPSC stage.

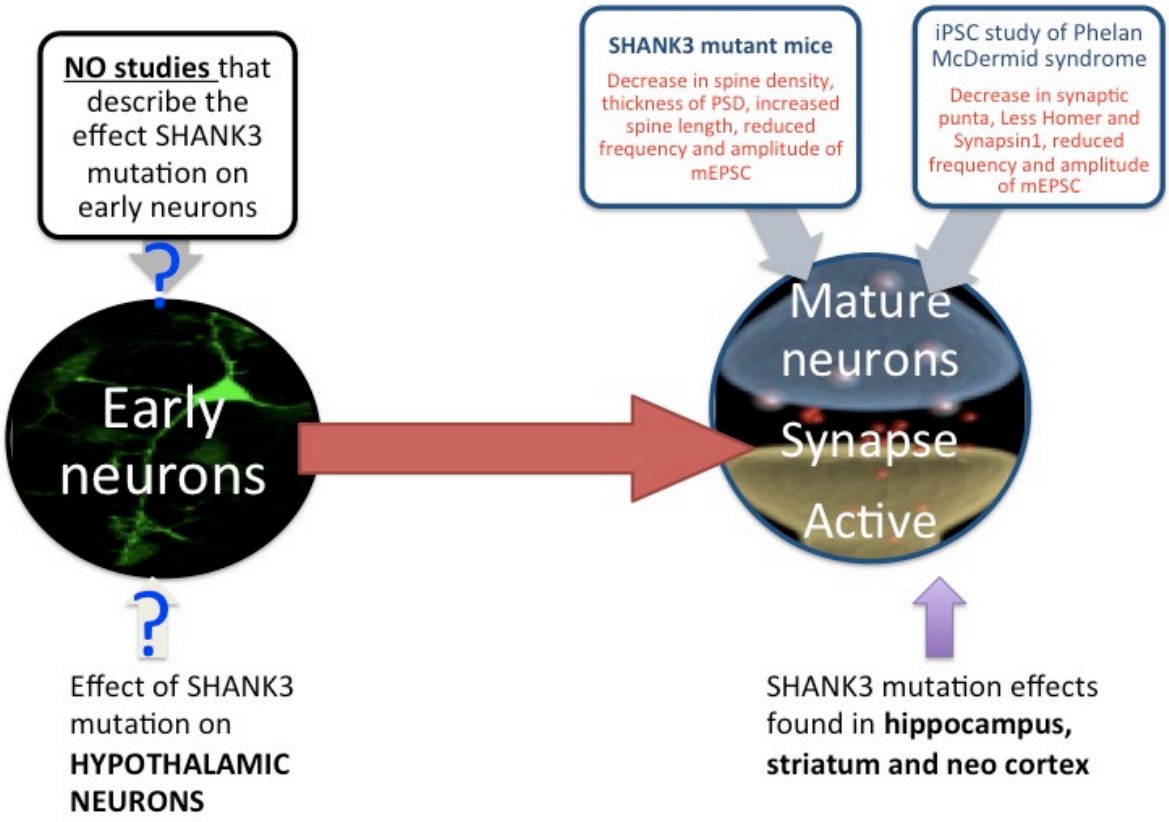

Figure 1.3: Project Rationale: The aim of this thesis is to discover the role of *SHANK3* in early development in hypothalamic neurons and how it contributes towards ASD.

As mentioned above most studies of *SHANK3* in autism focus on the synaptic phenotype, which develops at later stages of neuronal development (Figure 1.3). Currently, there are no studies that show the effects of *SHANK3* mutation on early neuronal development. Since, we have established that *SHANK3* is expressed during early stages (Figure 1.2) this study aims to fill this gap in our knowledge by investigating the role that *SHANK3* plays during early neuronal development and how disruption of this role may contribute to autism. Also, this builds on the hypothesis mentioned in figure1, which suggests that ASD candidate genes cause early neuronal abnormalities which leads to later synaptic dysfunction and combines the two main hypotheses for ASD - "the synaptic dysfunction hypothesis" and "the abnormal cellular growth hypothesis" - as the underlying mechanism for autism.

The second potential gap in our knowledge lies in the type of neurons most studies have focused on. In rodent models, we have seen effects of *Shank3* mutation on the hippocampus, striatum and neocortex (section 1.6). The iPSCs studies of ASD have focused on generating cortical neuronal lineages. None of these studies have looked at hypothalamic neurons. As mentioned in section 1.11, the hypothalamus produces various neurohormones, which are important for social behavior. Social behavior is a key aspect of ASD, as one of the main symptoms is impaired social interaction. Therefore, in this study we focus on the hypothalamic neurons and how they are affected in early development.

1.15 Aims of our study

Prof Jack Price's lab has generated iPSC lines from root hair biopsies from three categories of individual: autistic individuals carrying a deletion in the SHANK3 gene, neurotypical controls and sporadic ASD patient line. The *SHANK3* patient lines have been generated from two patients. The first patient is a four year old male diagnosed with autism, regression of motor skills, language and speech delay, who has a deletion from *SHANK3* exon4 to the next gene *ACR* (Acrosin). Acrosin is a protease enzyme that is released from the acromsome of spermatozoa (Zheng et al.,2012). The second *SHANK3* patient line is from a five-year-old female diagnosed with autism, social communication disorder and speech delay. The patient has a deletion extending from *SHANK3* exon4 to the next two genes *ACR* and *RABL2* (Ras oncogene family like 2). I carried out this deletion mapping using a TaqMan assay as part of my master's thesis project (Data shown in Supplementary table 1.0 and 2.0).

As the etiology of autism is poorly understood, iPSCs provide us with a unique opportunity that allows us not only to study the cellular mechanism behind autism but also to follow the developmental trajectory. Thus, the aim of this project is to discover cellular and molecular phenotypes associated with autism.
This study has three specific aims:

1. To compare the morphology of control neurons to *SHANK3* patient neurons at different stages of neuralisation. The structure of a neuron is critical for its function, as the size and shape of this cell defines its capacity to receive and send signals (Kulkarni et al., 2012).
2. To rescue the morphogenetic phenotypes discovered by enhancing the expression of *SHANK3*.
3. To assess via preliminary assays the underlying mechanisms behind the morphogenetic phenotypes discovered in Aim1.

These investigations will enable us to generate an in vitro system to help understand the cellular basis of ASD as well as provide a system that, in the future, can be used for drug screening.

Chapter 2

Methods

2.1 iPSC generation and characterization

Hair root were harvested from three autistic patients and three neurotypical controls. Keratinocytes were derived from the hair root biopsies and converted into iPSCs using lenti-viral reprogramming (Cocks et al., 2014). Dr. Graham Cocks did this in Prof. Jack Price's lab.

The autism lines were generated from two individuals with a heterozygous deletion in the *SHANK3* gene (see Table 2.1). The first patient was a 4-year-old male diagnosed with autism, regression of motor skills, language and speech delay. This individual carried a heterozygous deletion stretching from exon4 of the *SHANK3* gene to the *ACR* gene (Acrosin). The second patient was a 5-year-old female diagnosed with autism, social communication disorder and speech delay. This individual had a heterozygous deletion stretching from exon 4 to the neighboring genes *ACR* and *RABL2* (Rab-like protein 2A). The deletions were mapped out during my Master's thesis using Taqman assay (Supplementary table 1.0 and 2.0). The third autism patient line was generated from a male patient diagnosed with sporadic autism. Two clonal lines were generated from each patient and control line. Please see table 2.1 for more details.

Unlike the other cell lines used in this study, the control patient 2 clone 3 line was generated using sendai viral vector rather than lentiviral vectors (Table 2.1). The sendai virus contains single stranded negative anti-sense RNA, which replicates in the host cytoplasm. Therefore, there is no viral integration in the host cell.

Cell Line Name	iPSC Line Name	Patient Details
Control Patient 1 Clone 1 Control P1 C1	Control Male 242 CM242	Healthy Control Male
Control Patient 1 Clone 2 Control P1 C2	Control Male 205 CM205	Healthy Control Male
Control Patient 2 Clone 1 Control P2 C1	Control Male 322 CM322	Healthy Control Male
Control Patient 2 Clone 2 Control P2 C2	Control Male 315 CM315	Healthy Control Male
Control Patient 2 Clone 3 Control P2 C3	Control Male m336s CM336s	Healthy Control Male
Control Patient 3 Control P3	Control Female CF102	Healthy Control Female
ASD Patient 1 ASD P1	ASD Male ASD M101	Sporadic ASD Patient Male
ASD Patient 1 Clone 2 ASD P1 C2	ASD Male ASD M108	Sporadic ASD Patient Male
SHANK3 Patient 1 SHANK3 P1 C1	SHANK3 Male SHANK3 M103	SHANK3 deleted Male Patient
SHANK3 Patient 2 SHANK3 P1 C2	SHANK3 Male SHANK3 M107	SHANK3 deleted Male Patient
SHANK3 Patient 2 SHANK3 P2 C1	SHANK3 Female SHANK3 F109	SHANK3 deleted Female Patient
SHANK3 Patient 2 SHANK3 P2 C2	SHANK3 Female SHANK3 F107	SHANK3 deleted Female Patient
SHANK3 Patient 2 SHANK3 P2 C3	SHANK3 Female SHANK3 F103	SHANK3 deleted Female Patient

Table 2.1: Cell Lines: The cell lines used in this study.

2.2: iPSC Cell Culture

Vial of iPS cells, stored in liquid nitrogen, were thawed at 37°C and plated onto one Geltrex coated (Life Technologies, diluted in Dilbecco's Modified Eagle's Media F-12 (DMEM: F: 12); Sigma Aldrich and incubated for one hour at 37°C) well of a 6 well Nunclon^{TM} tissue culture dish (Thermo Scientific) in Essential 8^{TM} medium (Life Technologies). Cultures were then placed in a Binder CB150 incubator at 37°C, 5% O_2, 5% CO_2 and saturated humidity. The culture medium was then changed every 24 hours until the cells reached 50-80% confluence, when they were passaged at a dilution of 1:6 (1 well into 6 wells).

For passaging, media was removed by aspiration and cells were washed with pre-warmed Hank's Balanced Salt Solution HBSS without Ca^{2+} and Mg^{2+} (HBSS; Life technologies). The HBSS was removed by aspiration and then replaced with room temperature Versene (Life Technologies), which was left on for 4 minutes at 37°C. The Versene was then removed, the cells detached from the culture vessel using pre-warmed media (Essential 8^{TM} medium) and transferred into a geltrex-coated 6 well tissue culture dish. The volumes of the reagents used for passaging cells are detailed in Table 2.2.

Table 2.2: Volumes: Tissue culture reagents volumes for different vessels.

Vessel	Media	HBSS	Accutase
96 well plate	200µl	100µl	50µl
6 well plate	2 ml	2ml	1ml
12 well plate	1ml	1ml	500µl
24 well plate	500µl	500µl	200µl

2.3 Neuralisation

iPSCs were plated in 6 well plates (Nunclon^{TM} tissue culture) on to plates coated with Geltrex and treated with three inhibitors of SMAD (mothers against DPP homologs signaling) -1μM dorsomorphin + 10μM SB431542 + 5 μM XAV (SMAD inhibitors (SMADi) in N2:B27 (henceforth referred to as "neuralisation medium"). Plates were then incubated for 24 hours at 37°C (5% CO_2; 20% O_2). Medium was replaced every 24 hours until day 7, or until formation of a uniform neuroepithelial sheet occurred (Figure 2.1). At day 7, wells were rinsed with HBSS and 1mL/well cold (4˚C) Accutase (1 ml) was added. The plates were then transferred to the incubator for 2-5 minutes (37°C; 5% CO_2; 20% O_2), until cells could be removed by gentle pipetting. The collected cells were transferred into DMEM (1 ml) and centrifuged at 900 RPM for 5 minutes. Once the supernatant was removed, DMEM (1 ml) was added to resuspend the pellet and the cell suspension was again centrifuged at 900 RPM for 5 minutes. After removing the supernatant, neuralisation medium + 10μM ROCKi was added to the tube to dissolve the pellet. The cells were plated on to fresh 6 well gletrex coated plate and then incubated for 24 hours (37°C; 5% CO_2; 20% O_2) Following this, the medium was removed and replaced with 2mL/well N2:B27 only (i.e. no SMADi) and the medium was replaced every 24 hours until day 12**.** The cells were then passaged using the protocol described above. Further passaging was carried out at day 15 and 18. On day 19/20, the cells were terminally plated on to Laminin for neural differentiation. See Table 2.3 for source of materials used.

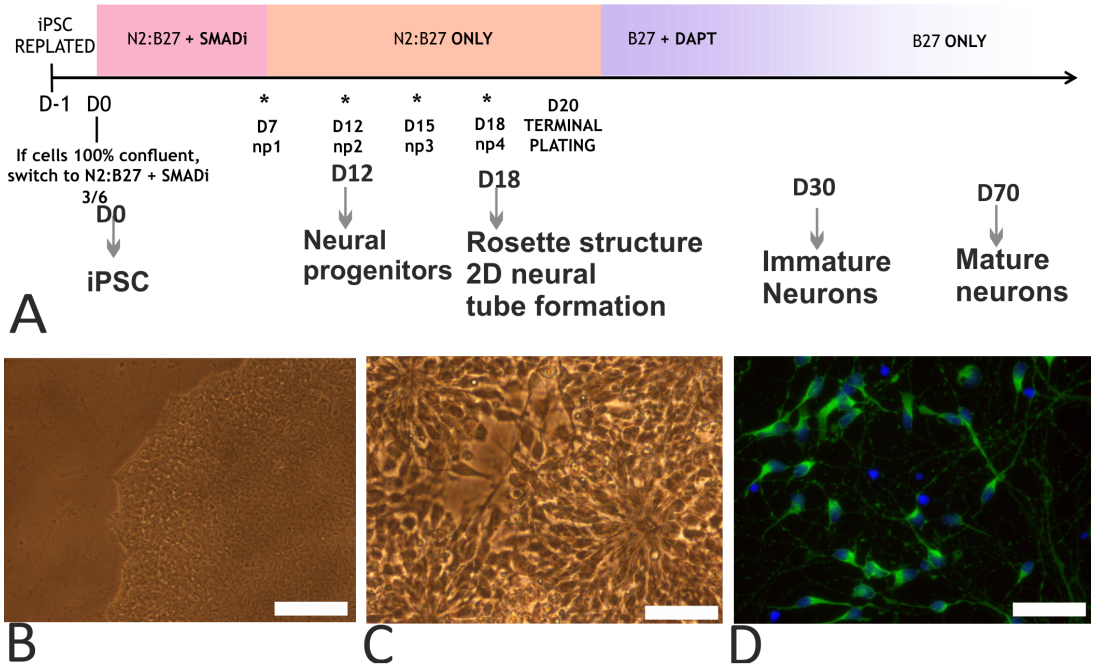

Figure 2.1: Neuralisation protocol. A. The neuralisation protocol summary. B. iPSC colony (Scale=100μm) C. Rosette structure (Scale=50μm) D. Tuj1 positive neurons at day 26 (Scale=50μm). D-1 (Day one, D0 (day 0)- iPSC stage, D7- (Day7) neural passage 1 (np1), D12-Day 12 neural passage 2 (np2), D15- Day 15 neural passage 3 (np3), D18-Day18 neural passage 4 (np4), D20-Day20 terminal plating of neural progenitors, D30-Day30 immature neurons and D70-Day70 mature neurons.

Table 2.3: Culture media and reagents

Culture media and reagents
Geltrex (Life Technologies; A1413302)
HBSS (Invitrogen; 14170146)
Versene (Lonza; BE17-711E)
E8 Medium (Life Technologies; A1517001)
ROCKi (Sigma; Y0503)
Accutase (Invitrogen; a1110501)
N2 Supplement (Life Technologies; 17502-048)
DMEM (Sigma; D6421)
B27 Supplement (Life Technologies; 17504-044)
Neurobasal Medium (Life Technologies; 21103-049)
Glutamax (Life Technologies; 35050-038)
SB431542 (Cambridge Bioscience; ZRD-SB-50)
Dorsomorphin (Sigma; P5499)
Laminin (Sigma; L2020)
DAPT (Abcam; ab120633)

2.4 Plating and Quality check for Neurons:

Plates were coated with poly-D-lysine (0.2mg/ml) in borate buffer (Thermo Scientific Pierce) and incubated (37°C; 5% CO_2; 5% O_2) overnight. The plates were rinsed with PBS and Laminin (Laminin from Engelbreth-Holm-Swarm murine sarcoma basement membrane Sigma L2020) was added at a concentration of 20µg/mL diluted in DMEM for plastic dishes (Nunclon™ tissue culture) and 30µg/mL diluted in DMEM for glass dishes (Greiner Bio One) and incubated (37°C; 5% CO_2; 5% O_2) overnight. Glass dishes were used for imaging studies while plastic dishes were used for protein studies.

Day 20 neurons were removed from the culture dish using Accutase as described previously and the cells resuspended in B27 medium supplemented with 10µM ROCKi and 10 µM DAPT. ROCKi inhibitor helps single cell survival and DAPT anti Notch signal molecule, which induces the neural progenitors to differentiate into neurons. The cells were counted using a haemocytometer and at a density of 1500-2000 cells/well of a 96 well plate. Following 24 hours of incubation, the medium was replaced with Neurobasal media (Life Technologies) and was supplemented with B27. B-27 was used because it is required for neuronal growth. Medium was then replaced twice a week but after the first week, only half the medium was replaced in each well. On day 25, quality control was carried out on each neuronal culture and if 90% of cells were not positive for the Neuronal specific marker B-iii tubulin (Tuj1) the culture was discarded.

2.5 Cryopreservation and Thawing of neural progenitors

In order to generate independent iPSC samples to replicate experiments, neural progenitors were generated as described above and then cryopreserved at day 19. Three independent iPSC samples were generated for each line.

Neural progenitors that were supposed to be cryopreserved were collected using Accutase, as described above then following two washes in HBSS the cells were resuspended in freezing medium (10% DMSO in B27/N2) and transferred to pre-labeled 1mL cryovials. The cryovials were transferred into Mr. Frosty™ Freezing Container (Thermos Scientific) and kept in -80°C freezer for 24 hours before being stored in liquid nitrogen until required.

The cryovials were thawed in a 37°C water bath. The vial contents was then transferred into a centrifuge tube (15 ml) and 5mL of 37°C B27/N2 medium + 10μM ROCKi added in a dropwise fashion. This cell suspension was then centrifuged at 900 RPM for 5 minutes, the pellet was resuspended in B27 and 10μM ROCKi (1 ml) and the cells were counted. Cells were plated on poly-d-lysine and laminin coated 96 well plates at a concentration of 2000 to 3000 cells per well of 96 well plate. Following 24 hours of incubation, the medium in each well was replaced with 100μL of Neurobasal media with B-27 plus 10 μM DAPT and 10μM ROCKi. To maintain these cultures the medium was replaced twice a week but after the first week, DAPT was removed from the medium and only half media changes were carried out. On day 25, we analyzed the cultures to determine the percentage of neurons present, as described above.

ROCKi is added on the day of passage and thawing. In the first 24 hours after passaging the cells are in single cell state, ROCKi helps this survival. After 24, we remove ROCKi from the medium as the cells need to clump and form a monolayer for neural induction to occur. Moreover, DAPT an anti notch signaling molecule is added for neuronal differentiation from neural progenitor. Only two doses of this are required as this is enough for neural progenitors to convert into neurons.

2.6 Immunocytochemistry for Confocal Microscopy

In order to study the neuron morphology of control and *SHANK3* neurons, GFP transfected neurons were analyzed at day 30 and 45 of neuralisation via confocal microscopy. Also to count the number of pre and post synaptic puncta, I used Immunocytochemistry and confocal imaging. This was done at day 70 of neuralisation.

For immunofluorescence analysis, cultures were grown on 24 well glass bottom culture plates (Greiner Bio One) that were fixed with 100% methanol at -20°C for 5 minutes on ice, and permeabilised with 0.1 % triton X 100 (Sigma) for 10 minutes. This was followed with three washes of phosphate buffered saline (PBS). Cultures were then incubated with the appropriate primary antibody (Table 2.4) diluted in normal donkey serum (NDS) at 4°C for 12 hours. Wherever the antibody classes permitted, cultures were incubated with various primary antibodies simultaneously. The culture plate was then washed three times with PBS and incubated for 1 hour at room temperature with the appropriate secondary antibody (Table 2.5). DAPI (4'-6 Diamindino-2-phenylindole) or Hoescht 2000 was added at a dilution of 1:2000 to stain the nucleus. In all experiments, to ensure that the observed staining was specific, controls were included in which primary antibodies were omitted or incorrect secondary antibodies were used.

Table 2.4: **Antibody list**

Antibody Used	Species/ Dilution	Company
Tuj1 (Neuronal specific Biii tubulin)	Mouse/1 in 1000	Covance
DCX (Double cortin)	Rabbit/ 1in 500	AbCam
CRH	Sheep/ 1 in 100	Novus Biologicals
GnRh1	Rabbit/ 1 in 500	Atlas
TH	Rabbit/1 in 1000	AbCam
Phalloidin	Cytopainter KIT	AbCam
G actin staining (Bovine pancreatic deoxyribonuclease DnaseI)	-	Life Tech
Shank3	Rabbit/ 1 in 100	Atlas
Myc	Mouse/ 1 in 5000	Cell signaling
Anti GFP	Rabbit/ 1 in 500	AbCam
Synaptophysin	Mouse/ 1 in 300	AbCam
Homer	Rabbit / 1 in 300	Synaptic systems
Puromycin	Mouse 1/1000	Kerafast

Table 2.5: Secondary antibody list

Secondary Antibodies	Species/Dilution	Company
Alexa 488	Mouse/ 1 in 500	Invitrogen
Alex 594	Rabbit/ 1 in 500	Invitrogen
Alexa 594	Mouse/ 1 in 500	Invitrogen
Alex 680	Mouse/ 1 in 500	Invitrogen
Oydessey 800	Rat/1 in 5000	Oydessey
Alexa 594	Sheep/ 1 in 500	Invitrogen

2.7 Immunocytochemistry for High Content Imaging

To measure the morphology of the neurons for the whole cell population, I used high content imaging. Cryopreserved neural progenitors from day 19 of neuralisation were thawed for this analysis. Differentiated neurons were grown on 96 well Nunclon^{TM} tissue culture plates coated with PDL and laminin. Then they were fixed with 4% para formaldehyde PFA for 20 minutes at room temperature, and permeabilised with 0.1 % triton X 100 (Sigma) for 10 minutes. This was followed with three washes of phosphate buffered saline (PBS). The cultures were incubated with the appropriate primary antibody (Table 2.4) in normal donkey serum (NDS) at 4°C for 12 hours. Wherever the antibody classes permitted, cultures were incubated with various primary antibodies

simultaneously. The plate was then washed three times with PBS and incubated for 1 hour at room temperature with the appropriate secondary antibody (Table 2.5). DAPI (4'-6 Diamindino-2-phenylindole) or Hoescht 2000 was added at dilution of 1:2000 to stain the nucleus. In all experiments, to ensure that the observed staining was specific, controls were included in which primary antibodies were omitted or incorrect secondary antibodies were used.

2.8 Actin staining

To compare the cytoskeletal organization of control and *SHANK3* patient neurons, the expression of F actin and G actin were investigated. Ten days after terminal plating onto PDL coated laminin 96 well dish, cells were fixed using 4% paraformaldehyde (PFA) for 20 minutes at room temperature, and then permeabilised with 0.1% triton X 100 (Sigma) for 10 minutes. This was followed with three washes of phosphate buffered saline (PBS). Phalloidin was used to visualize F actin filaments (Phalloidin CytoPainter F actin staining kit abcam 1121125) and Bovine pancreatic deoxyribonuclease (DNase1, 31,000 daltons life technologies) was used to visualize G actin. Both reagents were added for 30 minutes and then removed to add Hoechst 2000 to stain the nucleus. The fluorescence intensity was measured using high content imaging. The measured fluorescence intensity was normalized to total the number of nucleus present in the well, as determined by nuclear Hoechst staining. The following cell lines were compared: In this assay, I used three control lines and two shank3 lines, these were the following: Control P3, Control P2 C2, Control P1 C2 were compared to SHANK3 P1 C2 and SHANK3 P2 C1. The experiment was repeated three times (each independent experiment started from the iPSC stage). In total I compared 13500 control neurons to 10100 *SHANK3* neurons.

2.9 Neuronal morphological assessment via GFP transfections

The morphological properties of control and *SHANK3* neurons were compared by analyzing the number of primary, secondary and tertiary neurites, the primary neurite length and cell soma diameter. Here, the term neurite is used as a collective term for dendrites and axons that are formed by the cultured neurons.

To visualize neuronal morphology, iPSC derived neurons were transfected with an eGFP plasmid at two stages of neuralisation (Figure 2.1) at day 30 (immature neurons) and at day 45 (young neurons). To do this, Lipofectimine 2000 (life technologies) was mixed with the eGFP plasmid (2 µg) (Figure 2.2) and added to cells for 4 hours. After 4 hours, the media was changed and the neurons were assayed 48 hours later.

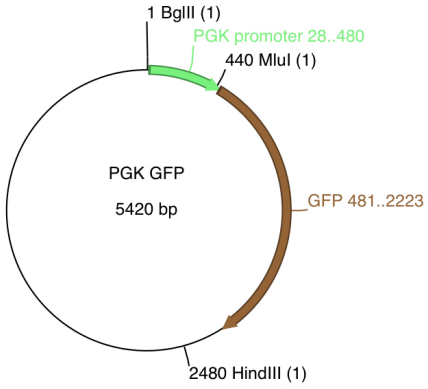

Figure 2.2: eGFP plasmid vector with a PGK (Phosphoglycerate kinase) mouse promoter.

Images were taken of eGFP expressing cells using the 10x objective on a Confocal Laser Scanning Microscope Leica TCS SP8 coupled with LAS AF lite software. The 488 nm laser was used along with the appropriate excitation and emission filters. Acquired images were converted into 8 bit tiff files and analyzed with Neuron J software version 7.3. Quantitative analysis was performed on images blinded for genotype from two control lines with one clonal replicate and two shank3 lines with one clonal replicate. The following cell lines were compared: Control P1 C1, Control P1 C2, and Control P2 C2 to SHANK3 P1 C2,

SHANK3 P1 C1 and SHANK3 P2 C2. The experiment was repeated three times (each independent experiment started from the iPSC stage). Total number of control cells that were examined was 4997, out of which 120 were positive for GFP. Therefore, transfection efficiency in the control neurons was 2.4%. Total number of *SHANK3* cells that were examined was 5200, out of which 122 were positive for GFP. Therefore, transfection efficiency in the *SHANK3* neurons was 2.3%.

2.10 Global Morphological analysis of control and *SHANK3* neurons (High content screening)

In order to measure the morphology of the whole neuronal population, high content screening was carried out using the Cellomics Cell Insight (Thermo scientific), using a program Cell Scan to analyze the cell soma area and mean number of neurite per neuron. In this assay, 5 control lines from three control patients were compared to 4 *SHANK3* lines from two *SHANK3* patients. These were as follows: Control P1 C1, Control P1 C2, Control P2 C1, Control P2 C2 and Control P3 were compared to SHANK3 P1 C1, SHANK3 P1 C2, SHANK3 P2 C2 and SHANK3 P2 C3. The experiment was repeated three times (each independent experiment started from the iPSC stage). The total numbers of neurons examined for the control were 26,000 and for *SHANK3* were 30,000.

The scans were performed in 96 well plate format (day 22, 25, 27 and 30 of neuralisation). Neurons were stained with DAP/Hoechst to stain for nuclei, this was then used by the cell insight to autofocus itself on the nuclei. To visualize the morphology of the neuron, neurons were stained with DCX (double cortin immature neuronal marker) and/or neuronal specific βiii tubulin (Table 2.4, and section 2.7). After scanning a minimum of 10 wells of a 96 well plate (1 field per well), the fluorescence exposure was fixed. A mini scan was then run to take raw

pictures (using a 10x objective), which formed the basis of programming the machine to analyze the cell soma area and neurite morphology.

In the following paragraph, I describe the programming protocol for the cell insight. Initially, the cell insight identified the nucleus. The first step is to smoothen the images that were taken during the mini scan. The smoothening reduces the sharpness of the intensity variations by redistributing their relative brightness over the immediate vicinity of the image. This reduces variation noise from the image. The image is of neuronal nuclei stained with DAPI/Hoescht. The second step was to set the thresholding to Isodata. Isodata is a dynamic method that utilizes a threshold calculated from the histogram of pixel intensities taken from individual points in the image. This method worked best when there was a clear distinction between the background and the object. Segmentation was applied to the image in order to identify individual objects. We used the intensity method that uses pixel intensity to separate objects. Successful segmentation required dominant intensity peaks for each object.

Once the nuclei were identified, the next step was to detect the cell bodies using DCX or tuj1 staining. Smoothing was applied to all images that were acquired during the mini scan after autofocus. Thresholding was set to “Fixed” so that the same threshold value was applied to each object in the image. The minimum cell body nucleus overlap was used to associate valid nuclei with cell bodies. This value was set to 100%, which meant that the entire nucleus must be within the cell body in order for it to be considered for analysis. We used the “Nuclei as seeds” method for segmentation between cells. This helped with segmentation between clusters of cells, as only cell bodies with one nucleus was considered. Next, “Cell Body demarcation” was selected. This process helped set up the boundaries that distinguish the cell soma from the neurites. The cell soma area was then validated using cell body nucleus count and cell soma area. The cell body nucleus count should give us a 1:1 ratio. For example, if there were 100 cells in the selected field, the number of nuclei should also be 100. The cell soma

area was set at any value between 50-600 um^2. The reason behind this is explained in section 2.11 below. Once the cell bodies were validated, the plates were scanned to measure the cell soma area only. The settings remained identical for all experiments.

Neurites were identified using the "Neurite identification modifier". The neurite identification modifier shifts the fluorescence threshold lower than that used for analyzing the cell bodies, as they are dimmer in nature. The next parameter selected was the "Neurite direction assay" parameter. In this, pixel number is used to find the direction of each segment. The last parameter used is the "Trace" within the cell body. This parameter assigns ownership of neurites to particular cell bodies. After the parameters were assigned, the plates were scanned for primary number of neurites, with the settings remaining identical for all experiments.

Figure 2.3 A(I-iii). shows an example of a tracing done by the cell insight, including both the cell soma and neurites. Please note that this is a representative picture taken from the machine while reprogramming. The cell insight is not capable of taking high-resolution images and does not provide any scale to the pictures.

In all analyses, at least 12 fields were scanned for each well of a 96 well plate and the well was rejected if there were more than 3 sparse fields in a well.

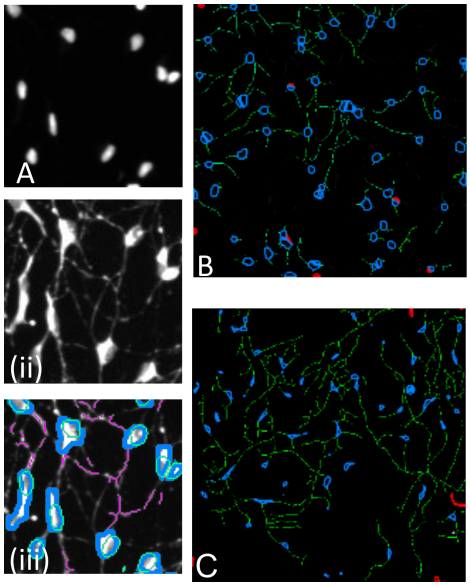

Figure 2.3: Cellomics scan: A. DAPI stained control neurons nuclei at day 30. (ii) and neurons (DCX). (iii) Tracing of the above two pictures where blue shows the cell soma outline, green shows the outline of nuclei and pink are the neurites. B. Control neurons after tracing. C. *SHANK3* neurons after tracing. Please note that the picture depicted here is a representation of the machine while reprogramming. The cell insight is not capable of taking high-resolution images and does not provide any scale to the pictures.

2.11 Manual counting and Error Rate

To identify and remove any false readings generated by the Cell Insight, three random *SHANK3* and control wells were selected and counted manually (blind to genotype). A histogram was generated from the manual count depicting the distribution of the cell soma area for both control and *SHANK3* at day 30 of neuralisation (Figure 2.4 B). The average error rate percentage is shown in Table 2.6. I manually counted the false positive neurons from the images taken by the cell insight for each cell soma area bin and divided it by the number of neurons in that well.

As you can see, there was a 100% false error rate for any cell soma area above 650 um^2. This was due to the cell insight sometimes including an adjoining neurite in the cell soma measurement (Figure 2.4 A.). Therefore, in our analysis

we excluded all values above 600 um^2. We also included this cell insight programming to measure cell soma area. During the programming of the cell insight, there is an option to set up reference values. For example, I can set up reference values for the cell soma area to be measured. I selected this as 50-600 um^2, so that the machine only selects for cell soma area between these values. The other error rate percentages (Table 2.6) were used to correct the data generated by the Cell Insight (presented in results chapter 3.2). Overall however, the manual counts confirmed the results obtained from the Cell Insight (compare Figure 2.4B with Figure 3.2.2).

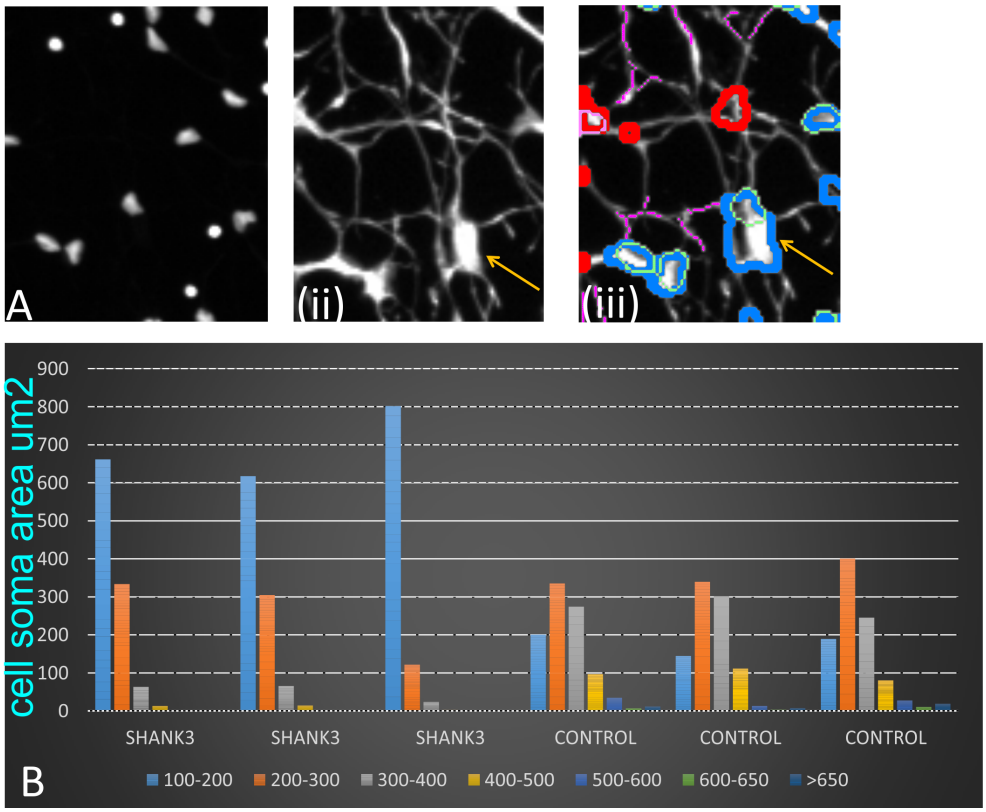

Figure 2.4: False reading done by the cell insight. A. DAPI stained nuclei from control neurons day 30. (ii) DCX positive neurons, the yellow arrow depicting the cell that has been false read. (iii) Yellow arrow showing the tracing of the false read neuron; it included the area next to cell soma. These type of cells were excluded from the data. B. Histogram showing the manual-count for different cell soma area bins. Please note that the picture depicted here (in A) is a representation of the machine while reprogramming. The cell insight is not capable of taking high-resolution images and does not provide any scale to the pictures.

CELL SOMA AREA bins (um^2)	Average error rate %
100-200	2.211244982
200-300	1.764033915
300-400	2.744800639
400-500	4.542722668
500-600	3.006815262
600-650	0.333333333
>650	100

Table 2.6: The average error rate percentage for the false positive cell shown by the cell insight.

2.12 Neurite Outgrowth

In order to compare neurite outgrowth, time-lapse videos were taken of *SHANK3* and control neurons. These neurons were grown on glass bottom PDL laminin coated ibidi dishes, until they reach day 29 of neuralisation, they were then imaged every hour for 48 hours using a Nikon Biostation IM-Q. Each image was converted into a 16bit tiff and analyzed using the neurite outgrowth application of metamorph offline software. In this assay, I compared 4 control lines from two control patients to 4 *SHANK3* patient lines from two *SHANK3* patients. These were as follows: Control P1 C1, Control P1 C2, Control P2 C1, Control P2 C2 were compared to SHANK3 P1 C1, SHANK3 P1 C2, SHANK3 P2 C1 and SHANK3 P2 C2. The experiment was repeated three times (each independent experiment started from the iPSC stage). In this assay, in total, I compared 51 control neurons to 59 *SHANK3* neurons.

Images were taken every hour from the Nikon Biostation and were individually evaluated. Also, each neuron in each image was tracked through the 12-hour period. The tracking was performed for only 12 hours due to time constraints.
The following parameters were then measured:

- Cell processes - total number of primary number of neurites.

- Mean process length - the average length of neurites.
- Cell branches - total number of secondary branches.
- Cell body area - the area of the cell soma
- Cell body position - the x and y coordinates of the centroid/centre of the cell body.

These parameters were then used to calculate different aspects of neurite outgrowth:

- **Rate of primary neurite formation -** we considered one neuron at a time. If there were 8 “Cell processes” at hour 1 and 9 at hour 2, there was a formation of 1 neurite. These were then averaged across 12 hours to gives us the rate of primary neurite formation (neurite/hour) for that neuron.
- **Rate of primary neurite elimination -** We considered one neuron at a time. If there were 10 “Cell processes” at hour 1 and 8 at hour 2, there was an elimination of 2 neurites. These were then averaged across 12 hours to gives us the rate of primary neurite elimination (neurite/ hour) for that neuron.
- **Extension rate -** the neurite length extension was calculated using the “Mean process length” parameter. If at hour 1 the mean process length was 20μm and at hour 2 the mean process length was 30μm, then the extension was 10μm. These were then averaged across 11 hours to give us the extension rate (μm/hr).
- **Retraction rate -** the neurite length retraction was also calculated using the “Mean process length” parameter. If at hour 1 the mean process length was 10μm and at hour 2 the mean process length was 5μm, then the retraction was 5μm. These were then averaged across 11 hours to give us the retraction rate (μm/hr).
- **Cell soma speed -** we used “Cell body position x and y coordinates” to calculate the distance of the cell body from one point to another. This was

done using the Pythagoras theorem [distance =√ $(x_2-x_1)^2+(y_2-y_1)^2$]. Once we calculated the distance for each hour, it was added then divided by 12 hours to estimate the speed per hour (μm/hr).

- **Change in cell soma area**- the cell soma area was recorded for each hour. This was then averaged across 12 hours to calculate the change in the cell soma area (μm^2/hr).
- **Rate of formation and elimination secondary branches** - we calculated this in the same way as we did the rate of primary neurite formation and elimination. However, instead of using the cell processes we used "Cell branches" parameter as it counts secondary branches.

2.13 Puromycin Assay

I measured and compared the global protein translation of control and *SHANK3* neurons at day 30. We used the Puromycin/ SUnSET assay to quantify this.
The neuronal culture was maintained for 30 days and 5mM of puromycin was added for 20 minutes to stop any translational activity. Puromycin is a structural analogue of aminoacyl tRNAs, it is incorporated into nascent polypeptide chains preventing their elongation (Nathan D 1969). The cells were then lysed and protein extracted for western blotting analysis using the puromycin antibody. I compared three controls and two *SHANK3* lines. This experiment has been repeated three times. These were as follows: Control P1 C1, Control P2 C2 and Control P3 were compared to SHANK3 P1 C1 and SHANK3 P2 C3. After sample preparation, the vials were blinded analyzed separately.

2.14 Preparation of Cell Lysates

To prepare cell lysates, cultures was washed twice with ice cold PBS (have you already defined this somewhere) then with 100μl of ice cold lysis buffer (50 mM Tris-HCL, pH7.5, 150nM Nacl, 1mM EDTA, 1% Triton X-100, protease inhibitor cocktail set III (Sigma,:1000) was added and the cells were scrapped into the

buffer. This lysate was then incubated on ice for 10 minutes and spun at 14000 rpm for 5 minutes. Before storage at -80°C, Laemmli buffer (Sigma) was added to the sample. SDS detergent in the Laemill buffer denatures the proteins and subunits to give an overall negative charge so that each can be separated by size. The bromophenol blue dye makes it easier to load samples.

When required for western blot the samples were thawed and boiled for 5 minutes at 95°C, then spun briefly at 14000rpm. To allow equal loading of the samples, a BCA protein assay kit (Thermo Scientific) was used, as instructed by the manufacturer, to quantify the amount of protein in each sample, which was 15µg per lane.

2.15 Electrophoresis and Dry transfer of proteins

Lysates, prepared as described above were run (15µg protein/lane) on pre-made NuPAGE Bis-Tris gel (Life technologies) for 30 minutes at 80V. The iBlot2 (Life technologies) was used for the protein transfer to the nitro-cellulose membrane. The membrane was blocked (Odyssey bloking buffer LI-COR biosciences) for an hour on the orbital shaker and primary antibodies were added (Table 2.4). This was left overnight in the cold room at 4°C. The next day, the membrane was washed three times with 0.5% Tween and the secondary antibody (Table 2.5) was added in the blocking buffer and left for an hour. The membrane was then washed three times with 0.5% Tween and once with PBS. The membrane was imaged using the Odyssey and the resolution was set at 50µm. The channels used were 700nm and 800nm and the intensity was set at 3.0.

2.16 Analysis of the western blot

The images taken from the Odyssey were converted into 8 bit tiffs and analyzed using Image J software. The boxes were drawn on the band of interest and

fluorescence intensity peaks were reported. These were then normalized to fluorescent values of Alpha actin present in each sample.

2.17 Synaptic Assays

For comparing the pre and post synaptic puncta staining cultures of *SHANK3* and control neurons were maintained for 65-70 days (see Figure 2.1) and then fixed and stained with the pre-synaptic marker Synaptophysin and post-synaptic marker Homer (table 2.4). In this assay, I used three control lines and two lines, these were the following: Control P3, Control P2 C2, Control P1 C2 were compared to P1 C2 and P2 C1. The experiment was repeated three times (each independent experiment started from the iPSC stage). In this assay, in total, I compared 46 control neurons to 42 neurons.

Images were taken from the 63x objective on a Leica TCS SP8 Confocal Laser Scanning Microscope coupled with LAS AF lite software. I used 386, 488 and 594 nm lasers, along with the appropriate excitation and emission filters. These settings were kept consistent while taking images from all cultures. Acquired images were converted into 8 bit tiff files and analyzed with Image J software version 7.3. Using Image J, I opened the files and selected at least two portions of neurites, length not exceeding 50μm. This region was added to ROI (region of interest) manager. Following this, I thresholded the images such that the synaptic puncta would turn black and the background would turn white. The thresholded images were then analyzed through “Analyze Particles”. The thresholding was done because the “Analyze Particles” software does not recognize images that are not thresholded. The size limit at this point was set up to 0.03-3 μm^2. This meant that only punctas with a size of 0.03 to 3 μm^2 would be measured. The summary from “Analyze particles” gave the total number of punctas observed in the region of interest. I repeated these steps until the whole neuron was captured. The data obtained was analyzed as the number of punctas/50μm.

Presynaptic and postsynaptic punctas were counted separately for control and neurons. Images were taken and blinded for analysis.

2.19 Shank3 overexpression vector generation

I wanted to overexpress human *SHANK3* gene in *SHANK3* patient lines to rescue the morphogenetic phenotype discovered in the earlier assays. For this experiment I wanted to transduce neurons with a viral vector. Therefore, the full-length human *SHANK3* gene ORF (artificially synthesized by Genewiz) was cloned into pCDH-EF1-MCS (CD502-1A System Biosciences). The vector map for *SHANK3* is shown in Figure 2.5. *SHANK3* N terminal was fused with Myc tag; this was used to identify which of the neurons were positively transduced for *SHANK3*. The Myc tag was used for two reasons, first it is 10 amino acid base tag, which is very small as the human *SHANK3* ORF is 5.3 kb, which is stretching the limit of lentiviral capacity. Second, is that the rat *Shank3* ORF has been previously cloned with N terminal Myc tag and does not disrupt the function of the gene (Nasbitt et al., 1999). Therefore, I picked the Myc tag to tag the *SHANK3* gene at the N terminal. Two other clones were generated, *SHANK3* gene without exon18 and Myc tag only vector without the *SHANK3* gene (Figure 2.5 b,c).

Exon 18 in the *SHANK3* gene is 24 bp long. *SHANK3* without exon 18 was generated because previous work in our laboratory indicated that the expression of *SHANK3* with exon18 increased during the transition from neural progenitors to neurons (data shown in Introduction, Section 1.12). These data also indicated that the *SHANK3* patient lines had a reduced expression of this exon. Since this expression of exon 18-containing isoforms immediately preceded the appearance of the morphogenetic phenotypes, we hypothesized that the failure to express exon 18 might be associated with these phenotypes. If this hypothesis is correct then a full length *SHANK3* without exon18 might fail to rescue the phenotype, where a construct including exon 18 would succeed.

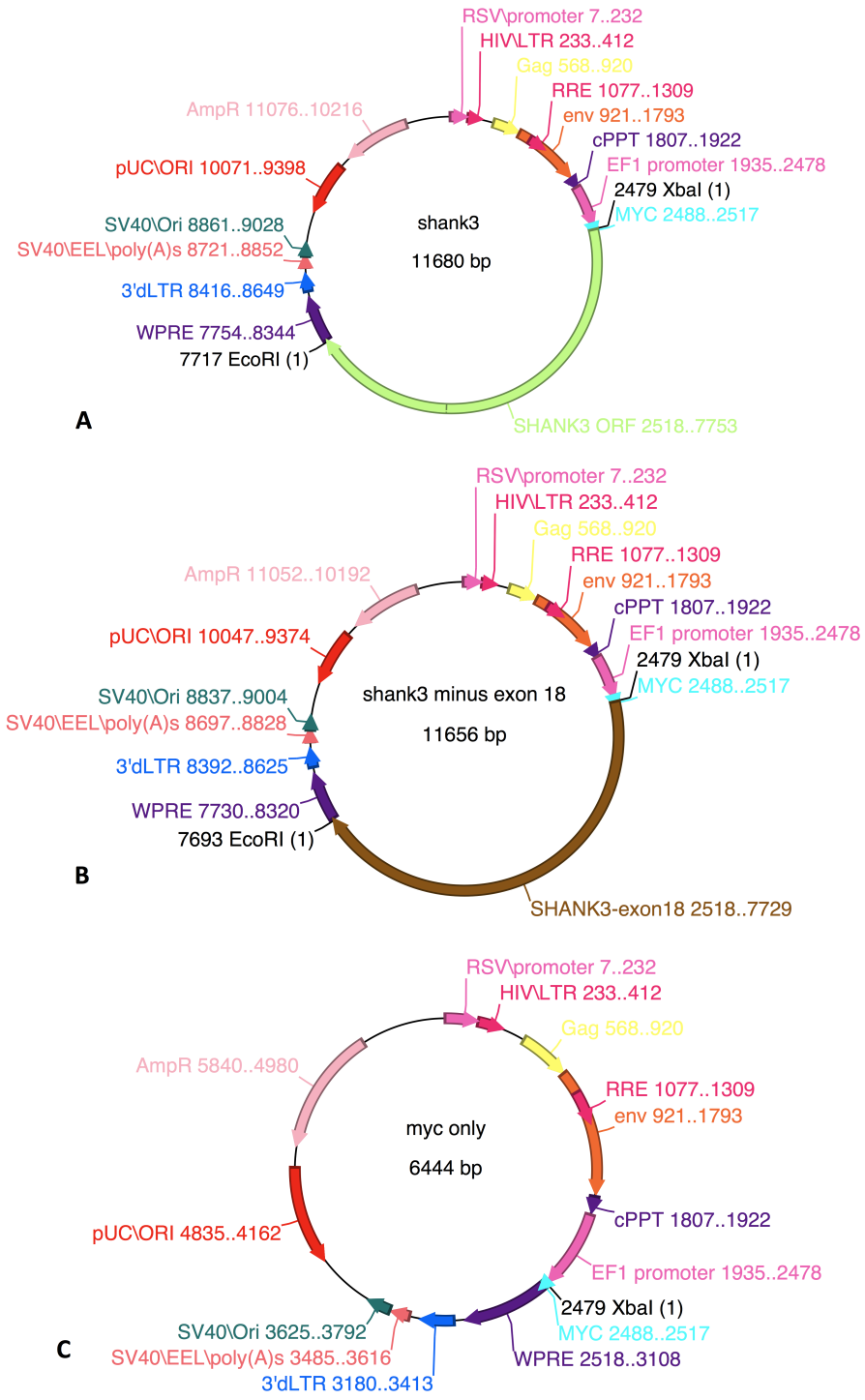

Figure 2.5: The *SHANK3* rescue vectors. A. Full length human *SHANK3* ORF with N terminal Myc tag cloned into lentiviral backbone. B. Human *SHANK3* without exon 18 with N terminal Myc tag cloned into lentiviral backbone. C. Myc tag only without *SHANK3*.

2.20 *SHANK3* lentiviral particle generation

The cloned vectors of *SHANK3* were transformed in lentivirus, to rescue the morphogenetic phenotype seen in *SHANK3* patient neurons.

Lentiviruses were generated with a three-plasmid transfection system using Lipofectamine LTX (Life Technologies) in HEK293FT cells as previously described (Kutner R et al., 2009). Twelve hours after transfection supernatants were collected. Viral particles were concentrated using Lenti-X concentrator (Clontech) according to manufacturer's instructions, then aliquoted (100μl), stored at -80°C until required. I made three viruses, first one with the full *SHANK3* ORF (*SHANK3* Plus 18), second *SHANK3* without exon 18 (*SHANK3* minus 18) and third was Myc tag only without *SHANK3* gene (Myc Only). The first virus was used to see if I could rescue the morphological phenotypes in the *SHANK3* patient neurons. The second virus was used to test the hypothesis that the specific failure to express exon 18 might be associated with morphogenetic phenotype (Introduction section 1.12). The third *virus* is supposed to act as negative control, such that the effect of rescue in *SHANK3* patient neurons would be due to *SHANK3* and not due to the myc tag.

To titer the concentration of virus to be used, I transduced a SHANK3 female patient line neurons (SHANK3 P2 C1) with different amounts of virus. These were 2, 5, 10, 20, 30 and 50μl. Approximately 80% of the cells in one well of 96 well dish were stained positive for Myc upon addition of 5μl of virus (Table 4.0).

To rescue the morphogenetic phenotypes seen in the *SHANK3* cells, I transduced *SHANK3* patient neurons (day 20/21) which were analyzed at day 30. At day 30 because, this is the day I see the morphogenetic phenotype differences between the control and *SHANK3* lines. I used high content screening, to see whether the overexpression of *SHANK3* in *SHANK3* patient neurons had rescued the morphological phenotype. To label neuronal cell bodies and processes, I stained for DCX and Myc (to identify for positively transduced

neurons) using the protocol described in section 2.7. The cell Insight was programmed to select the cells that were only positive for Myc, ensuring that it only selected transduced neurons. The timeline for this experiment is shown in Figure 2.6. We measured cell soma area and primary number of neurites per neuron with *SHANK3* rescue (plus 18), with *SHANK3* rescue (minus exon 18), only myc and no rescue (blank). The rescue was performed in two *SHANK3* patient lines namely SHANK3 P2 C1 and SHANK3 P1 C1. I repeated this experiment three times and the total number of neurons compared from all three experiments were as follows: SHANK3 P2 C1 before n=1.5X10^3, SHANK3 P2 C1 with rescue n=1.5X10^3, SHANK3 P2 C1 with rescue - exon18, SHANK3 P1 C2 before n=1.45 X10^3, SHANK3 P1 C2 with rescue n=1.98 X10^3, SHANK3 P1 C2 with rescue-18.

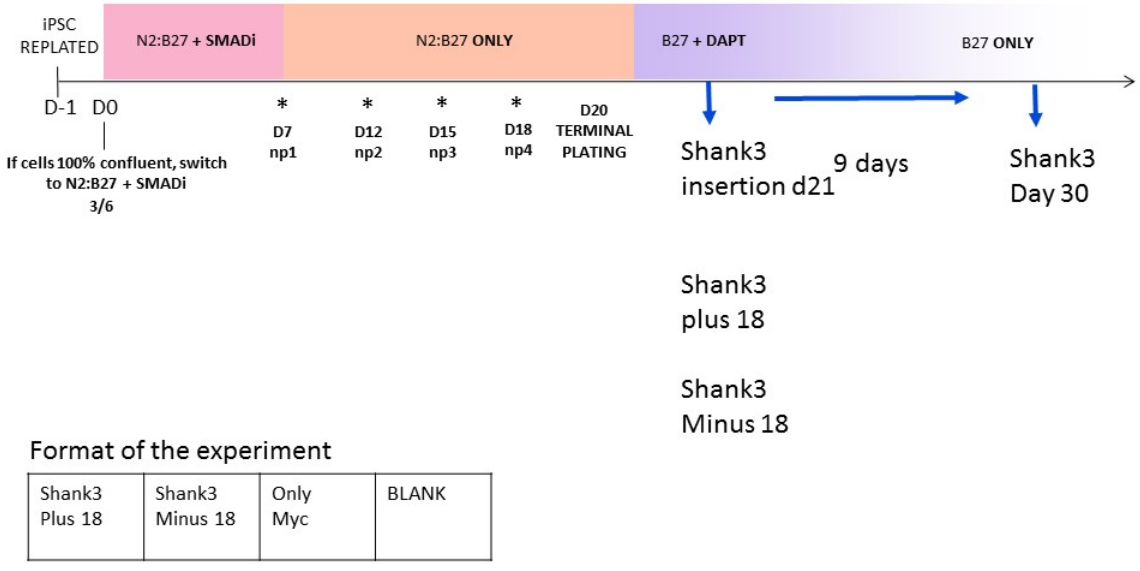

Format of the experiment

Shank3 Plus 18	Shank3 Minus 18	Only Myc	BLANK

Figure 2.6: Format of *SHANK3* rescue experiment.

2.21 Verification of *SHANK3* overexpression constructs

I used immunocytochemistry to verify that the *SHANK3* overexpression virus (plus 18) was actually expressing *SHANK3* and not something else. SHANK3 P2 C1 neurons were fixed and stained with *SHANK3* and Myc antibodies (Table 2.4). The Myc staining overlapped with SHANK3 antibody staining [Figure 2.7 A(I) –(iv)]. The Myc is tagged to N terminal of *SHANK3* and overlapping with the SHANK3 antibody means it is specific for SHANK3 protein and nothing else. I performed a control experiment for this. I repeated the above experiment with only Myc virus transduced neurons (NO *SHANK3*). In this case, there was no overlap seen between the SHANK3 antibody and Myc antibody [Figure 2.7 C(I) –(iv)]. This is exactly what we would expect. Since, the Myc only virus has no *SHANK3* gene in it, it is expected not to overlap with SHANK3 antibody. This assay was also used to verify *SHANK3* without exon 18 virus too [Figure 2.7 B(I) –(iv)].

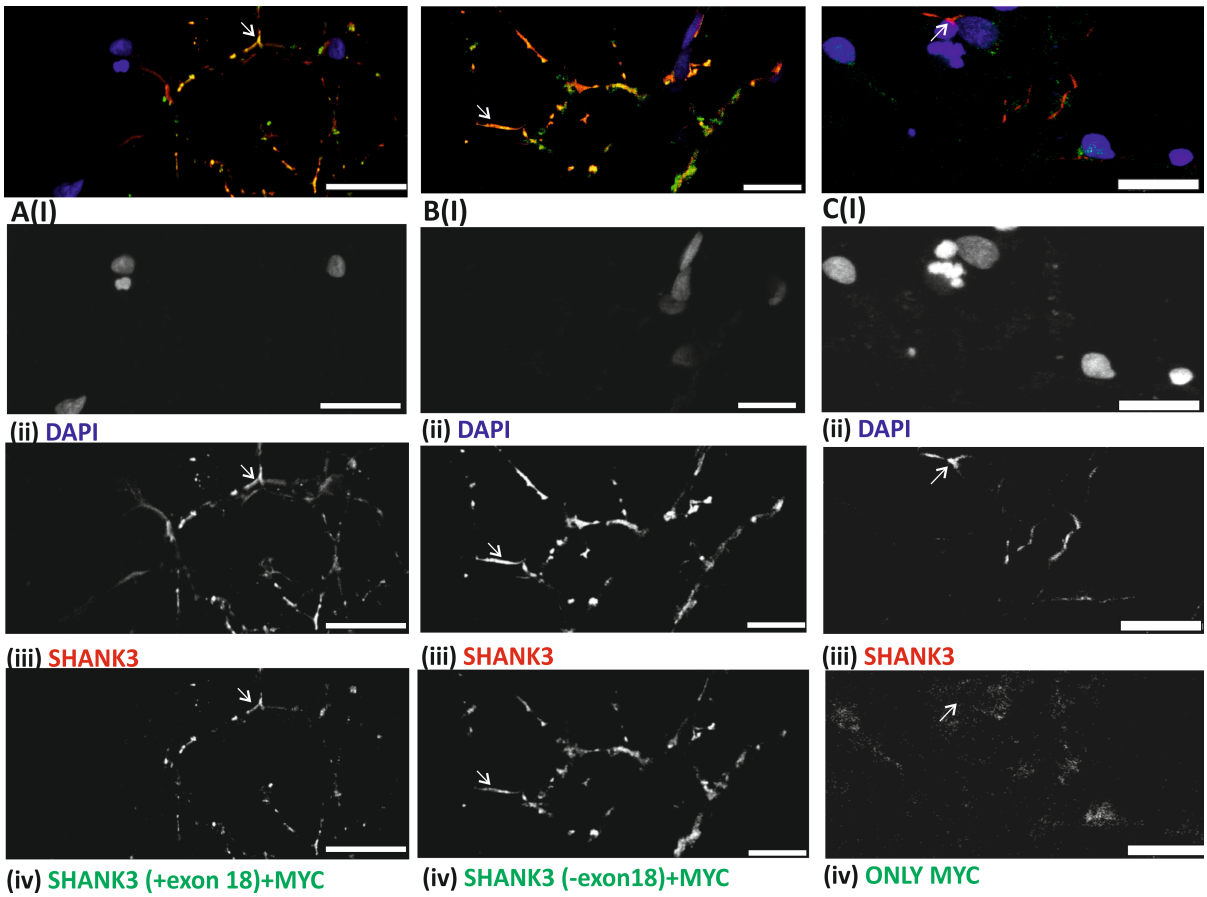

Figure 2.7: Verification of *SHANK3* overexpression virus via immunocytochemistry (Day 30 neurons). A(I) SHANK3 P2 C1 neuron transduced with Human *SHANK3* ORF plus exon 18 virus stained with (ii) DAPI, (iii)SHANK3 and (iv) SHANK3(plus exon18) MYC. The arrow indicates the overlapping of SHANK3 antibody with Myc antibody. B(I) SHANK3 P2 C1 neuron transduced with Human SHANK3 minus exon 18 virus stained with (ii) DAPI, (iii)SHANK3 and (iv) SHANK3(minus exon18) MYC. The arrow indicates the overlapping of SHANK3 antibody with Myc antibody. C(I) SHANK3 P2 C1 neuron transduced with only Myc virus stained with (ii) DAPI, (iii)SHANK3 and (iv) Only Myc. The arrow indicates no overlapping of SHANK3 antibody with Myc antibody. Scale=20μm.

2.22 Rescue cells via IGF1 and BDNF

To determine whether IGF1 or BDNF could rescue the morphological phenotypes of *SHANK3* patient neurons seen at day 30 of neuralisation (Chapter 3; Figure 3.2.2). I performed this experiment in two *SHANK3* patient lines with one clonal replicate of each and compared it to two control lines with one clone replicate of each. These were as follows: Control P1 C1, Control P1 C2, Control P2 C1 and Control P2 C2 were compared to SHANK3 P1 C1, SHANK3 P1 C2, SHANK3 P2 C2 and SHANK3 P2 C3.

iPSC derived neurons were grown on a 96 well plate in and IGF1 (20ng/ml) administered from day 23 of neuralisation to day 30 and BDNF (50ng/ml) from day 26 to day 30. The neurons were then fixed at day 30 and stained using the protocol described in section 2.7 – with DCX, Tuj1 and DAPI. Cell soma area and primary number of neurites per neuron were measured as described in section 2.10. All parameters were normalized to the cells grown without treatment.

2.23 ES culture

To further confirm that *SHANK3* was the cause of the morphological phenotypes seen in *SHANK3* patient neurons, I compared the morphology of neurons generated from a control male human es cell line with es cell lines where both copies of the *SHANK3* genes had been knocked out (es shank3-/-) and where only one copy had been knocked out (es shank3 +/-) (Tables 2.7, 4.2). These lines were provided by our collaborator, Dr Ravi Jagasia at Roche (F.Hoffmann-La Roche Ltd CNS Discovery Grenzacherstrasse CH-4070 Basel/Switzerland). The cell lines used are described in the table 2.7.

Vials were thawed from liquid nitrogen at 37°C and revived onto wells coated with Geltrex (Life Technologies). Cells were grown in Dilbecco's Modified Eagle's Media F-12 (DMEM: F: 12; Sigma Aldrich) in a binder CB150 incubator at 37°C, 5% O_2, 5% CO_2 and saturated humidity. For maintenance, cells were kept at 50%-80% confluence, which typically requires passage every week.

For passaging, media was removed by aspiration and cells were washed with pre-warmed Hank's Balanced Salt Solution HBSS without Ca^{2+} and Mg^{2+} (HBSS; Life technologies). The HBSS was removed by aspiration and replaced with room temperature Versene (Life Technologies), which was left on for 4 minutes at 37°C. The Versene was then aspirated off the cells detached from the plate with pre-warmed media and transferred into pre-coated a Geltrex coated 6 well tissue culture dish at a 1:6 dilution (1 well of cells into 6 wells). Growth media was then changed every 24 hours. See Table 2.2 for the volumes of reagents used.

I differentiated these cells into hypothalamic neurons in order to study the morphogenetic phenotype. The same protocol was used for IPSCs (see Section 2.2). To measure the changes in morphology of es derived neurons, we used high content screening on neurons at day 30 of neuralisation to analyse the cell soma area and primary number of neurites per neuron (see Sections 2.7 and 2.10).

Human ES cell Lines	**Patient Details**
es shank3 +/+	Control male es cell line no deletion
es shank3 -/+	es cell line heterozygous deletion of *SHANK3*
es shank3-/-	es cell line with homozygous deletion of *SHANK3*

Table 2.7: ES cell lines

2.24 Data analysis and statistics

All experiments were replicated at least three times using the iPS cell lines mentioned above. The sample size and description of the samples are reported in figure legends. In all cases, only the cultures that were 90% positive for Tuj1 expression were used. For manual analysis of the images, they were blinded and treated.

The statistical analysis used to compare the assays is reported in each figure legend. The normal distribution of data was checked using the Kolmogorov-Smirnov's test and all statistical analyses was carried out using Prism6 and SPSS.

Results

Chapter 3: Morphogenetic deficits reported in SHANK3 patient neurons

Brief overview

One of the greatest obstacles in our understanding of the etiology of neurodevelopmental diseases is the inaccessibility of human neural cell types. Various rodent studies of ASD including those using *Shank3* KO mice have successfully modeled autism-like phenotypes (Introduction section 1.6; Peca et al., 2012). These studies have provided some insights into the disease mechanisms. Nevertheless, they have not resulted in any clinical benefits for patients. This could be due to the inherent genetic and anatomical variations between rodents and humans.

Human cellular models can address these issues. One way of generating such a model is to reprogram somatic cells to generate induced pluripotent stem cells (iPSCs). iPSCs are adult cells that have been reprogrammed genetically to an embryonic stem cell like state. This reprogramming method was first described in 2006 (Takahashi and Yamanaka 2006) when mouse adult fibroblasts were converted into the pluripotent state by the retroviral transduction of four transcription factors Oct3/4, Klf4, c-Myc and Sox2. Later, Takahashi et al (2007) generated iPSCs from human adult dermal fibroblasts. Currently, various protocols have been established to generate iPSCs from other adult somatic cell types. For example blood, urine, amniotic cells and keratinocytes, as used in this thesis (Methods section 2.1).

In this project, the iPSCs used were generated using lenti viral reprogramming of keratinocytes with the Yamanaka factors (Oct4, Klf4, c-Myc and Sox2). These keratinocytes were derived from hair root biopsies from two autistic patients carrying a heterozygous deletion in the *SHANK3* gene (Cocks et al., 2014). Similarly, three control lines were produced from healthy individuals (Methods

section 2.1). The lines generated were expanded and neuralised to generate hypothalamic neurons. The protocol is outlined in the Methods section 2.3. The neurons produced from this protocol were both doublecortin (DCX) and neuronal specific β-iii-tubulin positive (Tuj1) as shown in Figure 3.1, 3.2.2.

Chapter 3

Background

The hypothalamus is a small brain structure located between the optic chiasm (OC) and anterior commissure (ac) and behind the organum vasculosum of the lamina terminalis (OVLT) (Swaab 2008). Its main function is to link the nervous system to the endocrine system through the pituitary. The hypothalamus releases a variety of neurohormones such as corticotropin-releasing hormone (CRH), gonadotropin releasing hormone (GnRH1), growth hormone-releasing hormone (GHRH), somatostatin (SST), thyrotropin-releasing hormone (TRH), oxytocin and vasopressin. These hormones play important roles in social behavior, motivation, circadian rhythms, response to stress and anxiety (Introduction Section 1.11).

There are very few biological studies that investigate the role of hypothalamus in autism. Recently, an MRI study was performed on 52 ASD children with 52 matched controls to compare the grey matter in different regions of the brain. Diminished grey matter was observed in the hypothalamus in ASD patients (Kurth et al., 2011), which is known to synthesize behaviorally relevant hormones. For instance, one of the key symptoms of autism is impaired social interaction. CRH is known to be released from the hypothalamus, and is responsible for our body's response to stress (Schulkin 2007). Elevated levels of CRH are associated with social withdrawal in primates (Erickson K et al., 2005). The current theory for autism patients is that they are thought to have higher levels of CRH (Schulkin 2007). Elevated levels of CRH and Neurotensin (NT) have been recently reported in serum of ASD children. Moreover, NT is a neuropeptide that has been implicated in the regulation of GnRH1 (Tsilioni et al., 2014). GnRH1 is also synthesized by the hypothalamus.

Due to the potential links between hypothalamic function and symptoms found in individuals suffering with autism, we have generated an in-vitro model to study human hypothalamic neurons, with and without mutations that are known to cause ASD. This model will then be used to compare the morphological features of the neurons during development.

We used 'dual SMAD inhibition' to direct iPSCs along a neuronal pathway. iPSCs were converted to neural progenitors following 8 days of growth in the smad inhibitor medium (Fig 3.1). By day 18, these cells formed the rosette structure (a radial arrangement of columnar cells that express many features of neuroepithelial cells that form the neural tube; Stice et al., 2008) and by day 30 DCX positive immature neurons could be identified.

In order to assess the types of neurons generated from this neuralisation protocol, Dr. Graham Cocks in our lab performed a microarray study with a control line at ten different stages of neuralisation from day 7 (early neural progenitors) to day 50 (synaptically active neurons). Figure 3.1 E, shows the expression of hypothalamic hormones. Between day 25 and day 30, an increase in the expression of hormones such GnRH1, CRH (corticotropin-releasing hormone) and SST (somatosatin) was observed. A low expression of *TBR1* (T-box brain1), a protein specifically expressed during cortical development in layer VI of the human cortex. This suggested that the neuralisation protocol was not producing cortical neurons.

As mentioned above, this assay was completed in one control line. I followed the same protocol for neuralising the rest of the lines. In the first section of this chapter, (Section 3.1) I performed a confirmatory experiment to verify the neurons derived from the rest of the iPSC lines gave us a similar pattern of hypothalamic expression.

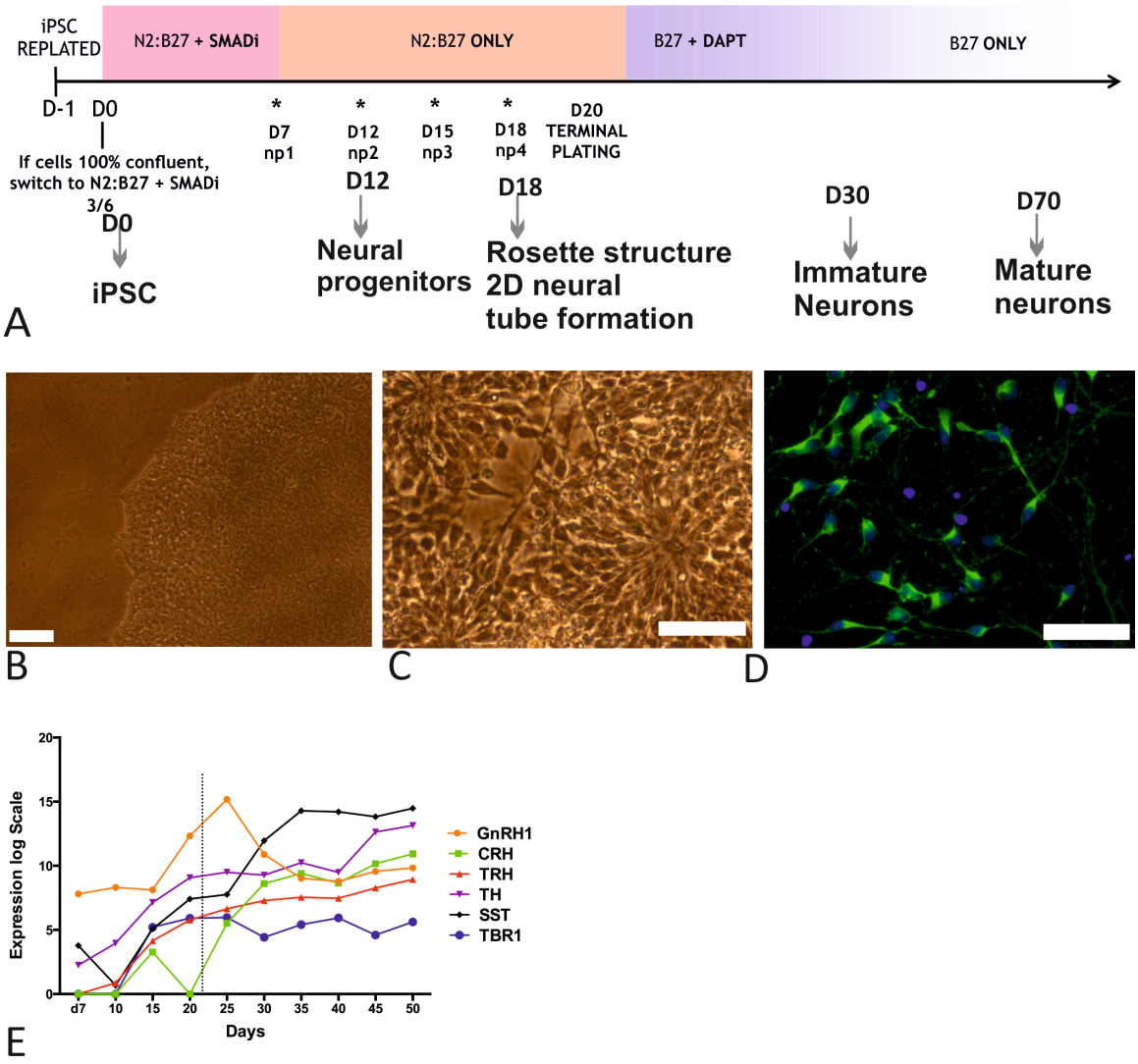

Figure 3.1: Neuralisation A. The chart depicts the neuralisation protocol used and indicates the five stages of neuralisation. These are the iPSC (day 0), the neural progenitors (Day12), the rosette structure (Day 18), the immature neurons (day 30) and the mature neuronal stage (Day 70). B. iPSC colony (Scale=50μm) C. Rosette structure (Scale=50μm) D. Neurons at day 26 postive for tuj1 (Scale=50μm). E. Microarray RNA study on a control line (Control P2 C3) at ten different stages of neuralisation. It shows the expression of various hypothalamic hormones. Micro array study was carried out by Dr. Graham Cocks (2015).

In the second section of this chapter, I describe the in-vitro experiments designed to characterize the development of *SHANK3* patient hypothalamic neurons. Specifically, I compare the morphological changes of control and *SHANK3* iPSC derived hypothalamic neurons.

As we know, one of the main features during the development of a neuron is the ability to form neurites. The neurites then form into dendrites and axon, which forms the basis of receiving and integrating signals. Previous studies have shown that the deficits in dendritic morphology including retractions, formations and eliminations of dendrites contribute to the miscommunication between neurons, which is one of the major underlying causes of ASD. (Kulkarni VA et al., 2012; Da.Silva JS et al., 2002). Also, described in the introduction section 1.3, one of the hypotheses regarding the molecular mechanism behind autism is miscommunication between neurons due to abnormal cellular growth.

Over the past decade, a number of studies have been associated with aberrant neuronal connectivity in psychiatric disorders such as ASD, schizophrenia and bipolar disorder. Morphometric and MRI studies have observed an increase in white matter volume in 2 to 4 years old autistic children (Schumann.et al 2004; Courchesne et al., 2001) and the suggested cause for this is irregular neuronal growth. In addition, studies have reported changes in dendritic arborization in Rett's syndrome, Fragile X syndrome and Timothy syndrome, all rare genetic forms of ASD (Brennand KJ et al., 2012). Dendrites represent the compartment of neurons that primarily collect and compute information. These structures are highly dynamic during development, a combination of intrinsic and extrinsic signals shape dendritic morphology (Gaia 2012). Thus, it is important to understand the impact of dendritic morphology during early development in ASD.

Among the various genetic variants associated with risk for ASD, variations within the *SHANK3* gene are known to be the most penetrant. About 2% of

people who have autism and intellectual disability carry mutation in *SHANK3* (Leblond C.S et. al 2014; Bentancur.C et al., 2013; Boccuto L et al., 2013; Durand C.M et. al 2007). SHANK3/Prosap2 is an integral scaffolding protein located in postsynaptic density (Sheng M et al., 2000; Nasbitt et al., 1999). Previous studies of *SHANK3* have linked its role to regulating synaptic protein, synapse transmission and plasticity [Introduction section 1.5 (b); Jiang et al., 2013; Shcheglovitov A et al., 2014].

However, most these studies of *SHANK3* focus on its role in the synapse, which occurs at later stages of development when the neuronal connections have been established. None of these studies focus on its role during early development. In addition to its function at the synapse, SHANK3 also binds to various actin-binding proteins such as Abp1, SPIN90, Cortactin and many more [Introduction section 1.5(c); Verpelli et al., 2012]. These play a critical part in cytoskeletal remodeling. Therefore, the loss of *SHANK3* is highly likely to play a role in the structural growth of neurons. Since ASD is a neurodevelopmental disorder, in the second section of this chapter (3.2), we focus on the role of *SHANK3* in the structural organization of the neuron during early development.

3.1: Verification of hypothalamic neurons

I used a panel of antibodies against cell-type specific hypothalamic neurohormones - GnRH1, CRH, and SST using the microarray as reference point. The antibodies used are listed in detail in Table 2.4. Both *SHANK3* and control cultures were fixed at day 26 of neuralisation. Cultures were stained with each hypothalamic marker in conjunction with neuronal specific β iii tubulin (Tuj1) (Figure 3.1.2 A and B). The percentages were calculated as shown below in table 3.1. The percentage was the total number of CRH/GnRH1 positive cells divided by the total number of neurons present.

Cell Line Name	Percentage CRH positive±SD	Cell Line Name	Percentages CRH positive±SD
Control Patient 1 Clone 1	62.467±15.144	ASD Patient 1	61.840±17.319
Control Patient 1 Clone 2	50.786±3.212	SHANK3 Patient 1 Clone 1	44.486±17.277
Control Patient 2 Clone 1	40.132±10.611	SHANK3 Patient 2 Clone 1	41.432±22.229
Control Patient 3	67.921±1.277	SHANK3 Patient 2 Clone 2	59.160±12.828
Control Patient 2 Clone 2	43.291±7.883	SHANK3 Patient 1 Clone 2	55.144±19.441
Cell Line Name	**Percentage GnRH1 positive±SD**	**Cell Line Name**	**Percentages GnRH1 positive±SD**
Control Patient 1 Clone 1	33.428±11.812	ASD Patient 1	30.906±7.942
Control Patient 1 Clone 2	43.968±4.029	SHANK3 Patient 1 Clone 1	31.794±2.689
Control Patient 2 Clone 1	31.0735±10.631	SHANK3 Patient 2 Clone 1	39.633±19.760
Control Patient 3	30.441±8.526	SHANK3 Patient 2 Clone 2	34.923±5.382
Control Patient 2 Clone 2	29.472±14.059	SHANK3 Patient 1 Clone 2	35.271±12.994

Table 3.1: Percentage of each neuronal type: This table describes the percentage of CRH and GnRH1 neurons generated from each cell line. The percentage was calculated as the total number of CRH/GnRH1 positive cells divided by the total number of neurons present. Details of each cell line can be found in Methods section 2.1.

As shown in Figure 3.1.2, both control and *SHANK3* cells were positive for GnRH1, and CRH with 50-60% neurons being CRH positive and 30-40% neurons being GnRH1 positive. SST could not be assayed because of inadequate antibodies. As mentioned previously, all staining was done with neuronal specific tubulin (Tuj1). Therefore, we have identified over 85% of the

neurons in our culture (Figure 3.1.2), although we have not discounted the possibility that some cells might double stained for GnRH1 and CRH together.

In addition to the *SHANK3* line, we also analyzed a sporadic ASD line for expression of these markers (ASD P1; Figure 3.1.2 C; Table 3.1). We saw 31% of cells positive for GnRH1 and 62% positive for CRH. These percentages were quite similar to what we saw in our *SHANK3* and control neurons.

These results indicate that the neuralisation procedure used gives reproducible results, in terms of percentages and type of neurons generated, across control *SHANK3* and ASD lines. This suggests that is this system is robust and, as such can be used to study the effects of autism-causing mutation on neuronal structure and function.

Our immunocytochemical analysis of the iPSCs lines showed that the expression of CRH and GnRH1 is consistent with the microarray data shown in Figure 3.1. Nonetheless, the microarray data also showed an expression TRH (thyrotropin-releasing hormone), SST and TH. These could account for the missing 15% of the unidentified cells in our culture.

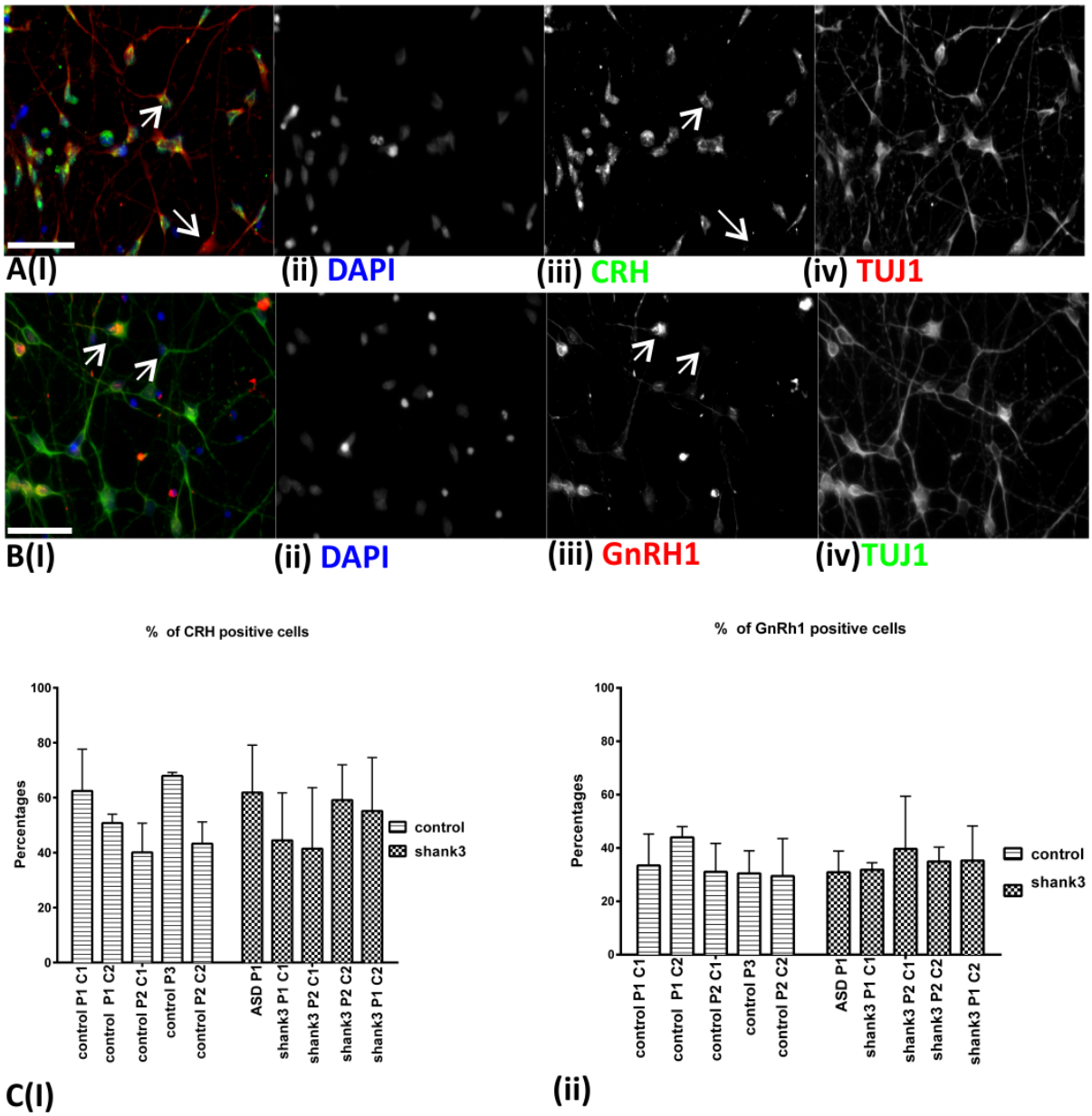

Figure 3.1.2: Characterization of the neurons generated from iPSCs: Neurons generated were Hypothalamic in nature. Neurons are at day 25/26 of neuralisation. A. (i) Control line stained with DAPI (blue), CRH (Green) and Tuj1 (red). B (i) Control line stained with DAPI (blue) GnRH1 (Red) and Tuj1 (green) positive. C(i) Control line stained with DAPI (blue) TH (Red) and Tuj1 (green) positive(Scale=50μm).(i) Percentage of CRH positive cells (ii) Percentage of GnRH1 positive cells (Scale=50μm). Data represented as mean±SD.

3.2: Morphological analysis of *SHANK3* patient neurons

3.2.1: Morphological analysis of single cell via eGFP

In order to investigate the morphological differences between the patient and the control iPSC generated hypothalamic neurons. At day 30 (immature neurons) and day 45 (young neurons) of neuralisation, the cells were transfected with eGFP and visualized with fluorescence microscopy (Figure 3.2; Table 3.2). The following cell lines were compared: Control P1 C1, Control P1 C2, and Control P2 C2 to SHANK3 P1 C2, SHANK3 P1 C1 and SHANK3 P2 C2.

Average neurite length (μm)	Control median	SHANK3 Median
Day 45 of Neuralisation	387.5, n=124	609.3, n=106 ***p=0.0001
Day 30 of Neuralisation	169.9, n=120	278.2, n=122 ***p=0.0002
Primary no.of neurites per neuron		
Day 45 of Neuralisation	3.44	4.94 ***p=0.0003
Day 30 of Neuralisation	2.250	3.986 **p=0.0012
Average cell soma diameter (μm)		
Day 45 of Neuralisation	17.68	12.50 *** p<0.001
Day 30 of Neuralisation	20.92	14.08 ,****p<0.0001

Table3.2: Morphological parameters assessed at different stages of neuralization. The table shows the median for each morphological parameter assessed at two stages of neuralisation, day 45 and day 30. Since morphological parameters did not pass the KS normality test, we compared medians. Day 45 Control neurons n=124; *SHANK3* neurons n=106, from all 3 biological replicates. We compared 2 control lines with 2 *SHANK3* lines, with one clonal replicate. Day 30 Control neurons n=120; *SHANK3* neurons n=122, from all 3 biological replicates. We compared 2 control lines with 2 *SHANK3* lines, with one clonal replicate

The transfection efficiency was the same in both lines at approximately 2% (Methods section 2.9). The following morphological features were assessed for both the patient and the control lines: Primary no. of neurites per neuron, average neurite length (μm) and average cell soma diameter (μm).

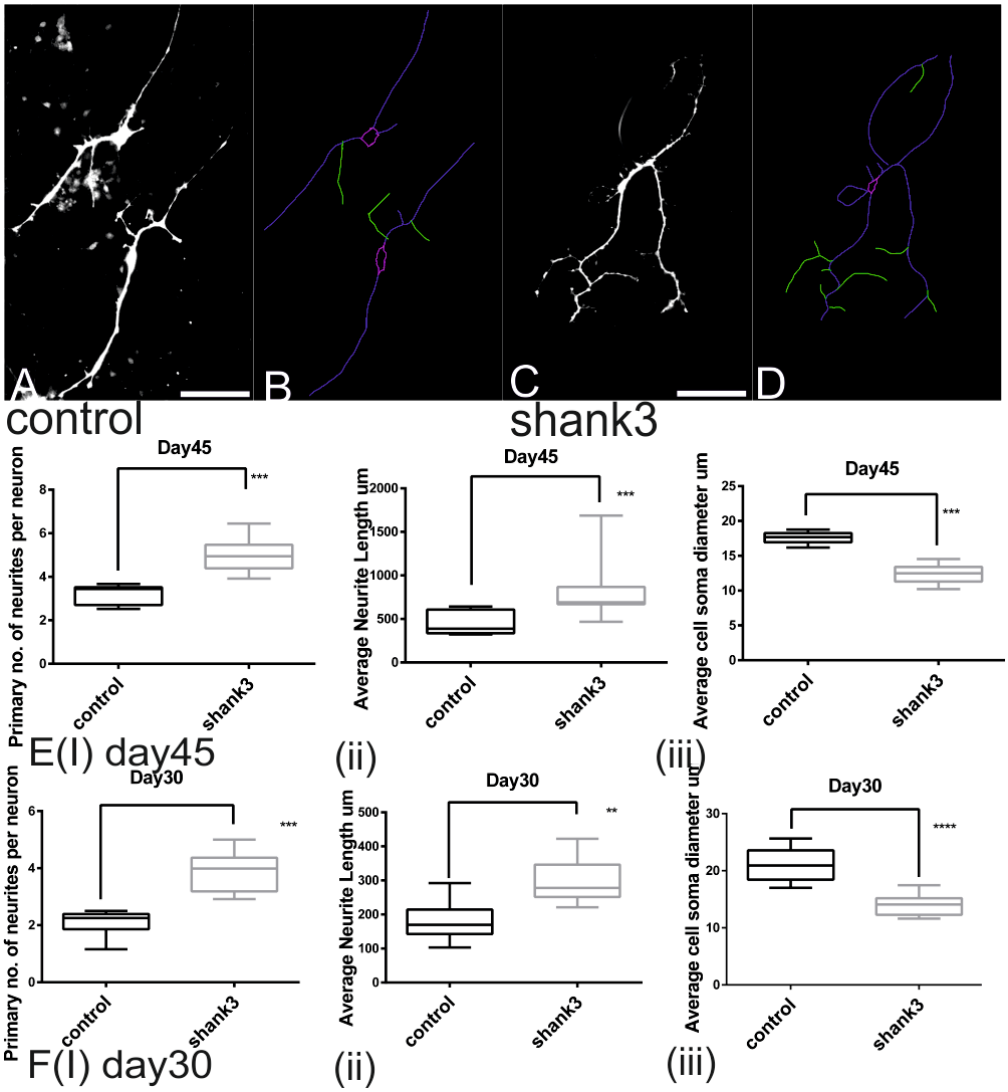

Figure 3.2: *SHANK3* patient neurons exhibit morphogenetic deficits

A. GFP transfected control neuron B. Tracing of the control neuron (Blue: Neurites, Pink: Cell body outline, Green: secondary branches) C. GFP transfected *SHANK3* neuron D. Tracing of *SHANK3* neuron. (45 days neurons, Scale=250μm) E. (i) Primary no. of neurites per neuron (ii) Average neurite length (μm). (iii) Average cell soma diameter (μm). Significant differences were observed in all three parameters; data shown for day 45 neurons. Data presented as box plots with min and max, ***p=0.0001, ***p=0.0003, *** p<0.001 respectively. Mann-Whitney U test was performed. (Control neurons n=124; *SHANK3* neurons n=106, from all 3 biological replicates. We compared 2 control lines with 2 *SHANK3* lines, with one clonal replicate).

F. (i) Primary no. of neurites per neuron (ii) Average neurite length (μm) (iii) Average cell soma diameter (μm). (30 days neurons). Significant differences were observed in all the three parameters; data shown for day 30 neurons. Data presented as box plots with min and max, ***p=0.0002, **p=0.0012,****p<0.0001 respectively; Mann-Whitney U test was performed. (Control neurons n=120; *SHANK3* neurons n=122, from all 3 biological replicates. We compared 2 control lines with 2 *SHANK3* lines, with one clonal replicate).

Morphological differences were found in the *SHANK3* neurons at day 30 (immature neurons) and day 45 (young neurons) of neuronal development. The cell soma diameter (μm) was smaller in the patient neurons while the neurite length (μm) and the mean number of neurites was higher at both stages, as shown via the box plots [Figure3.2.1 E (I-iii) and Figure F (I-iii)]. These data indicate that there are structural differences between the control and *SHANK3* neurons. These changes are consistent through different stages of neuralisation and occur at an earlier stage of development when the neurons are immature day 30.

3.2.2: Tracking morphological changes through neuronal development

Since GFP transfection only targeted 2% of the cell population, we wanted to test whether the observed morphological deficits occurred within the whole cell population and not just in a subset of the population. To answer this question we used a high content cytometry assay to compare cell soma area and number of primary neurite per neuron. This was carried out at four stages of neuralisation; day 22 (late neural progenitors), 25, 27 and 30 (immature neurons) [Table 3.2.1].

Morphological Parameters	**Control (mean±SEM)**	**SHANK3 (mean±SEM)**
Primary no. of neurite per neuron	n=26,000	n=30,000
Mean at day 22 of neuralisation	1.265±0.2168	1.204±0.244
Mean at day 25 of neuralisation	1.663±0.3	1.773±0.263
Mean at day 27 of neuralisation	1.7878±0.136	1.865±0.099
Mean at day 30 of neuralisation	1.3950±0.156	2.698±0.212 ***p=0.0002
Cell soma area μm^2		
Mean at day 22 of neuralisation	113.2±25.809	109.1±15.944
Mean at day 25 of neuralisation	157.7±34.47	129.6±19.187
Mean at day 27 of neuralisation	155.8±20.89	170.5±23.21
Mean at day 30 of neuralisation	308±40.89	150.6±20.86 ***p=0.0001

Table3.2.1: Morphological analysis using High content imaging. The table describes the mean±SEM for each morphological parameter assessed at various stages of neuralisation. We analyzed from 5 control lines and 4 *SHANK3* lines (3 control lines with two clonal replicates and 2 SHANK3 lines with one clonal replicate of each). We compared 5 control lines with 4 *SHANK3* lines; 3 control lines with two clonal replicates and 2 *SHANK3* lines with one clonal replicate of each. (Control neurons n=26.0X10^3; shank3 neurons n=30.0X10^3).

No morphological changes were observed from day 22 to day 27. However, at day 30 we observe a significant decrease in cell soma area and increase in primary number of neurites per neuron in the *SHANK3* patient lines compared to the control lines (Figure 3.2.2). This not only confirmed our pervious observation on day 30 immature neurons (section 3.2.1) but also defined a window for change in the development of *SHANK3* neurons (day 27 to day 30).

In this assay, 5 control lines from three control patients were compared to 4 *SHANK3* lines from two *SHANK3* patients. These were as follows: Control P1 C1, Control P1 C2, Control P2 C1, Control P2 C2 and Control P3 were compared to SHANK3 P1 C1, SHANK3 P1 C2, SHANK3 P2 C2 and SHANK3 P2 C3 (Figure 3.2.2).

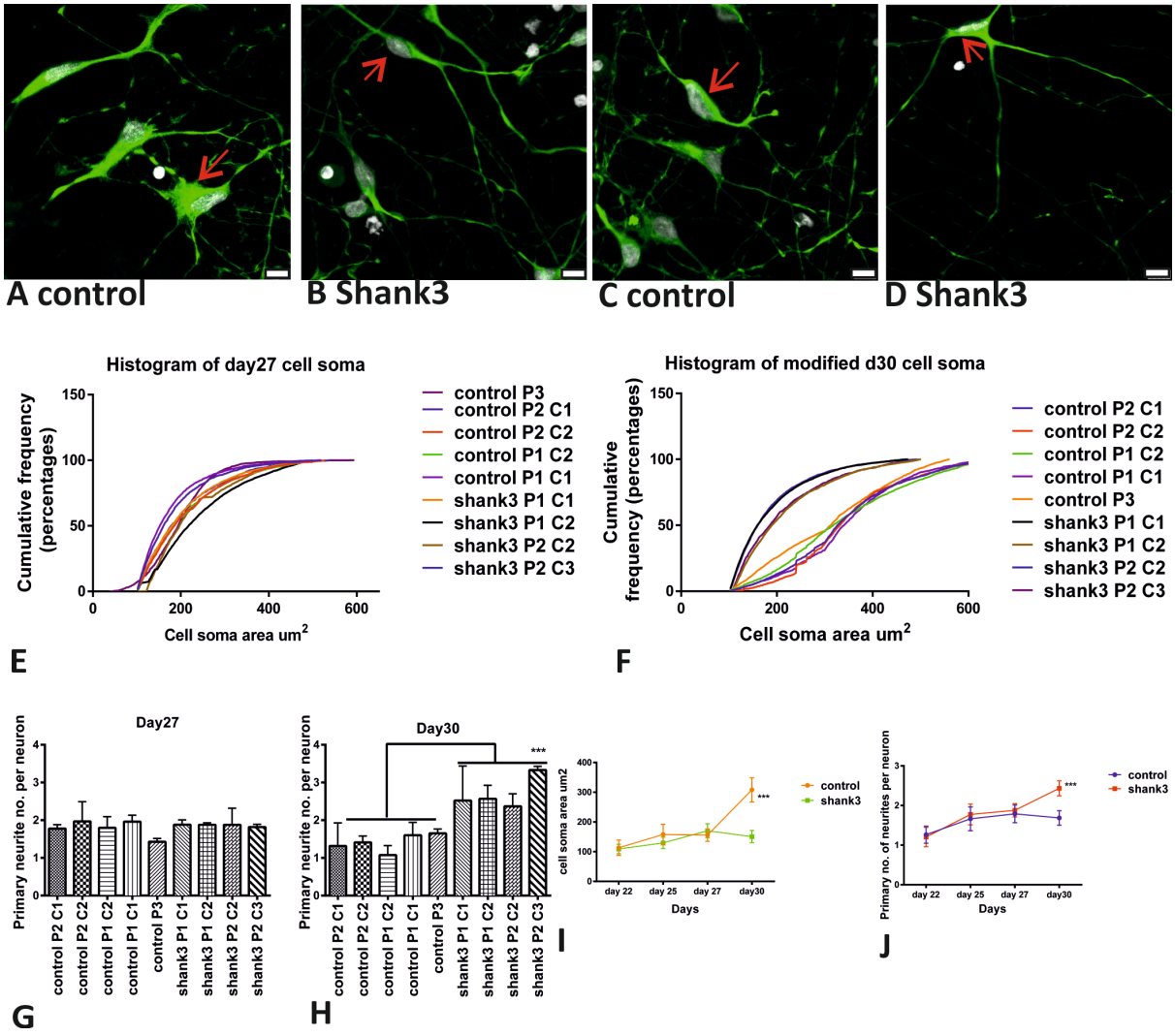

Figure 3.2.2: Morphological deficits found in immature *SHANK3* patient neurons

A. Control neurons cell soma B. Shank3 neurons cell soma C. Control neurons neurite D. Shank3 neurons neurite [Scale=10μm, day 30 neurons stained with DCX (green), DAPI (grey)]. E and F. are cumulative frequency distribution of cell soma area at day 27 and day 30. (**** $p<0.0001$, the Kolmogorov–Smirnov test was performed, Control neurons $n=26.0X10^3$; shank3 neurons $n=30.0X10^3$) G and H. are primary no. of neurites per neuron day 27 and day 30. Data represented as mean±SD, ***$p=0.0002$, the student t test was performed, Control neurons $n=26.0X10^3$; shank3 neurons $n=30.0X10^3$). I High content screening performed to find changes in cell soma area μm^2 from day 22 (late neural progenitors) to day 30 (immature neurons). Data represented as mean±sem, Mann-Whitney U test was performed for each time point, the only difference was seen at day 30 ***$p=0.0001$. J. High content screening performed to find out the primary no.of neurite per neuron from day 22 (late neural progenitors) to day 30 (immature neurons). Data represented as mean±sem. Unpaired student t test with Welch's correction was performed for each time point, the only difference was seen at day 30 ***$p=0.0002$. We performed 3 biological replicates. We compared 5 control lines with 4 *SHANK3* lines; 3 control lines with two clonal replicates and 2 *SHANK3* lines with one clonal replicate of each.

3.2.3: Neurite Outgrowth

Having established that *SHANK3* patient neurons exhibit abnormal neurite morphology (Figure 3.2 and 3.2.2), I now wished to explore neurite outgrowth in these cells in more detail. I therefore compared the rate of neurite formation (neurite/hr), elimination (neurite/hr), extension (μm/hr) and retraction (μm/hr) in control and *SHANK3* neurons at day 30 of neuralisation over a 12 hour period using time lapse imaging (Methods, section 2.12).

I studied 4 control lines from two control patients and 4 SHANK3 patient lines from two SHANK3 patients. These were as follows: Control P1 C1, Control P1 C2, Control P2 C1, Control P2 C2 were compared to SHANK3 P1 C1, SHANK3 P1 C2, SHANK3 P2 C1 and SHANK3 P2 C2 (Figure 3.2.3).

I found that the rate of formation of the primary neurite was significantly higher in *SHANK3* neurons than in control neurons, while the rate of primary neurite elimination was significantly lower (Figure 3.2.3 C,G and H; Table 3.2.2). There was, however, no change between the patient and control lines in the rate of secondary branch formation and elimination (Figure 3.2.3 I and J).

Similarly, when we analysed changes in the rate of extension and retraction of the primary neurite, the rate of extension of primary neurite length was significantly higher in *SHANK3* neurons, whereas the rate of primary neurite length retraction was significantly lower (Figure 3.2.3 D, E and F; Table 3.2.2).

Thus, we observed an increase in the rate of primary neurite formation and increase in neurite length extension in *SHANK3* patient neurons. This corroborates our previous experiments in section 3.2.1 and 3.2.2, which showed significant increases in the number of primary neurite number and length.

Table 3.2.2: Neurite Outgrowth: The table describes the mean±SEM for each neurite outgrowth parameter averaged from 4 control lines and 4 *SHANK3* lines (2 control lines and 2 *SHANK3* lines with one clonal replicate of each) assessed at day 30 of neuralisation. We compared 4 control lines with 4 *SHANK3* lines; 2 control lines with two clonal replicates and 2 *SHANK3* lines with one clonal replicate of each. (Control neurons n=51; SHANK3 neurons n=59, from all 3 biological replicates).

Neurite Outgrowth Parameters	**Control mean±SEM, n=51**	**SHANK3 mean±SEM, n=59**
Extension Rate µm/hr	31.60 ± 2.787	70.50±2.630, ****p<0.0001
Retraction rate µm/hr	58.32 ± 2.635	42.35 ± 3.291,**p=0.001
Neurite formation rate neurite/hr	0.4158 ± 0.02055	0.6555 ± 0.02538,****p<0.0001,
Neurite elimination rate neurite/hr	0.5809 ± 0.02885	0.3955 ± 0.01964,****p<0.0001,
Second branch formation branch/hr	3.018 ± 0.335	3.018 ± 0.335
Second branch elimination branch/hr	3.857 ± 0.5360	3.005 ± 0.3257
cell soma speed µm/hr	19.73 ± 0.6385	7.754 ± 0.5210, ****p<0.0001,
Avg. rate of change in cell soma area um^2/hr	139.9 ± 6.761	101.2 ± 3.751,**p=0.005

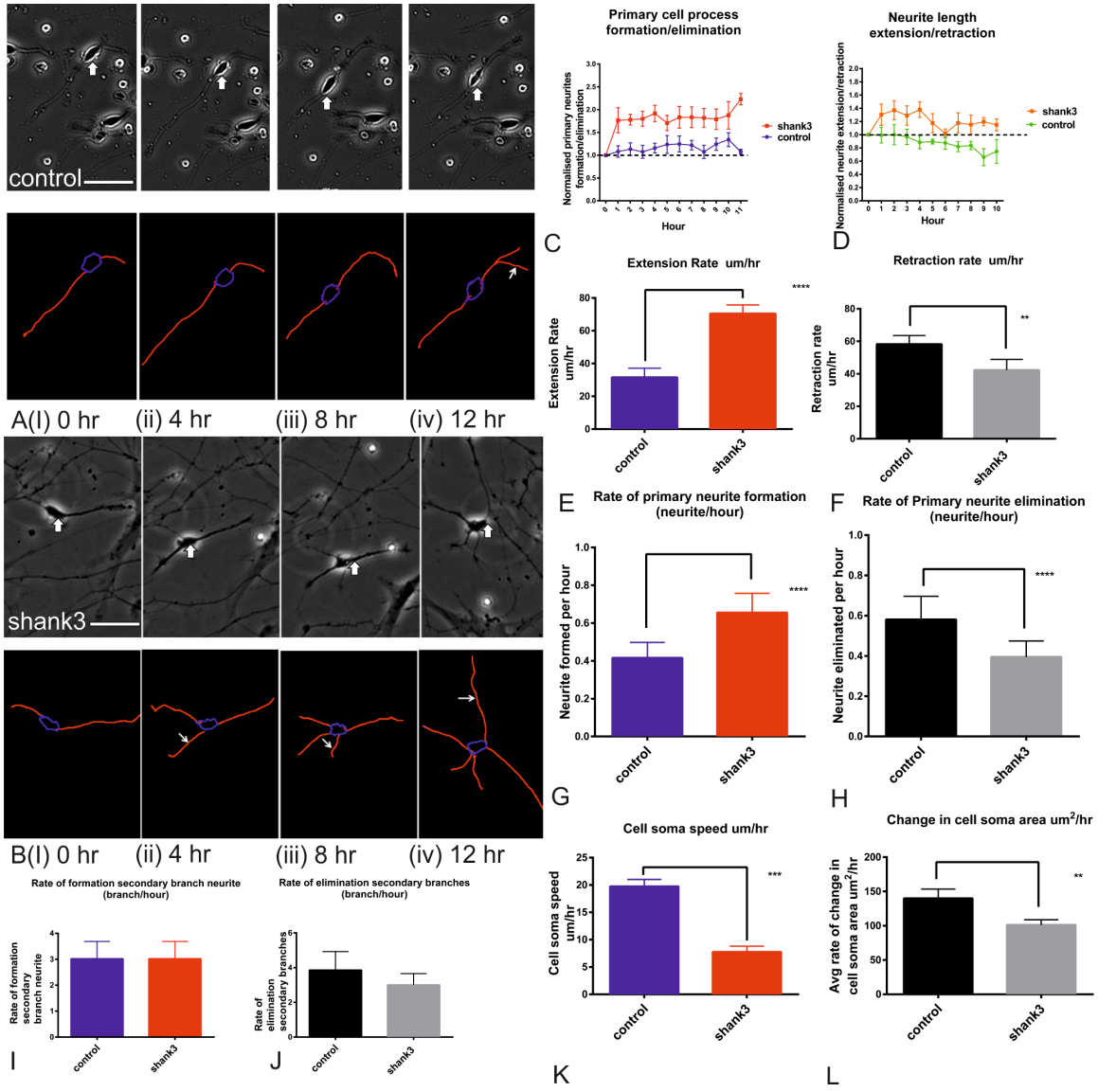

Figure 3.2.3: *SHANK3* patient neurons exhibit abnormal neurite outgrowth. A (i) Phase contrast image of control neuron and tracing (Red: Neurite, Blue: Cell body outline, Yellow: secondary branches) Neuron at zero hour (ii) fourth hour (iii) eighth hour (iv) twelfth hour. B(i) Phase contrast image of *SHANK3* neuron and tracing given below at zero hour (ii) fourth hour (iii) eighth hour (iv) twelfth hour (Scale = 50μm).C. Primary neurite of formation/ elimination rate were normalized to zero hour; above 1 represents the formation, below 1 represents elimination. Data presented as mean±sem.(Two way Anova performed, ****p<0.0001 b/w genotypes, ****p<0.0001 b/w genotypes and days). D. Neurite extension/ retraction rate of primary neurite were normalized to zero hour; above 1 represents the extension, below 1 represents retraction. Data presented as mean±sem. (****p<0.0001, Two way Anova performed). E. Extension rate (μm/hr) F. Retraction rate (μm/hr). G. Formation rate (neurite/hour) H. Elimination rate (neurite/hour). Data represented as mean±SD, ****p<0.0001, **p=0.001, ****p<0.0001, ****p<0.0001 respectively. Unpaired student t test with Welch's correction was performed. I. Rate of secondary branch formation (branch/hour). J. Rate of secondary branch elimination (branch/hour). K. Cell soma speed (μm/hr) L. Change in cell soma area μm^2/hr. Data represented as mean±SD. ****p<0.0001, **p=0.005 respectively, Unpaired student t test with Welch's correction was performed. (Control neurons

n=51; *SHANK3* neurons n=59, from all 3 biological replicates). We compared 4 control lines with 4 *SHANK3* lines; 2 control lines with two clonal replicates and 2 *SHANK3* lines with one clonal replicate of each.

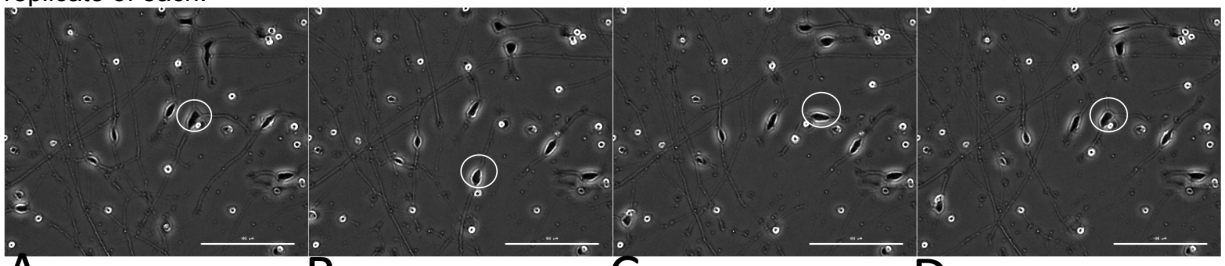

Figure 3.2.4: Cell soma movement: A. Depicts control neurons at day 30 at hour zero. B. control neuron at 4 hours C. Control neuron at 8 hour D. Control neuron at 12 hour. Scale= 100μm Please also see the CD attached at the back of this thesis, it contains the video of control and *SHANK3* neurons for 24 hours, picture taken every hour.

As described in section 3.1 of this chapter, approximately 30-35% of our cells were GnRH1 positive (Figure 3.1.2). During development of GnRH neurons, they pass through the nasal placode to several regions of the forebrain before reaching their final destination in the hypothalamus (Wray 2010). Recently, it has been shown that the migratory mechanism of GnRH1 neurons is through the movement of the cell soma. Briefly, guidance molecules cause the release of calcium in the cytoplasm, which reorganizes actin, microtubules and cytoskeletal elements. This causes contractions in the cell that linked to adhesive protein on the cell surface pulling the cell forward (Prakash J et al., 2012; Hutchins et al., 2013; Hutchins et al., 2014).

A similar phenomenon was observed in my experiments when carrying out time lapse imaging, the cell body moved from one position to another along with its neurites (Figure 3.2.4). In figure 3.2.4 B, the position of the control neuron is further down than the position it was at in figure 3.2.4 A. To analyze this, I calculated the speed of the cell soma movement in control and *SHANK3* neurons and discovered that the *SHANK3* neurons showed a significant decrease in cell soma speed (Figure 3.2.3 K). Therefore, the phenomenon I observed could be related to lesser migration of *SHANK3* patient neurons.

In our previous experiments, we have shown that the cell soma area of control neurons is much greater than *SHANK3* neurons (Figure 3.2.2). The next question I wanted to ask was whether the control cell soma size was inherently different than the *SHANK3* cells or is there expansion of the cell soma size. I tried to correlate this with time. I calculated the average rate of change in cell soma area over the period of twelve hours (μm^2/hr). This was found to be significantly lower in the *SHANK3* neurons (Figure 3.2.3 L). This indicated that the control neurons expand the cell soma area more with time than the *SHANK3* neurons. This suggests that there is a possible mechanism in the control neurons that causes them to expand with time such that its size increases. While the *SHANK3* patient neurons, due to the loss of *SHANK3*, have possibly lost this function of expansion. Thus, their cell size remains smaller. One of the possible mechanisms behind this I explore in chapter 5, which could be the loss of global protein synthesis in the *SHANK3* patient neurons.

3.3: Discussion

3.3 (a) ASD and Hypothalamus

In section 3.1 of this chapter, I have characterized the neurons derived from control, mutant *SHANK3* iPSC lines and the sporadic ASD line. The neuralisation protocol described gave us neurons that were positive for neuronal markers such as DCX and Tuj1. We identified over 85% of the neuronal population as hypothalamic neurons, although we have not formally excluded the possibility that neurons could be expressing both CRH and GnRH1. 50-60% of the neuronal population was positive for CRH and 30-40% of the neuronal population was positive for GnRH1.

There were no differences found in the neural induction of patient and control iPSC lines. Moreover, there was minimal variability found between the iPSCs lines in the percentages of the types of neurons generated. Therefore, we have

established a stable neuronal model to study the effects of autism in hypothalamic neurons.

As mentioned in the introduction section 1.11, the hypothalamus produces hormones, which impact greatly on social behavior. For example, increased levels of cortisol, testosterone and progesterone have all been reported in fetal development of autism (S Cohen et al., 2015). It is well known that CRH and GnRH hormones are precursors to cortisol and testosterone respectively (Quintanar J. Luis et al., 2013). Thus, it is essential we understand how hypothalamic neurons develop in humans with and without ASD.

3.3 (b) *SHANK3* haplo-insufficiency affects morphology of the neuron

The shape and structure of the neuron dictates its function. Dendritic branching and orientation further impact on this (Meinertzhagen et al., 2009). Furthermore, the development of morphological features of the neuron is dependent on genetic factors, electrical fields and chemical cues. In this study, we specifically address the role of *SHANK3* gene in autism during early development. I compared various aspects of neuron morphology in control versus *SHANK3* patient neurons.

These studies have revealed that the *SHANK3* neurons were morphologically compromised: having smaller cell bodies, more primary neurites and longer primary neurites than the control neurons. Moreover, the *SHANK3* neurons showed deficits in neurite extension and retraction. These results suggest that in neurons, *SHANK3* plays a role in the regulation of neuronal structure.

Smaller cell soma size has been consistently described in both post mortem and rodent models of ASD. For example, in Rett's and Fragile X syndrome both have shown a reduction in cell soma size in the cerebral cortex and hippocampal regions of the brain (Irwin et al., 2001; Bauman et al., 1995; Chen et al., 2001;

Kishi and Macklis 2004: Smrt et al., 2007, Asaka et al., 2006; Moretti et al., 2006; Nelson et al., 2006; Noutel et al., 2011; Castern et al., 2005). Decreased cell soma size has also been validated in iPSC models of the same diseases (Cheung et al 2011; Marchetto et al., 2010; Ananiev et al., 2011). These studies support our observations that *SHANK3* neurons have smaller cell somas.

Recently, Peca et al (2012) studied the *Shank3* KO mice, they traced Golgi-stained striatal medium spiny neurons and found increase in total dendritic length. Sholl analysis of the same neurons revealed neuronal hypertrophy as measured by increased dendritic arborization. Furthermore, they linked this back to significant volumetric enlargement of caudate in *Shank3* KO mice. An enlarged caudate in autistic patients' is associated with repetitive behavior (Hollander E et al., 2005; Langen et al., 2009). In our study, we saw a similar pattern of increase in neurite length (Figure 3.2) and increase in neurite number (Figure 3.2.2). Therefore, it is possible that increased brain volume seen in autistic patients could be due to the morphological changes we report here.

In the introduction section 1.3, we described the hypothesis that abnormal cellular growth causes aberrant connections between neurons, which leads to social deficits in autistic patients (Keown C et al., 2013). Through the above experiments we have also shown that the SHANK3 patients have abnormal neuronal growth, which is increased neurite number and neurite length. This could lead to synaptic and electrophysiological deficits that cause miscommunication between neurons (preliminary results of these experiments have been described in Chapter 5 of this thesis). This in turn could cause the social deficits that are commonly reported in autistic patients.

In this chapter, I have established a stable in-vitro system to analyze the effects of *SHANK3* in autism. I have revealed that the loss of *SHANK3* in patient neurons resulted in the neuronal morphology changes, which could be related back to autism. It is now important to confirm that these phenotypic differences

between cells derived from *SHANK3*-deletion patients and neurotypical individuals were genuinely due to *SHANK3* haploinsufficency. In the next chapter I use three different approaches to confirm this.

Chapter 4: Rescue of morphogenetic deficits in *SHANK3* patient neurons

Background

In the previous chapter, I presented data indicating that iPSC-derived neurons that carry a heterozygous deletion in *SHANK3* show developmental defects. These defects are evident as early as day 30 of neuralisation when these *SHANK3* patient neurons exhibit a decreased cell soma area, increased primary neurites and neurite outgrowth.

It is essential to verify that these phenotypic differences between cells derived from *SHANK3* patients and control were due to the *SHANK3* haplo-insufficiency. I therefore undertook three further studies. In the first study, I sought to rescue morphogenetic phenotype in *SHANK3* patient neurons by transducing into the cells a *SHANK3* expression construct. The second I studied a genome-edited male human embryonic stem cell line, comparing a homozygous deletion of *SHANK3*, a heterozygous deletion of *SHANK3* and a control line with no modifications. The third experiment used the growth factors IGF1 and BDNF as potential drugs to rescue the morphological phenotypes.

4.1 Enhancing the expression of *SHANK3* rescues the morphogenetic phenotype seen in *SHANK3* patient neurons.

In order to determine whether the phenotype observed in the *SHANK3* patient neurons could be rescued by overexpressing *SHANK3*, I infected the *SHANK3* patient neurons with a lentivirus overexpressing the full length *SHANK3* (ORF) where the N terminal had been fused to Myc (Figure 4.0 A; Methods section 2.19). Non-infected SHANK3 neuronal cultures were included as controls.

I used two *SHANK3* patient lines to show the rescue: SHANK3 patient 2 clone 1(SHANK3 P2 C1), and the male SHANK3 patient 1 clone 2 (SHANK3 P1 C2). These lines have previously revealed to have morphogenetic deficits at day 30 of neuralisation. They both showed a decrease in cell soma area and an increase in primary number of neurites (Figure 3.2.2). The neurons were infected at day 20/21 of neuralisation and the virus was removed after twenty-four hours. After the removal of the virus, media was changed every other day till day 30.

On day 30, neurons were fixed and stained for Myc and DCX (Doublecortin) using immunocytochemistry. Myc was used to identify neurons that were positively infected (as Myc is fused to N terminal of *SHANK3* overexpression construct) and DCX was used to identify immature neurons. I counted the proportion of neurons that were positive for Myc, these were about 80% as described in Table 4.0. Next, I programmed the high content imaging platform such that it only selected the neurons that were positively infected, in other words, positive for Myc staining. After the successful transduction of the neurons, I used high content imaging to measure the cell soma area (um^2) and primary number of neurites per neuron.

In the SHANK3 patient female line, (SHANK3 P2 C1) the overexpression of *SHANK3* rescued both the cell soma area and the primary number of neurites (Table 4.1). In the SHANK3 female patient the cell soma area of 30 day neurons

without rescue was 153.237 ±6.52 μm^2 after the enhanced expression of SHANK3 in the female patient neuron this increases up to 238.58±3.66 μm^2 (Figure 4.0 D). Similarly, in the SHANK3 male patient line (SHANK3 P1 C2) the enhanced expression of *SHANK3* increases the cell soma area from 180.38±3.23 (without rescue) to 250.422±4.07 μm^2 (Figure 4.0 E). Therefore, increasing the expression of *SHANK3* in *SHANK3* patient neurons rescued the cell soma morphogenetic phenotype.

We know from previous experiments that the loss *SHANK3* in *SHANK3* patient neurons results in the increased primary number of neurites (chapter 3 section 3.2). When we enhanced the expression of *SHANK3* in the SHANK3 female patient line we saw a significant decrease in the primary number of neurites (Figure 4.0 F) that is 2.36 ± 0.04 neurites were turned into 1.20±0.03 neurites. However, in the male SHANK3 patient line, the enhanced expression of *SHANK3* did not cause any change in the primary number of neurites (Figure 4.0 G; Table 4.1).

Cell Line	Total number of neurons DCX	Number of cells positive for Myc and DCX	Transduction percentage
SHANK3 P2 C1 with rescue	1885	1500	79.57%
SHANK3 P2 C1 with rescue -18	2278	1820	79.89%
SHANK3 P1 C2 with rescue	2470	1980	80.16%
SHANK3 P1 C2 with rescue-18	1751	1400	79.95%

Table 4.0: Neurons positive for Myc and transduction percentage.

LINES	CELL SOMA AREA (um^2 mean±SEM)
Shank3 P1 C2 without rescue	180.38±3.23
Shank3 P1 C2 rescue	250.422±4.07
Shank3 P1 C2 rescue EXON-18	250.918±3.55
Shank3 P2 C1 without rescue	153.237±6.52
Shank3 P2 C1 rescue	238.58±3.66
Shank3 P2 C1 rescue EXON-18	234.25±4.32

LINES	Primary neurite per neurons (mean±SEM)
Shank3 P2 C1 without rescue	2.36 ± 0.04
Shank3 P2 C1 rescue	1.20±0.03
Shank3 P2 C1 rescue EXON-18	1.36 ±0.02
Shank3 P1 C2 without rescue	1.82±0.138
Shank3 P1 C2 rescue	1.76±0.35
Shank3 P1 C2 rescue EXON-18	1.64±0.08

Table 4.1: Enhanced expression of *SHANK3* rescues morphogenetic phenotypes. The table above shows the mean±SEM of cell soma area (um^2) before rescue, after SHANK3 rescue and with SHANK3 rescue without exon18 for two different SHANK3 lines. The table at the bottom describes the mean±SEM of primary no. of neurite before rescue, with SHANK3 rescue and with SHANK3 rescue without exon18 for different SHANK3 lines. Red is SHANK3 male line and **Black** is the SHANK3 female line.

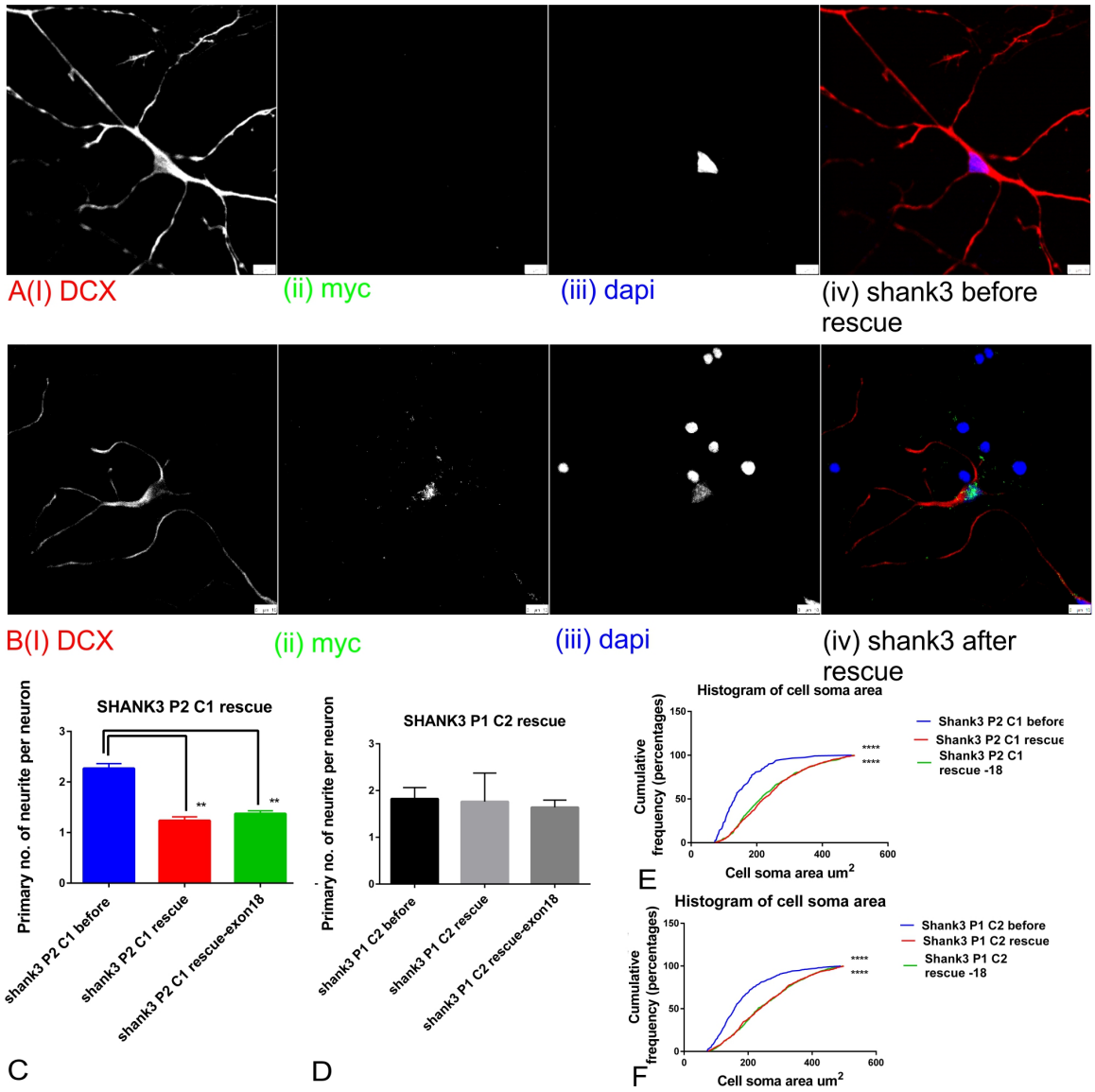

Figure 4.0: Overexpression of *SHANK3* rescues the morphogenetic phenotypes: A. Day 30 SHANK3 before rescue, (i) DCX (red) (ii) MYC (green) stained (iii) DAPI (blue), (Scale=10μm). B. Day30 SHANK3 neuron after rescue, (i) DCX (red) (ii) MYC (green) stained (iii) DAPI (blue), (Scale=10μm). C. Primary number of neurites per neuron SHANK3 Patient 2 Clone1 with and without rescue. D. Primary number of neurites per neuron SHANK3 Patient 1 Clone2 with and without rescue. Data represented as mean±SD. Data compared via unpaired student t test with Welch's correction. (**p=0.0026 SHANK3 P2 C1 before vs. SHANK3 P2 C1 rescue, **p=0.0066 SHANK3 P2 C1 before vs. SHANK3 P2 C1 rescue-18). E. Cumulative frequency distribution of cell soma area (μm^2) of SHANK3 Patient 2 clone 1 with and without rescue. F. Cumulative frequency distribution of cell soma area (μm^2) of SHANK3 Patient 1 clone 2 with and without rescue. Data compared via Kolmogorov-Smirnov test. (****p<0.0001 SHANK3 P2 C1 before vs. SHANK3 P2 C1 rescue, ****p<0.0001 SHANK3 P2 C1 before vs. SHANK3 P2 C1 rescue-18, ****p<0.0001 SHANK3 P1 C2 before vs. SHANK3 P1 C2 rescue and ****p<0.0001 SHANK3 P1 C2 before vs. SHANK3 P1 C2 rescue-18). I repeated this experiment three times and the total number of neurons compared from all three experiments were as follows: SHANK3 P2 C1 before n=1.5X103, SHANK3 P2 C1 with rescue n=1.5X103, SHANK3 P2 C1 with rescue - exon18, SHANK3 P1 C2 before n=1.45 X103, SHANK3 P1 C2 with rescue n=1.98 X103, SHANK3 P1 C2 with rescue-18.

I next wanted to determine whether the enhanced expression of SHANK3 in *SHANK3* patient neurons resulted in a completely wild-type phenotype. I compared the control female line to the SHANK3 female patient line with the rescue and the control male line to the SHANK3 male patient line with rescue (Figure 4.1). There was a significant shift in the cumulative frequency distribution in both the *SHANK3* patient lines with rescue [Figure 4.1 A (I) and (ii)]. A significant increase in the cell soma area is shown by both *SHANK3* patient lines with rescue as compared to *SHANK3* patient lines without rescue. Moreover, if we glance at the cumulative frequency distribution lines for both *SHANK3* patient lines with rescue we see that these distributions are moving towards the control and away from *SHANK3* patient lines without the rescue [Figure 4.1 A (I) and (ii)]. This suggested that the enhanced expression of SHANK3 in patient lines recues the cell soma phenotype. However, it does this only relatively as the cumulative distribution of cell soma area for the control and *SHANK3* patient lines with rescue do not completely overlap.

On the other hand, there was a significant decrease reported in the number of primary neurites per neuron in the SHANK3 female patient line with rescue [Figure 4.1, B (I)]. In the SHANK3 female patient line we have previously shown that there is an increase in the primary number of neurites as reflected in SHANK3 female patient without rescue. If we compare the SHANK3 female patient line with rescue to control we see that there is no significant difference between them [Figure 4.1, B (I)]. This suggests that the enhanced expression of *SHANK3* completely rescues the primary number of neurites in the female patient neurons. Since, there was no rescue seen in the primary number of neurites in the SHANK3 male patient line, I did not compare it to the controls.

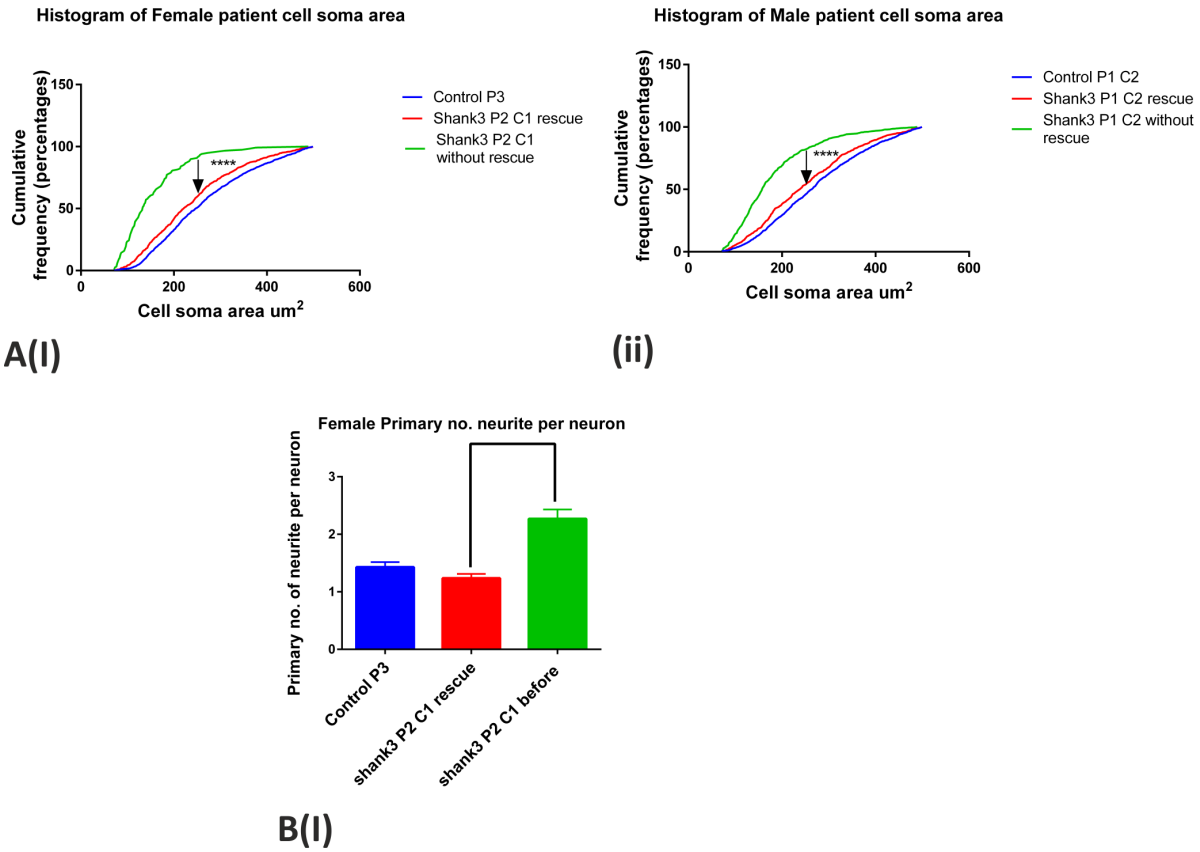

Figure 4.1: *SHANK3* rescue versus control: A. I compared the cell soma area (um^2) of female patient SHANK3 line (SHANK3 P2 C1; SHANK3 patient 2 clone 1) with rescue and without rescue to control female line (Control Patient 3). (ii) I compared the cell soma area (um^2) of male patient SHANK3 line (SHANK3 P1 C2; SHANK3 patient 1 clone 2) with rescue and without rescue to control male line (Control patient 1 clone 2). B (I). I compared the primary number of neurites per neuron of female patient SHANK3 line (SHANK3 P2 C1; SHANK3 patient 2 clone 1) with rescue and without rescue to control female patient line.

The *SHANK3* gene produces several protein isoforms in the human brain (Jiang et al., 2013). The protein domain structure of each isoform has been deduced from *mRNA* expression of different human promoters. To date, no protein isoforms have been validated because of lack of isoform specific antibodies (Introduction section 1.5, Figure 1.1).

Previous work in our laboratory indicates that the expression of *SHANK3* with exon18 increases during transition from neural progenitors to neurons (data shown in introduction section 1.12). These data also indicated that the *SHANK3* patient lines had a reduced expression of this exon. Since this expression of exon 18-containing isoforms immediately precedes the appearance of the morphogenetic phenotype, we hypothesized that the specific failure to express exon 18 might be associated with this phenotype. If this hypothesis were correct then a full length *SHANK3* without exon18 might fail to rescue the phenotype where a construct including exon 18 would succeed. In fact, both exon 18+ and exon 18- constructs rescued equally well (Figure 4.0 D to G; Table 4.1). In the both male and female *SHANK3* patient lines increasing the expression of SHANK3 rescue without exon 18 lead to increase in cell soma area, which was similar to SHANK3 full length rescue (Figure 4.0 D and E). Likewise, the overexpression of SHANK3 rescue without exon 18 resulted in the decrease of primary number of neurites in SHANK3 female patient line. While, no change in primary number of neurites was reported in the SHANK3 male patient line (Figure 4.0 F and G). Thus, the increase in expression of SHANK3 exon18 during transition from neural progenitors to neurons had no bearing on neuronal morphology.

4.2 Morphogenetic deficits reported in genetically modified human embryonic stem cells (es)

Above I have shown that increasing the expression of *SHANK3* in *SHANK3* patient neurons rescued morphogenetic phenotype. To further confirm that *SHANK3* was the cause of the morphological phenotypes seen in *SHANK3* patient neurons, I compared the morphology of neurons generated from a control male human es cell line with es cell lines where both copies of the *SHANK3* genes had been knocked out (es shank3-/-) and where only one copy had been knocked out (es shank3+/-) (Tables 2.7, 4.2).

These lines were provided by our collaborator, Dr. Ravi Jagasia at Roche (F.Hoffmann-La Roche Ltd CNS Discovery Grenzacherstrasse CH-4070 Basel/Switzerland). We converted these es cell lines into hypothalamic neurons using the neuralisation protocol (Methods section 2.3). These were then analyzed at three stages of neuralisation; day 25 (early neurons), 27 and 30 (immature neurons) using high content screening [Figure 4.2 A (I-iii)].

Figure 4.2 [B (I-iii); Table 4.2] shows the cumulative frequency distribution of cell soma area at day 25, 27 and 30 of neuralisation. There was a significant difference between the cell soma area in es shank3+/- and es shank3+/+ derived neurons, with this area being smaller in the former. Similarly, the cell soma area was significantly smaller in the es shank3-/- derived neurons than in the es shank3 +/+ derived neurons [Figure 4.2 B (I-iii)]. These differences were not only evident on day 30 of neuralisation as seen in the patient lines (Chapter 3, Figure 3.2.2), but also at day 25 and day 27.

Moreover, we also saw a difference in es cell-derived neurons in the number of primary neurites per neuron. Both the es shank3 +/- and es shank3-/- neurons showed an increase in the number of neurites present compared to the es shank3+/+ at all three stages analyzed [day 25, 27 and 30; Figure 4.2.1 B (I-iii),].

Although this was similar to what we see in the *SHANK3* patient lines, it also occurred at an earlier stage; from day 25 rather than day 30 (Chapter 3, section 3.2). However, a qualitative observation was made that the es cells neuralised somewhat faster than the iPSCs and this could possibly be the reason for the morphological phenotypes appearing earlier in es-derived neurons.

LINES	Primary neurite per neuron Day 25 (mean±SEM)	Primary neurite per neuron Day 27 (mean±SEM)	Primary neurite per neurons Day 30 (mean±SEM)
es shank3+/+, n=5100	1.69±0.084	1.64±0.1472	1.90±0.655
es shank3+/-, n=5000	3.03±0.141	2.76±0.188	3.00±0.131
es shank3-/-, n=5110	3.12±0.119	2.78±0.102	3.04±0.136
	cell soma area Day 25 (mean±SEM)	**cell soma area Day 27 (mean±SEM)**	**cell soma area Day 30 (mean±SEM)**
es shank3+/+, n=5100	289.8±3.38	303.845±1.947	272.600±1.949
es shank3+/-, n=5000	220.7±1.797	183.469±1.475	191.100±1.501
es shank3-/-, n=5110	188.1±1.551	190.294±1.343	206.4±3.117

Table 4.2: Morphological phenotypes of es derived neurons. The table below shows the mean±SEM for cell soma area (um^2) and primary neurites per neuron in hES derived neurons. This analysis was done on days 25, 27 and 30 of neuralisation. For P values please refer figures 4.2 and 4.2.1

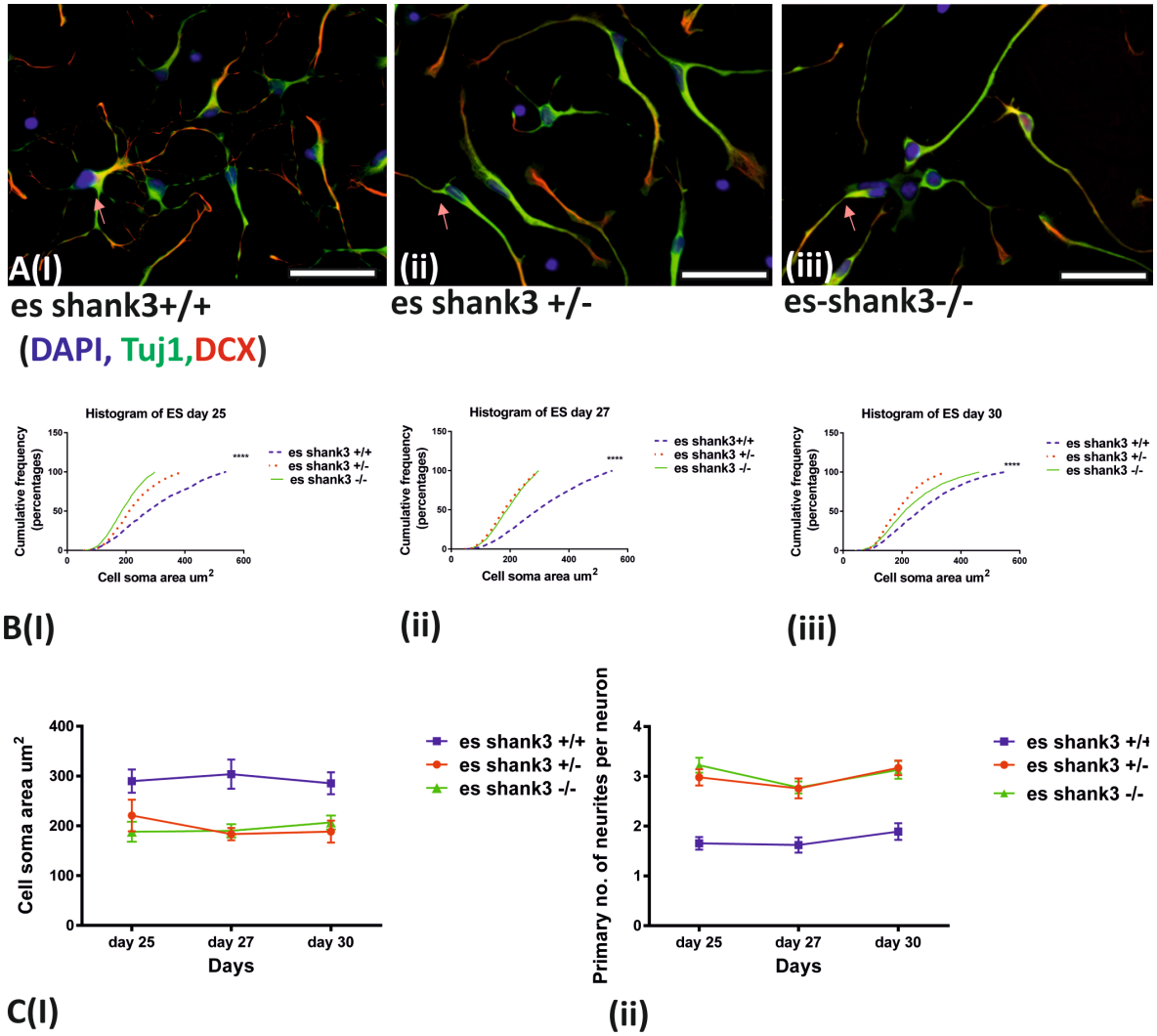

Figure 4.2: Morphogenetic deficits reported in genetically modified human embryonic stem cells (es). A (I-iii) day 30 es shank3+/+, es shank3+/- and es shank3/- derived neurons stained with DAPI, DCX and tuj1 (Scale bar=50μm). B (I) shows the cumulative frequency distribution of cell soma area (μm^2) of day 25 neurons (ii) day27 neurons (iii) and day 30 neurons. Comparison were made using the Kolmogorov-Smirnov test as es shank3+/+ vs. +/- and es shank3+/+vs. es shank3-/- for day 25, 27 and 30. Day 25 ES+/+ vs. es shank3+/- ****p<0.0001, day 25 es shank3+/+ vs. es shank3-/- ****p<0.0001, day 27 es shank3+/+ vs. es shank3+/- ****p<0.0001, day 27 es shank3+/+ vs. es shank3-/- ****p<0.0001 and day 30 es shank3+/+ vs. es shank3+/- ****p<0.0001, day 30 es shank3+/+ vs. es shank3-/- ****p<0.0001. C (I) shows the cell soma area changes through various neuralisation stages (day 25 to day 30). Data is represented as the Mean±sem. Freidman's Two-way Anova by ranks pairwise comparison ****p<0.0001 on all three stages of neuralisation. C (ii) shows the change in the number of primary neurites (day 25 to day 30). Data is presented as mean±sem, (es shank3 +/+ n= $5.1X10^3$, es shank3 +/- n=$5.0X10^3$, es shank3-/- n=$5.11X10^3$ from all 3 biological replicates). Data represented as mean±sem. Two way Anova with repeated measure performed at each time point, ***p<0.001 significant difference was found between genotypes and **p<0.005 there is an interaction between days and genotypes. Bonferroni's multiple comparisons test revealed ***p<0.001 es shank3 +/+ vs. es shank3 +/-, ***p<0.001 es shank3 +/+ vs. es shank3 -/- and p=1.0 es shank3 +/- and es shank3 -/-.

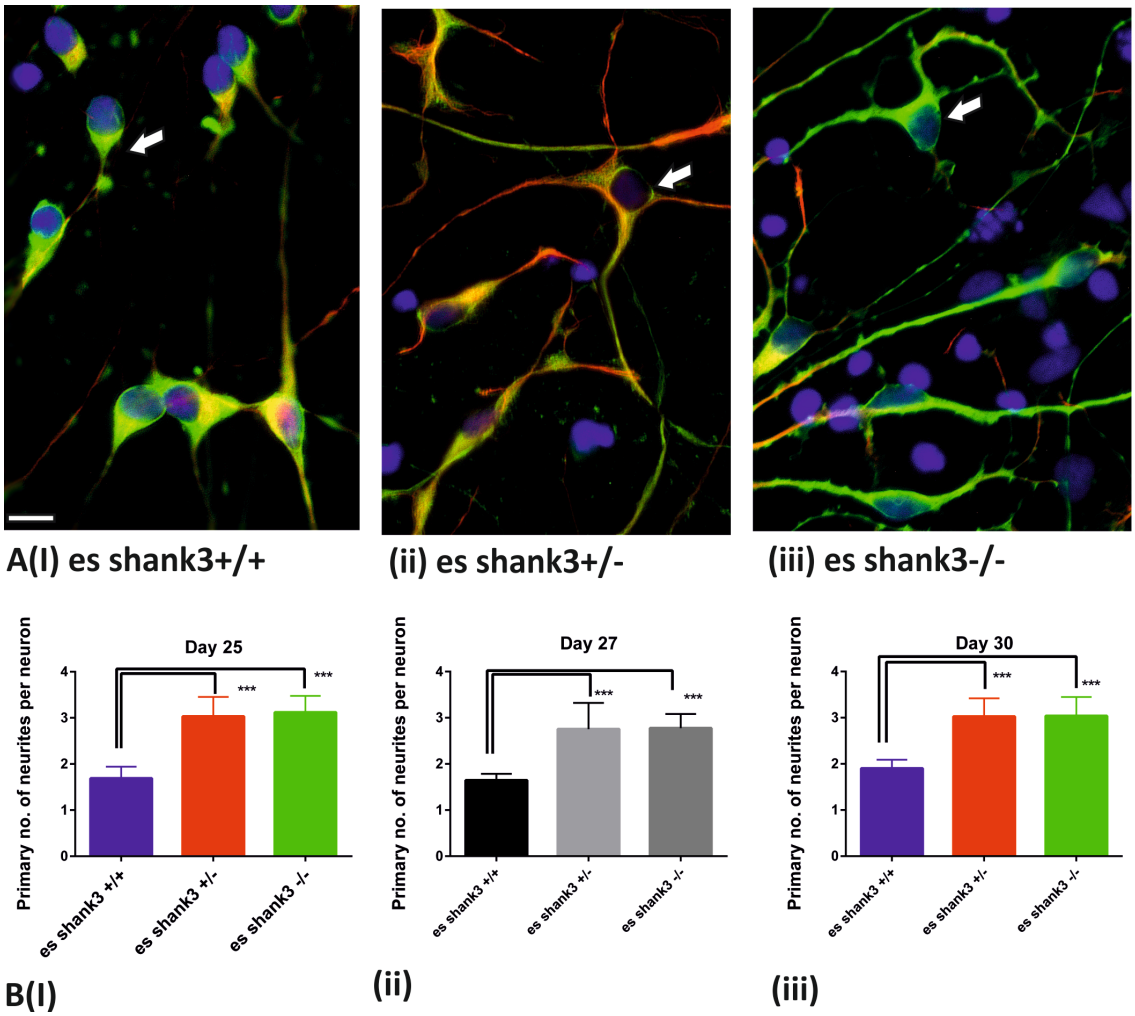

Figure 4.2.1: Neurite deficits reported in genetically modified human embryonic stem cells (es). Day 30 of neurons A (I) es shank3 +/+, (ii) es shank3 +/-, (iii) es shank3 -/- stained with DAPI, DCX and Tuj1 (Scale bar=10μm). B (I) Primary number of neurites per neuron day25, (ii) Primary number of neurites per neuron day27. (iii) Primary number of neurites per neuron day30. Data represented as mean±SD. Data compared via. Unpaired student t test with Welch's correction. . Day 25 es shank3 +/+ vs. es shank3 +/- ***p<0.001, day 25 es shank3 +/+ vs. es shank3 -/- ***p<0.001, day 27 es shank3+/+ vs. es shank3+/- ***p<0.001, day 27 es shank3+/+ vs. es shank3-/- ***p<0.001 and day 30 es shank3 +/+ vs. es shank3 +/- ***p<0.001, day 30 es+/+ vs. es-/- ***p<0.001. (es shank3 +/+ n= $5.1X10^3$, es shank3+/-n=$5.0X10^3$, es shank3-/- n=$5.11X10^3$ from all 3 biological replicates).

These experiments showed that the morphological phenotypes seen in the es shank3 -/- and es shank3 +/- derived neurons were similar to those observed in *SHANK3* patient neurons. These observations suggest that the decreased cell soma area and increased primary number of neurites observed in these neurons are caused by either the loss or the decrease in the expression of *SHANK3*.

4.3 Growth factors are unable to rescue *SHANK3* morphogenetic deficits

Recently, an iPSC model was used to study Phelan Mcdermid syndrome (PMDS), a syndrome caused by a deletion in the 22q.13 chromosomal region that includes the *SHANK3* gene (Shcheglovitov et al., 2013). This disorder is characterized by intellectual disability, seizures motor problems and autism (Shcheglovitov et al., 2013). The PMDS neurons generated from patient iPSCs revealed synaptic signaling deficits, and these were restored to normal with exposure to IGF1 (Shcheglovitov et al., 2013). They selected IGF1 as it promoted neurogenesis and synaptogenesis in hippocampal dentate gyrus during postnatal development of mice (O'Kusky JR et al., 2000). Recently, a small clinical trial is also underway to treat PMDS patients with IGF (clinicaltrails.gov/ct2/show/NCT01525901).

In addition, IGF1 partially reversed cellular phenotypes associated with Rett's syndrome a co-morbid disorder of ASD. It restored spine density, synaptic amplitude, and increased postsynaptic density protein 95 (PSD95) in mouse model of Rett's syndrome (Tropea D et al., 2009). Furthermore, a mouse model with *Shank3* KO was given daily intraperitoneal injections of human IGF1 for over two weeks. This rescued LTP (Long term potentiation) and motor performance in these mice (Bozdagi et al., 2013).

In most of the studies described above the IGF1 rescues the function at the synapse. In this study we report early morphogenetic deficits in *SHANK3* patient neurons. However, a key point to remember is that the structure of the neuron defines its capacity to receive and integrate synaptic signals (Hausser M 2001). Later, in this thesis (chapter 5, section 5.3), I describe pre- and post-synaptic puncta deficits in *SHANK3* patient neurons. This also suggests that the *SHANK3* haplo- insufficiency leads to morphological deficits in neurons which could cause synaptic discrepancies. Thus, in this experiment, we use IGF1 as potential drug to rescue the morphogenetic deficit, which might prevent the synaptic abnormalities from occurring.

During development BDNF is required for neuronal proliferation, neuronal migration, neuronal survival, neuronal protection, neuritogenesis, synapse formation, neuronal excitability and synaptic transmission, short- and long-term plasticity, axon guidance, axonal branching, dendritic growth, dendrite branching, modulation of excitatory and inhibitory synapses (Tapia-Arancibia, Lucia et al., 2004; Lee J et al., 2013; Bath KG et al., 2012; Waterhouse et al., 2012). Administration of BDNF in hypothalamic rat neurons in vitro has been shown to stimulate neurohormone synthesis, release and increased neuronal differentiation (Tapia-Arancibia, Lucia et al., 2004). Moreover, BDNF stimulates the differentiation somatostatin (SST) and cortisol releasing hormone (CRH) neurons (Loudes et al., 2000). Therefore, I also investigated whether this factor could rescue the morphological defects of *SHANK3* neurons.

To determine whether IGF1 or BDNF could rescue the morphological phenotypes of *SHANK3* patient neurons seen at day 30 of neuralisation (Chapter 3; Figure 3.2.2). I performed this experiment in two *SHANK3* patient lines with one clonal replicate of each and compared it to two control lines with one clone replicate of each. These were as follows: Control P1 C1, Control P1 C2, Control P2 C1 and Control P2 C2 were compared to SHANK3 P1 C1, SHANK3 P1 C2, SHANK3 P2 C2 and SHANK3 P2 C3.

IGF1 was administered at 20ng/ml for seven days starting from day 23 to day 30 (Figure 4.3 A). The concentration of IGF1 was chosen from the iPSC study on Phelan McDermid syndrome (Shcheglovitov et al., 2013). BDNF was administered at 50ng/ml for four days starting from day 26 to day 30 of neuralisation. Concentration of BDNF and time period was adapted from McAllister et al (1997). At day 30 cultures were fixed, stained with Tuj1 (neuronal specific ß-iii-tubulin) analyzed using high content imaging. Neither IGF1 nor BDNF had any effect on cell soma area or the mean number of primary neurites (Figure 4.3 B, C).

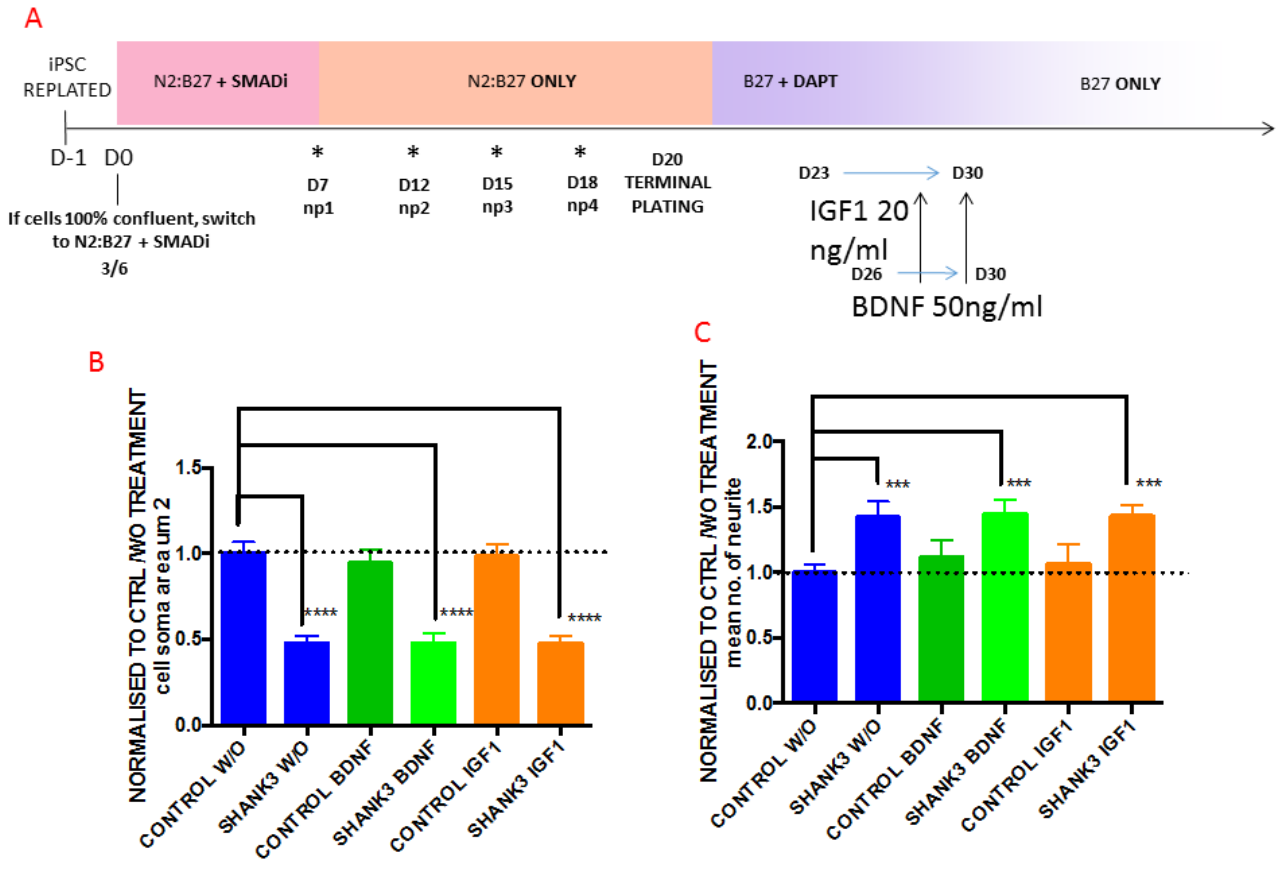

Figure 4.3: Effect of IGF1 and BDNF on the morphology of *SHANK* 3 patient neurons. A shows the neuralisation timeline and treatment schedule. The histograms compare the cell soma area (B) or Mean no. of neurites (C) of control and SHANK3 neurons with and without treatment with BDNF and IGF1. Data is presented as mean±SD. ****p<0.0001, one –way analysis of variance with Dunnet's multiple comparisons test. All values were normalised to the mean values acquired from control untreated neurons. I performed this experiment in two SHANK3 patient lines with one clonal replicate of each and compared it to two control lines with one clone replicate of each.

4.4: Discussion

In chapter 3, phenotypic analyses of *SHANK3* patient neurons at the morphological level revealed deficits in neuronal outgrowth and cell soma size. Here we have used enhanced expression studies and analysis of neurons derived from *SHANK3* KO human es cells to confirm that decrease in *SHANK3* expression is the primary cause of these deficits. This reveals that *SHANK3* plays a critical role in the formation of neurons, particularly its shape, size and structure.

Interestingly, in the female SHANK3 patient line enhanced expression of *SHANK3* rescued the primary number of neurites but this was not the case for neurons derived from the male SHANK3 patient line (Figure 4.0 F and G). Even though, the female *SHANK3* patient line has a longer mutation, which includes the genes *SHANK3*, *ACR* and *RABL2* (data for this is shown in supplementary Table 1.0 and 2.0) while the male SHANK3 patient line has a shorter deletion including the genes *SHANK3* and *ACR* only. They both have the same deletion in the *SHANK3* gene, therefore it is unlikely that the neurite morphology in the SHANK3 patient male line could be affected by this.

The other speculation we could make that there is some protein translational deficits in *SHANK3* patient lines. However, this also does not seem to be the case as firstly, the *SHANK3* rescue construct managed to successfully rescue cell soma area phenotype for both the male and female patient line. Secondly, global protein translational was measured in both the SHANK3 male and female patient line in chapter 5 (section 5.2) of this thesis. There were no differences found. The other possibility could be that *SHANK3* is translated or regulated differently in males than females. Currently, there is no evidence in the literature that supports this theory.

Lastly, although these patients have deletions in the *SHANK3* gene, other mutations and potentially other deletions and or duplications for other genes on

other chromosomes may also exist in these patients. Indeed, our understanding of ASD genetics clearly indicates that no one gene can account for the disorder and that multiple deficits in gene function and/or expression converge to cause the disease. Therefore, it is entirely possible that there are unknown mutations or altered expression of other genes specifically in the male line that even with *SHANK3* rescue experiment which bought *SHANK3* to a "normal" expression level, is still not enough to compensate for this additional factor that could contribute towards the neurite morphology. Hence, we currently have no explanations for the failure of *SHANK3* to rescue the neurite morphology phenotype in the SHANK3 male patient line.

Since, I could only rescue the cell soma area and not the primary number of neurites in the SHANK3 male patient line, I further verified my results using genetically modified male es lines. The results indicated that neurons derived from both homozygous and heterozygous es *SHANK3* KO lines showed the same morphological deficits as neurons derived from the *SHANK3* iPSC patient lines. It was interesting to that both es SHANK3-/- and es SHANK3+/+ lines reacted similarly. A two way repeated measured ANOVA performed, with posthoc Bonferroni test revealed a significance of 1 between the two lines [Figure 4.2 C (ii)]. This suggested like the iPSC cells the es cells even the loss of one copy of SHANK3 is detrimental to the neuron.

One might have thought that the loss of two copies of *SHANK3* would lead to more devastating effects that the loss one of copy of *SHANK3*. This however was not the case as they es SHANK3-/- and es SHANK3+/- lines reacted similarly.

As mentioned in the discussion section of chapter 3 (section 3.3), Peca et al (2012) reported that neurons isolated from the striatum of *Shank3* knockout mice showed an increase in dendritic arborization and dendritic length. These mice also displayed behavioral abnormalities such as excessive/repetitive grooming which lead to skin lesions. Therefore, this study provides a link between cellular

phenotype and behavioral phenotypes, which relates back to ASD patients since restricted repetitive behavior is one of the core symptoms of this disorder. We have now shown that the loss of *SHANK3* in human neurons also leads to neurite outgrowth irregularities and by analogy with the mouse studies these defects could lead to the behavioral symptoms such as restricted repetitive behavior often observed in autism.

In section 4.3, we attempted to use growth factors as drugs to restore the organizational deficits of the *SHANK3* patient neurons. IGF1 and BDNF were not able to restore these deficits. Nonetheless, I have developed a stable platform that could be used for high content screening for a new class of drugs. These drugs would be capable of pharmacological amelioration of neuronal phenotypes for treatment or even early prevention of ASD. Also, this assay can be used as a forward chemical genetics approach, to find the possible mechanism behind the morphological deficits we see in our *SHANK3* patient neurons. For example, a small chemical compound library could be tested with this method on the control lines. If we find a compound which mimics the *SHANK3* patient morphogenetic phenotype then the chemical analysis of that compound could lead us to understand how *SHANK3* affects neuronal structure. Currently, these experiments are ongoing in our lab.

Therefore, experiments described in this chapter have established that loss of *SHANK3* causes a reduction in neuronal cell soma size and increases neurite outgrowth. In the next chapter pilot experiments are described that investigate the preliminary possible mechanisms behind these phenotypes and how they relate back to *SHANK3*.

Chapter 5: The effects of *SHANK3* haplo-insufficiency on neuronal development

Background

In the earlier chapters, we have established that *SHANK3* haplo-insufficiency causes morphogenetic deficits in neurons. Nonetheless, we still do not understand how the loss of *SHANK3* in patient lines causes these deficits. In this chapter, I describe some of the preliminary experiments that address the possible mechanism(s) by which these defects could arise; by altering actin polymerization and causing translational defects. After this, I look at later developmental stage of the neuron, when synaptic markers are being expressed. Specifically, the change in number of pre- and post-synaptic markers.

In the Introduction (section 1.5c), I discussed how SHANK3 binds to various actin-binding proteins such as Abp1, Abi1, Cortactin, Sharpin, SPIN90 and Alpha fodrin (Verpelli et al., 2011). These actin-binding proteins play an important functional role in the assembly and disassembly of actin filaments and also modulate their organization into higher order networks (Winder et al., 2005). For example, Abp1 co-localizes with F actin and binds with SHANK3 to regulate dendritic spine morphology (Haekel et al., 2008). Further, it is known that the actin cytoskeleton plays an essential role in many cellular processes such as cell division, cell migration and neuronal polarization (Cooper GM 2000). For instance, actin-depolymerizing drugs were applied to rat hippocampal neurons in culture, resulting in multiple axon formation. The neurons produced had lost their polarity (Bradke et al., 1999).

I therefore hypothesize that the loss of *SHANK3* in patient neurons could cause an imbalance in one or more of the actin binding proteins that it interacts with, disturbing the normal polymerization of actin filaments thus leading to an imbalance of Filamentous (F) actin (Globular (G) actin, since G actin polymerizes

to form F actin (Figure 5). This imbalance could create neurite growth alterations as observed in patient neurons and described in chapter 3 of this thesis.

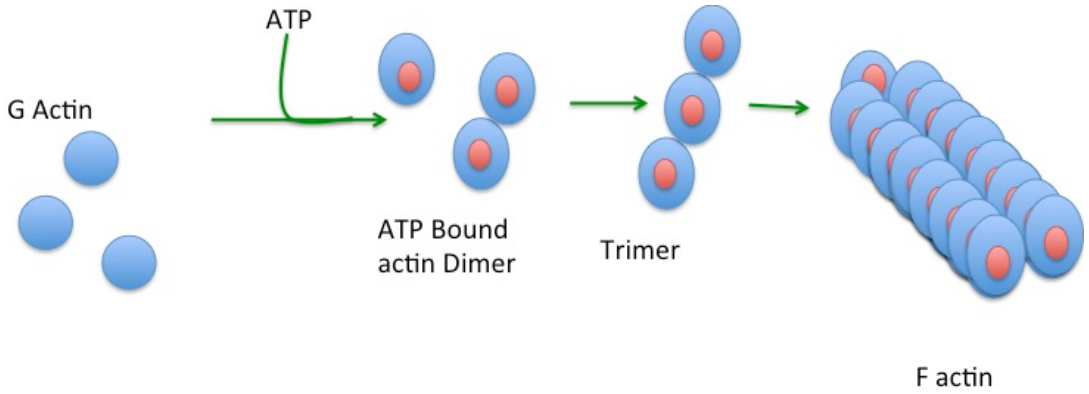

Figure 5: Polymerisation of G actin to form F actin: Diagram showing the conversion of G actin to F actin. G actin (Globular actin) when bound with an ATP can polymerize to form short oligomers (3 to 4 subunits). These oligomers then can act as stable seeds that elongates into F actin (Filamentous actin).

One of the hypotheses that has emerged from previous studies is that there could be enhanced translation in autism, which creates a chemical imbalance in the brain (Introduction section 1.3.3; Santini et al., 2012; Kelleher et al., 2008). For example, mutations in the genes TSC1 (Hamartin) and TSC2 (tuberin) are known monogenic causes of ASD. TSC1/2 inhibit the activity of mTORC1 (rapamycin sensitive mTOR raptor complex), which is downstream of PI3 kinase cascade. This cascade is involved in cellular growth (Kelleher et al., 2008). The mTORC1 activation is dependent on protein translation. Rodent studies have shown that the inactivation of TSC1/2 up regulates mTORC1 activity. This leads to an increase in protein translation. In the same studies they reported that the loss of TSC1/2 impacts neuron morphology, increased cell soma size and dendritic spines were seen (Meike et al., 2007; Tavazoie et al., 2005; Ehninger et al., 2008). Thus, suggesting that the loss of TSC1/2 function enhances translation in neurons, which causes an increase in cell soma size.

Following the reverse logic, in our *SHANK3* patient neurons we report that there is a decrease in cell soma area, we could postulate that there might be a decrease in protein translation which could cause this phenotype. To test this possibility I have used the SUnSET (surface sensing of translation) to quantify

and compare global protein synthesis in *SHANK3* patient and control lines (Section 5.2). This will indicate whether there are any protein translational deficits in the patient neurons that may contribute to cell size changes observed (Figure 3.2.2).

After assessing the preliminary mechanism behind the morphogenetic phenotype of *SHANK3* patient lines, I wanted to ask whether this early morphogenetic phenotype affected synaptic development. In section 5.3, I therefore explore the changes in the synaptic puncta in control versus *SHANK3*.

SHANK3 is among the first proteins to be expressed during the formation of the post-synaptic density (PSD). In the PSD, it helps anchor subcomplexes such as PSD95, Homer and GKAP (Grabruker et al., 2011; Boecker et. 2002; Hayashi et al., 2009; Carbonetto S 2013). SHANK3 has multiple functional domains, notably SH3, SAM, PDZ, ankyrin repeats and the proline rich domain (Jiang et al., 2013). The SAM domain has been known to help in synaptic localization and assembly of SHANK3 into multi-molecular sheets (Carbonetto S 2013). Metabotropic glutamate receptors (mGluR5) bind via homer which links back to the proline-rich domain of SHANK3 (Verpelli et al., 2011). NMDA and AMPA receptors bind via PSD95 and GKAP, which in turn bind to the PDZ domain of SHANK3 (Jiang et al., 2013). These interactions of SHANK3 with other PSD molecules suggests that SHANK3 plays an important role in bringing together signaling molecules into scaffolds which help in downstream receptor activation. For instance, the knockdown of *Shank3* in rat hippocampal neurons leads to the loss NMDA receptor hypofunction (Duffney et al., 2013).

Various mouse *Shank3* knockout studies have reported disruption in synaptic physiology and altered synaptic protein expression. For example, decreases in GluA1, Homer 1b/c, GKAP, GluN2A and SHANK2 have been reported (Bozdagi et al., 2010; Wang et al., 2011; Peca et al., 2011; Yang et al., 2012; Schmeisser et al., 201). The loss of these proteins resulted in reduction of AMPAR-mediated transmission; decreased mEPSC amplitude and frequency were also described

(Bozdagi et al., 2010; Wang et al., 2011; Peca et al., 2011; Yang et al., 2012; Schmeisser et al., 2012).

In section 5.3, I will describe experiments designed to understand how the loss of *SHANK3* in patient neurons may have an impact on the synapse by studying both control and *SHANK3* iPSC derived mature neurons at day 70 of neuralisation. We mainly focus our study on how the decrease in SHANK3 in the patient neurons contribute to change in presynaptic and postsynaptic puncta.

Therefore, this chapter describes how the *SHANK3* haplo-insufficiency in *SHANK3* patient neurons causes changes in actin modeling, protein translation and synaptic puncta.

5.1: Do the levels of F and G actin change in *SHANK3* patient neurons?

In the following experiment, I compare if the endogenous levels of G and F actin differ in *SHANK3* patient and control neurons. These different actin forms were detected using the fluorescent probes DnaseI (G actin) and Phalloidin (F actin) and the fluorescent intensity measured using high content screening (see Methods, Section 2.7). The fluorescence intensity was normalized to total number of nuclei. The experiments were carried out at day 30 of neuralisation (immature neurons), as it was at this stage of development that the morphogenetic phenotype first (day 30, figure 3.2.2) appeared in *SHANK3* patient neurons. I compared three control lines and two shank3 lines, these were the following: Control P3, Control P2 C2, Control P1 C2 were compared to SHANK3 P1 C2 and SHANK3 P2 C1.

As shown in Figure 5.1 (iii and iv), both the G actin and F actin fluorescence staining was significantly higher in control than in *SHANK3* neurons. For example, the normalized fluorescence intensity for DnaseI staining [G actin; figure 5.1 (I) and (ii)] for control was 0.25 ± 0.039, while for *SHANK3* it was 0.042 ± 0.004. Therefore, there is approximately six times higher G actin in control than in *SHANK3* neurons. Likewise, the normalised fluorescence intensity for Phalloidin staining (F actin) measured in control was 0.15 ± 0.018, while for *SHANK3* patient neurons was 0.070 ± 0.007. Hence, there is approximately two times higher F actin in control than in *SHANK3* neurons.

Thus, this suggested that both the amount of G and F actin was lower in the patient neurons at this stage of neuralisation.

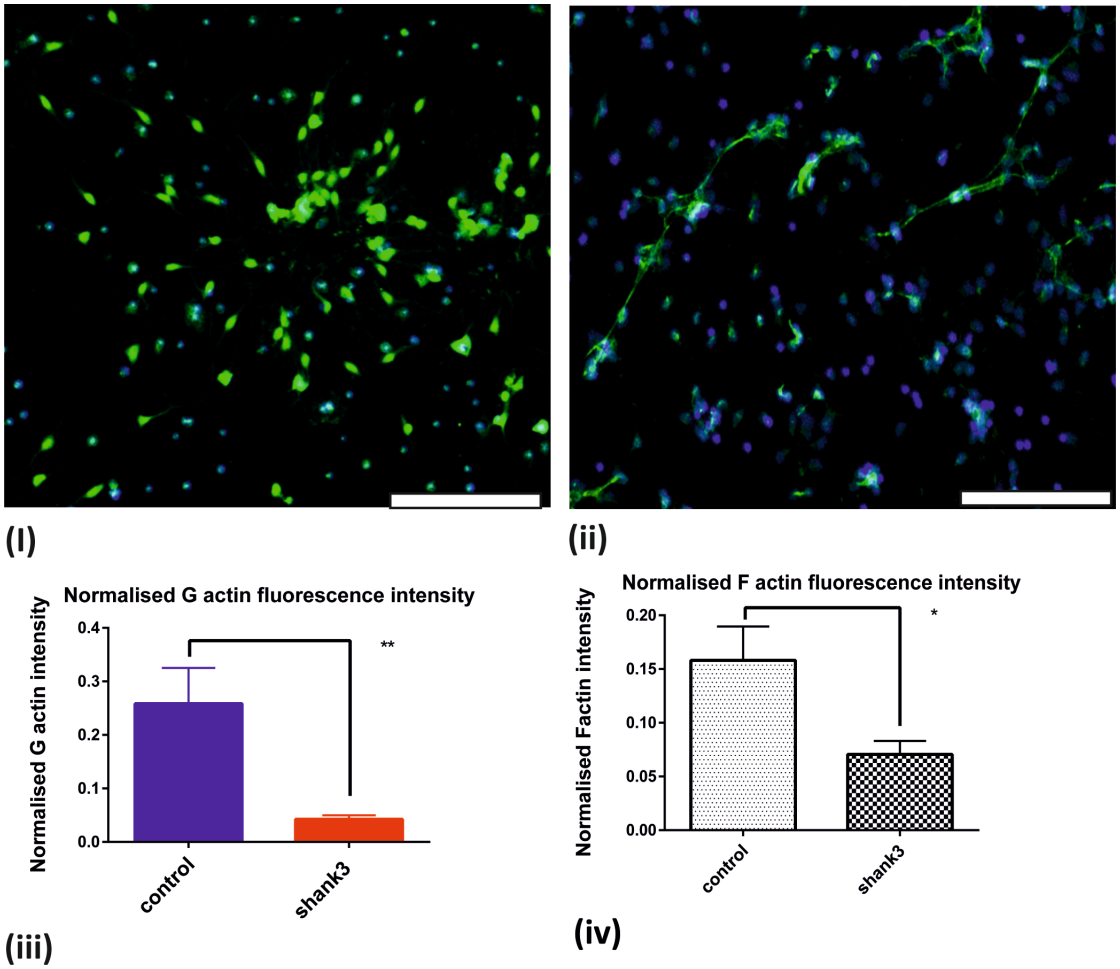

Figure 5.1: Levels of F and G actin in control and *SHANK3* neurons at day 30. (I) G actin staining in Control neurons, (ii) G actin staining in SHANK3 neurons, (iii) G actin fluorescence intensity normalized to the number of nuclei present, (iv) F actin (Phalloidin) fluorescence intensity normalized to the number of nuclei present. Data was collected from $13.5X10^3$ control neurons and $10.1X10^3$ SHANK3 neurons, from all 3 biological repeats for 3 control lines and 2 SHANK3 lines and presented as mean±SD. A significant decrease in both G-actin (**p= 0.0051) and F actin (*p= 0.011) .Scale bar in (i) and (ii) = 150 μm. Statistical analysis was carried out using unpaired student t test with Welch's correction. (Control neurons $n=13.5X10^3$ and SHANK3 neurons $n=10.1X10^3$, from 3 biological replicates. We compared 3 control lines with 2 SHANK3 lines). Please note the Phalloidin images could not be taken, as the microscope was broken.

5.2 Does global protein synthesis vary in *SHANK3* patient neurons?

We hypothesized that the smaller cell soma size observed in *SHANK3* neurons might be a protein translational deficit. To test this hypothesis, we performed a SUnSET assay (see Methods, Section 2.13) to compare the global protein synthesis in control and *SHANK3* neurons. The cell lines used in this assay were as follows: Control P1 C1, Control P2 C2 and Control P3 were compared to SHANK3 P1 C1, SHANK3 P2 C3 and ASD P1.

Briefly, puromycin was added to day 30 neurons for twenty minutes, when being a structural analogue of aminoacyl tRNAs it is incorporated into nascent polypeptide chains preventing their elongation (Nathan D 1969). The cells were then lysed and protein extracted for western blotting using a puromycin antibody. The amount of puromycin detected can then be used to determine the amount of translation occurring in the cells (Schmidt et al., 2009).

Figure 5.2 A, shows the amount of total protein synthesized from three control and two *SHANK3* lines. Equal amount of protein was added to each lane that was 15μg. This was measured using the BCA Assay as described in methods section 2.14. This was replicated three times and total protein intensity measured from the western blot was normalized to the acetylated tubulin commonly found in neurons. The analysis revealed that there were no differences in protein synthesis between the control and the *SHANK3* neurons (Figure 5.2 A and B; actual intensity values are given in Table 5.1).

Puromycin expression intensity/Alpha tubulin expression intensity	**Control mean±SEM**	**SHANK3 mean±SEM**
control vs. shank3	1.517 ± 0.2359	1.474 ± 0.1906
control vs. ASD	1.517 ± 0.2359	1.011 ± 0.2259

Table 5.1: Protein translational changes. The table describes the mean±SEM for puromycin expression intensity normalised to alpha tubulin expression intensity. We compared 3 control lines with 2 SHANK3 lines. We compared 3 control lines with 1 sporadic ASD line.

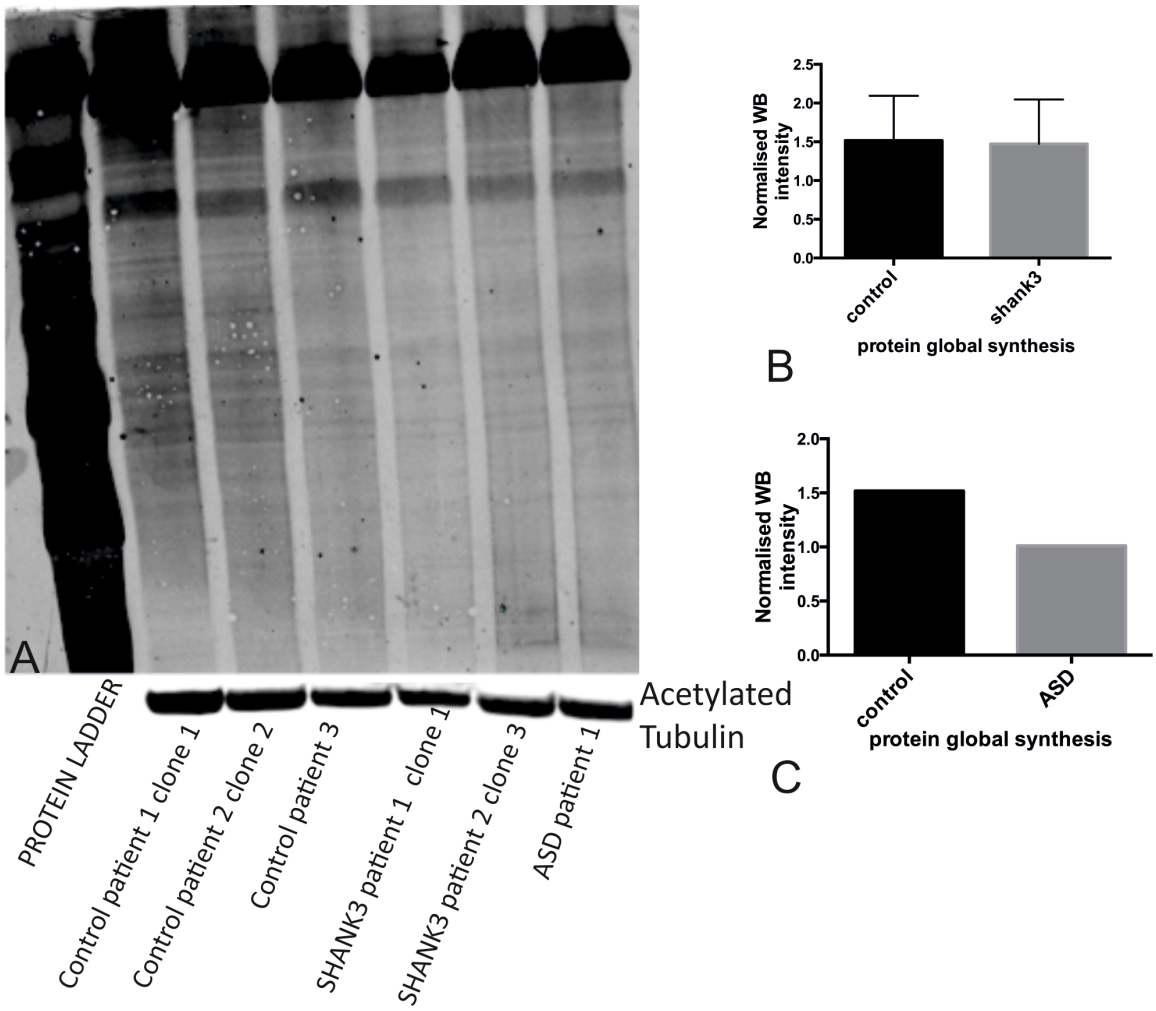

Figure 5.2: Protein translational changes in day 30 neurons. A. Western blot for puromycin and alpha tubulin carried out on lysates from control, *SHANK3* neurons and from neurons generated from a sporadic ASD line at day 30 of neuralisation. B. Puromycin expression intensity normalised to acetylated tubulin expression intensity for control vs. *SHANK3*. C. Puromycin expression intensity normalised to alpha tubulin expression intensity for control vs. ASD.
Control lines, n = 3; *SHANK3* lines, n=2; sporadic ASD line, n=1. Data represented as mean±SD. p=0.888 (B) (Unpaired student-t test with Welch's correction).

I also compared protein synthesis in our sporadic ASD patient neurons (Figure 5.2 C, actual intensity values are given in Table 5.2). This was done because in section 5.4 of this thesis, I reported that the cell soma size of the neurons generated from the sporadic ASD line was smaller than those of control neurons (see Figure 5.4). Therefore, I also wanted to investigate whether changes in global protein synthesis might explain this phenotype. A decrease in protein synthesis was observed sporadic ASD patient neurons compared to control neurons, but the significance of this result could not be determined since statistical analysis could not be performed as we have only one sporadic ASD patient line.

5.3: Are there changes in the number synaptic puncta in *SHANK3* patient neurons?

As a first step towards investigating whether the morphogenetic deficits observed in early in development in *SHANK3* patient neurons affect synaptic development, I compared the expression synaptic markers in 70 day-old neurons for both control and *SHANK3* patient neurons. I used three control lines and two shank3 lines, these were the following: Control P3, Control P2 C2, Control P1 C2 were compared to SHANK3 P1 C2 and SHANK3 P2 C1.

Synaptophysin, an integral membrane glycoprotein that occurs in presynaptic vesicles at excitatory synapses (Meittinen 1987) was used as a pre-synaptic marker (Figure 5.3A). As a post-synaptic marker, I used Homer1 which is a known postsynaptic density protein involved in the targeting glutamate receptors (Figure 5.3B). Also, SHANK3's proline rich domain binds to Homer1, which in turn binds mGLuR1 and mGLuR5 (Metabotropic glutamate receptor 1 and 5; see Introduction section 1.5b). To quantify expression, I used confocal imaging to count the number of pre- and post-synaptic puncta present per 50μm of neurite (Figure 5.3C).

There was an increase in the synaptophysin and Homer1 puncta in the control as compared to *SHANK3* patient neurons [Figure 5.3 C (I) and (ii)]. The average synpatophysin puncta per 50µm of neurite for control was 208.4 ± 13.98 while for SHANK3 it was 94.69 ± 6.698. This suggest that there are twice the number of presynaptic marker for control than *SHANK3*. Similarly, the average Homer1 puncta per 50µm of neurite for control was 180.3 ± 10.89 on the other hand for *SHANK3*, it was 70.61 ± 5.955. This suggests that there twice the amount Homer1 present in control than the *SHANK3* neurons. Thus, there were significant differences were found in expression of both pre- and post- synaptic markers (Figure 5.3C).

This leads us to the conclusion that *SHANK3* patient neurons show deficits in both pre and postsynaptic number.

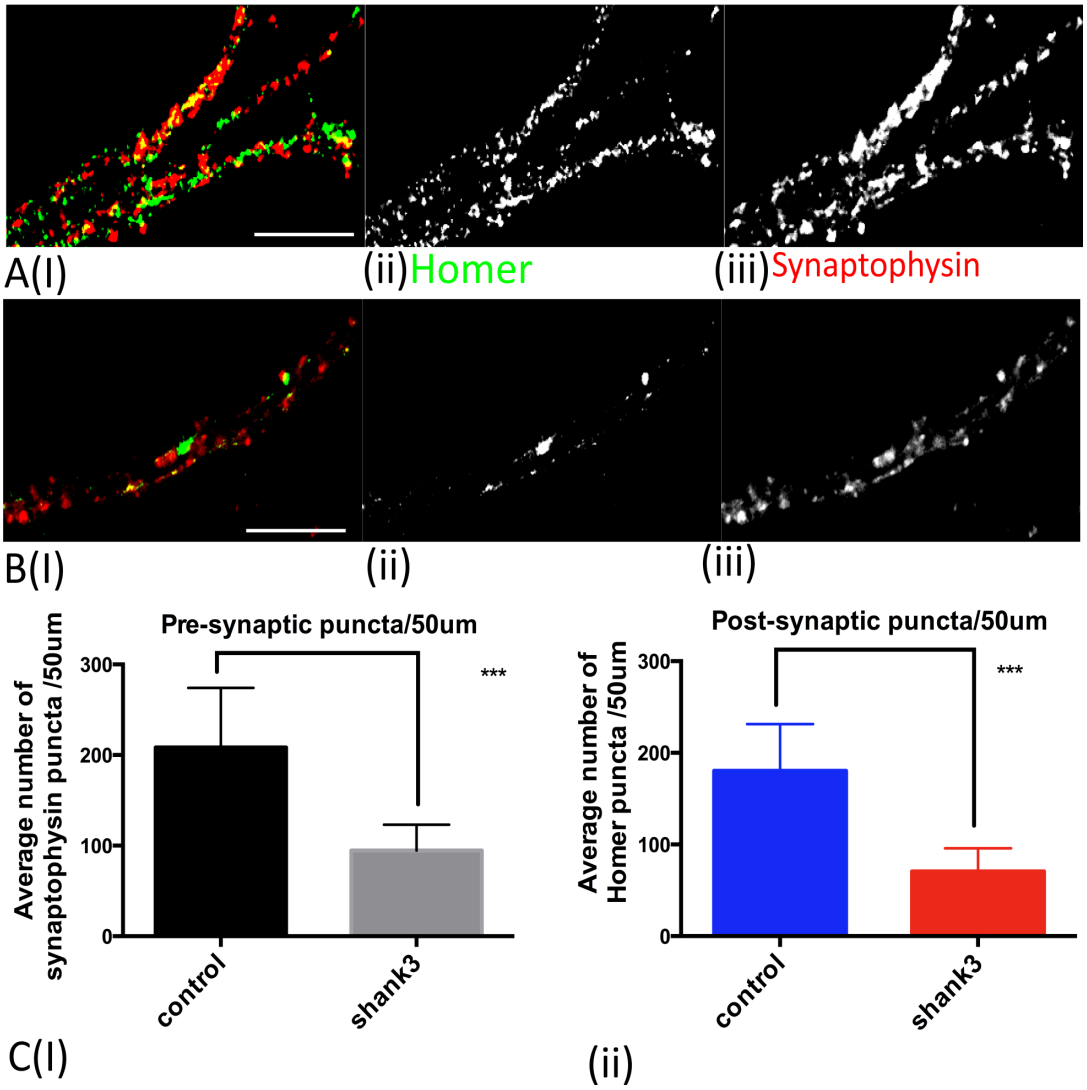

Figure 5.3: Changes in the number of synaptic puncta in day 70 neurons: A, Day 70 control neurons stained with Synaptophysin (Presynaptic marker) and Homer1 (Postsynaptic marker). B (I) Day 70 SHANK3 neuron stained with Synaptophysin (Presynaptic marker) and Homer (Postsynaptic marker). C(I) The average number of Synpatophysin puncta per 50µm, (ii) The average number of Homer1 puncta per 50µm. Significant differences in expression of both Synaptophysin and Homer1 were found ***p<0.001 (Unpaired student t test with Welch's correction). Data is expressed as mean±SD, A, B, Scale bar=10µm. We compared 4 control lines with 4 SHANK3 lines; 2 control lines with two clonal replicates and 2 SHANK3 lines with one clonal replicate of each. (Control neurons n=46; SHANK3 neurons n=41, from 3 biological replicates).

5.4: Cell soma changes in sporadic ASD patients

Recently, in our lab we generated one sporadic ASD patient iPSC line. I therefore wanted to test this sporadic ASD generated neurons that had similar morphogenetic phenotypes to the *SHANK3* patient neurons. This will allow help determine if there are any common cellular mechanisms that contribute to the symptoms of ASD seen in both the genetic and sporadic form.

I used high content screening to assess the number of primary neurites and cell soma area at day 27 and 30 of neuralisation. I compared three control lines to two sporadic ASD lines derived from one patient. These were the following: Control P1 C1, Control P2 C2, and Control P1 C2 were compared to ASD P1 and ASD P1 C2. This analysis showed that there were no differences in the number of primary neurites between the control and ASD [Figure 5.4 (iii)], yet, there was a decrease in the cell soma area in the ASD patient lines (Figure 5.4 i, ii). In figure 5.4(I), the cumulative frequency distribution graphs show that there is no difference between control and ASD at day 27. At day 30, the ASD distribution remains the same whereas the control neuron cell soma area distribution expands up to 600μm^2 [Figure 5.4 (ii)]. This suggests that there might be some cell soma deficits in the sporadic ASD patients.

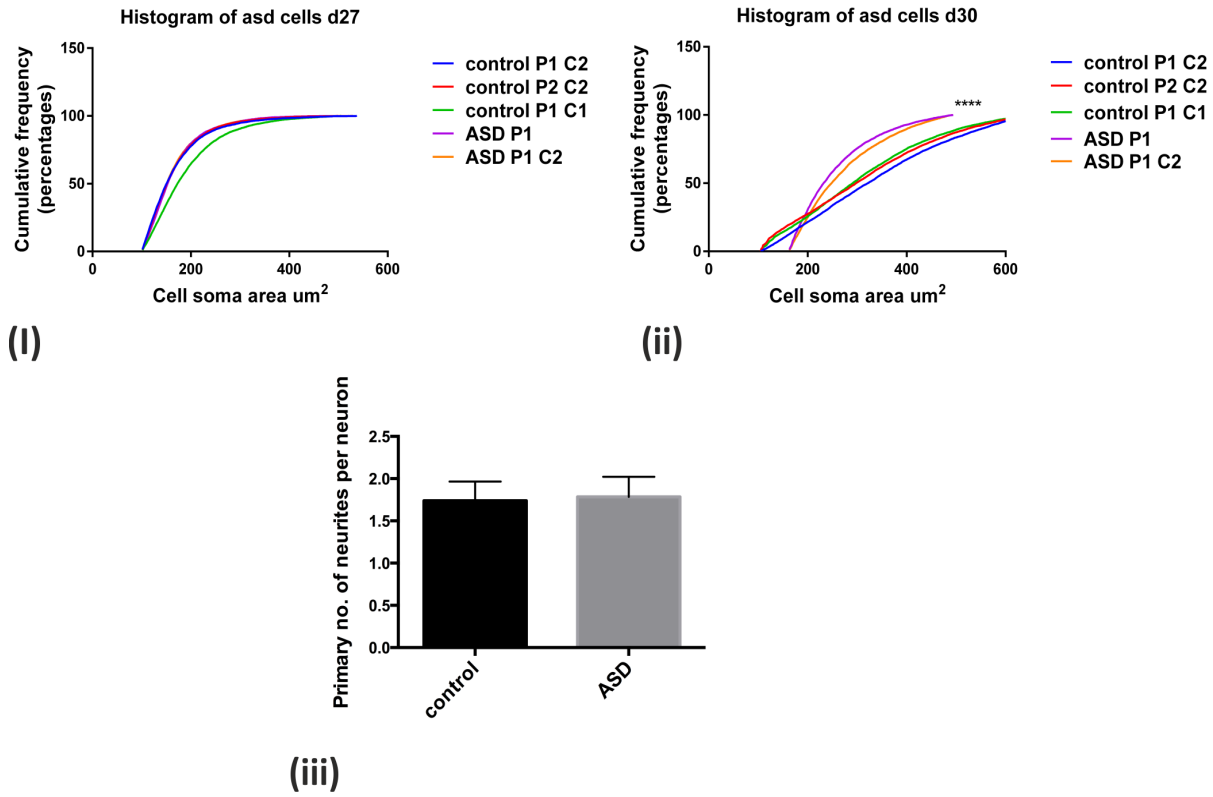

Figure 5.4: Change in cell soma area in sporadic ASD patient neurons: (I) Cumulative frequency distribution of cell soma area at day 27. (ii) Cumulative frequency distribution of cell soma area at day 30. (iii) Primary number of neurites per neuron at day30 control versus ASD. We performed 3 biological replicates. We compared 3 control lines with 2 ASD lines. The 2 ASD lines were clones from the same patient.

5.5 Discussion

In this chapter, we discovered that the *SHANK3* haplo-insufficiency in *SHANK3* patient neurons causes actin changes, such as loss F and G actin. Nonetheless, SHANK3 deficiency in patient neurons did not induce any protein translational deficits. In the next assay I tried to understand how change in morphology impacts synaptic development. I measured the number of synaptic puncta at day 70 of neuralisation. It was shown that the *SHANK3* patient neurons have lesser pre and postsynaptic puncta.

Lastly, we tested a sporadic ASD line to see if it showed any morphogenetic deficits as in *SHANK3* patient neurons. We found a decrease in cell soma area in the sporadic ASD patient line. This suggested that a smaller cell body could be thought of as a global cellular phenotype of ASD.

5.5 (a): Association of actin to SHANK3

In the introduction section 1.5c of this thesis, we described that SHANK3 played a dynamic role in cytoskeleton modeling. It does this by either binding to actin directly or indirectly through various actin-binding proteins. For instance, SHANK3 binds to IRSp53 (the insulin receptor substrate of 53kDa) via proline rich domain and PDZ domain (Kreienkamp 2008). F actin is modulated through IRSp53 in the dendrites through the WAVE2 complex (Choi et al., 2005). Therefore, we measured the levels of actin in our *SHANK3* patient neurons to understand how it relates to the increased number of primary neurites, as shown in the *SHANK3* patient neurons. Both G and F actin were increased in control neurons as compared to *SHANK3* patient neurons at day 30. Since the amount of G actin is lower in *SHANK3*, it stands to reason that there would be less F actin, as G actin polymerizes to form F actin (Figure 5; Lodish Harvey et al., 2000).

A previous study by Durand et al (2012) has linked alterations in F actin levels with alterations in *SHANK3* expression. They studied the effects of *SHANK3*

overexpression on spine morphology in rat hippocampal neurons. The study showed an increased spine density and, not only did the F actin co-localize with *SHANK3* in the spines but also there was an increase in its levels. Moreover, the increase in *SHANK3* expression caused increase in the width of spines. This suggested an actin dependent mechanism for spine growth and enlargement.

Two *de novo* human *SHANK3* mutations (R12C and R3000C) were modeled in rodent hippocampal and cerebellar neurons (Durand et al 2012; Grabrucker et al., 2011). Both mutations showed a decrease in spines, which were then associated with a decrease in F actin. Furthermore, the frequency of mEPSCs (spontaneous excitatory post synaptic current) was decreased in these mutations. A network of both long and short F actin filaments is present in the dendritic spine underneath the PSD. Its function is to stabilize postsynaptic proteins and modulate spine head in response to synaptic signaling (Hotulainen, Pirta et al., 2010; Honkura et al., 2008; Kuni T et al., 2006). Thus, the authors proposed that the loss of *SHANK3* causes loss of dendritic spines due to a decrease in F actin. This disrupts the spine's ability to respond to postsynaptic signaling, which leads to aberrant electrophysiological changes that might underpin the behavioral symptoms of ASD.

F actin staining has also been performed on various brain regions from *Shank3* deficient mice. A significant decrease in F actin staining was observed in the prefrontal cortex and hippocampus (Duffney L et al., 2015). Similarly, we report that *SHANK3* patient hypothalamic neurons at day 30 show a decrease in F and G actin.

In addition, the *Shank3* deficient mice also showed social impairment and excessive self-grooming, both hallmarks of ASD, along with reduced NMDAR-EPSCs in the prefrontal cortex (Duffney L et al., 2015). Alterations in NMDAR function are thought to be the underlying cause of these social deficits (Won et al., 2012; Duffney L et al., 2013; Duffney L et al., 2015). Several studies have

reported that *SHANK3* connects to NMDARs using actin cytoskeleton (Duffney L et al., 2013; Rycroft et al., 2004; Michailidis et al., 2007). Increased actin depolymerization leads to the loss of F actin that causes the disruption NMDAR membrane delivery leading to fewer NMDAR receptors (Rosenmund et al., 1997; Duffney L et al., 2013). This implies that *SHANK3* deficiency causes a decrease in F actin, which leads to hypofunction of NMDARs that in turn might triggers social deficits. As it has been reported that drugs acting on various NMDAR sites enhance its function and lead to significant recovery of social deficits in *SHANK2* mutant mice and other ASD animal models (Won et al., 2012; Moskal et al.,2011).

Moreover, combined biochemical and molecular studies of SHANK3 have described many actin-binding partners such as SPIN90, profilin1 and 2, Mena, βpix, αfodrin, SPAR and Sharpin (Verpelli C et al., 2012; Han Kihoon et al., 2013). For example, Arp2/3 (Actin-related protein 2/3 complex) mediates the nucleation of actin filaments to form branches (Krause M et al., 2014). SPIN90 a known binder of SHANK3 activates Arp2/3 without preformed F actin filaments (Nolen Brad 2015). SPIN90 and Arp2/3 complex together initiate lamellopodia formation, which is the basis of neurite outgrowth (Kim DJ et al., 2006). Therefore, it is highly possible that the loss of *SHANK3* might interrupt SPIN90, which can result in the neurite outgrowth deficits that have been reported in previous chapters (I discuss other possible mechanisms in depth in Chapter 6, the general discussion part of the thesis).

Taken together the rodent studies above support our culture experiments on *SHANK3* patient hypothalamic neurons, where we also saw a significant decrease in F actin and G actin. Thus, we can hypothesize that the deficiency of *SHANK3* in *SHANK3* patient neurons leads to a decrease in G and F actin, which could result in neurite outgrowth deficits and be the foundation of synaptic dysfunction.

5.5 (b): Global protein synthesis is not altered in *SHANK3* patient neurons

No global protein translational deficits seen in *SHANK3* patient neurons suggesting that, at this stage of neuronal development, *SHANK3* does not play a role in protein translation. Indeed, previous studies have suggested an increase in protein translation in autism, particularly at the synapse (Kelleher et al., 2008). However, it is worth noting that our analysis was carried at a stage of neuronal development long before neurons are synaptically active. Preliminary data for the sporadic ASD line does show a decrease in protein translation rather than an increase, although this result will need to be confirmed by analyzing additional lines.

5.5 (c): Synaptic changes associated with *SHANK3* patient neurons

At later stages of development (day 70), the *SHANK3* patient neurons show a reduced number of synaptic punctas. I observed a decrease in synaptophysin (pre-synaptic) and Homer1 (post synaptic marker) as shown in figure 5.3.

A similar occurrence has been reported in patients with Phelan McDermid Syndrome (PMDS). PMDS is a global developmental delay disorder, commonly known as 22q13 deletion syndrome. This region of the chromosome includes the gene *SHANK3* and, as might be expected, most PMDS patients have autism (Shcheaglovitiv et al., 2013). A study on neurons generated from PMDS iPSCs revealed that these cells have a decrease in number of synaptic punctas of Homer1 and Synapsin (Shcheaglovitiv et al., 2013). Synapsin is found in the presynaptic vesicles of excitatory synapses and Homer1 is found at the postsynaptic terminal. Hence, both pre and post-excitatory synaptic markers were reduced indicating that there were fewer excitatory synapses in PMDS neurons. The spontaneous EPSCs were also measured in these neurons and both their frequency and amplitude were found to be significantly reduced relative to controls (Shcheaglovitiv et al., 2013). The impairment of excitatory synaptic

transmission in PMDS neurons is linked to lesser number of synapses. If there are lesser number of presynaptic punctas, there will be a lesser release of neurotransmitter which would result in lesser receptor binding in the plasma membrane of the post synaptic terminal. No secondary pathways would activate to initiate excitatory response. Thus, leading to an impaired synaptic transmission.

Furthermore, this can also be connected to the “synaptic hypothesis” as the underlying mechanism of autism (Introduction, Section 1.3.1), which suggests that a decrease in synaptic number causes synaptic dysfunction, which leads to autistic symptoms.

Many rodent studies of *Shank3* KO have also reported electrophysiological disruptions, such as reduction in amplitude and frequency of EPSCs, paired pulse ratio, fiber volley and population spikes in hippocampal neurons (Jiang et al., 2013). However, in striatal *Shank3* KO rodent neurons only EPSCs were affected and not the paired pulse ratio. This suggested that different regions of the brain may respond differently to the loss of *Shank3* (Peca et al., 2012). In addition to the synaptic phenotype, *Shank3* KO rodents also exhibit autism like behavior such as social reclusiveness and repetitive behavior in terms of excessive social grooming. The conclusion we can draw is that the loss of *Shank3* disrupts synaptic transmission and this leads to autistic symptoms.

In the introduction (1.3.2), I proposed that that the fundamental cellular mechanism behind autism is abnormal cellular growth, and this causes synaptic dysfunction, which leads to symptoms of autism. For instance, Peca et al. (2012) described increased dendritic length and arborization of striatal neurons in *Shank3* KO mice. The same neurons also revealed decrease in frequency and amplitude of mEPSC. Moreover, these *Shank3* KO mice displayed autistic behavior like excessive self-injurious and grooming behavior. Therefore,

establishing a pattern, where aberrant neuronal structure leads to changes in synaptic transmission, which could cause autistic behavior.

Similarly, in our study, the decrease in Homer1 and Synaptophysin could indicate that *SHANK3* patient hypothalamic neurons have significantly fewer excitatory synapses than controls. These could lead to electrophysiological deficits. Therefore, in our *SHANK3* patient neurons, the hypothesis is that *SHANK3* haplo-insufficiency causes morphogenetic deficits leading to changes in both the number and expression of synaptic markers. These could affect synaptic transmission, which could produce autistic symptoms.

In conclusion, published data and the data presented in this chapter suggest that loss of *SHANK3* results in abnormal neuronal structure that causes synaptic dysfunction, which leads to behavioral changes.

5.5 (d): Decrease in cell soma area a global ASD phenotype

In the *SHANK3* patient neurons we reported a decrease in cell soma area (Chapter 3, section 3.2). Similarly, we tested whether the sporadic ASD line showed a similar morphogenetic deficit. During our analysis we found that the sporadic ASD line also shows a decrease in cell soma area (Figure 5.4).

Recently, a study characterized the volume of neuronal nucleus and cytoplasm of autistic subjects in sixteen different brain regions (Wegiel et al., 2015). Post mortem tissue was obtained and analyzed. In this study, they not only examined tissue from early childhood, but also studied tissue from autistic adolescents and autistic adults. They observed the following pattern of nuclear and cytoplasmic changes. First, severe volume deficits were reported in both the nucleus and cytoplasm. These deficits were shown in thirteen out of the sixteen brain regions that were examined. Second, all these deficits were reported in early childhood from the ages of four to eight. Thus, suggesting developmental abnormalities begin before the age of three. Third, there was a significant increase in the

volumes of both the cytoplasm and nucleus during adolescence (11 to 23 ages) in eleven of the sixteen brain regions examined. This increase in nuclear and cytoplasm volume bought it closer to the level of control samples. No volumetric changes were observed in controls throught the various stages of development. In addition, no volume modifications were reported in adult autistic brains (Wegiel et al., 2015). Therefore, this indicates that the ASD patient nucleus and cell soma takes longer to develop, as the initial volume was smaller during early childhood and then increased to normal levels at later stages of adolescents. Also, these volumetric changes in neuronal soma were correlated with changes in chromatin organization, which impacts neuronal development and maturation.

Thus, these observations suggest that in people suffering from autism neurons fail to develop normally and if the neurons don't mature properly they are bound to have functional deficits, which could lead to autism (Wegiel et al., 2015).

Another interesting fact found in the Wegiel et al (2015) study was the size of the neurons. If we make the assumption that the neuron cell soma is a sphere and convert these cytoplasmic volumes into area, the area ranges from 112μm^2 to 600 μm^2 for the control cohort (ages 4-8) and for the ASD cohort the area was from 87μm^2 to 477μm^2. Similarly, in our study of iPSC generated neurons I reported the following cell soma area ranges: for control cohort 105μm^2 to 600μm^2, for the sporadic ASD patient 163μm^2 to 492μm^2 and for the *SHANK3* patient neurons 103μm^2 to 476μm^2. Not only do these findings validate our data but also suggest a common cellular mechanism that effects the development of the cell body of a neuron.

An additional study of human neural progenitor cells originating from the fetal cerebral cortex was reported. The exposure of these cells to the serum of a 3 year old autistic donors. This increased the percentage of small sized neurons (Mazur-Kolecka et al., 2007). Hence, suggesting that neuronal size deficits occur in autistic children and begin from early development.

Co-morbid studies of autism like Rett's syndrome and Fragile X syndrome have also reported cell soma size deficits (Brennand et al., 2012). Similarly, our study has shown a decrease cell soma area in both sporadic ASD and *SHANK3* patient neurons.

Taking all of these studies into account, a decrease in cell soma area could be thought of as a global cellular phenotype of ASD. Having said that, we still need to confirm this phenotype in multiple sporadic ASD lines, as our data is only from one individual.

In conclusion, I have described pilot experiments that could provide us with a possible mechanism on how the morphogenetic deficits occur in the *SHANK3* patient neurons. The neurite outgrowth deficits in the *SHANK3* patient neurons could be linked to the loss of F and G actin, which involves a SHANK3-actin-binding, mediated mechanism. We also found out that the morphogenetic deficits in the *SHANK3* patient neurons could contribute to synaptic development. As I reported a decrease in pre and postsynaptic number; this could have an implication in normal synaptic transmission, which could lead to autistic behavioral changes. Finally, the decrease in cell soma area in the sporadic ASD line shows a global ASD phenotype. This insinuates a common cellular mechanism that contributes to the symptoms of ASD, seen in both the genetic and sporadic form.

Chapter 6
General Discussion

In this thesis, I described experiments showing that *SHANK3* patient hypothalamic neurons show morphogenetic deficits early in development and these can be rescued by enhancing the *SHANK3* expression. Later in development, these neurons also exhibit synaptic deficits, such as a decrease in pre and postsynaptic density. This also has been reported previously in Phelan McDermid Syndrome iPSC generated neurons (Shcheglovitov et al., 2014)
Neurons generated from sporadic ASD iPSCs were also observed to have a smaller soma size when compared with control neurons, raising the possibility that this soma size change could be a global ASD phenotype.

Reduced expression of *SHANK3* expression causes the morphogenetic changes as mentioned above, therefore in order to develop effective treatments, it is important to understand the mechanisms by which these defects arise.
The first four sections of this chapter 6, will discuss the possible mechanisms behind the morphogenetic phenotypes as observed in *SHANK3* patient neurons. The last section will discuss the possible translational research approaches.

6.1: How can *SHANK3* influence neurite outgrowth?

Dynamic re-arrangement of cytoskeletal components is essential for the process of neurite outgrowth (Yuh Nung et al., 2010). As described in the introduction (Section 1.5), the SHANK3/PROSAP2 protein has various binding partners. Some of these include actin cytoskeletal proteins. Recently, gene ontology and pathway analysis in rodents have suggested that regulation of actin cytoskeleton is the principal role of the Shank3 protein (Han et al., 2013). Actin cytoskeleton is important for maintaining the cell's shape and function. Moreover, overexpression of *Shank3* in cultured mouse hippocampal neurons showed that Shank3

localized to the growth cones, suggesting that it might participate in neurite extension (Durand et al., 2012).

Through immunoprecipitation and yeast two-hybrid screening, SHANK3 has been found to interact directly with two subunits of the Arp2/3 complex (Actin-Related Proteins ARP2 and ARP3), namely ARPC2 and ARPC5L (K. Han et al., 2013). The Arp2/3 complex consists of seven subunits that initiate nucleation and branching of F actin. This helps form neurites in neurons (Campellone KG et al., 2010).

It was shown in a rodent model of *Shank3* duplication that ARPC2 binds with SHANK3, which would suggest that SHANK3 could act as a scaffold that brings WASF1, cortactin and ARPC2 to facilitate actin rearrangement (Figure 6.1; K.Han et al., 2013; Proepper C et al., 2007; Naisbitt S et al., 1999). As we know, actin plays a major role in many important cellular processes, including, cell signaling, cell motility, cell division, organelle and vesicle movement, and the establishment of cell junctions and cell shape (Doherty, Gary J et al., 2008). Therefore, one could explore the various aspects of this scaffold in order to understand the role of Arp2/3 complex in neurite outgrowth. In particular, does this SHANK3 –cortactin-WASF1-Arp2/3 complex exist in human neurons? Also, how does it impact actin re-arrangement in *SHANK3* patient versus control neurons and does it contribute to the phenotype I see in our cells? To answer such questions, we could assess gene and protein expression (for cortactin, WASF1 and Arp2/3) using real time PCR and western blots, followed by assessing the binding of this complex via immunoprecipitation in both control and SHANK3 neurons. This could point us in the direction of the mechanism behind the neurite changes I saw in *SHANK3* patient neurons.

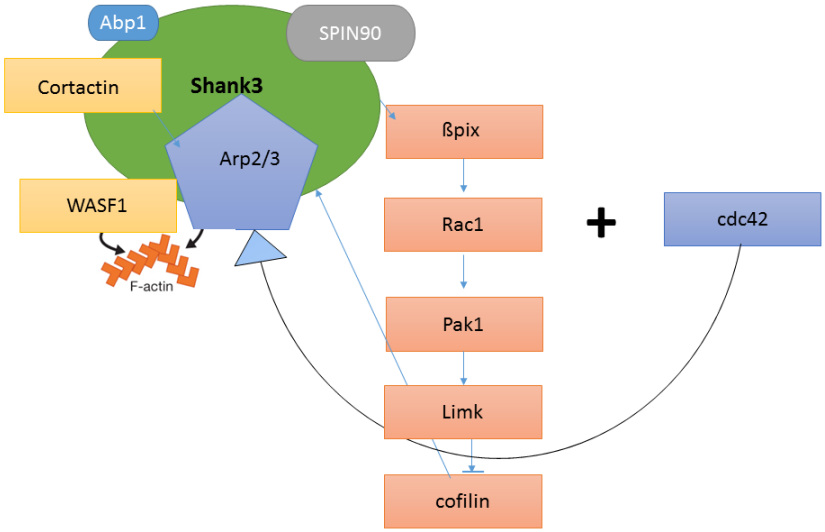

Figure 6.1: Proposed mechanism of SHANK3 in actin regulation: The Diagram above illustrates the various SHANK3 interactions with other proteins which help regulate F actin. SHANK3 binds to ßpix which binds Rac1, Pak1 and activates Limk which inhibits cofilin, cofilin causes disassembles actin filaments. The disassembled actin can be used by the Arp2/3 complex to make new branches (Duffney L et al., 2015).

Two key players in actin dynamics are Rac1 (Ras-Related C3 Botulinum Toxin Substrate 1) and Cdc42 (Cell division control protein 42 homolog). They act as coordinators in neurite outgrowth, spine development, dendrite initiation, elongation and branching complexity (Duffney L et al., 2013). It has been shown that βPIX, the guanine nucleotide exchange factor for Rac1 coupled with PAK, interacts with *SHANK3* at the synapse (Manser et al., 1998; Park et al., 2003). A recent study indicated that *Shank3*-deficent mice exhibit a decrease in the levels of βPIX and that this, in turn, leads to a decrease in Rac1 activity. This further resulted in a decrease in the levels of downstream targets such as PAK1/2/3 [(P21 Protein (Cdc42/Rac)-Activated Kinase 1)] and LIMK (LIM Domain Kinase 1). A key downstream target of PAK1/2/3 and LIMK is cofilin, an actin-depolymerizing factor that is inactivated when phosphorylated by LIMK at Serine3 (Bamburg et al., 1999; Duffney L et al., 2013;Duffney L et al., 2015. So when levels of LIMK decrease, more cofilin remains in the active state resulting

in increased depolymerisation of actin (Figure 6.1). Duffney L et al., 2015 showed that *Shank3* deficient mice had decreased levels of F actin and behavioral deficits. They found that this was due to a decrease in *SHANK3*, which cause a decrease in the expression Rac1-PAK1-LIMK pathway. This all lead to an increase in cofilin. So, they used an endogenous inhibitor of cofilin (Ser3-phosphorylated cofilin to stabilize actin filaments. This stabilized F actin and rescued the behavioral deficits reported in *Shank3* deficient mice (Duffney L et al., 2015).

The next question that arises is: how does this link back to the increased number of primary neurites I see in our *SHANK3* patient cell lines? To answer this question, we would first need to understand the mechanism behind how Arp2/3 complex modulates actin to forms branches.

In chapter 5, I discussed that G actin polymerizes into F actin (Figure 5). The F actin has two ends pointed and barbed. The barbed end grows faster than the pointed end. Three G actin monomers are associated together in order to generate F actin filament. This process is called nucleation, and the actin filament generated is known as a primer (Krause M et al., 2014; Achard, V. et al., 2010). The role of Arp2/3 complex in generating branches is as follows, when activated the Arp2/3 complex binds to preexisting actin filament (primer), and undergoes a conformational changes. The conformational change is such that it mimics the barbed end of the F actin filament, from which an actin filament (primer) can be elongated (Figure 6.2 A). Elongation of actin filaments (primer) is the addition of monomeric form of G actin at the barbed end. The new actin filament generated through this process is anchored via the pointed end to preexisting actin filament. Thus, the Arp2/3 complex can create actin branch networks (Krause M et al., 2014). The elongation process can be blocked by capping proteins. However, elongation can be enhanced with the help of elongation proteins such as ENA/VASP and Formin (Krause M et al., 2014).

As described above, the Arp2/3 complex binds to the side of pre-existing F actin filaments called primers. This causes it to undergo conformational changes to elongate actin filaments to (Polland TD 2007; Krause M et al., 2014). There are currently three proposed mechanisms suggested for Arp2/3 that cause the elongation of actin filaments (primers) into branches. These are shown in Figure 6.2B. For the purpose of this discussion, I am mainly concentrating on the cofilin pathway as it links back to *SHANK3*.

In the cofilin-mediated pathway, cofilin severs the actin filaments, which generates more actin filaments or primers. These uncapped filaments are elongated by the Arp2/3 complex. This process helps forms neurites (Ichetovkin I et al., 2002; Chen Q et al., 2013; Krause M et al., 2014). Indeed, in the brains of cofilin knock out mice, drastic cortical hypoplasia and ventricle expansion is observed. Morphologically, phenotypes such as reduced axonal tract formation, irregular neuronal migration and complete ablation of neurite processes were also reported (Flynn et al., 2012).

I have already discussed how lack of *SHANK3* results in an increase in activation of cofilin. Therefore, I can postulate that this causes increased severing of F actin filaments that could then be elongated via the Arp2/3 complex, leading to increase in the number of neurites I see in our patient neurons. To confirm this, cofilin inhibitors could be added to *SHANK3* patient neurons, more cofilin would be inhibited leading to fewer neurites. This would be detected using immunocytochemistry via high content imaging.

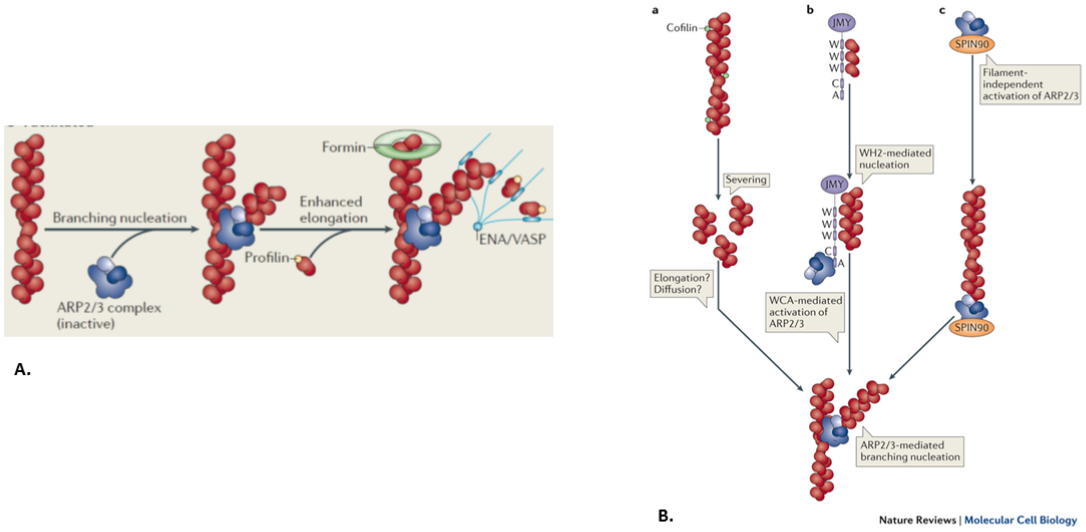

Figure 6.2: Priming of Arp2/3 complex leading to elongation. A. Shows the Arp2/3 conformational change leading to elongation, creating new branches. B. The diagram above explains the three possible mechanisms through which Arp2/3 forms new branches .Adapted from Krause M et al., 2014.

Another protein that links *SHANK3* (Figure 6.1) to actin complex is Abp1 (Haeckel A et al., 2008). Abp1 binds to SHANK3 and helps the Apr2/3 complex elongation. Both cortactin and Abp1 play a role in neurite outgrowth. It has been shown that the depletion of Abp1 results in increased axonal length during the early stages of development in rodents (Pinoyl R et al., 2007; Hering H et al., 2003). Since SHANK3 binds to Abp1, we could consider that the decrease of *SHANK3* in patient neurons would lead to a decrease in Abp1, which would increase neurite length. Again, to fully consider this as an explanation, we verify the interaction between SHANK3 and Abp1 in hiPSC-generated neurons via co-immunoprecipitation. I could then increase the expression of Abp1 using a genetic construct like I did for *SHANK3* (Chapter4; Figure 4.0) and see whether this recues the neurite outgrowth phenotype.

Densin -180 binds to the SH3 domain and N terminal ANK domain of SHANK3 protein to antagonize dendritic branching. SHANK3 binds to the C terminus of densin-180, making the PDZ domain of densin-180 inaccessible to δcatenin. δcantenin binds with densin-180 and is required for the formation of new branches (Quitsch et al., 2005). Moreover, it has been shown that the overexpression of densin-180 causes excessive neuronal branching in rodent hippocampal neurons. These same neurons were then transfected with SHANK3, which lead to abrogation of dendrite formation and also lead to translocation of densin-180 to postsynaptic clusters (Quitsch et al., 2005). The hypothesis for increase in primary number of neurites as reported in SHANK3 patient neurons would be as follows: *SHANK3* deficiency leads to more densin-180 being accessible to bind to δcatenin which causes an increase in neurite formation. The experiment to test this hypothesis would be to block the binding of densin-180 and δcatenin. This can be done by using the δcatenin inhibitor, namely PP2 (kinase inhibitor). It has been shown in PC12 cells that overexpression of δcatenin leads to neurite formation which is disrupted by kinase inhibition (Martinez, M. C et al., 2003). Therefore, using immunocytochemistry and high content screening, I can administer the PP2, to see if it decreases neurite formation in *SHANK3* patient neurons.

In conclusion, the above section discusses several possible ways in which the loss of *SHANK3* would lead to the morphological alterations observed in our *SHANK3* patient neurons. These potential mechanisms would need to be further investigated to fully understand the role of *SHANK3* in the structural development of the neuron and to develop potential drug therapies for autism.

6.2: How is neuronal migration linked to SHANK3?

My research revealed that the rate of cell soma movement is significantly lower in the *SHANK3* patient neurons than the control neurons (Figure 3.2.3 and 3.2.4) and I suggested that this might reflect changes in neuronal migration. This

section discusses the three possible mechanisms by which immature neurons migrate and how it can linked to *SHANK3* haplo-insufficiency.

In Chapter 3, I reported that the neuralisation protocol used in this thesis generates GnRH1 positive neurons (Figure 3.2.1). The first two possible mechanisms focus on the GnRH neuron in particular, as they are known to migrate from the olfactory placode to the hypothalamus (Wierman, Margaret E et al., 2011).

The first mechanism describes that gonadotropes, endocrine cells in the anterior pituitary, release the hormone GnRH that phosphorylates Cortactin (cortical actin binding protein, Figure 6.3 A). Phosphorylation of cortactin activates the protein. Cortactin is a protein often found in the periphery of the cell that is activated by external stimuli and promotes actin polymerization (Navaratil et al., 2014). This protein is involved in the formation of lamellipodia and is therefore involved in the process cell migration (Navaratil et al., 2014). Cortactin is a known binder of *SHANK3* [Introduction, Section 1.5(c); Verpelli et al., 2012] and links to Arp2/3 complex to promote cell soma locomotion (Navaratil et al., 2014). Thus, a potential explanation for *SHANK3* patient neurons showing less cell soma movement, could be that decrease in *SHANK3* causes a decrease in cortactin. Hence, resulting in less of cortactin being available to form a complex with Arp2/3. This could result in lesser cellular locomotion, particularly in *SHANK3* patient GnRH positive neurons.

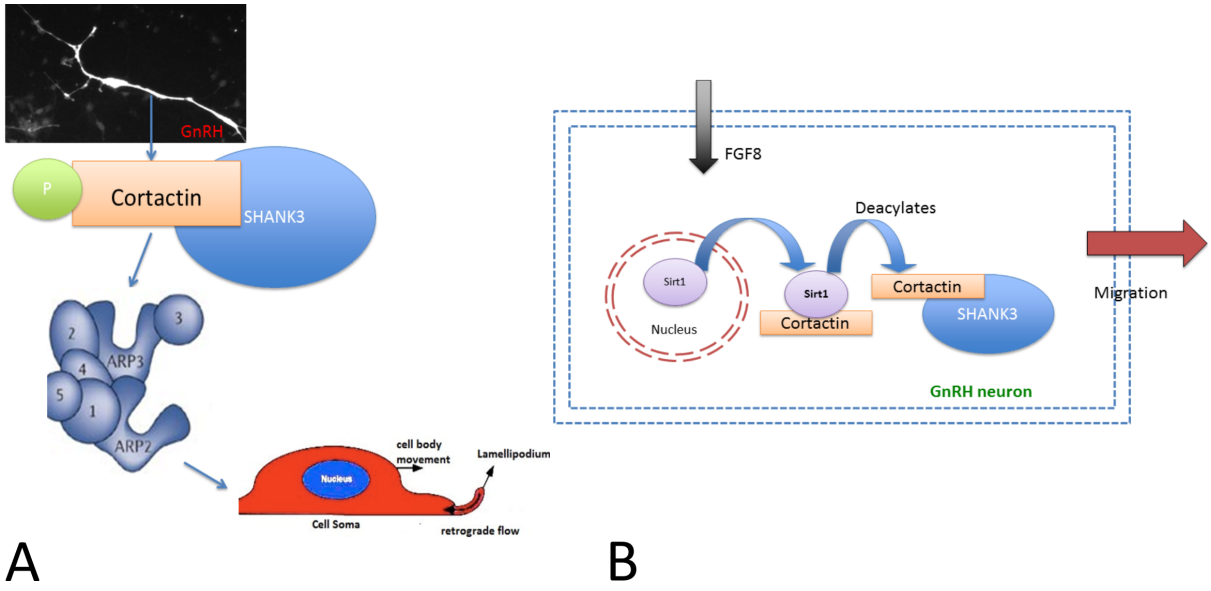

Figure 6.3: Possible mechanisms of GnRH neuron migration. A GnRH neuron releases GnRH which causes phosphorylation of cortactin to enable it to bind to the Arp2/3 complex increasing the formation of lamellipodia. B. FGF8 induces Sirt1 translocation from the nucleus to the cytoplasm where it deacetylates cortactin, to enable it to bind to the Arp2/3 complex which causes the GnRH neuron to migrate. From previous studies I know that cortactin binds to SHANK3 via its proline rich domain. (L Cramer 1997; Santé et al., 2015; Navaratil et al., 2014)

The second mechanism through which GnRH neurons migrate is shown in figure 6.3B. Here, FGF8 (fibroblast growth factor8) causes the Sirt1 (Sirtuin1) gene to translocate from the nucleus to cytoplasm. Sirt1 deacetylates and activates cortactin (Santé et al., 2015), which binds to SHANK3 to promote cell migration (Nasbitt et al., 1999). Since *SHANK3* binds to cortactin and the SHANK3 patient neurons have less *SHANK3*, they would be expected to have less cortactin, which in turn could lead the lower levels of migration observed in *SHANK3* patient neurons (Chapter 3, Section 3.2.3).

There is a distinct possibility that these two migration mechanisms involving the cortactin pathway are linked. It has been shown that FGF8 regulates the release of GnRH during early embryonic development (Falardeau J et al., 2008; Tsai et al., 2005). Therefore, the proposed mechanism would be that FGF8 increases the expression of GnRH hormone and induces Sirt1. They both activate cortactin

that binds to *SHANK3*. The cortactin-*SHANK3* complex binds to Arp2/3 complex which helps in cellular migration.

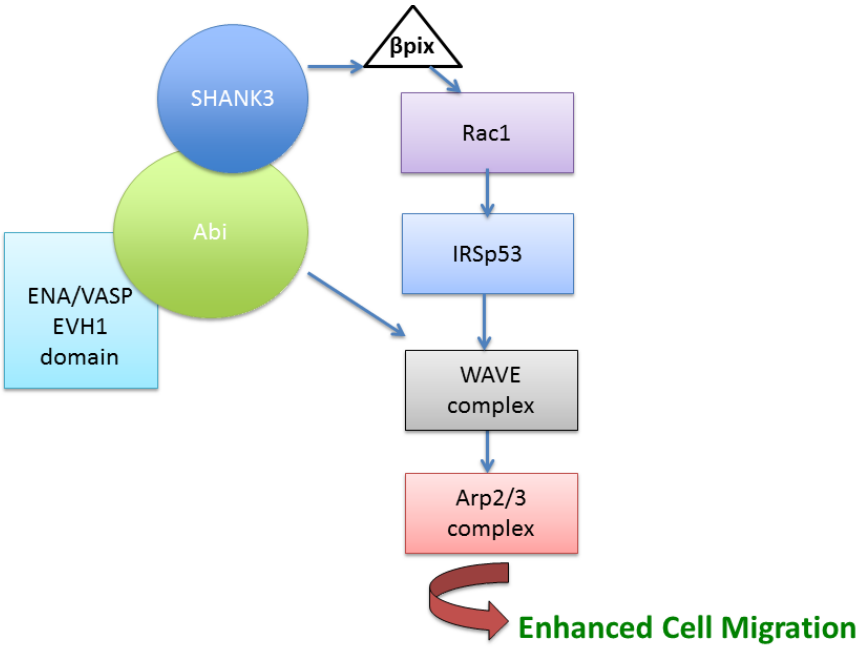

Figure 6.4: SHANK3-Abi complex triggers activation of Arp2/3 complex for cellular migration. Abi binds to the EVH1 domain of ENA/VASP. This activates the WAVE complex leading to the activation of the Arp2/3 complex (Chen X et al., 2014).

The third mechanism (Figure 6.4) for cellular migration relating to SHANK3, involves the Abi protein (Abelson interactor). The Abi proline rich domain binds to the EVH1 domain of ENA/ VASP proteins (Chen XJ et al., 2014) and these proteins are involved in cell motility through their ability to activate the WAVE regulatory complex (WRC) (Chen XJ et al., 2014). Therefore, Abi binds SHANK3 (C Proepper et al., 2007) and ENA/VASP, which activates WRC, initiating the Arp2/3 complex resulting in actin polymerization and leading to cell migration. As we know, SHANK3 binds to Abi and in *SHANK3* patient neurons there is less *SHANK3*, therefore there could also be reduced levels of Abi. This would result in

less of this protein being available to bind to ENA/VASP leading to reduced activation of both the WRC and Arp2/3 complexes. Altogether, this could cause reduced cellular migration in *SHANK3* patient neurons.

An interesting point to note is that, SHANK3 binds to βpix, which mediates cofilin through Rac1 (see Section 6.1). This was the mechanism proposed to be behind the neurite morphology seen in *SHANK3* patient neurons. The βpix and Rac1 pathway also activates the WRC complex, leading to activation of the Arp2/3 complex (Figure 6.4). This suggests that these two pathways are interlinked and could likely contribute to both increased primary number of neurites and decreased cell soma movement in the *SHANK3* patient neurons.

6.3: Cell soma size and Autism

The smaller cell soma size phenotype has been described in cortical and subcortical regions of the brain for both syndromic and non-syndromic autism (Bauman and Kemper 1995; 2005; Van Kooten et al., 2005; Casanova et al., 2002; 2006; Wegiel et al., 2010; 2015). There are currently three main hypotheses that explain why the cell soma is smaller in autistic patients.

The first is of “development arrest or delayed development” (Wegiel et al. 2010, 2015) where cell soma and nuclear volume were reported to be smaller during the first stages of development (4 to 8 years) but become normalized to control levels by the age of puberty (14 to 23 years). This suggests a development or growth delay in autism patients.

The second hypothesis is “abiotrophy”; this simply implies that there are regressive changes in the cell that causes it to wither (Casanova et al., 2013). These regressive changes are thought to be due to oxidative stress, reduced protein synthesis, lack of nutrients and growth factors. In autism, abiotrophy has been reported mainly in the cerebellum (Basson et al., 2013). Autistic children

often report deficits in motor coordination, this could be because of deficits in the cerebellum (Becker et al., 2013).

Moreover, increased oxidative stress, which causes abiotrophy has been related to autism (Chauhan A et al., 2006; Ghanizadeh et al., 2012). Additionally, it was observed that autistic children have 20-40% lower levels of glutathione in plasma. Glutathione is the main antioxidant found in the brain used for neutralizing reactive oxygen species. Due to lower levels of glutathione in plasma, there are more oxygen reactive species, which leads to oxidative stress causing the withering of the cell (Kern et al., 2011). This could then result in a decrease in cell soma.

The third hypothesis simply suggests that the smaller cell size is due to hyper connectivity of the brain (Casanova et al., 2011, 2013). In essence, the smaller cell soma is a compensation mechanism for the longer-range projections, which are metabolically expensive (Casanova et al., 2011, 2013). This fits perfectly with our study, as I report that there is a decrease in cell soma area but an increase in neurite length and number, in our *SHANK3* patient neurons. The maintenance of longer neurites requires a lot more nutrients and energy resulting in a smaller cell soma in the *SHANK3* patient neurons. Additionally, mitochondrial, the organelle that produces energy in the cell has been reported dysfunctional in autistic children (Rossignol, D A et al., 2012).

In conclusion, all three hypotheses have merits and experiments would be designed to specifically address which of these hypotheses is the cause of the decrease in cell soma area. The hypothesis that relates most to the phenotype seen in the *SHANK3* patient line, is the third one as it connects the change in cell soma area to neurite outgrowth.
In the next section, I look at the mechanism related to *SHANK3* that could influence the cell soma area phenotype.

6.4: Possible mechanism on how *SHANK3* contributes to cell soma size

The size of cell soma is determined by both intrinsic and extrinsic signals (Alison C Lloyd 2013). Very few studies have characterized regulatory pathways that control cell growth. There are two possible mechanisms through which SHANK3 could influence this pathway such that, it disrupts cell soma morphology (see Figure 6.5).

The first mechanism involves IGF1 (insulin growth factor1) activating the PI3K/AKT/mTORC1 pathway to facilitate neuronal growth (Wang, Y et al., 2014). Various studies have shown that IGF1 rescues the phenotypes produced by *SHANK3* deficiency such as decrease in synaptic puncta and synaptic transmission deficits (Shcheglovitov et al., 2013; Bozdagi et al., 2013). Thus, suggesting a link between IGF1 and *SHANK3*, although the mechanism behind this link is, at present, unknown. I hypothesize that the SHANK3 haplo-insufficiency in *SHANK3* patient neurons causes a reduction in the levels of IGF1, leading to smaller cell size. I tested this hypothesis analyzing the change in cell soma area after the administration of IGF1 (Chapter 4, section 4.3). However, I was not able to rescue the cell soma area phenotype in the *SHANK3* patient neurons. This does not mean that the hypothesis is not valid, as there could be some dosage issue, which due time constraints could not be tested. For example, I could increase the concentration of IGF1 used and/or increase the dosage period to determine whether this results in rescue of the cell soma area phenotype.

In the above section I describe abiotrophy as one of the causes of decreased cell soma size in autism. One of the main pathways regulated by growth factors and oxidative stress is the mTORC1 pathway (Alison C Lloyd 2013). Thus, another potential cause of the observed decrease in soma size could be an increase in oxidative stress in the *SHANK3* patient neurons that inhibits the mTORC1

pathway (Sengupta et al., 2010). To determine whether this is feasible, the oxidative stress of the cell should be measured. This can be done by high content screening of neurons at the various stages of neuralisation. For instance, the application of a fluorogenic probe to cells that are non-fluorescent in a reduced oxidative state but turn bright green, orange or red upon oxidation (CellROX® Deep Red Reagent ThermoScientific). This intensity can then be measured as the readout of oxidative stress in neurons. This approach could not only inform us about their oxidative stress but also allow us to correlate it to the development of our soma phenotype.

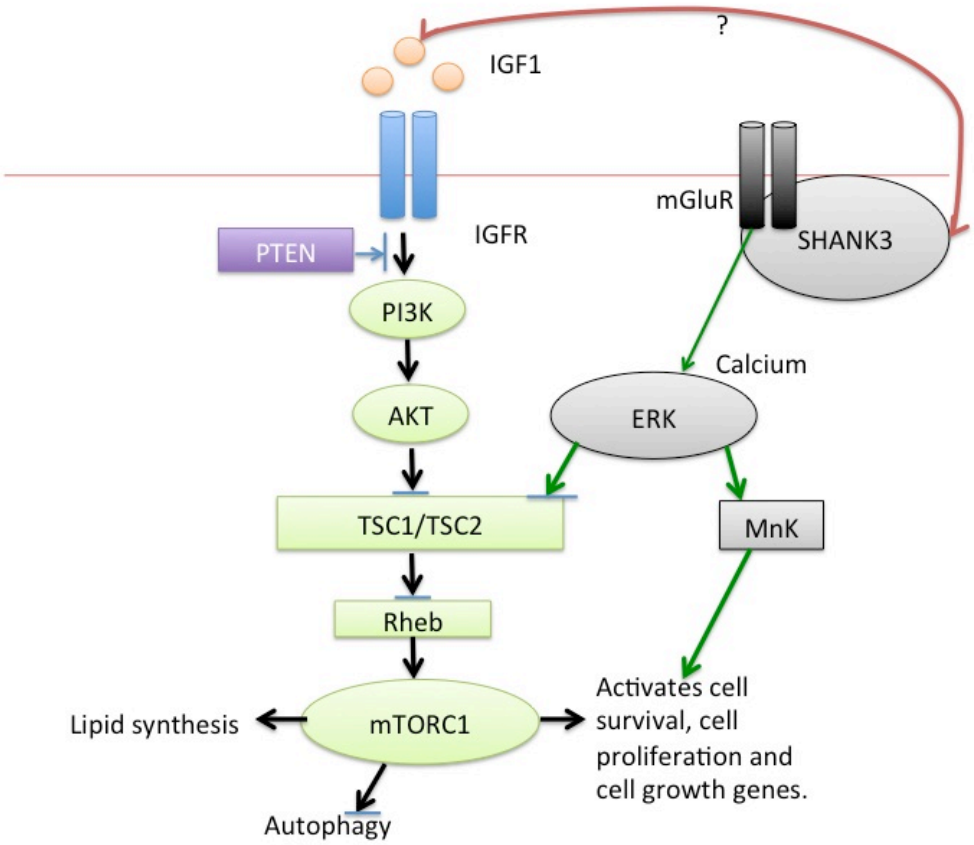

Figure 6.5: Possible mechanisms linking SHANK3 to cell growth: IGF1 activates the PI3K/AKT pathway which in turn results in mTOR activation. This leads to activation of genes that promote cell growth and proliferation. Various research studies have shown that IGF1 rescues phenotypes associated with the loss of SHANK3, linking these two protein through an unknown mechanism. SHANK3 may also influence the PI3K/AKT pathway via mGluRs that are known to bind SHANK3 through its proline rich domain via Homer1. mGluRs cause the release of calcium from endoplasmic reticulum which activates the ERK pathway. This in turn leads activation of cell proliferation (growth too) genes through via mTORC1 and MnK (Alison C Lloyd 2013; Kelleher et al., 2008; Holbro et al., 2009).

An alternative means by which *SHANK3* could influence cell growth is via the interaction of its activation of metabotropic glutamate receptors (mGluRs). This activation of mGluRs leads to calcium release from the endoplasmic reticulum, which initiates ERK signaling leading to activation of the mTORC1 pathway. In this scenario, a decrease in *SHANK3* would cause less activation of mGluR receptors, leading to a reduction in the activation of the mTORC1 pathway and hence a decrease in cell growth. For this hypothesis to be plausible, I would assess mGluR expression and activity throughout the various stages of neural development and determine whether this correlates with *SHANK3* expression and the development of the cell soma phenotype. This could be achieved via qPCR to discover when mGluR expression occurs during the neuralisation process, co-immunoprecipitation assay to confirm that *SHANK3* binds to mGluR at that stage, and to check if there are any changes in the level of protein or *mRNA* levels of mGluR between the control and *SHANK3* patient neurons. If there is a decrease in expression levels of mGluR, then I can rescue the cell soma area phenotype with an mGluR agonist. There is also the possibility that the expression levels of mGluR are normal, but it is the activation itself that is affected. This can be tested by stimulating both the control and *SHANK3* neurons with mGluR agonists and check if it increases the expression of mGluRs after stimulation.

6.5: Possible drug targets for ASD

There are only two drugs that are given to improve symptoms associated with ASD by the US FDA; aripiprazole (Abilify) and risperidone (Risperdal). Both of these act as dopamine antagonists and are given for correcting irritability and obsessive behavior (McPheeters et al., 2011). None of these target social and/or cognitive impairments in ASD. In the section below, I discuss a number of potential candidates' drugs for autism specific symptoms. Most of the drug candidates described below relate back to mechanisms behind the morphogenetic phenotypes seen in *SHANK3* patient neurons.

6.5 (a) Glutamate receptor agonists

mGluR1 and mGLuR5 are metabotropic glutamate receptors that are physically connected to NMDARs via Homer1-SHANK3 and GKAP-PSD95 interactions (Verpelli et al., 2011; Naisbitt et al., 1999). Also, mGluRs are known to functionally potentiate NMDAR function (Won et al., 2013). There are two potential theories on why agonists of this receptor could possibly work as a drug for *SHANK3* caused Autism.

First, the loss of *Shank3* in mutant mice is known to reduce the expression of both metabotropic and ionotropic glutamate receptors mGluR5, GluA1, GluN2A, GluN2B, and GluA2 (Table 1.3; Verpelli et al., 2011; Wang et al., 2011; Yang et al., 2012; Bozdagi et al., 2010; Peca et al., 2011; Schmeisser et al., 2012). This loss of expression causes synaptic deficits such as decrease in frequency of EPSCs (Verpelli et al., 2011). Therefore, treatment with a glutamate receptor agonist might restore the expression levels to normal and alleviate the deficits in synaptic transmission. In the schizophrenia model of rat, the mGluR agonists increased the expression of NMDAR and enhanced its transmission (Dong et al., 2011).

Second, mGluR activation releases calcium from the endoplasmic reticulum, which leads to the activation of the ERK pathway leading to cell growth (see Section 6.4, Holbro et al., 2009). Also, we know that knockdown of SHANK3 in mice leads to a decrease in mGuR5 expression (Verpelli et al., 2011). I hypothesize that this may lead to a reduction in activation of mTORC1 pathway via the ERK pathway and cause a decrease in cell soma area (section 6.4). Hence, an increase in mGluR activation via treatment with mGluR agonists could increase the activity of the ERK pathway, leading to growth of the cell soma of *SHANK3* patient neurons.

There are a large number of mGluR5 allosteric modulators available and four of these are known to cross the blood brain barrier (William DL et al., 2005; Gregory KJ et al., 2011) - CDPPB, MPPA (2-(3-mercaptopropyl) pentanedioic acid), ADX47273 (Acidovorax avenae subsp. avenae ATCC) and VU0092273 [(4-Hydroxypiperidin-1-yl)(4-phenylethynyl) phenyl methanone] (Won et al., 2013). Treatment of wild type mice with CDPPB and ADX47273 result in an enhanced performance in novel object recognition, learning and memory tasks. In cells, these drugs facilitate LTP and LTD in the hippocampus (Ayala et al, 2009; Liu et al., 2008; Uslaner et al., 2009). Treatment with CDPPB of a mouse model of autism and intellectual disability, due to the heterozygous deletion of TSC2 leads, resulted in a rescue of the cognitive impairment (Auerbach et al., 2011; Won et al., 2013). Also, social deficits in *Shank2*$^{-/-}$ mice were alleviated with CDPPB (Won et al., 2012). Thus, I could use CDPBB as a potential drug to rescue the morphogenetic phenotype seen in *SHANK3* patient neurons.

6.5 (b) Cofilin inhibitors

Shank3 deficient mice exhibit autism like social deficits and repetitive behavior as well as significantly diminished NMDA receptor function (Duffney et al., 2013). These behavioral phenotypes were associated with actin filament loss and reduced activity of the Rac1/PAK pathway leading to an increase in cofilin activity (Figure 6.1; Duffney et al., 2015; 2013). Using this information, I propose that reduced Rac1 activity would result in increased cofilin activity and that this could result in an increased number of primary neuritis, as seen in the *SHANK3* patient neurons (section 6.1). A Cofilin inhibitor was shown to rescue both the social deficits and NMDA synaptic dysfunction in *Shank3* deficient mice (Duffney et al., 2015), it would be reasonable, as a next step, to ask whether cofilin inhibitors such as Cytochalasin-D and/or Cucurbitacin E (Shoji Ket al., 2012; Nakashima et al., 2010) could rescue the morphogenetic phenotype observed in our *SHANK3* patient neurons. I reason that these drugs will decrease cofilin activity and this will stop the excessive severing of F actin filaments, resulting in the stabilization

of neurites in the *SHANK3* patient neurons (section 6.1). The first experiment I would perform, is to test if cofilin is increased in human SHANK3 deficient patient neurons, as *SHANK3* deficiency might have a different effect on human neurons than *Shank3* mutant rodent neurons. This could easily be assessed via western blotting [Examples of good coflin antibodies -Cofilin (D3F9) XP® Rabbit mAb and anti-Cofilin antibody (ab42824)]. Secondly, if we can confirm that there is an increase in cofilin levels, we can then use these inhibitors on *SHANK3* patient neurons to see if it rescues the neurite related morphogenetic deficits.

6.5 (c) Oxytocin

Oxytocin is a neuropeptide hormone released from the magnocellular cells of the hypothalamus (Won et al., 2013). Oxytocin is mainly associated with social behavior including affiliation, pair bonding, aggression and maternity (Won et al., 2013; Liu et al., 2010; Jacob et al., 2007). Oxytocin receptor (OXTRs) knockout mice display autistic behavior and also several mutations in OTXRs are associated with ASD. Nasal administration of oxytocin improved social interaction and communication and reduced self-injurious repetitive behavior in ASD individuals (Kosaka et al., 2012; Andari et al., 2010). Though, the molecular pathway of this is not fully understood, we can still apply this drug to the *SHANK3* patient neurons to see if this rescues the observed morphogenetic deficit and study the cellular mechanism through which it acts. This will lead to a better understanding of the action of oxytocin in neurons and could also be used as a potential drug for *SHANK3* related autism.

In conclusion, this thesis presents the novel idea that *SHANK3* haplo-insufficiency causes early structural deficits in neurons. This project has not only defined a critical period during development when cellular deficits occur in ASD but has also determined a period for successful rescue of these. I have provided some evidence that these early morphogenetic deficits can later produce changes in the number of synapses, which is commonly reported in autism (Jiang et al., 2013). Moreover, I have successfully modeled autism using iPSCs and identified robust neuronal phenotypes that can be used for future drug screening.

Bibliography

Achard, V., Martiel, J.-L., Michelot, A., Guérin, C., Reymann, A.-C., Blanchoin, L., & Boujemaa-Paterski, R. (2010). A "primer"-based mechanism underlies branched actin filament network formation and motility. *Current Biology : CB*, *20*(5), 423–8. http://doi.org/10.1016/j.cub.2009.12.056

Allan, C. M. (2013). RABL-regulated pathways: a new tale in sperm function. *Asian Journal of Andrology*, *15*(1), 87–8. http://doi.org/10.1038/aja.2012.137

Amaral, D. G., Schumann, C. M., & Nordahl, C. W. (2008). Neuroanatomy of autism. *Trends in Neurosciences*, *31*(3), 137–45. http://doi.org/10.1016/j.tins.2007.12.005

Ananiev, G., Williams, E. C., Li, H., & Chang, Q. (2011). Isogenic pairs of wild type and mutant induced pluripotent stem cell (iPSC) lines from Rett syndrome patients as in vitro disease model. *PloS One*, *6*(9), e25255. http://doi.org/10.1371/journal.pone.0025255

Andari, E., Duhamel, J.-R., Zalla, T., Herbrecht, E., Leboyer, M., & Sirigu, A. (2010). Promoting social behavior with oxytocin in high-functioning autism spectrum disorders. *Proceedings of the National Academy of Sciences of the United States of America*, *107*(9), 4389–94. http://doi.org/10.1073/pnas.0910249107

Antar, L. N., Dictenberg, J. B., Plociniak, M., Afroz, R., & Bassell, G. J. (2005). Localization of FMRP-associated mRNA granules and requirement of microtubules for activity-dependent trafficking in hippocampal neurons. *Genes, Brain, and Behavior*, *4*(6), 350–9. http://doi.org/10.1111/j.1601-183X.2005.00128.x

Arber, C., Precious, S. V, Cambray, S., Risner-Janiczek, J. R., Kelly, C., Noakes, Z., … Li, M. (2015). Activin A directs striatal projection neuron differentiation of human pluripotent stem cells. *Development (Cambridge, England)*, *142*(7), 1375–86. http://doi.org/10.1242/dev.117093

Asaka, Y., Jugloff, D. G. M., Zhang, L., Eubanks, J. H., & Fitzsimonds, R. M. (2006). Hippocampal synaptic plasticity is impaired in the Mecp2-null mouse model of Rett syndrome. *Neurobiology of Disease*, *21*(1), 217–27. http://doi.org/10.1016/j.nbd.2005.07.005

Auerbach, B. D., Osterweil, E. K., & Bear, M. F. (2011). Mutations causing syndromic autism define an axis of synaptic pathophysiology. *Nature*, *480*(7375), 63–8. http://doi.org/10.1038/nature10658

Ayala, J. E., Chen, Y., Banko, J. L., Sheffler, D. J., Williams, R., Telk, A. N., … Conn, P. J. (2009). mGluR5 positive allosteric modulators facilitate both hippocampal LTP and LTD and enhance spatial learning. *Neuropsychopharmacology : Official Publication of the American College of Neuropsychopharmacology*, *34*(9), 2057–71. http://doi.org/10.1038/npp.2009.30

Backman, S. A., Stambolic, V., & Mak, T. W. (2002). PTEN function in mammalian cell size regulation. *Current Opinion in Neurobiology*, *12*(5), 516–522. http://doi.org/10.1016/S0959-4388(02)00354-9

Baird, G., Cass, H., & Slonims, V. (2003). Diagnosis of autism. *BMJ (Clinical Research Ed.)*, *327*(7413), 488–93. http://doi.org/10.1136/bmj.327.7413.488

Baird, G., Simonoff, E., Pickles, A., Chandler, S., Loucas, T., Meldrum, D., & Charman, T. (2006a). Prevalence of disorders of the autism spectrum in a population cohort of children in South Thames: the Special Needs and Autism Project (SNAP). *The Lancet*, *368*(9531). Retrieved from https://kclpure.kcl.ac.uk/portal/en/publications/prevalence-of-disorders-of-the-autism-spectrum-in-a-population-cohort-of-children-in-south-thames-the-special-needs-and-autism-project-snap(5a0ab4da-87b2-4e77-8c8d-e3bac57f3ce7).html

Baird, G., Simonoff, E., Pickles, A., Chandler, S., Loucas, T., Meldrum, D., & Charman, T. (2006b). Prevalence of disorders of the autism spectrum in a population cohort of children in South Thames: the Special Needs and Autism Project (SNAP). *Lancet*, *368*(9531), 210–5. http://doi.org/10.1016/S0140-6736(06)69041-7

Bakos, J., Bacova, Z., Grant, S. G., Castejon, A. M., & Ostatnikova, D. (2015). Are Molecules Involved in Neuritogenesis and Axon Guidance Related to Autism Pathogenesis? *Neuromolecular Medicine*. http://doi.org/10.1007/s12017-015-8357-7

Bamburg, J. R. (1999). Proteins of the ADF/cofilin family: essential regulators of actin dynamics. *Annual Review of Cell and Developmental Biology*, *15*, 185–230. http://doi.org/10.1146/annurev.cellbio.15.1.185

Baron-Cohen, S., Auyeung, B., Nørgaard-Pedersen, B., Hougaard, D. M., Abdallah, M. W., Melgaard, L., … Lombardo, M. V. (2015). Elevated fetal steroidogenic activity in autism. *Molecular Psychiatry*, *20*(3), 369–76. http://doi.org/10.1038/mp.2014.48

Bassell, G. J., & Warren, S. T. (2008). Fragile X syndrome: loss of local mRNA regulation alters synaptic development and function. *Neuron*, *60*(2), 201–14. http://doi.org/10.1016/j.neuron.2008.10.004

Basson, M. A., & Wingate, R. J. (2013). Congenital hypoplasia of the cerebellum: developmental causes and behavioral consequences. *Frontiers in Neuroanatomy*, *7*, 29. http://doi.org/10.3389/fnana.2013.00029

Bath, K. G., Akins, M. R., & Lee, F. S. (2012). BDNF control of adult SVZ neurogenesis. *Developmental Psychobiology*, *54*(6), 578–89. http://doi.org/10.1002/dev.20546

Bauman, M., & Kemper, T. L. (1985). Histoanatomic observations of the brain in early infantile autism. *Neurology*, *35*(6), 866–74. Retrieved from http://www.ncbi.nlm.nih.gov/pubmed/4000488

Bauman, M. L., & Kemper, T. L. Neuroanatomic observations of the brain in autism: a review and future directions. *International Journal of Developmental Neuroscience : The Official Journal of the International Society for Developmental Neuroscience*, *23*(2-3), 183–7. http://doi.org/10.1016/j.ijdevneu.2004.09.006

Bauman, M. L., Kemper, T. L., & Arin, D. M. (1995). Pervasive neuroanatomic abnormalities of the brain in three cases of Rett's syndrome. *Neurology*, *45*(8), 1581–6. Retrieved from http://www.ncbi.nlm.nih.gov/pubmed/7644058

Becker, E. B. E., & Stoodley, C. J. (2013). *Neurobiology of Autism*. *International review of neurobiology* (Vol. 113). Elsevier. http://doi.org/10.1016/B978-0-12-418700-9.00001-0

Belmonte, M. K., Allen, G., Beckel-Mitchener, A., Boulanger, L. M., Carper, R. A., & Webb, S. J. (2004). Autism and abnormal development of brain connectivity. *The Journal of Neuroscience : The Official Journal of the Society for Neuroscience*, *24*(42), 9228–31. http://doi.org/10.1523/JNEUROSCI.3340-04.2004

Berkel, S., Marshall, C. R., Weiss, B., Howe, J., Roeth, R., Moog, U., … Rappold, G. A. (2010). Mutations in the SHANK2 synaptic scaffolding gene in autism spectrum disorder and mental retardation. *Nature Genetics*, *42*(6), 489–91. http://doi.org/10.1038/ng.589

Betancur, C. (2011). Etiological heterogeneity in autism spectrum disorders: more than 100 genetic and genomic disorders and still counting. *Brain Research*, *1380*, 42–77. http://doi.org/10.1016/j.brainres.2010.11.078

Betancur, C., & Buxbaum, J. D. (2013). SHANK3 haploinsufficiency: a "common" but underdiagnosed highly penetrant monogenic cause of autism spectrum disorders. *Molecular Autism*, *4*(1), 17. http://doi.org/10.1186/2040-2392-4-17

Bhattacharyya, A., McMillan, E., Wallace, K., Tubon, T. C., Capowski, E. E., & Svendsen, C. N. (2008). Normal Neurogenesis but Abnormal Gene Expression in Human Fragile X Cortical Progenitor Cells. *Stem Cells and Development*, *17*(1), 107–17. http://doi.org/10.1089/scd.2007.0073

Blundell, J., Blaiss, C. A., Etherton, M. R., Espinosa, F., Tabuchi, K., Walz, C., … Powell, C. M. (2010). Neuroligin-1 deletion results in impaired spatial memory and increased repetitive behavior. *The Journal of Neuroscience : The Official Journal of the Society for Neuroscience*, *30*(6), 2115–29. http://doi.org/10.1523/JNEUROSCI.4517-09.2010

Boccuto, L., Lauri, M., Sarasua, S. M., Skinner, C. D., Buccella, D., Dwivedi, A., … Schwartz, C. E. (2013). Prevalence of SHANK3 variants in patients with different subtypes of autism spectrum disorders. *European Journal of Human Genetics : EJHG*, *21*(3), 310–6. http://doi.org/10.1038/ejhg.2012.175

Boeckers, T. M., Bockmann, J., Kreutz, M. R., & Gundelfinger, E. D. (2002). ProSAP/Shank proteins - a family of higher order organizing molecules of the postsynaptic density with an emerging role in human neurological disease. *Journal of Neurochemistry*, *81*(5), 903–10. Retrieved from http://www.ncbi.nlm.nih.gov/pubmed/12065602

Boeckers, T. M., Kreutz, M. R., Winter, C., Zuschratter, W., Smalla, K. H., Sanmarti-Vila, L., … Gundelfinger, E. D. (1999). Proline-rich synapse-associated protein-1/cortactin binding protein 1 (ProSAP1/CortBP1) is a PDZ-domain protein

highly enriched in the postsynaptic density. *The Journal of Neuroscience : The Official Journal of the Society for Neuroscience*, *19*(15), 6506–18. Retrieved from http://www.ncbi.nlm.nih.gov/pubmed/10414979

Boissart, C., Poulet, A., Georges, P., Darville, H., Julita, E., Delorme, R., … Benchoua, A. (2013). Differentiation from human pluripotent stem cells of cortical neurons of the superficial layers amenable to psychiatric disease modeling and high-throughput drug screening. *Translational Psychiatry*, *3*, e294. http://doi.org/10.1038/tp.2013.71

Bonaglia, M. C., Giorda, R., Borgatti, R., Felisari, G., Gagliardi, C., Selicorni, A., & Zuffardi, O. (2001). Disruption of the ProSAP2 gene in a t(12;22)(q24.1;q13.3) is associated with the 22q13.3 deletion syndrome. *American Journal of Human Genetics*, *69*(2), 261–8. http://doi.org/10.1086/321293

Bonaglia, M. C., Giorda, R., Mani, E., Aceti, G., Anderlid, B.-M., Baroncini, A., … Zuffardi, O. (2006). Identification of a recurrent breakpoint within the SHANK3 gene in the 22q13.3 deletion syndrome. *Journal of Medical Genetics*, *43*(10), 822–8. http://doi.org/10.1136/jmg.2005.038604

Boulting, G. L., Kiskinis, E., Croft, G. F., Amoroso, M. W., Oakley, D. H., Wainger, B. J., … Eggan, K. (2011). A functionally characterized test set of human induced pluripotent stem cells. *Nature Biotechnology*, *29*(3), 279–86. http://doi.org/10.1038/nbt.1783

Bourgeron, T. (2009). A synaptic trek to autism. *Current Opinion in Neurobiology*, *19*(2), 231–4. http://doi.org/10.1016/j.conb.2009.06.003

Bozdagi, O., Sakurai, T., Papapetrou, D., Wang, X., Dickstein, D. L., Takahashi, N., … Buxbaum, J. D. (2010). Haploinsufficiency of the autism-associated Shank3 gene leads to deficits in synaptic function, social interaction, and social communication. *Molecular Autism*, *1*(1), 15. http://doi.org/10.1186/2040-2392-1-15

Bozdagi, O., Tavassoli, T., & Buxbaum, J. D. (2013). Insulin-like growth factor-1 rescues synaptic and motor deficits in a mouse model of autism and developmental delay. *Molecular Autism*, *4*(1), 9. http://doi.org/10.1186/2040-2392-4-9

Bradke, F. (1999). The Role of Local Actin Instability in Axon Formation. *Science*, *283*(5409), 1931–1934. http://doi.org/10.1126/science.283.5409.1931

Brennand, K. J., Simone, A., Tran, N., & Gage, F. H. (2012). Modeling psychiatric disorders at the cellular and network levels. *Molecular Psychiatry*, *17*(12), 1239–53. http://doi.org/10.1038/mp.2012.20

Brodal, P. (2004). *The Central Nervous System: Structure and Function*. Oxford University Press, USA. Retrieved from https://books.google.com/books?hl=en&lr=&id=WdATFQ0YUrMC&pgis=1

Brugha, T. S., McManus, S., Bankart, J., Scott, F., Purdon, S., Smith, J., … Meltzer, H. (2011). Epidemiology of autism spectrum disorders in adults in the community in England. *Archives of General Psychiatry*, *68*(5), 459–65. http://doi.org/10.1001/archgenpsychiatry.2011.38

Burbach, J. P. H., Luckman, S. M., Murphy, D., & Gainer, H. (2001). Gene Regulation in the Magnocellular Hypothalamo-Neurohypophysial System. *Physiol Rev*, *81*(3), 1197–1267. Retrieved from http://physrev.physiology.org/content/81/3/1197

Campellone, K. G., & Welch, M. D. (2010). A nucleator arms race: cellular control of actin assembly. *Nature Reviews. Molecular Cell Biology*, *11*(4), 237–51. http://doi.org/10.1038/nrm2867

Carbonetto, S. (2014). A blueprint for research on Shankopathies: a view from research on autism spectrum disorder. *Developmental Neurobiology*, *74*(2), 85–112. http://doi.org/10.1002/dneu.22150

Casanova, M. F., Buxhoeveden, D. P., Switala, A. E., & Roy, E. (2002). Minicolumnar pathology in autism. *Neurology*, *58*(3), 428–432. http://doi.org/10.1212/WNL.58.3.428

Casanova, M. F., El-Baz, A., & Switala, A. (2011). Laws of conservation as related to brain growth, aging, and evolution: symmetry of the minicolumn. *Frontiers in Neuroanatomy*, *5*, 66. http://doi.org/10.3389/fnana.2011.00066

Casanova, M. F., van Kooten, I., Switala, A. E., van Engeland, H., Heinsen, H., Steinbusch, H. W. M., … Schmitz, C. (2006). Abnormalities of cortical minicolumnar organization in the prefrontal lobes of autistic patients. *Clinical Neuroscience Research*, *6*(3-4), 127–133. http://doi.org/10.1016/j.cnr.2006.06.003

Castrén, M., Tervonen, T., Kärkkäinen, V., Heinonen, S., Castrén, E., Larsson, K., … Akerman, K. (2005). Altered differentiation of neural stem cells in fragile X syndrome. *Proceedings of the National Academy of Sciences of the United States of America*, *102*(49), 17834–9. http://doi.org/10.1073/pnas.0508995102

Chambers, S. M., Fasano, C. A., Papapetrou, E. P., Tomishima, M., Sadelain, M., & Studer, L. (2009). Highly efficient neural conversion of human ES and iPS cells by dual inhibition of SMAD signaling. *Nature Biotechnology*, *27*(3), 275–280. http://doi.org/10.1038/nbt.1529

Chapleau, C. A., Calfa, G. D., Lane, M. C., Albertson, A. J., Larimore, J. L., Kudo, S., … Pozzo-Miller, L. (2009). Dendritic spine pathologies in hippocampal pyramidal neurons from Rett syndrome brain and after expression of Rett-associated MECP2 mutations. *Neurobiology of Disease*, *35*(2), 219–33. http://doi.org/10.1016/j.nbd.2009.05.001

Chauhan, A., & Chauhan, V. (2006). Oxidative stress in autism. *Pathophysiology : The Official Journal of the International Society for Pathophysiology / ISP*, *13*(3), 171–81. http://doi.org/10.1016/j.pathophys.2006.05.007

Chen, Q., & Pollard, T. D. (2013). Actin filament severing by cofilin dismantles actin patches and produces mother filaments for new patches. *Current Biology : CB*, *23*(13), 1154–62. http://doi.org/10.1016/j.cub.2013.05.005

Chen, R. Z., Akbarian, S., Tudor, M., & Jaenisch, R. (2001). Deficiency of methyl-CpG binding protein-2 in CNS neurons results in a Rett-like phenotype in mice. *Nature Genetics*, *27*(3), 327–31. http://doi.org/10.1038/85906

Chen, X. J., Squarr, A. J., Stephan, R., Chen, B., Higgins, T. E., Barry, D. J., … Way, M. (2014). Ena/VASP proteins cooperate with the WAVE complex to regulate the actin cytoskeleton. *Developmental Cell*, *30*(5), 569–84. http://doi.org/10.1016/j.devcel.2014.08.001

Cheung, A. Y. L., Horvath, L. M., Grafodatskaya, D., Pasceri, P., Weksberg, R., Hotta, A., … Ellis, J. (2011). Isolation of MECP2-null Rett Syndrome patient hiPS cells and isogenic controls through X-chromosome inactivation. *Human Molecular Genetics*, *20*(11), 2103–15. http://doi.org/10.1093/hmg/ddr093

Choi, J., Ko, J., Racz, B., Burette, A., Lee, J.-R., Kim, S., … Kim, E. (2005). Regulation of dendritic spine morphogenesis by insulin receptor substrate 53, a downstream effector of Rac1 and Cdc42 small GTPases. *The Journal of Neuroscience : The Official Journal of the Society for Neuroscience*, *25*(4), 869–79. http://doi.org/10.1523/JNEUROSCI.3212-04.2005

Cocks, G., Curran, S., Gami, P., Uwanogho, D., Jeffries, A. R., Kathuria, A., … Price, J. (2014). The utility of patient specific induced pluripotent stem cells for the modelling of Autistic Spectrum Disorders. *Psychopharmacology*, *231*(6), 1079–88. http://doi.org/10.1007/s00213-013-3196-4

Comery, T. A., Harris, J. B., Willems, P. J., Oostra, B. A., Irwin, S. A., Weiler, I. J., & Greenough, W. T. (1997). Abnormal dendritic spines in fragile X knockout mice: maturation and pruning deficits. *Proceedings of the National Academy of Sciences of the United States of America*, *94*(10), 5401–4. Retrieved from http://www.pubmedcentral.nih.gov/articlerender.fcgi?artid=24690&tool=pmcentrez&rendertype=abstract

Cooper, G. M. (2000). Structure and Organization of Actin Filaments. Sinauer Associates. Retrieved from http://www.ncbi.nlm.nih.gov/books/NBK9908/

Courchesne, E., Karns, C. M., Davis, H. R., Ziccardi, R., Carper, R. A., Tigue, Z. D., … Courchesne, R. Y. (2001). Unusual brain growth patterns in early life in patients with autistic disorder: an MRI study. *Neurology*, *57*(2), 245–54. Retrieved from http://www.ncbi.nlm.nih.gov/pubmed/11468308

Cramer, L. P. (1997). Molecular mechanism of actin-dependent retrograde flow in lamellipodia of motile cells. *Frontiers in Bioscience : A Journal and Virtual Library*, *2*, d260–70. Retrieved from http://www.ncbi.nlm.nih.gov/pubmed/9206973

da Silva, J. S., & Dotti, C. G. (2002). Breaking the neuronal sphere: regulation of the actin cytoskeleton in neuritogenesis. *Nature Reviews. Neuroscience*, *3*(9), 694–704. http://doi.org/10.1038/nrn918

Dani, V. S., Chang, Q., Maffei, A., Turrigiano, G. G., Jaenisch, R., & Nelson, S. B. (2005). Reduced cortical activity due to a shift in the balance between excitation and inhibition in a mouse model of Rett syndrome. *Proceedings of the National Academy of Sciences of the United States of America*, *102*(35), 12560–5. http://doi.org/10.1073/pnas.0506071102

Darnell, J. C., & Klann, E. (2013). The translation of translational control by FMRP: therapeutic targets for FXS. *Nature Neuroscience*, *16*(11), 1530–6. http://doi.org/10.1038/nn.3379

De Rubeis, S., He, X., Goldberg, A. P., Poultney, C. S., Samocha, K., Ercument Cicek, A., … Buxbaum, J. D. (2014). Synaptic, transcriptional and chromatin genes disrupted in autism. *Nature*, *515*(7526), 209–215. http://doi.org/10.1038/nature13772

Dementieva, Y. A., Vance, D. D., Donnelly, S. L., Elston, L. A., Wolpert, C. M., Ravan, S. A., … Cuccaro, M. L. (2005). Accelerated head growth in early development of individuals with autism. *Pediatric Neurology*, *32*(2), 102–8. http://doi.org/10.1016/j.pediatrneurol.2004.08.005

Devine, M. J., Ryten, M., Vodicka, P., Thomson, A. J., Burdon, T., Houlden, H., … Kunath, T. (2011). Parkinson's disease induced pluripotent stem cells with triplication of the α-synuclein locus. *Nature Communications*, *2*, 440. http://doi.org/10.1038/ncomms1453

Dhara, S. K., & Stice, S. L. (2008). Neural differentiation of human embryonic stem cells. *Journal of Cellular Biochemistry*, *105*(3), 633–40. http://doi.org/10.1002/jcb.21891

Di Sante, G., Wang, L., Wang, C., Jiao, X., Casimiro, M. C., Chen, K., … Pestell, R. G. (2015). Sirt1-deficient mice have hypogonadotropic hypogonadism due to defective GnRH neuronal migration. *Molecular Endocrinology (Baltimore, Md.)*, *29*(2), 200–12. http://doi.org/10.1210/me.2014-1228

Doers, M. E., Musser, M. T., Nichol, R., Berndt, E. R., Baker, M., Gomez, T. M., … Bhattacharyya, A. (2014). iPSC-derived forebrain neurons from FXS individuals show defects in initial neurite outgrowth. *Stem Cells and Development*, *23*(15), 1777–87. http://doi.org/10.1089/scd.2014.0030

Doherty, G. J., & McMahon, H. T. (2008). Mediation, modulation, and consequences of membrane-cytoskeleton interactions. *Annual Review of Biophysics*, *37*, 65–95. http://doi.org/10.1146/annurev.biophys.37.032807.125912

Duffney, L. J., Wei, J., Cheng, J., Liu, W., Smith, K. R., Kittler, J. T., & Yan, Z. (2013). Shank3 deficiency induces NMDA receptor hypofunction via an actin-dependent mechanism. *The Journal of Neuroscience : The Official Journal of the Society for Neuroscience*, *33*(40), 15767–78. http://doi.org/10.1523/JNEUROSCI.1175-13.2013

Duffney, L. J., Zhong, P., Wei, J., Matas, E., Cheng, J., Qin, L., … Yan, Z. (2015). Autism-like Deficits in Shank3-Deficient Mice Are Rescued by Targeting Actin Regulators. *Cell Reports*. http://doi.org/10.1016/j.celrep.2015.04.064

Durand, C. M., Betancur, C., Boeckers, T. M., Bockmann, J., Chaste, P., Fauchereau, F., … Bourgeron, T. (2007). Mutations in the gene encoding the synaptic scaffolding protein SHANK3 are associated with autism spectrum disorders. *Nature Genetics*, *39*(1), 25–7. http://doi.org/10.1038/ng1933

Durand, C. M., Perroy, J., Loll, F., Perrais, D., Fagni, L., Bourgeron, T., … Sans, N. (2012). SHANK3 mutations identified in autism lead to modification of dendritic spine morphology via an actin-dependent mechanism. *Molecular Psychiatry*, *17*(1), 71–84. http://doi.org/10.1038/mp.2011.57

Ehninger, D., Han, S., Shilyansky, C., Zhou, Y., Li, W., Kwiatkowski, D. J., … Silva, A. J. (2008). Reversal of learning deficits in a Tsc2+/− mouse model of tuberous sclerosis. *Nature Medicine*, *14*(8), 843–848. http://doi.org/10.1038/nm1788

Eigenmann, D. E., Xue, G., Kim, K. S., Moses, A. V, Hamburger, M., & Oufir, M. (2013). Comparative study of four immortalized human brain capillary endothelial cell lines, hCMEC/D3, hBMEC, TY10, and BB19, and optimization of culture conditions, for an in vitro blood-brain barrier model for drug permeability studies. *Fluids and Barriers of the CNS*, *10*(1), 33. http://doi.org/10.1186/2045-8118-10-33

El-Fishawy, P., & State, M. W. (2010). The genetics of autism: key issues, recent findings, and clinical implications. *The Psychiatric Clinics of North America*, *33*(1), 83–105. http://doi.org/10.1016/j.psc.2009.12.002

Erceg, S., Lukovic, D., Moreno-Manzano, V., Stojkovic, M., & Bhattacharya, S. S. (2012). Derivation of cerebellar neurons from human pluripotent stem cells. *Current Protocols in Stem Cell Biology*, *Chapter 1*, Unit 1H.5. http://doi.org/10.1002/9780470151808.sc01h05s20

Erickson, K., Gabry, K. E., Lindell, S., Champoux, M., Schulkin, J., Gold, P., … Higley, J. D. (2005). Social withdrawal behaviors in nonhuman primates and changes in neuroendocrine and monoamine concentrations during a separation paradigm. *Developmental Psychobiology*, *46*(4), 331–9. http://doi.org/10.1002/dev.20061

Falardeau, J., Chung, W. C. J., Beenken, A., Raivio, T., Plummer, L., Sidis, Y., … Pitteloud, N. (2008). Decreased FGF8 signaling causes deficiency of gonadotropin-releasing hormone in humans and mice. *The Journal of Clinical Investigation*, *118*(8), 2822–31. http://doi.org/10.1172/JCI34538

Fasano, C. A., Chambers, S. M., Lee, G., Tomishima, M. J., & Studer, L. (2010). Efficient derivation of functional floor plate tissue from human embryonic stem cells. *Cell Stem Cell*, *6*(4), 336–47. http://doi.org/10.1016/j.stem.2010.03.001

Fingar, D. C., Salama, S., Tsou, C., Harlow, E., & Blenis, J. (2002). Mammalian cell size is controlled by mTOR and its downstream targets S6K1 and 4EBP1/eIF4E. *Genes & Development*, *16*(12), 1472–87. http://doi.org/10.1101/gad.995802

Flynn, K. C., Hellal, F., Neukirchen, D., Jacob, S., Tahirovic, S., Dupraz, S., … Bradke, F. (2012). ADF/cofilin-mediated actin retrograde flow directs neurite formation in the developing brain. *Neuron*, *76*(6), 1091–107. http://doi.org/10.1016/j.neuron.2012.09.038

Ganten, D., & Pfaff, D. (Eds.). (1990). *Behavioral Aspects of Neuroendocrinology* (Vol. 10). Berlin, Heidelberg: Springer Berlin Heidelberg. http://doi.org/10.1007/978-3-642-75837-9

Gauthier, J., Spiegelman, D., Piton, A., Lafrenière, R. G., Laurent, S., St-Onge, J., … Rouleau, G. A. (2009). Novel de novo SHANK3 mutation in autistic patients. *American Journal of Medical Genetics. Part B, Neuropsychiatric Genetics : The Official Publication of the International Society of Psychiatric Genetics*, *150B*(3), 421–4. http://doi.org/10.1002/ajmg.b.30822

Ghosh, A., Michalon, A., Lindemann, L., Fontoura, P., & Santarelli, L. (2013). Drug discovery for autism spectrum disorder: challenges and opportunities. *Nature Reviews. Drug Discovery*, *12*(10), 777–90. http://doi.org/10.1038/nrd4102

Gkogkas, C. G., Khoutorsky, A., Ran, I., Rampakakis, E., Nevarko, T., Weatherill, D. B., … Sonenberg, N. (2013). Autism-related deficits via dysregulated eIF4E-dependent translational control. *Nature*, *493*(7432), 371–7. http://doi.org/10.1038/nature11628

Goldsmith, A. D., Sarin, S., Lockery, S., & Hobert, O. (2010). Developmental control of lateralized neuron size in the nematode Caenorhabditis elegans. *Neural Development*, *5*(1), 33. http://doi.org/10.1186/1749-8104-5-33

Grabrucker, A. M., Knight, M. J., Proepper, C., Bockmann, J., Joubert, M., Rowan, M., … Boeckers, T. M. (2011). Concerted action of zinc and ProSAP/Shank in synaptogenesis and synapse maturation. *The EMBO Journal*, *30*(3), 569–81. http://doi.org/10.1038/emboj.2010.336

Grabrucker, A. M., Schmeisser, M. J., Schoen, M., & Boeckers, T. M. (2011). Postsynaptic ProSAP/Shank scaffolds in the cross-hair of synaptopathies. *Trends in Cell Biology*, *21*(10), 594–603. http://doi.org/10.1016/j.tcb.2011.07.003

Gregory, K. J., Dong, E. N., Meiler, J., & Conn, P. J. (2011). Allosteric modulation of metabotropic glutamate receptors: structural insights and therapeutic potential. *Neuropharmacology*, *60*(1), 66–81. http://doi.org/10.1016/j.neuropharm.2010.07.007

Guilmatre, A., Huguet, G., Delorme, R., & Bourgeron, T. (2014). The emerging role of SHANK genes in neuropsychiatric disorders. *Developmental Neurobiology*, *74*(2), 113–22. http://doi.org/10.1002/dneu.22128

Haeckel, A., Ahuja, R., Gundelfinger, E. D., Qualmann, B., & Kessels, M. M. (2008a). The actin-binding protein Abp1 controls dendritic spine morphology and is important for spine head and synapse formation. *The Journal of Neuroscience : The Official Journal of the Society for Neuroscience*, *28*(40), 10031–44. http://doi.org/10.1523/JNEUROSCI.0336-08.2008

Haeckel, A., Ahuja, R., Gundelfinger, E. D., Qualmann, B., & Kessels, M. M. (2008b). The actin-binding protein Abp1 controls dendritic spine morphology and is important for spine head and synapse formation. *The Journal of Neuroscience : The Official Journal of the Society for Neuroscience*, *28*(40), 10031–44. http://doi.org/10.1523/JNEUROSCI.0336-08.2008

Hallmayer, J., Cleveland, S., Torres, A., Phillips, J., Cohen, B., Torigoe, T., … Risch, N. (2011). Genetic heritability and shared environmental factors among twin pairs with autism. *Archives of General Psychiatry*, *68*(11), 1095–102. http://doi.org/10.1001/archgenpsychiatry.2011.76

Han, K., Holder, J. L., Schaaf, C. P., Lu, H., Chen, H., Kang, H., … Zoghbi, H. Y. (2013). SHANK3 overexpression causes manic-like behaviour with unique pharmacogenetic properties. *Nature*, *503*(7474), 72–7. http://doi.org/10.1038/nature12630

Häusser, M. (2001). Synaptic function: Dendritic democracy. *Current Biology*, *11*(1), R10–R12. http://doi.org/10.1016/S0960-9822(00)00034-8

Hayashi, M. K., Tang, C., Verpelli, C., Narayanan, R., Stearns, M. H., Xu, R.-M., … Hayashi, Y. (2009). The postsynaptic density proteins Homer and Shank form a polymeric network structure. *Cell*, *137*(1), 159–71. http://doi.org/10.1016/j.cell.2009.01.050

He, B. J., Shulman, G. L., Snyder, A. Z., & Corbetta, M. (2007). The role of impaired neuronal communication in neurological disorders. *Current Opinion in Neurology*, *20*(6), 655–60. http://doi.org/10.1097/WCO.0b013e3282f1c720

Hering, H., & Sheng, M. (2003a). Activity-Dependent Redistribution and Essential Role of Cortactin in Dendritic Spine Morphogenesis. *J. Neurosci.*, *23*(37), 11759–11769. Retrieved from http://www.jneurosci.org/content/23/37/11759.long

Hering, H., & Sheng, M. (2003b). Activity-Dependent Redistribution and Essential Role of Cortactin in Dendritic Spine Morphogenesis. *J. Neurosci.*, *23*(37), 11759–11769. Retrieved from http://www.jneurosci.org/content/23/37/11759.short

Holbro, N., Grunditz, A., & Oertner, T. G. (2009). Differential distribution of endoplasmic reticulum controls metabotropic signaling and plasticity at hippocampal synapses. *Proceedings of the National Academy of Sciences of the United States of America*, *106*(35), 15055–60. http://doi.org/10.1073/pnas.0905110106

Hollander, E., Anagnostou, E., Chaplin, W., Esposito, K., Haznedar, M. M., Licalzi, E., … Buchsbaum, M. (2005). Striatal volume on magnetic resonance imaging and repetitive behaviors in autism. *Biological Psychiatry*, *58*(3), 226–32. http://doi.org/10.1016/j.biopsych.2005.03.040

Hollander, E., Bartz, J., Chaplin, W., Phillips, A., Sumner, J., Soorya, L., … Wasserman, S. (2007). Oxytocin increases retention of social cognition in autism. *Biological Psychiatry*, *61*(4), 498–503. http://doi.org/10.1016/j.biopsych.2006.05.030

Honkura, N., Matsuzaki, M., Noguchi, J., Ellis-Davies, G. C. R., & Kasai, H. (2008). The subspine organization of actin fibers regulates the structure and plasticity of dendritic spines. *Neuron*, *57*(5), 719–29. http://doi.org/10.1016/j.neuron.2008.01.013

Hoos, M. D., Vitek, M. P., Ridnour, L. A., Wilson, J., Jansen, M., Everhart, A., … Colton, C. A. (2014). The impact of human and mouse differences in NOS2 gene expression on the brain's redox and immune environment. *Molecular Neurodegeneration*, *9*(1), 50. http://doi.org/10.1186/1750-1326-9-50

Hotulainen, P., & Hoogenraad, C. C. (2010). Actin in dendritic spines: connecting dynamics to function. *The Journal of Cell Biology*, *189*(4), 619–29. http://doi.org/10.1083/jcb.201003008

Hung, A. Y., Futai, K., Sala, C., Valtschanoff, J. G., Ryu, J., Woodworth, M. A., … Sheng, M. (2008). Smaller dendritic spines, weaker synaptic transmission, but enhanced spatial learning in mice lacking Shank1. *The Journal of Neuroscience : The Official Journal of the Society for Neuroscience*, *28*(7), 1697–708. http://doi.org/10.1523/JNEUROSCI.3032-07.2008

Hutchins, B. I., Klenke, U., & Wray, S. (2013). Calcium release-dependent actin flow in the leading process mediates axophilic migration. *The Journal of Neuroscience : The Official Journal of the Society for Neuroscience*, *33*(28), 11361–71. http://doi.org/10.1523/JNEUROSCI.3758-12.2013

Hutchins, B. I., & Wray, S. (2014). Capture of microtubule plus-ends at the actin cortex promotes axophilic neuronal migration by enhancing microtubule tension in the leading process. *Frontiers in Cellular Neuroscience*, *8*, 400. http://doi.org/10.3389/fncel.2014.00400

Ichetovkin, I., Grant, W., & Condeelis, J. (2002). Cofilin produces newly polymerized actin filaments that are preferred for dendritic nucleation by the Arp2/3 complex. *Current Biology : CB*, *12*(1), 79–84. Retrieved from http://www.ncbi.nlm.nih.gov/pubmed/11790308

Imaging the Brain in Autism. (2013) (p. 387). Springer Science & Business Media. Retrieved from https://books.google.com/books?id=IZ5GAAAAQBAJ&pgis=1

Inoue, H., Nagata, N., Kurokawa, H., & Yamanaka, S. (2014). iPS cells: a game changer for future medicine. *The EMBO Journal*, *33*(5), 409–17. http://doi.org/10.1002/embj.201387098

Irwin, S. A., Patel, B., Idupulapati, M., Harris, J. B., Crisostomo, R. A., Larsen, B. P., … Greenough, W. T. (2001). Abnormal dendritic spine characteristics in the temporal and visual cortices of patients with fragile-X syndrome: a quantitative examination. *American Journal of Medical Genetics*, *98*(2), 161–7. Retrieved from http://www.ncbi.nlm.nih.gov/pubmed/11223852

Jacob, S., Brune, C. W., Carter, C. S., Leventhal, B. L., Lord, C., & Cook, E. H. (2007). Association of the oxytocin receptor gene (OXTR) in Caucasian children and adolescents with autism. *Neuroscience Letters*, *417*(1), 6–9. http://doi.org/10.1016/j.neulet.2007.02.001

Jaeger, I., Arber, C., Risner-Janiczek, J. R., Kuechler, J., Pritzsche, D., Chen, I.-C., … Li, M. (2011). Temporally controlled modulation of FGF/ERK signaling directs midbrain dopaminergic neural progenitor fate in mouse and human pluripotent stem cells. *Development (Cambridge, England)*, *138*(20), 4363–74. http://doi.org/10.1242/dev.066746

Jan, Y.-N., & Jan, L. Y. (2010). Branching out: mechanisms of dendritic arborization. *Nature Reviews. Neuroscience*, *11*(5), 316–28. http://doi.org/10.1038/nrn2836

Jiang, Y.-H., & Ehlers, M. D. (2013). Modeling autism by SHANK gene mutations in mice. *Neuron*, *78*(1), 8–27. http://doi.org/10.1016/j.neuron.2013.03.016

Kelleher, R. J., & Bear, M. F. (2008). The autistic neuron: troubled translation? *Cell*, *135*(3), 401–6. http://doi.org/10.1016/j.cell.2008.10.017

Keown, C. L., Shih, P., Nair, A., Peterson, N., Mulvey, M. E., & Müller, R.-A. (2013). Local Functional Overconnectivity in Posterior Brain Regions Is Associated with Symptom Severity in Autism Spectrum Disorders. *Cell Reports*, *5*(3), 567–572. http://doi.org/10.1016/j.celrep.2013.10.003

Kern, J. K., Geier, D. A., Adams, J. B., Garver, C. R., Audhya, T., & Geier, M. R. (2011). A clinical trial of glutathione supplementation in autism spectrum disorders. *Medical Science Monitor : International Medical Journal of Experimental and Clinical Research*, *17*(12), CR677–82. Retrieved from http://www.pubmedcentral.nih.gov/articlerender.fcgi?artid=3628138&tool=pmcentrez&rendertype=abstract

Kim, D. J., Kim, S. H., Lim, C. S., Choi, K. Y., Park, C. S., Sung, B. H., … Song, W. K. (2006). Interaction of SPIN90 with the Arp2/3 complex mediates lamellipodia and actin comet tail formation. *The Journal of Biological Chemistry*, *281*(1), 617–25. http://doi.org/10.1074/jbc.M504450200

Kim, S.-M., Choi, K. Y., Cho, I. H., Rhy, J. H., Kim, S. H., Park, C.-S., … Song, W. K. (2009). Regulation of dendritic spine morphology by SPIN90, a novel Shank binding partner. *Journal of Neurochemistry*, *109*(4), 1106–17. http://doi.org/10.1111/j.1471-4159.2009.06039.x

Kishi, N., & Macklis, J. D. (2004). MECP2 is progressively expressed in post-migratory neurons and is involved in neuronal maturation rather than cell fate decisions. *Molecular and Cellular Neurosciences*, *27*(3), 306–21. http://doi.org/10.1016/j.mcn.2004.07.006

Kleijer, K. T. E., Schmeisser, M. J., Krueger, D. D., Boeckers, T. M., Scheiffele, P., Bourgeron, T., … Burbach, J. P. H. (2014). Neurobiology of autism gene products: towards pathogenesis and drug targets. *Psychopharmacology*, *231*(6), 1037–62. http://doi.org/10.1007/s00213-013-3403-3

Kolevzon, A., Cai, G., Soorya, L., Takahashi, N., Grodberg, D., Kajiwara, Y., … Buxbaum, J. D. (2011). Analysis of a purported SHANK3 mutation in a boy with autism: clinical impact of rare variant research in neurodevelopmental disabilities. *Brain Research*, *1380*, 98–105. http://doi.org/10.1016/j.brainres.2010.11.005

Kosaka, H., Munesue, T., Ishitobi, M., Asano, M., Omori, M., Sato, M., … Wada, Y. (2012). Long-term oxytocin administration improves social behaviors in a girl with autistic disorder. *BMC Psychiatry*, *12*, 110. http://doi.org/10.1186/1471-244X-12-110

Kouser, M., Speed, H. E., Dewey, C. M., Reimers, J. M., Widman, A. J., Gupta, N., … Powell, C. M. (2013). Loss of predominant Shank3 isoforms results in hippocampus-dependent impairments in behavior and synaptic transmission. *The Journal of Neuroscience : The Official Journal of the Society for Neuroscience*, *33*(47), 18448–68. http://doi.org/10.1523/JNEUROSCI.3017-13.2013

Krause, M., & Gautreau, A. (2014). Steering cell migration: lamellipodium dynamics and the regulation of directional persistence. *Nature Reviews Molecular Cell Biology*, *15*(9), 577–590. http://doi.org/10.1038/nrm3861

Kreienkamp, H.-J. (2008). Scaffolding proteins at the postsynaptic density: shank as the architectural framework. *Handbook of Experimental Pharmacology*, (186), 365–80. http://doi.org/10.1007/978-3-540-72843-6_15

Kulkarni, V. A., & Firestein, B. L. (2012). The dendritic tree and brain disorders. *Molecular and Cellular Neurosciences*, *50*(1), 10–20. http://doi.org/10.1016/j.mcn.2012.03.005

Kumari, D., Swaroop, M., Southall, N., Huang, W., Zheng, W., & Usdin, K. (2015). High-Throughput Screening to Identify Compounds That Increase Fragile X Mental Retardation Protein Expression in Neural Stem Cells Differentiated From Fragile X Syndrome Patient-Derived Induced Pluripotent Stem Cells. *Stem Cells Translational Medicine*, *4*(7), 800–8. http://doi.org/10.5966/sctm.2014-0278

Kuriu, T., Inoue, A., Bito, H., Sobue, K., & Okabe, S. (2006). Differential control of postsynaptic density scaffolds via actin-dependent and -independent mechanisms. *The Journal of Neuroscience : The Official Journal of the Society for Neuroscience*, *26*(29), 7693–706. http://doi.org/10.1523/JNEUROSCI.0522-06.2006

Kutner, R. H., Zhang, X.-Y., & Reiser, J. (2009). Production, concentration and titration of pseudotyped HIV-1-based lentiviral vectors. *Nature Protocols*, *4*(4), 495–505. http://doi.org/10.1038/nprot.2009.22

LaFlamme, B. (2015). Genetic modules for autism. *Nature Genetics*, *47*(2), 105–105. http://doi.org/10.1038/ng.3210

Lancaster, M. A., Renner, M., Martin, C.-A., Wenzel, D., Bicknell, L. S., Hurles, M. E., … Knoblich, J. A. (2013). Cerebral organoids model human brain development and microcephaly. *Nature*, *501*(7467), 373–9. http://doi.org/10.1038/nature12517

Langen, M., Schnack, H. G., Nederveen, H., Bos, D., Lahuis, B. E., de Jonge, M. V, … Durston, S. (2009). Changes in the developmental trajectories of striatum in autism. *Biological Psychiatry*, *66*(4), 327–33. http://doi.org/10.1016/j.biopsych.2009.03.017

Leblond, C. S., Nava, C., Polge, A., Gauthier, J., Huguet, G., Lumbroso, S., … Bourgeron, T. (2014). Meta-analysis of SHANK Mutations in Autism Spectrum Disorders: a gradient of severity in cognitive impairments. *PLoS Genetics*, *10*(9), e1004580. http://doi.org/10.1371/journal.pgen.1004580

Lechan, R. M., & Toni, R. (2013, February 22). Functional Anatomy of the Hypothalamus and Pituitary. MDText.com, Inc. Retrieved from http://www.ncbi.nlm.nih.gov/books/NBK279126/

Lee, J., Duan, W., & Mattson, M. P. (2002). Evidence that brain-derived neurotrophic factor is required for basal neurogenesis and mediates, in part, the enhancement of neurogenesis by dietary restriction in the hippocampus of adult mice. *Journal of Neurochemistry*, *82*(6), 1367–75. Retrieved from http://www.ncbi.nlm.nih.gov/pubmed/12354284

Leo Kanner's 1943 paper on autism —. (n.d.). Retrieved July 2, 2015, from http://sfari.org/news-and-opinion/classic-paper-reviews/2007/leo-kanners-1943-paper-on-autism-commentary-by-gerald-fischbach

Lim, S., Naisbitt, S., Yoon, J., Hwang, J.-I., Suh, P.-G., Sheng, M., & Kim, E. (1999). Characterization of the Shank Family of Synaptic Proteins: MULTIPLE GENES, ALTERNATIVE SPLICING, AND DIFFERENTIAL EXPRESSION IN BRAIN AND DEVELOPMENT. *Journal of Biological Chemistry*, *274*(41), 29510–29518. http://doi.org/10.1074/jbc.274.41.29510

Liu, F., Grauer, S., Kelley, C., Navarra, R., Graf, R., Zhang, G., … Marquis, K. L. (2008). ADX47273 [S-(4-fluoro-phenyl)-{3-[3-(4-fluoro-phenyl)-[1,2,4]-oxadiazol-5-yl]-piperidin-1-yl}-methanone]: a novel metabotropic glutamate receptor

5-selective positive allosteric modulator with preclinical antipsychotic-like and procognitive activities. *The Journal of Pharmacology and Experimental Therapeutics*, *327*(3), 827–39. http://doi.org/10.1124/jpet.108.136580

Liu, J., Koscielska, K. A., Cao, Z., Hulsizer, S., Grace, N., Mitchell, G., … Hagerman, P. J. (2012). Signaling defects in iPSC-derived fragile X premutation neurons. *Human Molecular Genetics*, *21*(17), 3795–805. http://doi.org/10.1093/hmg/dds207

Liu, X., Kawamura, Y., Shimada, T., Otowa, T., Koishi, S., Sugiyama, T., … Sasaki, T. (2010). Association of the oxytocin receptor (OXTR) gene polymorphisms with autism spectrum disorder (ASD) in the Japanese population. *Journal of Human Genetics*, *55*(3), 137–41. http://doi.org/10.1038/jhg.2009.140

Lloyd, A. C. (2013). The regulation of cell size. *Cell*, *154*(6), 1194–205. http://doi.org/10.1016/j.cell.2013.08.053

Lodish, H., Berk, A., Zipursky, S. L., Matsudaira, P., Baltimore, D., & Darnell, J. (2000). The Dynamics of Actin Assembly. W. H. Freeman. Retrieved from http://www.ncbi.nlm.nih.gov/books/NBK21594/

Lombardi, L. M., Baker, S. A., & Zoghbi, H. Y. (2015). MECP2 disorders: from the clinic to mice and back. *The Journal of Clinical Investigation*, *125*(8), 2914–23. http://doi.org/10.1172/JCI78167

Lord, C. (2011). Epidemiology: How common is autism? *Nature*, *474*(7350), 166–8. http://doi.org/10.1038/474166a

Loudes, C., Petit, F., Kordon, C., & Faivre-Bauman, A. (2000). Brain-derived neurotrophic factor but not neurotrophin-3 enhances differentiation of somatostatin neurons in hypothalamic cultures. *Neuroendocrinology*, *72*(3), 144–53. http://doi.org/54581

Lozano, R., Rosero, C. A., & Hagerman, R. J. (2014). Fragile X spectrum disorders. *Intractable & Rare Diseases Research*, *3*(4), 134–146. http://doi.org/10.5582/irdr.2014.01022

Luikenhuis, S., Giacometti, E., Beard, C. F., & Jaenisch, R. (2004). Expression of MeCP2 in postmitotic neurons rescues Rett syndrome in mice. *Proceedings of the National Academy of Sciences of the United States of America*, *101*(16), 6033–8. http://doi.org/10.1073/pnas.0401626101

Majzoub, J. A. (2006). Corticotropin-releasing hormone physiology. *European Journal of Endocrinology*, *155*(suppl_1), S71–S76. http://doi.org/10.1530/eje.1.02247

Mameza, M. G., Dvoretskova, E., Bamann, M., Hönck, H.-H., Güler, T., Boeckers, T. M., … Kreienkamp, H.-J. (2013). SHANK3 gene mutations associated with autism facilitate ligand binding to the Shank3 ankyrin repeat region. *The Journal of Biological Chemistry*, *288*(37), 26697–708. http://doi.org/10.1074/jbc.M112.424747

Manser, E., Loo, T. H., Koh, C. G., Zhao, Z. S., Chen, X. Q., Tan, L., … Lim, L. (1998). PAK kinases are directly coupled to the PIX family of nucleotide exchange factors. *Molecular Cell*, *1*(2), 183–92. Retrieved from http://www.ncbi.nlm.nih.gov/pubmed/9659915

Marchetto, M. C. N., Carromeu, C., Acab, A., Yu, D., Yeo, G. W., Mu, Y., … Muotri, A. R. (2010). A model for neural development and treatment of Rett syndrome using human induced pluripotent stem cells. *Cell*, *143*(4), 527–39. http://doi.org/10.1016/j.cell.2010.10.016

Martinez, M. C. (2003). Dual regulation of neuronal morphogenesis by a -catenin-cortactin complex and Rho. *The Journal of Cell Biology*, *162*(1), 99–111. http://doi.org/10.1083/jcb.200211025

Maunakea, A. K., Nagarajan, R. P., Bilenky, M., Ballinger, T. J., D'Souza, C., Fouse, S. D., … Costello, J. F. (2010). Conserved role of intragenic DNA methylation in regulating alternative promoters. *Nature*, *466*(7303), 253–7. http://doi.org/10.1038/nature09165

Mazur-Kolecka, B., Cohen, I. L., Jenkins, E. C., Kaczmarski, W., Flory, M., & Frackowiak, J. (2007). Altered development of neuronal progenitor cells after stimulation with autistic blood sera. *Brain Research*, *1168*, 11–20. http://doi.org/10.1016/j.brainres.2007.06.084

McAllister, A. K., Katz, L. C., & Lo, D. C. (1997). Opposing Roles for Endogenous BDNF and NT-3 in Regulating Cortical Dendritic Growth. *Neuron*, *18*(5), 767–778. http://doi.org/10.1016/S0896-6273(00)80316-5

McPheeters, M. L., Warren, Z., Sathe, N., Bruzek, J. L., Krishnaswami, S., Jerome, R. N., & Veenstra-Vanderweele, J. (2011). A systematic review of medical treatments for children with autism spectrum disorders. *Pediatrics*, *127*(5), e1312–21. http://doi.org/10.1542/peds.2011-0427

Meikle, L., Talos, D. M., Onda, H., Pollizzi, K., Rotenberg, A., Sahin, M., … Kwiatkowski, D. J. (2007). A mouse model of tuberous sclerosis: neuronal loss of Tsc1 causes dysplastic and ectopic neurons, reduced myelination, seizure activity, and limited survival. *The Journal of Neuroscience : The Official Journal of the Society for Neuroscience*, *27*(21), 5546–58. http://doi.org/10.1523/JNEUROSCI.5540-06.2007

Meinertzhagen, I. A., Takemura, S., Lu, Z., Huang, S., Gao, S., Ting, C.-Y., & Lee, C.-H. (2009). From form to function: the ways to know a neuron. *Journal of Neurogenetics*, *23*(1-2), 68–77. http://doi.org/10.1080/01677060802610604

Michailidis, I. E., Helton, T. D., Petrou, V. I., Mirshahi, T., Ehlers, M. D., & Logothetis, D. E. (2007). Phosphatidylinositol-4,5-bisphosphate regulates NMDA receptor activity through alpha-actinin. *The Journal of Neuroscience : The Official Journal of the Society for Neuroscience*, *27*(20), 5523–32. http://doi.org/10.1523/JNEUROSCI.4378-06.2007

Miettinen, M. (1987). Synaptophysin and neurofilament proteins as markers for neuroendocrine tumors. *Archives of Pathology & Laboratory Medicine*, *111*(9), 813–8. Retrieved from http://www.ncbi.nlm.nih.gov/pubmed/2820344

Moessner, R., Marshall, C. R., Sutcliffe, J. S., Skaug, J., Pinto, D., Vincent, J., … Scherer, S. W. (2007). Contribution of SHANK3 mutations to autism spectrum disorder. *American Journal of Human Genetics*, *81*(6), 1289–97. http://doi.org/10.1086/522590

Moretti, P., Levenson, J. M., Battaglia, F., Atkinson, R., Teague, R., Antalffy, B., … Zoghbi, H. Y. (2006). Learning and memory and synaptic plasticity are impaired in a mouse model of Rett syndrome. *The Journal of Neuroscience : The Official Journal of the Society for Neuroscience*, *26*(1), 319–27. http://doi.org/10.1523/JNEUROSCI.2623-05.2006

Moskal, J. R., Burgdorf, J., Kroes, R. A., Brudzynski, S. M., & Panksepp, J. (2011). A novel NMDA receptor glycine-site partial agonist, GLYX-13, has therapeutic potential for the treatment of autism. *Neuroscience and Biobehavioral Reviews*, *35*(9), 1982–8. http://doi.org/10.1016/j.neubiorev.2011.06.006

Naisbitt, S., Kim, E., Tu, J. C., Xiao, B., Sala, C., Valtschanoff, J., … Sheng, M. (1999). Shank, a Novel Family of Postsynaptic Density Proteins that Binds to the NMDA Receptor/PSD-95/GKAP Complex and Cortactin. *Neuron*, *23*(3), 569–582. http://doi.org/10.1016/S0896-6273(00)80809-0

Naisbitt, S., Kim, E., Tu, J. C., Xiao, B., Sala, C., Valtschanoff, J., … Sheng, M. (1999). Shank, a novel family of postsynaptic density proteins that binds to the NMDA receptor/PSD-95/GKAP complex and cortactin. *Neuron*, *23*(3), 569–82. Retrieved from http://www.ncbi.nlm.nih.gov/pubmed/10433268

Nakashima, S., Matsuda, H., Kurume, A., Oda, Y., Nakamura, S., Yamashita, M., & Yoshikawa, M. (2010). Cucurbitacin E as a new inhibitor of cofilin phosphorylation in human leukemia U937 cells. *Bioorganic & Medicinal Chemistry Letters*, *20*(9), 2994–7. http://doi.org/10.1016/j.bmcl.2010.02.062

Narsinh, K. H., Plews, J., & Wu, J. C. (2011). Comparison of human induced pluripotent and embryonic stem cells: fraternal or identical twins? *Molecular Therapy : The Journal of the American Society of Gene Therapy*, *19*(4), 635–8. http://doi.org/10.1038/mt.2011.41

NATHANS, D. INHIBITION OF PROTEIN SYNTHESIS BY PUROMYCIN. *Federation Proceedings*, *23*, 984–9. Retrieved from http://www.ncbi.nlm.nih.gov/pubmed/14209831

Navratil, A. M., Dozier, M. G., Whitesell, J. D., Clay, C. M., & Roberson, M. S. (2014). Role of cortactin in dynamic actin remodeling events in gonadotrope cells. *Endocrinology*, *155*(2), 548–57. http://doi.org/10.1210/en.2012-1924

Nelson, E. D., Kavalali, E. T., & Monteggia, L. M. (2006). MeCP2-dependent transcriptional repression regulates excitatory neurotransmission. *Current Biology : CB*, *16*(7), 710–6. http://doi.org/10.1016/j.cub.2006.02.062

Nemirovsky, S. I., Córdoba, M., Zaiat, J. J., Completa, S. P., Vega, P. A., González-Morón, D., … Kauffman, M. A. (2015). Whole genome sequencing reveals a de novo SHANK3 mutation in familial autism spectrum disorder. *PloS One*, *10*(2), e0116358. http://doi.org/10.1371/journal.pone.0116358

Nolen, B. (2015). WISH/DIP/SPIN90 Proteins Activate Arp2/3 Complex to Create Linear Actin Filaments that Seed Assembly of Branched Actin Networks. *Biophysical Journal*, *108*(2), 188a. http://doi.org/10.1016/j.bpj.2014.11.1040

Noutel, J., Hong, Y. K., Leu, B., Kang, E., & Chen, C. (2011). Experience-dependent retinogeniculate synapse remodeling is abnormal in MeCP2-deficient mice. *Neuron*, *70*(1), 35–42. http://doi.org/10.1016/j.neuron.2011.03.001

O'Kusky, J. R., Ye, P., & D'Ercole, A. J. (2000). Insulin-like growth factor-I promotes neurogenesis and synaptogenesis in the hippocampal dentate gyrus during postnatal development. *The Journal of Neuroscience : The Official Journal of the Society for Neuroscience*, *20*(22), 8435–42. Retrieved from http://www.ncbi.nlm.nih.gov/pubmed/11069951

Onore, C., Careaga, M., & Ashwood, P. (2012). The role of immune dysfunction in the pathophysiology of autism. *Brain, Behavior, and Immunity*, *26*(3), 383–92. http://doi.org/10.1016/j.bbi.2011.08.007

Pantaleón F, G., & Juvier R, T. (2015). [Molecular basis of Rett syndrome: A current look]. *Revista Chilena de Pediatria*. http://doi.org/10.1016/j.rchipe.2015.07.001

Park, E., Na, M., Choi, J., Kim, S., Lee, J.-R., Yoon, J., … Kim, E. (2003). The Shank family of postsynaptic density proteins interacts with and promotes synaptic accumulation of the beta PIX guanine nucleotide exchange factor for Rac1 and Cdc42. *The Journal of Biological Chemistry*, *278*(21), 19220–9. http://doi.org/10.1074/jbc.M301052200

Parkash, J., Cimino, I., Ferraris, N., Casoni, F., Wray, S., Cappy, H., … Giacobini, P. (2012). Suppression of β1-integrin in gonadotropin-releasing hormone cells disrupts migration and axonal extension resulting in severe reproductive alterations. *The Journal of Neuroscience : The Official Journal of the Society for Neuroscience*, *32*(47), 16992–7002. http://doi.org/10.1523/JNEUROSCI.3057-12.2012

Patkar, S., Tate, R., Modo, M., Plevin, R., & Carswell, H. V. O. (2012). Conditionally immortalised neural stem cells promote functional recovery and brain plasticity after transient focal cerebral ischaemia in mice. *Stem Cell Research*, *8*(1), 14–25. http://doi.org/10.1016/j.scr.2011.07.001

Peça, J., Feliciano, C., Ting, J. T., Wang, W., Wells, M. F., Venkatraman, T. N., … Feng, G. (2011). Shank3 mutant mice display autistic-like behaviours and striatal dysfunction. *Nature*, *472*(7344), 437–42. http://doi.org/10.1038/nature09965

Perrier, A. L., Tabar, V., Barberi, T., Rubio, M. E., Bruses, J., Topf, N., … Studer, L. (2004). Derivation of midbrain dopamine neurons from human embryonic stem cells. *Proceedings of the National Academy of Sciences of the United States of America*, *101*(34), 12543–8. http://doi.org/10.1073/pnas.0404700101

Pinyol, R., Haeckel, A., Ritter, A., Qualmann, B., & Kessels, M. M. (2007). Regulation of N-WASP and the Arp2/3 complex by Abp1 controls neuronal morphology. *PloS One*, *2*(5), e400. http://doi.org/10.1371/journal.pone.0000400

Pollard, T. D. (2007). Regulation of actin filament assembly by Arp2/3 complex and formins. *Annual Review of Biophysics and Biomolecular Structure*, *36*, 451–77. http://doi.org/10.1146/annurev.biophys.35.040405.101936

Proepper, C., Johannsen, S., Liebau, S., Dahl, J., Vaida, B., Bockmann, J., … Boeckers, T. M. (2007). Abelson interacting protein 1 (Abi-1) is essential for dendrite morphogenesis and synapse formation. *The EMBO Journal*, *26*(5), 1397–409. http://doi.org/10.1038/sj.emboj.7601569

Qualmann, B., Boeckers, T. M., Jeromin, M., Gundelfinger, E. D., & Kessels, M. M. (2004). Linkage of the actin cytoskeleton to the postsynaptic density via direct interactions of Abp1 with the ProSAP/Shank family. *The Journal of Neuroscience : The Official Journal of the Society for Neuroscience*, *24*(10), 2481–95. http://doi.org/10.1523/JNEUROSCI.5479-03.2004

Quintanar, J. L., & Guzmán-Soto, I. (2013). Hypothalamic neurohormones and immune responses. *Frontiers in Integrative Neuroscience*, *7*, 56. http://doi.org/10.3389/fnint.2013.00056

Quitsch, A., Berhörster, K., Liew, C. W., Richter, D., & Kreienkamp, H.-J. (2005). Postsynaptic shank antagonizes dendrite branching induced by the leucine-rich repeat protein Densin-180. *The Journal of Neuroscience : The Official Journal of the Society for Neuroscience*, *25*(2), 479–87. http://doi.org/10.1523/JNEUROSCI.2699-04.2005

Ransdell, J. L., Faust, T. B., & Schulz, D. J. (2010). Correlated Levels of mRNA and Soma Size in Single Identified Neurons: Evidence for Compartment-specific Regulation of Gene Expression. *Frontiers in Molecular Neuroscience*, *3*, 116. http://doi.org/10.3389/fnmol.2010.00116

Raynaud, F., Janossy, A., Dahl, J., Bertaso, F., Perroy, J., Varrault, A., … Homburger, V. (2013). Shank3-Rich2 interaction regulates AMPA receptor recycling and synaptic long-term potentiation. *The Journal of Neuroscience : The Official Journal of the Society for Neuroscience*, *33*(23), 9699–715. http://doi.org/10.1523/JNEUROSCI.2725-12.2013

Raynaud, F., Moutin, E., Schmidt, S., Dahl, J., Bertaso, F., Boeckers, T. M., … Fagni, L. (2014). Rho-GTPase-activating protein interacting with Cdc-42-interacting protein 4 homolog 2 (Rich2): a new Ras-related C3 botulinum toxin substrate 1 (Rac1) GTPase-activating protein that controls dendritic spine morphogenesis. *The Journal of Biological Chemistry*, *289*(5), 2600–9. http://doi.org/10.1074/jbc.M113.534636

Richnau, N., & Aspenström, P. (2001). Rich, a rho GTPase-activating protein domain-containing protein involved in signaling by Cdc42 and Rac1. *The Journal of Biological Chemistry*, *276*(37), 35060–70. http://doi.org/10.1074/jbc.M103540200

Román, G. C., Ghassabian, A., Bongers-Schokking, J. J., Jaddoe, V. W. V, Hofman, A., de Rijke, Y. B., … Tiemeier, H. (2013). Association of gestational maternal hypothyroxinemia and increased autism risk. *Annals of Neurology*, *74*(5), 733–42. http://doi.org/10.1002/ana.23976

Rosenmund, C., & Westbrook, G. L. (1993). Calcium-induced actin depolymerization reduces NMDA channel activity. *Neuron*, *10*(5), 805–14. Retrieved from http://www.ncbi.nlm.nih.gov/pubmed/7684233

Rossignol, D. A., & Frye, R. E. (2012). Mitochondrial dysfunction in autism spectrum disorders: a systematic review and meta-analysis. *Molecular Psychiatry*, *17*(3), 290–314. http://doi.org/10.1038/mp.2010.136

Rycroft, B. K., & Gibb, A. J. (2004). Regulation of single NMDA receptor channel activity by alpha-actinin and calmodulin in rat hippocampal granule cells. *The Journal of Physiology*, *557*(Pt 3), 795–808. http://doi.org/10.1113/jphysiol.2003.059212

Salimi, A., Nadri, S., Ghollasi, M., Khajeh, K., & Soleimani, M. (2014). Comparison of different protocols for neural differentiation of human induced pluripotent stem cells. *Molecular Biology Reports*, *41*(3), 1713–21. http://doi.org/10.1007/s11033-014-3020-1

Santini, E., Huynh, T. N., MacAskill, A. F., Carter, A. G., Pierre, P., Ruggero, D., … Klann, E. (2013). Exaggerated translation causes synaptic and behavioural aberrations associated with autism. *Nature*, *493*(7432), 411–5. http://doi.org/10.1038/nature11782

Schmeisser, M. J., Ey, E., Wegener, S., Bockmann, J., Stempel, A. V., Kuebler, A., … Boeckers, T. M. (2012). Autistic-like behaviours and hyperactivity in mice lacking ProSAP1/Shank2. *Nature*, *486*(7402), 256–60. http://doi.org/10.1038/nature11015

Schmidt, E. K., Clavarino, G., Ceppi, M., & Pierre, P. (2009a). SUnSET, a nonradioactive method to monitor protein synthesis. *Nature Methods*, *6*(4), 275–7. http://doi.org/10.1038/nmeth.1314

Schmidt, E. K., Clavarino, G., Ceppi, M., & Pierre, P. (2009b). SUnSET, a nonradioactive method to monitor protein synthesis. *Nature Methods*, *6*(4), 275–7. http://doi.org/10.1038/nmeth.1314

Schuetz, G., Rosário, M., Grimm, J., Boeckers, T. M., Gundelfinger, E. D., & Birchmeier, W. (2004). The neuronal scaffold protein Shank3 mediates signaling and biological function of the receptor tyrosine kinase Ret in epithelial cells. *The Journal of Cell Biology*, *167*(5), 945–52. http://doi.org/10.1083/jcb.200404108

Schulkin, J. (2007). Autism and the amygdala: an endocrine hypothesis. *Brain and Cognition*, *65*(1), 87–99. http://doi.org/10.1016/j.bandc.2006.02.009

Schumann, C. M., Hamstra, J., Goodlin-Jones, B. L., Lotspeich, L. J., Kwon, H., Buonocore, M. H., … Amaral, D. G. (2004). The amygdala is enlarged in children but not adolescents with autism; the hippocampus is enlarged at all ages. *The Journal of Neuroscience : The Official Journal of the Society for Neuroscience*, *24*(28), 6392–401. http://doi.org/10.1523/JNEUROSCI.1297-04.2004

Sengupta, S., Peterson, T. R., & Sabatini, D. M. (2010). Regulation of the mTOR complex 1 pathway by nutrients, growth factors, and stress. *Molecular Cell*, *40*(2), 310–22. http://doi.org/10.1016/j.molcel.2010.09.026

Shao, K., Koch, C., Gupta, M. K., Lin, Q., Lenz, M., Laufs, S., … Wagner, W. (2013). Induced pluripotent mesenchymal stromal cell clones retain donor-derived differences in DNA methylation profiles. *Molecular Therapy : The Journal of the American Society of Gene Therapy*, *21*(1), 240–50. http://doi.org/10.1038/mt.2012.207

Shcheglovitov, A., Shcheglovitova, O., Yazawa, M., Portmann, T., Shu, R., Sebastiano, V., … Dolmetsch, R. E. (2013a). SHANK3 and IGF1 restore synaptic deficits in neurons from 22q13 deletion syndrome patients. *Nature*, *503*(7475), 267–71. http://doi.org/10.1038/nature12618

Shcheglovitov, A., Shcheglovitova, O., Yazawa, M., Portmann, T., Shu, R., Sebastiano, V., … Dolmetsch, R. E. (2013b). SHANK3 and IGF1 restore synaptic deficits in neurons from 22q13 deletion syndrome patients. *Nature*, *503*(7475), 267–71. http://doi.org/10.1038/nature12618

Sheng, M., & Kim, E. (2000). The Shank family of scaffold proteins. *Journal of Cell Science*, *113 (Pt 1*, 1851–6. Retrieved from http://www.ncbi.nlm.nih.gov/pubmed/10806096

Shepherd, G. M. G. (2013). Corticostriatal connectivity and its role in disease. *Nature Reviews. Neuroscience*, *14*(4), 278–91. http://doi.org/10.1038/nrn3469

Sheridan, S. D., Theriault, K. M., Reis, S. A., Zhou, F., Madison, J. M., Daheron, L., … Haggarty, S. J. (2011). Epigenetic characterization of the FMR1 gene and aberrant neurodevelopment in human induced pluripotent stem cell models of fragile X syndrome. *PloS One*, *6*(10), e26203. http://doi.org/10.1371/journal.pone.0026203

Shi, Y., Kirwan, P., & Livesey, F. J. (2012). Directed differentiation of human pluripotent stem cells to cerebral cortex neurons and neural networks. *Nature Protocols*, *7*(10), 1836–46. http://doi.org/10.1038/nprot.2012.116

Shoji, K., Ohashi, K., Sampei, K., Oikawa, M., & Mizuno, K. (2012). Cytochalasin D acts as an inhibitor of the actin-cofilin interaction. *Biochemical and Biophysical Research Communications*, *424*(1), 52–7. http://doi.org/10.1016/j.bbrc.2012.06.063

Smith, S. M., & Vale, W. W. (2006). The role of the hypothalamic-pituitary-adrenal axis in neuroendocrine responses to stress. *Dialogues in Clinical Neuroscience*, *8*(4), 383–95. Retrieved from http://www.pubmedcentral.nih.gov/articlerender.fcgi?artid=3181830&tool=pmcentrez&rendertype=abstract

Smrt, R. D., Eaves-Egenes, J., Barkho, B. Z., Santistevan, N. J., Zhao, C., Aimone, J. B., … Zhao, X. (2007). Mecp2 deficiency leads to delayed maturation and altered gene expression in hippocampal neurons. *Neurobiology of Disease*, *27*(1), 77–89. http://doi.org/10.1016/j.nbd.2007.04.005

Spratt, E. G., Nicholas, J. S., Brady, K. T., Carpenter, L. A., Hatcher, C. R., Meekins, K. A., … Charles, J. M. (2012). Enhanced cortisol response to stress in children in autism. *Journal of Autism and Developmental Disorders*, *42*(1), 75–81. http://doi.org/10.1007/s10803-011-1214-0

Sterneckert, J. L., Reinhardt, P., & Schöler, H. R. (2014). Investigating human disease using stem cell models. *Nature Reviews. Genetics*, *15*(9), 625–39. http://doi.org/10.1038/nrg3764

Suvrathan, A., Hoeffer, C. A., Wong, H., Klann, E., & Chattarji, S. (2010). Characterization and reversal of synaptic defects in the amygdala in a mouse model of fragile X syndrome. *Proceedings of the National Academy of Sciences of the United States of America*, *107*(25), 11591–6. http://doi.org/10.1073/pnas.1002262107

Swaab, D. F. (2008). Sexual orientation and its basis in brain structure and function. *Proceedings of the National Academy of Sciences of the United States of America*, *105*(30), 10273–4. http://doi.org/10.1073/pnas.0805542105

Takahashi, K., Tanabe, K., Ohnuki, M., Narita, M., Ichisaka, T., Tomoda, K., & Yamanaka, S. (2007). Induction of pluripotent stem cells from adult human fibroblasts by defined factors. *Cell*, *131*(5), 861–72. http://doi.org/10.1016/j.cell.2007.11.019

Takahashi, K., & Yamanaka, S. (2006). Induction of pluripotent stem cells from mouse embryonic and adult fibroblast cultures by defined factors. *Cell*, *126*(4), 663–76. http://doi.org/10.1016/j.cell.2006.07.024

Tapia-Arancibia, L., Rage, F., Givalois, L., & Arancibia, S. (2004). Physiology of BDNF: focus on hypothalamic function. *Frontiers in Neuroendocrinology*, *25*(2), 77–107. http://doi.org/10.1016/j.yfrne.2004.04.001

Tavazoie, S. F., Alvarez, V. A., Ridenour, D. A., Kwiatkowski, D. J., & Sabatini, B. L. (2005). Regulation of neuronal morphology and function by the tumor suppressors Tsc1 and Tsc2. *Nature Neuroscience*, *8*(12), 1727–34. http://doi.org/10.1038/nn1566

Tavosanis, G. (2012). Dendritic structural plasticity. *Developmental Neurobiology*, *72*(1), 73–86. http://doi.org/10.1002/dneu.20951

Tornero, D., Wattananit, S., Grønning Madsen, M., Koch, P., Wood, J., Tatarishvili, J., … Kokaia, Z. (2013). Human induced pluripotent stem cell-derived cortical neurons integrate in stroke-injured cortex and improve functional recovery. *Brain : A Journal of Neurology*, *136*(Pt 12), 3561–77. http://doi.org/10.1093/brain/awt278

Tropea, D., Giacometti, E., Wilson, N. R., Beard, C., McCurry, C., Fu, D. D., … Sur, M. (2009). Partial reversal of Rett Syndrome-like symptoms in MeCP2 mutant mice. *Proceedings of the National Academy of Sciences of the United States of America*, *106*(6), 2029–34. http://doi.org/10.1073/pnas.0812394106

Tsai, P.-S., Moenter, S. M., Postigo, H. R., El Majdoubi, M., Pak, T. R., Gill, J. C., … Weiner, R. I. (2005). Targeted expression of a dominant-negative fibroblast growth factor (FGF) receptor in gonadotropin-releasing hormone (GnRH) neurons reduces FGF responsiveness and the size of GnRH neuronal population. *Molecular Endocrinology (Baltimore, Md.)*, *19*(1), 225–36. http://doi.org/10.1210/me.2004-0330

Tsilioni, I., Dodman, N., Petra, A. I., Taliou, A., Francis, K., Moon-Fanelli, A., … Theoharides, T. C. (2014). Elevated serum neurotensin and CRH levels in children with autistic spectrum disorders and tail-chasing Bull Terriers with a phenotype similar to autism. *Translational Psychiatry*, *4*, e466. http://doi.org/10.1038/tp.2014.106

Tu, J. C., Xiao, B., Naisbitt, S., Yuan, J. P., Petralia, R. S., Brakeman, P., … Worley, P. F. (1999). Coupling of mGluR/Homer and PSD-95 complexes by the Shank family of postsynaptic density proteins. *Neuron*, *23*(3), 583–92. Retrieved from http://www.ncbi.nlm.nih.gov/pubmed/10433269

Uchino, S., Wada, H., Honda, S., Nakamura, Y., Ondo, Y., Uchiyama, T., … Kohsaka, S. (2006). Direct interaction of post-synaptic density-95/Dlg/ZO-1 domain-containing synaptic molecule Shank3 with GluR1 alpha-amino-3-hydroxy-5-methyl-4-isoxazole propionic acid receptor. *Journal of Neurochemistry*, *97*(4), 1203–14. http://doi.org/10.1111/j.1471-4159.2006.03831.x

Uchino, S., & Waga, C. (2013). SHANK3 as an autism spectrum disorder-associated gene. *Brain & Development*, *35*(2), 106–10. http://doi.org/10.1016/j.braindev.2012.05.013

Urbach, A., Bar-Nur, O., Daley, G. Q., & Benvenisty, N. (2010). Differential modeling of fragile X syndrome by human embryonic stem cells and induced pluripotent stem cells. *Cell Stem Cell*, *6*(5), 407–11. http://doi.org/10.1016/j.stem.2010.04.005

Uslaner, J. M., Parmentier-Batteur, S., Flick, R. B., Surles, N. O., Lam, J. S. H., McNaughton, C. H., … Hutson, P. H. Dose-dependent effect of CDPPB, the mGluR5 positive allosteric modulator, on recognition memory is associated with GluR1 and CREB phosphorylation in the prefrontal cortex and hippocampus. *Neuropharmacology*, *57*(5-6), 531–8. http://doi.org/10.1016/j.neuropharm.2009.07.022

van Kooten, I. A. J., Palmen, S. J. M. C., von Cappeln, P., Steinbusch, H. W. M., Korr, H., Heinsen, H., … Schmitz, C. (2008). Neurons in the fusiform gyrus are fewer and smaller in autism. *Brain : A Journal of Neurology*, *131*(Pt 4), 987–99. http://doi.org/10.1093/brain/awn033

Veenstra-VanderWeele, J., & Cook, E. H. (2004). Molecular genetics of autism spectrum disorder. *Molecular Psychiatry*, *9*(9), 819–32. http://doi.org/10.1038/sj.mp.4001505

Verpelli, C., Dvoretskova, E., Vicidomini, C., Rossi, F., Chiappalone, M., Schoen, M., … Sala, C. (2011a). Importance of Shank3 protein in regulating metabotropic glutamate receptor 5 (mGluR5) expression and signaling at synapses. *The Journal of Biological Chemistry*, *286*(40), 34839–50. http://doi.org/10.1074/jbc.M111.258384

Verpelli, C., Dvoretskova, E., Vicidomini, C., Rossi, F., Chiappalone, M., Schoen, M., … Sala, C. (2011b). Importance of Shank3 protein in regulating metabotropic glutamate receptor 5 (mGluR5) expression and signaling at synapses. *The Journal of Biological Chemistry*, *286*(40), 34839–50. http://doi.org/10.1074/jbc.M111.258384

Verpelli, C., Schmeisser, M. J., Sala, C., & Boeckers, T. M. (2012). Scaffold proteins at the postsynaptic density. *Advances in Experimental Medicine and Biology*, *970*, 29–61. http://doi.org/10.1007/978-3-7091-0932-8_2

Waga, C., Okamoto, N., Ondo, Y., Fukumura-Kato, R., Goto, Y.-I., Kohsaka, S., & Uchino, S. (2011). Novel variants of the SHANK3 gene in Japanese autistic patients with severe delayed speech development. *Psychiatric Genetics*, *21*(4), 208–11. http://doi.org/10.1097/YPG.0b013e328341e069

Wagner, A. R., Luan, Q., Liu, S.-L., & Nolen, B. J. (2013). Dip1 defines a class of Arp2/3 complex activators that function without preformed actin filaments. *Current Biology : CB*, *23*(20), 1990–8. http://doi.org/10.1016/j.cub.2013.08.029

Wang, L., Meece, K., Williams, D. J., Lo, K. A., Zimmer, M., Heinrich, G., … Leibel, R. L. (2015). Differentiation of hypothalamic-like neurons from human pluripotent stem cells. *The Journal of Clinical Investigation*, *125*(2), 796–808. http://doi.org/10.1172/JCI79220

Wang, X., McCoy, P. A., Rodriguiz, R. M., Pan, Y., Je, H. S., Roberts, A. C., … Jiang, Y.-H. (2011). Synaptic dysfunction and abnormal behaviors in mice lacking major isoforms of Shank3. *Human Molecular Genetics*, *20*(15), 3093–108. http://doi.org/10.1093/hmg/ddr212

Wang, Y., Wang, W., Li, D., Li, M., Wang, P., Wen, J., … Yin, Y. (2014). IGF-1 alleviates NMDA-induced excitotoxicity in cultured hippocampal neurons against autophagy via the NR2B/PI3K-AKT-mTOR pathway. *Journal of Cellular Physiology*, *229*(11), 1618–29. http://doi.org/10.1002/jcp.24607

Waterhouse, E. G., An, J. J., Orefice, L. L., Baydyuk, M., Liao, G.-Y., Zheng, K., … Xu, B. (2012). BDNF promotes differentiation and maturation of adult-born neurons through GABAergic transmission. *The Journal of Neuroscience : The Official Journal of the Society for Neuroscience*, *32*(41), 14318–30. http://doi.org/10.1523/JNEUROSCI.0709-12.2012

Wegiel, J., Flory, M., Kuchna, I., Nowicki, K., Ma, S. Y., Imaki, H., … Brown, W. T. (2015). Neuronal nucleus and cytoplasm volume deficit in children with autism and volume increase in adolescents and adults. *Acta Neuropathologica Communications*, *3*, 2. http://doi.org/10.1186/s40478-015-0183-5

Wegiel, J., Kuchna, I., Nowicki, K., Imaki, H., Wegiel, J., Marchi, E., … Wisniewski, T. (2010). The neuropathology of autism: defects of neurogenesis and neuronal migration, and dysplastic changes. *Acta Neuropathologica*, *119*(6), 755–70. http://doi.org/10.1007/s00401-010-0655-4

Welsh, J. P., Ahn, E. S., & Placantonakis, D. G. Is autism due to brain desynchronization? *International Journal of Developmental Neuroscience : The Official Journal of the International Society for Developmental Neuroscience*, *23*(2-3), 253–63. http://doi.org/10.1016/j.ijdevneu.2004.09.002

Whitlock, K. E. (2005). Origin and development of GnRH neurons. *Trends in Endocrinology and Metabolism: TEM*, *16*(4), 145–51. http://doi.org/10.1016/j.tem.2005.03.005

Wierman, M. E., Kiseljak-Vassiliades, K., & Tobet, S. (2011). Gonadotropin-releasing hormone (GnRH) neuron migration: initiation, maintenance and cessation as critical steps to ensure normal reproductive function. *Frontiers in Neuroendocrinology*, *32*(1), 43–52. http://doi.org/10.1016/j.yfrne.2010.07.005

Williams, D. L., & Lindsley, C. W. (2005). Discovery of positive allosteric modulators of metabotropic glutamate receptor subtype 5 (mGluR5). *Current Topics in Medicinal Chemistry*, *5*(9), 825–46. Retrieved from http://www.ncbi.nlm.nih.gov/pubmed/16178729

Wilson, P. G., & Stice, S. S. (2006). Development and differentiation of neural rosettes derived from human embryonic stem cells. *Stem Cell Reviews*, *2*(1), 67–77. http://doi.org/10.1007/s12015-006-0011-1

Winder, S. J., & Ayscough, K. R. (2005). Actin-binding proteins. *Journal of Cell Science*, *118*(Pt 4), 651–4. http://doi.org/10.1242/jcs.01670

Won, H., Lee, H.-R., Gee, H. Y., Mah, W., Kim, J.-I., Lee, J., … Kim, E. (2012). Autistic-like social behaviour in Shank2-mutant mice improved by restoring NMDA receptor function. *Nature*, *486*(7402), 261–5. http://doi.org/10.1038/nature11208

Won, H., Mah, W., & Kim, E. (2013). Autism spectrum disorder causes, mechanisms, and treatments: focus on neuronal synapses. *Frontiers in Molecular Neuroscience*, *6*, 19. http://doi.org/10.3389/fnmol.2013.00019

Wray, S. (2010). From nose to brain: development of gonadotrophin-releasing hormone-1 neurones. *Journal of Neuroendocrinology*, *22*(7), 743–53. http://doi.org/10.1111/j.1365-2826.2010.02034.x

Xi, D., Li, Y.-C., Snyder, M. A., Gao, R. Y., Adelman, A. E., Zhang, W., … Gao, W.-J. (2011). Group II metabotropic glutamate receptor agonist ameliorates MK801-induced dysfunction of NMDA receptors via the Akt/GSK-3β pathway in adult rat prefrontal cortex. *Neuropsychopharmacology : Official Publication of the American College of Neuropsychopharmacology*, *36*(6), 1260–74. http://doi.org/10.1038/npp.2011.12

Yang, M., Bozdagi, O., Scattoni, M. L., Wöhr, M., Roullet, F. I., Katz, A. M., … Crawley, J. N. (2012). Reduced excitatory neurotransmission and mild autism-relevant phenotypes in adolescent Shank3 null mutant mice. *The Journal of Neuroscience : The Official Journal of the Society for Neuroscience*, *32*(19), 6525–41. http://doi.org/10.1523/JNEUROSCI.6107-11.2012

Yao, I., Hata, Y., Hirao, K., Deguchi, M., Ide, N., Takeuchi, M., & Takai, Y. (1999). Synamon, a novel neuronal protein interacting with synapse-associated protein 90/postsynaptic density-95-associated protein. *The Journal of Biological Chemistry*, *274*(39), 27463–6. Retrieved from http://www.ncbi.nlm.nih.gov/pubmed/10488079

Yau, V. M., Lutsky, M., Yoshida, C. K., Lasley, B., Kharrazi, M., Windham, G., … Croen, L. A. (2015). Prenatal and neonatal thyroid stimulating hormone levels and autism spectrum disorders. *Journal of Autism and Developmental Disorders*, *45*(3), 719–30. http://doi.org/10.1007/s10803-014-2227-2

Zheng, J.-J., Yang, X., Zhang, L.-Y., Fei, Q.-J., Pan, C.-S., Ni, W.-H., … Huang, X.-F. (2012). [Sperm DNA damage and sperm-nucleoprotein transition correlate to acrosin activity and seminal parameters]. *Zhonghua Nan Ke Xue = National Journal of Andrology*, *18*(10), 925–9. Retrieved from http://www.ncbi.nlm.nih.gov/pubmed/23297503

Zoghbi, H. Y. (2003). Postnatal neurodevelopmental disorders: meeting at the synapse? *Science (New York, N.Y.)*, *302*(5646), 826–30. http://doi.org/10.1126/science.1089071

Achard, V., Martiel, J.-L., Michelot, A., Guérin, C., Reymann, A.-C., Blanchoin, L., & Boujemaa-Paterski, R. (2010). A “primer”-based mechanism underlies branched actin filament network formation and motility. *Current Biology : CB*, *20*(5), 423–8. http://doi.org/10.1016/j.cub.2009.12.056

Allan, C. M. (2013). RABL-regulated pathways: a new tale in sperm function. *Asian Journal of Andrology*, *15*(1), 87–8. http://doi.org/10.1038/aja.2012.137

Amaral, D. G., Schumann, C. M., & Nordahl, C. W. (2008). Neuroanatomy of autism. *Trends in Neurosciences*, *31*(3), 137–45. http://doi.org/10.1016/j.tins.2007.12.005

Ananiev, G., Williams, E. C., Li, H., & Chang, Q. (2011). Isogenic pairs of wild type and mutant induced pluripotent stem cell (iPSC) lines from Rett syndrome patients as in vitro disease model. *PloS One*, *6*(9), e25255. http://doi.org/10.1371/journal.pone.0025255

Andari, E., Duhamel, J.-R., Zalla, T., Herbrecht, E., Leboyer, M., & Sirigu, A. (2010). Promoting social behavior with oxytocin in high-functioning autism spectrum disorders. *Proceedings of the National Academy of Sciences of the United States of America*, *107*(9), 4389–94. http://doi.org/10.1073/pnas.0910249107

Antar, L. N., Dictenberg, J. B., Plociniak, M., Afroz, R., & Bassell, G. J. (2005). Localization of FMRP-associated mRNA granules and requirement of microtubules for activity-dependent trafficking in hippocampal neurons. *Genes, Brain, and Behavior*, *4*(6), 350–9. http://doi.org/10.1111/j.1601-183X.2005.00128.x

Arber, C., Precious, S. V, Cambray, S., Risner-Janiczek, J. R., Kelly, C., Noakes, Z., … Li, M. (2015). Activin A directs striatal projection neuron differentiation of human pluripotent stem cells. *Development (Cambridge, England)*, *142*(7), 1375–86. http://doi.org/10.1242/dev.117093

Asaka, Y., Jugloff, D. G. M., Zhang, L., Eubanks, J. H., & Fitzsimonds, R. M. (2006). Hippocampal synaptic plasticity is impaired in the Mecp2-null mouse model of Rett syndrome. *Neurobiology of Disease*, *21*(1), 217–27. http://doi.org/10.1016/j.nbd.2005.07.005

Auerbach, B. D., Osterweil, E. K., & Bear, M. F. (2011). Mutations causing syndromic autism define an axis of synaptic pathophysiology. *Nature*, *480*(7375), 63–8. http://doi.org/10.1038/nature10658

Ayala, J. E., Chen, Y., Banko, J. L., Sheffler, D. J., Williams, R., Telk, A. N., … Conn, P. J. (2009). mGluR5 positive allosteric modulators facilitate both hippocampal LTP and LTD and enhance spatial learning. *Neuropsychopharmacology : Official Publication of the American College of Neuropsychopharmacology*, *34*(9), 2057–71. http://doi.org/10.1038/npp.2009.30

Backman, S. A., Stambolic, V., & Mak, T. W. (2002). PTEN function in mammalian cell size regulation. *Current Opinion in Neurobiology*, *12*(5), 516–522. http://doi.org/10.1016/S0959-4388(02)00354-9

Baird, G., Cass, H., & Slonims, V. (2003). Diagnosis of autism. *BMJ (Clinical Research Ed.)*, *327*(7413), 488–93. http://doi.org/10.1136/bmj.327.7413.488

Baird, G., Simonoff, E., Pickles, A., Chandler, S., Loucas, T., Meldrum, D., & Charman, T. (2006a). Prevalence of disorders of the autism spectrum in a population cohort of children in South Thames: the Special Needs and Autism Project (SNAP). *The Lancet*, *368*(9531). Retrieved from https://kclpure.kcl.ac.uk/portal/en/publications/prevalence-of-disorders-of-the-autism-spectrum-in-a-population-cohort-of-children-in-south-thames-the-special-needs-and-autism-project-snap(5a0ab4da-87b2-4e77-8c8d-e3bac57f3ce7).html

Baird, G., Simonoff, E., Pickles, A., Chandler, S., Loucas, T., Meldrum, D., & Charman, T. (2006b). Prevalence of disorders of the autism spectrum in a population cohort of children in South Thames: the Special Needs and Autism Project (SNAP). *Lancet*, *368*(9531), 210–5. http://doi.org/10.1016/S0140-6736(06)69041-7

Bakos, J., Bacova, Z., Grant, S. G., Castejon, A. M., & Ostatnikova, D. (2015). Are Molecules Involved in Neuritogenesis and Axon Guidance Related to Autism Pathogenesis? *Neuromolecular Medicine*. http://doi.org/10.1007/s12017-015-8357-7

Bamburg, J. R. (1999). Proteins of the ADF/cofilin family: essential regulators of actin dynamics. *Annual Review of Cell and Developmental Biology*, *15*, 185–230. http://doi.org/10.1146/annurev.cellbio.15.1.185

Baron-Cohen, S., Auyeung, B., Nørgaard-Pedersen, B., Hougaard, D. M., Abdallah, M. W., Melgaard, L., … Lombardo, M. V. (2015). Elevated fetal steroidogenic activity in autism. *Molecular Psychiatry*, *20*(3), 369–76. http://doi.org/10.1038/mp.2014.48

Bassell, G. J., & Warren, S. T. (2008). Fragile X syndrome: loss of local mRNA regulation alters synaptic development and function. *Neuron*, *60*(2), 201–14. http://doi.org/10.1016/j.neuron.2008.10.004

Basson, M. A., & Wingate, R. J. (2013). Congenital hypoplasia of the cerebellum: developmental causes and behavioral consequences. *Frontiers in Neuroanatomy*, *7*, 29. http://doi.org/10.3389/fnana.2013.00029

Bath, K. G., Akins, M. R., & Lee, F. S. (2012). BDNF control of adult SVZ neurogenesis. *Developmental Psychobiology*, *54*(6), 578–89. http://doi.org/10.1002/dev.20546

Bauman, M., & Kemper, T. L. (1985). Histoanatomic observations of the brain in early infantile autism. *Neurology*, *35*(6), 866–74. Retrieved from http://www.ncbi.nlm.nih.gov/pubmed/4000488

Bauman, M. L., & Kemper, T. L. Neuroanatomic observations of the brain in autism: a review and future directions. *International Journal of Developmental Neuroscience : The Official Journal of the International Society for Developmental Neuroscience*, *23*(2-3), 183–7. http://doi.org/10.1016/j.ijdevneu.2004.09.006

Bauman, M. L., Kemper, T. L., & Arin, D. M. (1995). Pervasive neuroanatomic abnormalities of the brain in three cases of Rett's syndrome. *Neurology*, *45*(8), 1581–6. Retrieved from http://www.ncbi.nlm.nih.gov/pubmed/7644058

Becker, E. B. E., & Stoodley, C. J. (2013). *Neurobiology of Autism*. *International review of neurobiology* (Vol. 113). Elsevier. http://doi.org/10.1016/B978-0-12-418700-9.00001-0

Belmonte, M. K., Allen, G., Beckel-Mitchener, A., Boulanger, L. M., Carper, R. A., & Webb, S. J. (2004). Autism and abnormal development of brain connectivity. *The Journal of Neuroscience : The Official Journal of the Society for Neuroscience*, *24*(42), 9228–31. http://doi.org/10.1523/JNEUROSCI.3340-04.2004

Berkel, S., Marshall, C. R., Weiss, B., Howe, J., Roeth, R., Moog, U., … Rappold, G. A. (2010). Mutations in the SHANK2 synaptic scaffolding gene in autism spectrum disorder and mental retardation. *Nature Genetics*, *42*(6), 489–91. http://doi.org/10.1038/ng.589

Betancur, C. (2011). Etiological heterogeneity in autism spectrum disorders: more than 100 genetic and genomic disorders and still counting. *Brain Research*, *1380*, 42–77. http://doi.org/10.1016/j.brainres.2010.11.078

Betancur, C., & Buxbaum, J. D. (2013). SHANK3 haploinsufficiency: a “common” but underdiagnosed highly penetrant monogenic cause of autism spectrum disorders. *Molecular Autism*, *4*(1), 17. http://doi.org/10.1186/2040-2392-4-17

Bhattacharyya, A., McMillan, E., Wallace, K., Tubon, T. C., Capowski, E. E., & Svendsen, C. N. (2008). Normal Neurogenesis but Abnormal Gene Expression in Human Fragile X Cortical Progenitor Cells. *Stem Cells and Development*, *17*(1), 107–17. http://doi.org/10.1089/scd.2007.0073

Blundell, J., Blaiss, C. A., Etherton, M. R., Espinosa, F., Tabuchi, K., Walz, C., … Powell, C. M. (2010). Neuroligin-1 deletion results in impaired spatial memory and increased repetitive behavior. *The Journal of Neuroscience : The Official Journal of the Society for Neuroscience*, *30*(6), 2115–29. http://doi.org/10.1523/JNEUROSCI.4517-09.2010

Boccuto, L., Lauri, M., Sarasua, S. M., Skinner, C. D., Buccella, D., Dwivedi, A., … Schwartz, C. E. (2013). Prevalence of SHANK3 variants in patients with different subtypes of autism spectrum disorders. *European Journal of Human Genetics : EJHG*, *21*(3), 310–6. http://doi.org/10.1038/ejhg.2012.175

Boeckers, T. M., Bockmann, J., Kreutz, M. R., & Gundelfinger, E. D. (2002). ProSAP/Shank proteins - a family of higher order organizing molecules of the postsynaptic density with an emerging role in human neurological disease. *Journal of Neurochemistry*, *81*(5), 903–10. Retrieved from http://www.ncbi.nlm.nih.gov/pubmed/12065602

Boeckers, T. M., Kreutz, M. R., Winter, C., Zuschratter, W., Smalla, K. H., Sanmarti-Vila, L., … Gundelfinger, E. D. (1999). Proline-rich synapse-associated protein-1/cortactin binding protein 1 (ProSAP1/CortBP1) is a PDZ-domain protein highly enriched in the postsynaptic density. *The Journal of Neuroscience : The Official Journal of the Society for Neuroscience*, *19*(15), 6506–18. Retrieved from http://www.ncbi.nlm.nih.gov/pubmed/10414979

Boissart, C., Poulet, A., Georges, P., Darville, H., Julita, E., Delorme, R., … Benchoua, A. (2013). Differentiation from human pluripotent stem cells of cortical neurons of the superficial layers amenable to psychiatric disease modeling and high-throughput drug screening. *Translational Psychiatry*, *3*, e294. http://doi.org/10.1038/tp.2013.71

Bonaglia, M. C., Giorda, R., Borgatti, R., Felisari, G., Gagliardi, C., Selicorni, A., & Zuffardi, O. (2001). Disruption of the ProSAP2 gene in a t(12;22)(q24.1;q13.3) is associated with the 22q13.3 deletion syndrome. *American Journal of Human Genetics*, *69*(2), 261–8. http://doi.org/10.1086/321293

Bonaglia, M. C., Giorda, R., Mani, E., Aceti, G., Anderlid, B.-M., Baroncini, A., … Zuffardi, O. (2006). Identification of a recurrent breakpoint within the SHANK3 gene in the 22q13.3 deletion syndrome. *Journal of Medical Genetics*, *43*(10), 822–8. http://doi.org/10.1136/jmg.2005.038604

Boulting, G. L., Kiskinis, E., Croft, G. F., Amoroso, M. W., Oakley, D. H., Wainger, B. J., … Eggan, K. (2011). A functionally characterized test set of human induced pluripotent stem cells. *Nature Biotechnology*, *29*(3), 279–86. http://doi.org/10.1038/nbt.1783

Bourgeron, T. (2009). A synaptic trek to autism. *Current Opinion in Neurobiology*, *19*(2), 231–4. http://doi.org/10.1016/j.conb.2009.06.003

Bozdagi, O., Sakurai, T., Papapetrou, D., Wang, X., Dickstein, D. L., Takahashi, N., … Buxbaum, J. D. (2010). Haploinsufficiency of the autism-associated Shank3 gene leads to deficits in synaptic function, social interaction, and social communication. *Molecular Autism*, *1*(1), 15. http://doi.org/10.1186/2040-2392-1-15

Bozdagi, O., Tavassoli, T., & Buxbaum, J. D. (2013). Insulin-like growth factor-1 rescues synaptic and motor deficits in a mouse model of autism and developmental delay. *Molecular Autism*, *4*(1), 9. http://doi.org/10.1186/2040-2392-4-9

Bradke, F. (1999). The Role of Local Actin Instability in Axon Formation. *Science*, *283*(5409), 1931–1934. http://doi.org/10.1126/science.283.5409.1931

Brennand, K. J., Simone, A., Tran, N., & Gage, F. H. (2012). Modeling psychiatric disorders at the cellular and network levels. *Molecular Psychiatry*, *17*(12), 1239–53. http://doi.org/10.1038/mp.2012.20

Brodal, P. (2004). *The Central Nervous System: Structure and Function*. Oxford University Press, USA. Retrieved from https://books.google.com/books?hl=en&lr=&id=WdATFQ0YUrMC&pgis=1

Brugha, T. S., McManus, S., Bankart, J., Scott, F., Purdon, S., Smith, J., … Meltzer, H. (2011). Epidemiology of autism spectrum disorders in adults in the community in England. *Archives of General Psychiatry*, *68*(5), 459–65. http://doi.org/10.1001/archgenpsychiatry.2011.38

Burbach, J. P. H., Luckman, S. M., Murphy, D., & Gainer, H. (2001). Gene Regulation in the Magnocellular Hypothalamo-Neurohypophysial System. *Physiol Rev*, *81*(3), 1197–1267. Retrieved from http://physrev.physiology.org/content/81/3/1197

Campellone, K. G., & Welch, M. D. (2010). A nucleator arms race: cellular control of actin assembly. *Nature Reviews. Molecular Cell Biology*, *11*(4), 237–51. http://doi.org/10.1038/nrm2867

Carbonetto, S. (2014). A blueprint for research on Shankopathies: a view from research on autism spectrum disorder. *Developmental Neurobiology*, *74*(2), 85–112. http://doi.org/10.1002/dneu.22150

Casanova, M. F., Buxhoeveden, D. P., Switala, A. E., & Roy, E. (2002). Minicolumnar pathology in autism. *Neurology*, *58*(3), 428–432. http://doi.org/10.1212/WNL.58.3.428

Casanova, M. F., El-Baz, A., & Switala, A. (2011). Laws of conservation as related to brain growth, aging, and evolution: symmetry of the minicolumn. *Frontiers in Neuroanatomy*, *5*, 66. http://doi.org/10.3389/fnana.2011.00066

Casanova, M. F., van Kooten, I., Switala, A. E., van Engeland, H., Heinsen, H., Steinbusch, H. W. M., … Schmitz, C. (2006). Abnormalities of cortical minicolumnar organization in the prefrontal lobes of autistic patients. *Clinical Neuroscience Research*, *6*(3-4), 127–133. http://doi.org/10.1016/j.cnr.2006.06.003

Castrén, M., Tervonen, T., Kärkkäinen, V., Heinonen, S., Castrén, E., Larsson, K., … Akerman, K. (2005). Altered differentiation of neural stem cells in fragile X syndrome. *Proceedings of the National Academy of Sciences of the United States of America*, *102*(49), 17834–9. http://doi.org/10.1073/pnas.0508995102

Chambers, S. M., Fasano, C. A., Papapetrou, E. P., Tomishima, M., Sadelain, M., & Studer, L. (2009). Highly efficient neural conversion of human ES and iPS cells by dual inhibition of SMAD signaling. *Nature Biotechnology*, *27*(3), 275–280. http://doi.org/10.1038/nbt.1529

Chapleau, C. A., Calfa, G. D., Lane, M. C., Albertson, A. J., Larimore, J. L., Kudo, S., … Pozzo-Miller, L. (2009). Dendritic spine pathologies in hippocampal pyramidal neurons from Rett syndrome brain and after expression of Rett-associated MECP2 mutations. *Neurobiology of Disease*, *35*(2), 219–33. http://doi.org/10.1016/j.nbd.2009.05.001

Chauhan, A., & Chauhan, V. (2006). Oxidative stress in autism. *Pathophysiology : The Official Journal of the International Society for Pathophysiology / ISP*, *13*(3), 171–81. http://doi.org/10.1016/j.pathophys.2006.05.007

Chen, Q., & Pollard, T. D. (2013). Actin filament severing by cofilin dismantles actin patches and produces mother filaments for new patches. *Current Biology : CB*, *23*(13), 1154–62. http://doi.org/10.1016/j.cub.2013.05.005

Chen, R. Z., Akbarian, S., Tudor, M., & Jaenisch, R. (2001). Deficiency of methyl-CpG binding protein-2 in CNS neurons results in a Rett-like phenotype in mice. *Nature Genetics*, *27*(3), 327–31. http://doi.org/10.1038/85906

Chen, X. J., Squarr, A. J., Stephan, R., Chen, B., Higgins, T. E., Barry, D. J., … Way, M. (2014). Ena/VASP proteins cooperate with the WAVE complex to regulate the actin cytoskeleton. *Developmental Cell*, *30*(5), 569–84. http://doi.org/10.1016/j.devcel.2014.08.001

Cheung, A. Y. L., Horvath, L. M., Grafodatskaya, D., Pasceri, P., Weksberg, R., Hotta, A., … Ellis, J. (2011). Isolation of MECP2-null Rett Syndrome patient hiPS cells and isogenic controls through X-chromosome inactivation. *Human Molecular Genetics*, *20*(11), 2103–15. http://doi.org/10.1093/hmg/ddr093

Choi, J., Ko, J., Racz, B., Burette, A., Lee, J.-R., Kim, S., … Kim, E. (2005). Regulation of dendritic spine morphogenesis by insulin receptor substrate 53, a downstream effector of Rac1 and Cdc42 small GTPases. *The Journal of Neuroscience : The Official Journal of the Society for Neuroscience*, *25*(4), 869–79. http://doi.org/10.1523/JNEUROSCI.3212-04.2005

Cocks, G., Curran, S., Gami, P., Uwanogho, D., Jeffries, A. R., Kathuria, A., … Price, J. (2014). The utility of patient specific induced pluripotent stem cells for the modelling of Autistic Spectrum Disorders. *Psychopharmacology*, *231*(6), 1079–88. http://doi.org/10.1007/s00213-013-3196-4

Comery, T. A., Harris, J. B., Willems, P. J., Oostra, B. A., Irwin, S. A., Weiler, I. J., & Greenough, W. T. (1997). Abnormal dendritic spines in fragile X knockout mice: maturation and pruning deficits. *Proceedings of the National Academy of Sciences of the United States of America*, *94*(10), 5401–4. Retrieved from http://www.pubmedcentral.nih.gov/articlerender.fcgi?artid=24690&tool=pmcentrez&rendertype=abstract

Cooper, G. M. (2000). Structure and Organization of Actin Filaments. Sinauer Associates. Retrieved from http://www.ncbi.nlm.nih.gov/books/NBK9908/

Courchesne, E., Karns, C. M., Davis, H. R., Ziccardi, R., Carper, R. A., Tigue, Z. D., … Courchesne, R. Y. (2001). Unusual brain growth patterns in early life in patients with autistic disorder: an MRI study. *Neurology*, *57*(2), 245–54. Retrieved from http://www.ncbi.nlm.nih.gov/pubmed/11468308

Cramer, L. P. (1997). Molecular mechanism of actin-dependent retrograde flow in lamellipodia of motile cells. *Frontiers in Bioscience : A Journal and Virtual Library*, *2*, d260–70. Retrieved from http://www.ncbi.nlm.nih.gov/pubmed/9206973

da Silva, J. S., & Dotti, C. G. (2002). Breaking the neuronal sphere: regulation of the actin cytoskeleton in neuritogenesis. *Nature Reviews. Neuroscience*, *3*(9), 694–704. http://doi.org/10.1038/nrn918

Dani, V. S., Chang, Q., Maffei, A., Turrigiano, G. G., Jaenisch, R., & Nelson, S. B. (2005). Reduced cortical activity due to a shift in the balance between excitation and inhibition in a mouse model of Rett syndrome. *Proceedings of the National Academy of Sciences of the United States of America*, *102*(35), 12560–5. http://doi.org/10.1073/pnas.0506071102

Darnell, J. C., & Klann, E. (2013). The translation of translational control by FMRP: therapeutic targets for FXS. *Nature Neuroscience*, *16*(11), 1530–6. http://doi.org/10.1038/nn.3379

De Rubeis, S., He, X., Goldberg, A. P., Poultney, C. S., Samocha, K., Ercument Cicek, A., … Buxbaum, J. D. (2014). Synaptic, transcriptional and chromatin genes disrupted in autism. *Nature*, *515*(7526), 209–215. http://doi.org/10.1038/nature13772

Dementieva, Y. A., Vance, D. D., Donnelly, S. L., Elston, L. A., Wolpert, C. M., Ravan, S. A., … Cuccaro, M. L. (2005). Accelerated head growth in early development of individuals with autism. *Pediatric Neurology*, *32*(2), 102–8. http://doi.org/10.1016/j.pediatrneurol.2004.08.005

Devine, M. J., Ryten, M., Vodicka, P., Thomson, A. J., Burdon, T., Houlden, H., … Kunath, T. (2011). Parkinson's disease induced pluripotent stem cells with triplication of the α-synuclein locus. *Nature Communications*, *2*, 440. http://doi.org/10.1038/ncomms1453

Dhara, S. K., & Stice, S. L. (2008). Neural differentiation of human embryonic stem cells. *Journal of Cellular Biochemistry*, *105*(3), 633–40. http://doi.org/10.1002/jcb.21891

Di Sante, G., Wang, L., Wang, C., Jiao, X., Casimiro, M. C., Chen, K., … Pestell, R. G. (2015). Sirt1-deficient mice have hypogonadotropic hypogonadism due to defective GnRH neuronal migration. *Molecular Endocrinology (Baltimore, Md.)*, *29*(2), 200–12. http://doi.org/10.1210/me.2014-1228

Doers, M. E., Musser, M. T., Nichol, R., Berndt, E. R., Baker, M., Gomez, T. M., … Bhattacharyya, A. (2014). iPSC-derived forebrain neurons from FXS individuals show defects in initial neurite outgrowth. *Stem Cells and Development*, *23*(15), 1777–87. http://doi.org/10.1089/scd.2014.0030

Doherty, G. J., & McMahon, H. T. (2008). Mediation, modulation, and consequences of membrane-cytoskeleton interactions. *Annual Review of Biophysics*, *37*, 65–95. http://doi.org/10.1146/annurev.biophys.37.032807.125912

Duffney, L. J., Wei, J., Cheng, J., Liu, W., Smith, K. R., Kittler, J. T., & Yan, Z. (2013). Shank3 deficiency induces NMDA receptor hypofunction via an actin-dependent mechanism. *The Journal of Neuroscience : The Official Journal of the Society for Neuroscience*, *33*(40), 15767–78. http://doi.org/10.1523/JNEUROSCI.1175-13.2013

Duffney, L. J., Zhong, P., Wei, J., Matas, E., Cheng, J., Qin, L., … Yan, Z. (2015). Autism-like Deficits in Shank3-Deficient Mice Are Rescued by Targeting Actin Regulators. *Cell Reports*. http://doi.org/10.1016/j.celrep.2015.04.064

Durand, C. M., Betancur, C., Boeckers, T. M., Bockmann, J., Chaste, P., Fauchereau, F., … Bourgeron, T. (2007). Mutations in the gene encoding the synaptic scaffolding protein SHANK3 are associated with autism spectrum disorders. *Nature Genetics*, *39*(1), 25–7. http://doi.org/10.1038/ng1933

Durand, C. M., Perroy, J., Loll, F., Perrais, D., Fagni, L., Bourgeron, T., … Sans, N. (2012). SHANK3 mutations identified in autism lead to modification of dendritic spine morphology via an actin-dependent mechanism. *Molecular Psychiatry*, *17*(1), 71–84. http://doi.org/10.1038/mp.2011.57

Ehninger, D., Han, S., Shilyansky, C., Zhou, Y., Li, W., Kwiatkowski, D. J., … Silva, A. J. (2008). Reversal of learning deficits in a Tsc2+/− mouse model of tuberous sclerosis. *Nature Medicine*, *14*(8), 843–848. http://doi.org/10.1038/nm1788

Eigenmann, D. E., Xue, G., Kim, K. S., Moses, A. V, Hamburger, M., & Oufir, M. (2013). Comparative study of four immortalized human brain capillary endothelial cell lines, hCMEC/D3, hBMEC, TY10, and BB19, and optimization of culture conditions, for an in vitro blood-brain barrier model for drug permeability studies. *Fluids and Barriers of the CNS*, *10*(1), 33. http://doi.org/10.1186/2045-8118-10-33

El-Fishawy, P., & State, M. W. (2010). The genetics of autism: key issues, recent findings, and clinical implications. *The Psychiatric Clinics of North America*, *33*(1), 83–105. http://doi.org/10.1016/j.psc.2009.12.002

Erceg, S., Lukovic, D., Moreno-Manzano, V., Stojkovic, M., & Bhattacharya, S. S. (2012). Derivation of cerebellar neurons from human pluripotent stem cells. *Current Protocols in Stem Cell Biology*, *Chapter 1*, Unit 1H.5. http://doi.org/10.1002/9780470151808.sc01h05s20

Erickson, K., Gabry, K. E., Lindell, S., Champoux, M., Schulkin, J., Gold, P., … Higley, J. D. (2005). Social withdrawal behaviors in nonhuman primates and changes in neuroendocrine and monoamine concentrations during a separation paradigm. *Developmental Psychobiology*, *46*(4), 331–9. http://doi.org/10.1002/dev.20061

Falardeau, J., Chung, W. C. J., Beenken, A., Raivio, T., Plummer, L., Sidis, Y., … Pitteloud, N. (2008). Decreased FGF8 signaling causes deficiency of gonadotropin-releasing hormone in humans and mice. *The Journal of Clinical Investigation*, *118*(8), 2822–31. http://doi.org/10.1172/JCI34538

Fasano, C. A., Chambers, S. M., Lee, G., Tomishima, M. J., & Studer, L. (2010). Efficient derivation of functional floor plate tissue from human embryonic stem cells. *Cell Stem Cell*, *6*(4), 336–47. http://doi.org/10.1016/j.stem.2010.03.001

Fingar, D. C., Salama, S., Tsou, C., Harlow, E., & Blenis, J. (2002). Mammalian cell size is controlled by mTOR and its downstream targets S6K1 and 4EBP1/eIF4E. *Genes & Development*, *16*(12), 1472–87. http://doi.org/10.1101/gad.995802

Flynn, K. C., Hellal, F., Neukirchen, D., Jacob, S., Tahirovic, S., Dupraz, S., … Bradke, F. (2012). ADF/cofilin-mediated actin retrograde flow directs neurite formation in the developing brain. *Neuron*, *76*(6), 1091–107. http://doi.org/10.1016/j.neuron.2012.09.038

Ganten, D., & Pfaff, D. (Eds.). (1990). *Behavioral Aspects of Neuroendocrinology* (Vol. 10). Berlin, Heidelberg: Springer Berlin Heidelberg. http://doi.org/10.1007/978-3-642-75837-9

Gauthier, J., Spiegelman, D., Piton, A., Lafrenière, R. G., Laurent, S., St-Onge, J., … Rouleau, G. A. (2009). Novel de novo SHANK3 mutation in autistic patients. *American Journal of Medical Genetics. Part B, Neuropsychiatric Genetics : The Official Publication of the International Society of Psychiatric Genetics*, *150B*(3), 421–4. http://doi.org/10.1002/ajmg.b.30822

Ghosh, A., Michalon, A., Lindemann, L., Fontoura, P., & Santarelli, L. (2013). Drug discovery for autism spectrum disorder: challenges and opportunities. *Nature Reviews. Drug Discovery*, *12*(10), 777–90. http://doi.org/10.1038/nrd4102

Gkogkas, C. G., Khoutorsky, A., Ran, I., Rampakakis, E., Nevarko, T., Weatherill, D. B., … Sonenberg, N. (2013). Autism-related deficits via dysregulated eIF4E-dependent translational control. *Nature*, *493*(7432), 371–7. http://doi.org/10.1038/nature11628

Goldsmith, A. D., Sarin, S., Lockery, S., & Hobert, O. (2010). Developmental control of lateralized neuron size in the nematode Caenorhabditis elegans. *Neural Development*, *5*(1), 33. http://doi.org/10.1186/1749-8104-5-33

Grabrucker, A. M., Knight, M. J., Proepper, C., Bockmann, J., Joubert, M., Rowan, M., … Boeckers, T. M. (2011). Concerted action of zinc and ProSAP/Shank in synaptogenesis and synapse maturation. *The EMBO Journal*, *30*(3), 569–81. http://doi.org/10.1038/emboj.2010.336

Grabrucker, A. M., Schmeisser, M. J., Schoen, M., & Boeckers, T. M. (2011). Postsynaptic ProSAP/Shank scaffolds in the cross-hair of synaptopathies. *Trends in Cell Biology*, *21*(10), 594–603. http://doi.org/10.1016/j.tcb.2011.07.003

Gregory, K. J., Dong, E. N., Meiler, J., & Conn, P. J. (2011). Allosteric modulation of metabotropic glutamate receptors: structural insights and therapeutic potential. *Neuropharmacology*, *60*(1), 66–81. http://doi.org/10.1016/j.neuropharm.2010.07.007

Guilmatre, A., Huguet, G., Delorme, R., & Bourgeron, T. (2014). The emerging role of SHANK genes in neuropsychiatric disorders. *Developmental Neurobiology*, *74*(2), 113–22. http://doi.org/10.1002/dneu.22128

Haeckel, A., Ahuja, R., Gundelfinger, E. D., Qualmann, B., & Kessels, M. M. (2008a). The actin-binding protein Abp1 controls dendritic spine morphology and is important for spine head and synapse formation. *The Journal of Neuroscience : The Official Journal of the Society for Neuroscience*, *28*(40), 10031–44. http://doi.org/10.1523/JNEUROSCI.0336-08.2008

Haeckel, A., Ahuja, R., Gundelfinger, E. D., Qualmann, B., & Kessels, M. M. (2008b). The actin-binding protein Abp1 controls dendritic spine morphology and is important for spine head and synapse formation. *The Journal of Neuroscience : The Official Journal of the Society for Neuroscience*, *28*(40), 10031–44. http://doi.org/10.1523/JNEUROSCI.0336-08.2008

Hallmayer, J., Cleveland, S., Torres, A., Phillips, J., Cohen, B., Torigoe, T., … Risch, N. (2011). Genetic heritability and shared environmental factors among twin pairs with autism. *Archives of General Psychiatry*, *68*(11), 1095–102. http://doi.org/10.1001/archgenpsychiatry.2011.76

Han, K., Holder, J. L., Schaaf, C. P., Lu, H., Chen, H., Kang, H., … Zoghbi, H. Y. (2013). SHANK3 overexpression causes manic-like behaviour with unique pharmacogenetic properties. *Nature*, *503*(7474), 72–7. http://doi.org/10.1038/nature12630

Häusser, M. (2001). Synaptic function: Dendritic democracy. *Current Biology*, *11*(1), R10–R12. http://doi.org/10.1016/S0960-9822(00)00034-8

Hayashi, M. K., Tang, C., Verpelli, C., Narayanan, R., Stearns, M. H., Xu, R.-M., … Hayashi, Y. (2009). The postsynaptic density proteins Homer and Shank form a polymeric network structure. *Cell*, *137*(1), 159–71. http://doi.org/10.1016/j.cell.2009.01.050

He, B. J., Shulman, G. L., Snyder, A. Z., & Corbetta, M. (2007). The role of impaired neuronal communication in neurological disorders. *Current Opinion in Neurology*, *20*(6), 655–60. http://doi.org/10.1097/WCO.0b013e3282f1c720

Hering, H., & Sheng, M. (2003a). Activity-Dependent Redistribution and Essential Role of Cortactin in Dendritic Spine Morphogenesis. *J. Neurosci.*, *23*(37), 11759–11769. Retrieved from http://www.jneurosci.org/content/23/37/11759.long

Hering, H., & Sheng, M. (2003b). Activity-Dependent Redistribution and Essential Role of Cortactin in Dendritic Spine Morphogenesis. *J. Neurosci.*, *23*(37), 11759–11769. Retrieved from http://www.jneurosci.org/content/23/37/11759.short

Holbro, N., Grunditz, A., & Oertner, T. G. (2009). Differential distribution of endoplasmic reticulum controls metabotropic signaling and plasticity at hippocampal synapses. *Proceedings of the National Academy of Sciences of the United States of America*, *106*(35), 15055–60. http://doi.org/10.1073/pnas.0905110106

Hollander, E., Anagnostou, E., Chaplin, W., Esposito, K., Haznedar, M. M., Licalzi, E., … Buchsbaum, M. (2005). Striatal volume on magnetic resonance imaging and repetitive behaviors in autism. *Biological Psychiatry*, *58*(3), 226–32. http://doi.org/10.1016/j.biopsych.2005.03.040

Hollander, E., Bartz, J., Chaplin, W., Phillips, A., Sumner, J., Soorya, L., … Wasserman, S. (2007). Oxytocin increases retention of social cognition in autism. *Biological Psychiatry*, *61*(4), 498–503. http://doi.org/10.1016/j.biopsych.2006.05.030

Honkura, N., Matsuzaki, M., Noguchi, J., Ellis-Davies, G. C. R., & Kasai, H. (2008). The subspine organization of actin fibers regulates the structure and plasticity of dendritic spines. *Neuron*, *57*(5), 719–29. http://doi.org/10.1016/j.neuron.2008.01.013

Hoos, M. D., Vitek, M. P., Ridnour, L. A., Wilson, J., Jansen, M., Everhart, A., … Colton, C. A. (2014). The impact of human and mouse differences in NOS2 gene expression on the brain's redox and immune environment. *Molecular Neurodegeneration*, *9*(1), 50. http://doi.org/10.1186/1750-1326-9-50

Hotulainen, P., & Hoogenraad, C. C. (2010). Actin in dendritic spines: connecting dynamics to function. *The Journal of Cell Biology*, *189*(4), 619–29. http://doi.org/10.1083/jcb.201003008

Hung, A. Y., Futai, K., Sala, C., Valtschanoff, J. G., Ryu, J., Woodworth, M. A., … Sheng, M. (2008). Smaller dendritic spines, weaker synaptic transmission, but enhanced spatial learning in mice lacking Shank1. *The Journal of Neuroscience : The Official Journal of the Society for Neuroscience*, *28*(7), 1697–708. http://doi.org/10.1523/JNEUROSCI.3032-07.2008

Hutchins, B. I., Klenke, U., & Wray, S. (2013). Calcium release-dependent actin flow in the leading process mediates axophilic migration. *The Journal of Neuroscience : The Official Journal of the Society for Neuroscience*, *33*(28), 11361–71. http://doi.org/10.1523/JNEUROSCI.3758-12.2013

Hutchins, B. I., & Wray, S. (2014). Capture of microtubule plus-ends at the actin cortex promotes axophilic neuronal migration by enhancing microtubule tension in the leading process. *Frontiers in Cellular Neuroscience*, *8*, 400. http://doi.org/10.3389/fncel.2014.00400

Ichetovkin, I., Grant, W., & Condeelis, J. (2002). Cofilin produces newly polymerized actin filaments that are preferred for dendritic nucleation by the Arp2/3 complex. *Current Biology : CB*, *12*(1), 79–84. Retrieved from http://www.ncbi.nlm.nih.gov/pubmed/11790308

Imaging the Brain in Autism. (2013) (p. 387). Springer Science & Business Media. Retrieved from https://books.google.com/books?id=IZ5GAAAAQBAJ&pgis=1

Inoue, H., Nagata, N., Kurokawa, H., & Yamanaka, S. (2014). iPS cells: a game changer for future medicine. *The EMBO Journal*, *33*(5), 409–17. http://doi.org/10.1002/embj.201387098

Irwin, S. A., Patel, B., Idupulapati, M., Harris, J. B., Crisostomo, R. A., Larsen, B. P., … Greenough, W. T. (2001). Abnormal dendritic spine characteristics in the temporal and visual cortices of patients with fragile-X syndrome: a quantitative examination. *American Journal of Medical Genetics*, *98*(2), 161–7. Retrieved from http://www.ncbi.nlm.nih.gov/pubmed/11223852

Jacob, S., Brune, C. W., Carter, C. S., Leventhal, B. L., Lord, C., & Cook, E. H. (2007). Association of the oxytocin receptor gene (OXTR) in Caucasian children and adolescents with autism. *Neuroscience Letters*, *417*(1), 6–9. http://doi.org/10.1016/j.neulet.2007.02.001

Jaeger, I., Arber, C., Risner-Janiczek, J. R., Kuechler, J., Pritzsche, D., Chen, I.-C., … Li, M. (2011). Temporally controlled modulation of FGF/ERK signaling directs midbrain dopaminergic neural progenitor fate in mouse and human pluripotent stem cells. *Development (Cambridge, England)*, *138*(20), 4363–74. http://doi.org/10.1242/dev.066746

Jan, Y.-N., & Jan, L. Y. (2010). Branching out: mechanisms of dendritic arborization. *Nature Reviews. Neuroscience*, *11*(5), 316–28. http://doi.org/10.1038/nrn2836

Jiang, Y.-H., & Ehlers, M. D. (2013). Modeling autism by SHANK gene mutations in mice. *Neuron*, *78*(1), 8–27. http://doi.org/10.1016/j.neuron.2013.03.016

Kelleher, R. J., & Bear, M. F. (2008). The autistic neuron: troubled translation? *Cell*, *135*(3), 401–6. http://doi.org/10.1016/j.cell.2008.10.017

Keown, C. L., Shih, P., Nair, A., Peterson, N., Mulvey, M. E., & Müller, R.-A. (2013). Local Functional Overconnectivity in Posterior Brain Regions Is Associated with Symptom Severity in Autism Spectrum Disorders. *Cell Reports*, *5*(3), 567–572. http://doi.org/10.1016/j.celrep.2013.10.003

Kern, J. K., Geier, D. A., Adams, J. B., Garver, C. R., Audhya, T., & Geier, M. R. (2011). A clinical trial of glutathione supplementation in autism spectrum disorders. *Medical Science Monitor : International Medical Journal of Experimental and Clinical Research*, *17*(12), CR677–82. Retrieved from http://www.pubmedcentral.nih.gov/articlerender.fcgi?artid=3628138&tool=pmcentrez&rendertype=abstract

Kim, D. J., Kim, S. H., Lim, C. S., Choi, K. Y., Park, C. S., Sung, B. H., … Song, W. K. (2006). Interaction of SPIN90 with the Arp2/3 complex mediates lamellipodia and actin comet tail formation. *The Journal of Biological Chemistry*, *281*(1), 617–25. http://doi.org/10.1074/jbc.M504450200

Kim, S.-M., Choi, K. Y., Cho, I. H., Rhy, J. H., Kim, S. H., Park, C.-S., … Song, W. K. (2009). Regulation of dendritic spine morphology by SPIN90, a novel Shank binding partner. *Journal of Neurochemistry*, *109*(4), 1106–17. http://doi.org/10.1111/j.1471-4159.2009.06039.x

Kishi, N., & Macklis, J. D. (2004). MECP2 is progressively expressed in post-migratory neurons and is involved in neuronal maturation rather than cell fate decisions. *Molecular and Cellular Neurosciences*, *27*(3), 306–21. http://doi.org/10.1016/j.mcn.2004.07.006

Kleijer, K. T. E., Schmeisser, M. J., Krueger, D. D., Boeckers, T. M., Scheiffele, P., Bourgeron, T., … Burbach, J. P. H. (2014). Neurobiology of autism gene products: towards pathogenesis and drug targets. *Psychopharmacology*, *231*(6), 1037–62. http://doi.org/10.1007/s00213-013-3403-3

Kolevzon, A., Cai, G., Soorya, L., Takahashi, N., Grodberg, D., Kajiwara, Y., … Buxbaum, J. D. (2011). Analysis of a purported SHANK3 mutation in a boy with autism: clinical impact of rare variant research in neurodevelopmental disabilities. *Brain Research*, *1380*, 98–105. http://doi.org/10.1016/j.brainres.2010.11.005

Kosaka, H., Munesue, T., Ishitobi, M., Asano, M., Omori, M., Sato, M., … Wada, Y. (2012). Long-term oxytocin administration improves social behaviors in a girl with autistic disorder. *BMC Psychiatry*, *12*, 110. http://doi.org/10.1186/1471-244X-12-110

Kouser, M., Speed, H. E., Dewey, C. M., Reimers, J. M., Widman, A. J., Gupta, N., … Powell, C. M. (2013). Loss of predominant Shank3 isoforms results in hippocampus-dependent impairments in behavior and synaptic transmission. *The Journal of Neuroscience : The Official Journal of the Society for Neuroscience*, *33*(47), 18448–68. http://doi.org/10.1523/JNEUROSCI.3017-13.2013

Krause, M., & Gautreau, A. (2014). Steering cell migration: lamellipodium dynamics and the regulation of directional persistence. *Nature Reviews Molecular Cell Biology*, *15*(9), 577–590. http://doi.org/10.1038/nrm3861

Kreienkamp, H.-J. (2008). Scaffolding proteins at the postsynaptic density: shank as the architectural framework. *Handbook of Experimental Pharmacology*, (186), 365–80. http://doi.org/10.1007/978-3-540-72843-6_15

Kulkarni, V. A., & Firestein, B. L. (2012). The dendritic tree and brain disorders. *Molecular and Cellular Neurosciences*, *50*(1), 10–20. http://doi.org/10.1016/j.mcn.2012.03.005

Kumari, D., Swaroop, M., Southall, N., Huang, W., Zheng, W., & Usdin, K. (2015). High-Throughput Screening to Identify Compounds That Increase Fragile X Mental Retardation Protein Expression in Neural Stem Cells Differentiated From Fragile X Syndrome Patient-Derived Induced Pluripotent Stem Cells. *Stem Cells Translational Medicine*, *4*(7), 800–8. http://doi.org/10.5966/sctm.2014-0278

Kuriu, T., Inoue, A., Bito, H., Sobue, K., & Okabe, S. (2006). Differential control of postsynaptic density scaffolds via actin-dependent and -independent mechanisms. *The Journal of Neuroscience : The Official Journal of the Society for Neuroscience*, *26*(29), 7693–706. http://doi.org/10.1523/JNEUROSCI.0522-06.2006

Kutner, R. H., Zhang, X.-Y., & Reiser, J. (2009). Production, concentration and titration of pseudotyped HIV-1-based lentiviral vectors. *Nature Protocols*, *4*(4), 495–505. http://doi.org/10.1038/nprot.2009.22

LaFlamme, B. (2015). Genetic modules for autism. *Nature Genetics*, *47*(2), 105–105. http://doi.org/10.1038/ng.3210

Lancaster, M. A., Renner, M., Martin, C.-A., Wenzel, D., Bicknell, L. S., Hurles, M. E., … Knoblich, J. A. (2013). Cerebral organoids model human brain development and microcephaly. *Nature*, *501*(7467), 373–9. http://doi.org/10.1038/nature12517

Langen, M., Schnack, H. G., Nederveen, H., Bos, D., Lahuis, B. E., de Jonge, M. V, … Durston, S. (2009). Changes in the developmental trajectories of striatum in autism. *Biological Psychiatry*, *66*(4), 327–33. http://doi.org/10.1016/j.biopsych.2009.03.017

Leblond, C. S., Nava, C., Polge, A., Gauthier, J., Huguet, G., Lumbroso, S., … Bourgeron, T. (2014). Meta-analysis of SHANK Mutations in Autism Spectrum Disorders: a gradient of severity in cognitive impairments. *PLoS Genetics*, *10*(9), e1004580. http://doi.org/10.1371/journal.pgen.1004580

Lechan, R. M., & Toni, R. (2013, February 22). Functional Anatomy of the Hypothalamus and Pituitary. MDText.com, Inc. Retrieved from http://www.ncbi.nlm.nih.gov/books/NBK279126/

Lee, J., Duan, W., & Mattson, M. P. (2002). Evidence that brain-derived neurotrophic factor is required for basal neurogenesis and mediates, in part, the enhancement of neurogenesis by dietary restriction in the hippocampus of adult mice. *Journal of Neurochemistry*, *82*(6), 1367–75. Retrieved from http://www.ncbi.nlm.nih.gov/pubmed/12354284

Leo Kanner's 1943 paper on autism —. (n.d.). Retrieved July 2, 2015, from http://sfari.org/news-and-opinion/classic-paper-reviews/2007/leo-kanners-1943-paper-on-autism-commentary-by-gerald-fischbach

Lim, S., Naisbitt, S., Yoon, J., Hwang, J.-I., Suh, P.-G., Sheng, M., & Kim, E. (1999). Characterization of the Shank Family of Synaptic Proteins: MULTIPLE GENES, ALTERNATIVE SPLICING, AND DIFFERENTIAL EXPRESSION IN BRAIN AND DEVELOPMENT. *Journal of Biological Chemistry*, *274*(41), 29510–29518. http://doi.org/10.1074/jbc.274.41.29510

Liu, F., Grauer, S., Kelley, C., Navarra, R., Graf, R., Zhang, G., … Marquis, K. L. (2008). ADX47273 [S-(4-fluoro-phenyl)-{3-[3-(4-fluoro-phenyl)-[1,2,4]-oxadiazol-5-yl]-piperidin-1-yl}-methanone]: a novel metabotropic glutamate receptor 5-selective positive allosteric modulator with preclinical antipsychotic-like and procognitive activities. *The Journal of Pharmacology and Experimental Therapeutics*, *327*(3), 827–39. http://doi.org/10.1124/jpet.108.136580

Liu, J., Koscielska, K. A., Cao, Z., Hulsizer, S., Grace, N., Mitchell, G., … Hagerman, P. J. (2012). Signaling defects in iPSC-derived fragile X premutation neurons. *Human Molecular Genetics*, *21*(17), 3795–805. http://doi.org/10.1093/hmg/dds207

Liu, X., Kawamura, Y., Shimada, T., Otowa, T., Koishi, S., Sugiyama, T., … Sasaki, T. (2010). Association of the oxytocin receptor (OXTR) gene polymorphisms with autism spectrum disorder (ASD) in the Japanese population. *Journal of Human Genetics*, *55*(3), 137–41. http://doi.org/10.1038/jhg.2009.140

Lloyd, A. C. (2013). The regulation of cell size. *Cell*, *154*(6), 1194–205. http://doi.org/10.1016/j.cell.2013.08.053

Lodish, H., Berk, A., Zipursky, S. L., Matsudaira, P., Baltimore, D., & Darnell, J. (2000). The Dynamics of Actin Assembly. W. H. Freeman. Retrieved from http://www.ncbi.nlm.nih.gov/books/NBK21594/

Lombardi, L. M., Baker, S. A., & Zoghbi, H. Y. (2015). MECP2 disorders: from the clinic to mice and back. *The Journal of Clinical Investigation*, *125*(8), 2914–23. http://doi.org/10.1172/JCI78167

Lord, C. (2011). Epidemiology: How common is autism? *Nature*, *474*(7350), 166–8. http://doi.org/10.1038/474166a

Loudes, C., Petit, F., Kordon, C., & Faivre-Bauman, A. (2000). Brain-derived neurotrophic factor but not neurotrophin-3 enhances differentiation of somatostatin neurons in hypothalamic cultures. *Neuroendocrinology*, *72*(3), 144–53. http://doi.org/54581

Lozano, R., Rosero, C. A., & Hagerman, R. J. (2014). Fragile X spectrum disorders. *Intractable & Rare Diseases Research*, *3*(4), 134–146. http://doi.org/10.5582/irdr.2014.01022

Luikenhuis, S., Giacometti, E., Beard, C. F., & Jaenisch, R. (2004). Expression of MeCP2 in postmitotic neurons rescues Rett syndrome in mice. *Proceedings of the National Academy of Sciences of the United States of America*, *101*(16), 6033–8. http://doi.org/10.1073/pnas.0401626101

Majzoub, J. A. (2006). Corticotropin-releasing hormone physiology. *European Journal of Endocrinology*, *155*(suppl_1), S71–S76. http://doi.org/10.1530/eje.1.02247

Mameza, M. G., Dvoretskova, E., Bamann, M., Hönck, H.-H., Güler, T., Boeckers, T. M., … Kreienkamp, H.-J. (2013). SHANK3 gene mutations associated with autism facilitate ligand binding to the Shank3 ankyrin repeat region. *The Journal of Biological Chemistry*, *288*(37), 26697–708. http://doi.org/10.1074/jbc.M112.424747

Manser, E., Loo, T. H., Koh, C. G., Zhao, Z. S., Chen, X. Q., Tan, L., … Lim, L. (1998). PAK kinases are directly coupled to the PIX family of nucleotide exchange factors. *Molecular Cell*, *1*(2), 183–92. Retrieved from http://www.ncbi.nlm.nih.gov/pubmed/9659915

Marchetto, M. C. N., Carromeu, C., Acab, A., Yu, D., Yeo, G. W., Mu, Y., … Muotri, A. R. (2010). A model for neural development and treatment of Rett syndrome using human induced pluripotent stem cells. *Cell*, *143*(4), 527–39. http://doi.org/10.1016/j.cell.2010.10.016

Martinez, M. C. (2003). Dual regulation of neuronal morphogenesis by a -catenin-cortactin complex and Rho. *The Journal of Cell Biology*, *162*(1), 99–111. http://doi.org/10.1083/jcb.200211025

Maunakea, A. K., Nagarajan, R. P., Bilenky, M., Ballinger, T. J., D'Souza, C., Fouse, S. D., … Costello, J. F. (2010). Conserved role of intragenic DNA methylation in regulating alternative promoters. *Nature*, *466*(7303), 253–7. http://doi.org/10.1038/nature09165

Mazur-Kolecka, B., Cohen, I. L., Jenkins, E. C., Kaczmarski, W., Flory, M., & Frackowiak, J. (2007). Altered development of neuronal progenitor cells after stimulation with autistic blood sera. *Brain Research*, *1168*, 11–20. http://doi.org/10.1016/j.brainres.2007.06.084

McAllister, A. K., Katz, L. C., & Lo, D. C. (1997). Opposing Roles for Endogenous BDNF and NT-3 in Regulating Cortical Dendritic Growth. *Neuron*, *18*(5), 767–778. http://doi.org/10.1016/S0896-6273(00)80316-5

McPheeters, M. L., Warren, Z., Sathe, N., Bruzek, J. L., Krishnaswami, S., Jerome, R. N., & Veenstra-Vanderweele, J. (2011). A systematic review of medical treatments for children with autism spectrum disorders. *Pediatrics*, *127*(5), e1312–21. http://doi.org/10.1542/peds.2011-0427

Meikle, L., Talos, D. M., Onda, H., Pollizzi, K., Rotenberg, A., Sahin, M., … Kwiatkowski, D. J. (2007). A mouse model of tuberous sclerosis: neuronal loss of Tsc1 causes dysplastic and ectopic neurons, reduced myelination, seizure activity, and limited survival. *The Journal of Neuroscience : The Official Journal of the Society for Neuroscience*, *27*(21), 5546–58. http://doi.org/10.1523/JNEUROSCI.5540-06.2007

Meinertzhagen, I. A., Takemura, S., Lu, Z., Huang, S., Gao, S., Ting, C.-Y., & Lee, C.-H. (2009). From form to function: the ways to know a neuron. *Journal of Neurogenetics*, *23*(1-2), 68–77. http://doi.org/10.1080/01677060802610604

Michailidis, I. E., Helton, T. D., Petrou, V. I., Mirshahi, T., Ehlers, M. D., & Logothetis, D. E. (2007). Phosphatidylinositol-4,5-bisphosphate regulates NMDA receptor activity through alpha-actinin. *The Journal of Neuroscience : The Official Journal of the Society for Neuroscience*, *27*(20), 5523–32. http://doi.org/10.1523/JNEUROSCI.4378-06.2007

Miettinen, M. (1987). Synaptophysin and neurofilament proteins as markers for neuroendocrine tumors. *Archives of Pathology & Laboratory Medicine*, *111*(9), 813–8. Retrieved from http://www.ncbi.nlm.nih.gov/pubmed/2820344

Moessner, R., Marshall, C. R., Sutcliffe, J. S., Skaug, J., Pinto, D., Vincent, J., … Scherer, S. W. (2007). Contribution of SHANK3 mutations to autism spectrum disorder. *American Journal of Human Genetics*, *81*(6), 1289–97. http://doi.org/10.1086/522590

Moretti, P., Levenson, J. M., Battaglia, F., Atkinson, R., Teague, R., Antalffy, B., … Zoghbi, H. Y. (2006). Learning and memory and synaptic plasticity are impaired in a mouse model of Rett syndrome. *The Journal of Neuroscience : The Official Journal of the Society for Neuroscience*, *26*(1), 319–27. http://doi.org/10.1523/JNEUROSCI.2623-05.2006

Moskal, J. R., Burgdorf, J., Kroes, R. A., Brudzynski, S. M., & Panksepp, J. (2011). A novel NMDA receptor glycine-site partial agonist, GLYX-13, has therapeutic potential for the treatment of autism. *Neuroscience and Biobehavioral Reviews*, *35*(9), 1982–8. http://doi.org/10.1016/j.neubiorev.2011.06.006

Naisbitt, S., Kim, E., Tu, J. C., Xiao, B., Sala, C., Valtschanoff, J., … Sheng, M. (1999). Shank, a Novel Family of Postsynaptic Density Proteins that Binds to the NMDA Receptor/PSD-95/GKAP Complex and Cortactin. *Neuron*, *23*(3), 569–582. http://doi.org/10.1016/S0896-6273(00)80809-0

Naisbitt, S., Kim, E., Tu, J. C., Xiao, B., Sala, C., Valtschanoff, J., … Sheng, M. (1999). Shank, a novel family of postsynaptic density proteins that binds to the NMDA receptor/PSD-95/GKAP complex and cortactin. *Neuron*, *23*(3), 569–82. Retrieved from http://www.ncbi.nlm.nih.gov/pubmed/10433268

Nakashima, S., Matsuda, H., Kurume, A., Oda, Y., Nakamura, S., Yamashita, M., & Yoshikawa, M. (2010). Cucurbitacin E as a new inhibitor of cofilin phosphorylation in human leukemia U937 cells. *Bioorganic & Medicinal Chemistry Letters*, *20*(9), 2994–7. http://doi.org/10.1016/j.bmcl.2010.02.062

Narsinh, K. H., Plews, J., & Wu, J. C. (2011). Comparison of human induced pluripotent and embryonic stem cells: fraternal or identical twins? *Molecular Therapy : The Journal of the American Society of Gene Therapy*, *19*(4), 635–8. http://doi.org/10.1038/mt.2011.41

NATHANS, D. INHIBITION OF PROTEIN SYNTHESIS BY PUROMYCIN. *Federation Proceedings*, *23*, 984–9. Retrieved from http://www.ncbi.nlm.nih.gov/pubmed/14209831

Navratil, A. M., Dozier, M. G., Whitesell, J. D., Clay, C. M., & Roberson, M. S. (2014). Role of cortactin in dynamic actin remodeling events in gonadotrope cells. *Endocrinology*, *155*(2), 548–57. http://doi.org/10.1210/en.2012-1924

Nelson, E. D., Kavalali, E. T., & Monteggia, L. M. (2006). MeCP2-dependent transcriptional repression regulates excitatory neurotransmission. *Current Biology : CB*, *16*(7), 710–6. http://doi.org/10.1016/j.cub.2006.02.062

Nemirovsky, S. I., Córdoba, M., Zaiat, J. J., Completa, S. P., Vega, P. A., González-Morón, D., … Kauffman, M. A. (2015). Whole genome sequencing reveals a de novo SHANK3 mutation in familial autism spectrum disorder. *PloS One*, *10*(2), e0116358. http://doi.org/10.1371/journal.pone.0116358

Nolen, B. (2015). WISH/DIP/SPIN90 Proteins Activate Arp2/3 Complex to Create Linear Actin Filaments that Seed Assembly of Branched Actin Networks. *Biophysical Journal*, *108*(2), 188a. http://doi.org/10.1016/j.bpj.2014.11.1040

Noutel, J., Hong, Y. K., Leu, B., Kang, E., & Chen, C. (2011). Experience-dependent retinogeniculate synapse remodeling is abnormal in MeCP2-deficient mice. *Neuron*, *70*(1), 35–42. http://doi.org/10.1016/j.neuron.2011.03.001

O'Kusky, J. R., Ye, P., & D'Ercole, A. J. (2000). Insulin-like growth factor-I promotes neurogenesis and synaptogenesis in the hippocampal dentate gyrus during postnatal development. *The Journal of Neuroscience : The Official Journal of the Society for Neuroscience*, *20*(22), 8435–42. Retrieved from http://www.ncbi.nlm.nih.gov/pubmed/11069951

Onore, C., Careaga, M., & Ashwood, P. (2012). The role of immune dysfunction in the pathophysiology of autism. *Brain, Behavior, and Immunity*, *26*(3), 383–92. http://doi.org/10.1016/j.bbi.2011.08.007

Pantaleón F, G., & Juvier R, T. (2015). [Molecular basis of Rett syndrome: A current look]. *Revista Chilena de Pediatria*. http://doi.org/10.1016/j.rchipe.2015.07.001

Park, E., Na, M., Choi, J., Kim, S., Lee, J.-R., Yoon, J., … Kim, E. (2003). The Shank family of postsynaptic density proteins interacts with and promotes synaptic accumulation of the beta PIX guanine nucleotide exchange factor for Rac1 and Cdc42. *The Journal of Biological Chemistry*, *278*(21), 19220–9. http://doi.org/10.1074/jbc.M301052200

Parkash, J., Cimino, I., Ferraris, N., Casoni, F., Wray, S., Cappy, H., … Giacobini, P. (2012). Suppression of β1-integrin in gonadotropin-releasing hormone cells disrupts migration and axonal extension resulting in severe reproductive alterations. *The Journal of Neuroscience : The Official Journal of the Society for Neuroscience*, *32*(47), 16992–7002. http://doi.org/10.1523/JNEUROSCI.3057-12.2012

Patkar, S., Tate, R., Modo, M., Plevin, R., & Carswell, H. V. O. (2012). Conditionally immortalised neural stem cells promote functional recovery and brain plasticity after transient focal cerebral ischaemia in mice. *Stem Cell Research*, *8*(1), 14–25. http://doi.org/10.1016/j.scr.2011.07.001

Peça, J., Feliciano, C., Ting, J. T., Wang, W., Wells, M. F., Venkatraman, T. N., … Feng, G. (2011). Shank3 mutant mice display autistic-like behaviours and striatal dysfunction. *Nature*, *472*(7344), 437–42. http://doi.org/10.1038/nature09965

Perrier, A. L., Tabar, V., Barberi, T., Rubio, M. E., Bruses, J., Topf, N., … Studer, L. (2004). Derivation of midbrain dopamine neurons from human embryonic stem cells. *Proceedings of the National Academy of Sciences of the United States of America*, *101*(34), 12543–8. http://doi.org/10.1073/pnas.0404700101

Pinyol, R., Haeckel, A., Ritter, A., Qualmann, B., & Kessels, M. M. (2007). Regulation of N-WASP and the Arp2/3 complex by Abp1 controls neuronal morphology. *PloS One*, *2*(5), e400. http://doi.org/10.1371/journal.pone.0000400

Pollard, T. D. (2007). Regulation of actin filament assembly by Arp2/3 complex and formins. *Annual Review of Biophysics and Biomolecular Structure*, *36*, 451–77. http://doi.org/10.1146/annurev.biophys.35.040405.101936

Proepper, C., Johannsen, S., Liebau, S., Dahl, J., Vaida, B., Bockmann, J., … Boeckers, T. M. (2007). Abelson interacting protein 1 (Abi-1) is essential for dendrite morphogenesis and synapse formation. *The EMBO Journal*, *26*(5), 1397–409. http://doi.org/10.1038/sj.emboj.7601569

Qualmann, B., Boeckers, T. M., Jeromin, M., Gundelfinger, E. D., & Kessels, M. M. (2004). Linkage of the actin cytoskeleton to the postsynaptic density via direct interactions of Abp1 with the ProSAP/Shank family. *The Journal of Neuroscience : The Official Journal of the Society for Neuroscience*, *24*(10), 2481–95. http://doi.org/10.1523/JNEUROSCI.5479-03.2004

Quintanar, J. L., & Guzmán-Soto, I. (2013). Hypothalamic neurohormones and immune responses. *Frontiers in Integrative Neuroscience*, *7*, 56. http://doi.org/10.3389/fnint.2013.00056

Quitsch, A., Berhörster, K., Liew, C. W., Richter, D., & Kreienkamp, H.-J. (2005). Postsynaptic shank antagonizes dendrite branching induced by the leucine-rich repeat protein Densin-180. *The Journal of Neuroscience : The Official Journal of the Society for Neuroscience*, *25*(2), 479–87. http://doi.org/10.1523/JNEUROSCI.2699-04.2005

Ransdell, J. L., Faust, T. B., & Schulz, D. J. (2010). Correlated Levels of mRNA and Soma Size in Single Identified Neurons: Evidence for Compartment-specific Regulation of Gene Expression. *Frontiers in Molecular Neuroscience*, *3*, 116. http://doi.org/10.3389/fnmol.2010.00116

Raynaud, F., Janossy, A., Dahl, J., Bertaso, F., Perroy, J., Varrault, A., … Homburger, V. (2013). Shank3-Rich2 interaction regulates AMPA receptor recycling and synaptic long-term potentiation. *The Journal of Neuroscience : The Official Journal of the Society for Neuroscience*, *33*(23), 9699–715. http://doi.org/10.1523/JNEUROSCI.2725-12.2013

Raynaud, F., Moutin, E., Schmidt, S., Dahl, J., Bertaso, F., Boeckers, T. M., … Fagni, L. (2014). Rho-GTPase-activating protein interacting with Cdc-42-interacting protein 4 homolog 2 (Rich2): a new Ras-related C3 botulinum toxin substrate 1 (Rac1) GTPase-activating protein that controls dendritic spine morphogenesis. *The Journal of Biological Chemistry*, *289*(5), 2600–9. http://doi.org/10.1074/jbc.M113.534636

Richnau, N., & Aspenström, P. (2001). Rich, a rho GTPase-activating protein domain-containing protein involved in signaling by Cdc42 and Rac1. *The Journal of Biological Chemistry*, *276*(37), 35060–70. http://doi.org/10.1074/jbc.M103540200

Román, G. C., Ghassabian, A., Bongers-Schokking, J. J., Jaddoe, V. W. V, Hofman, A., de Rijke, Y. B., … Tiemeier, H. (2013). Association of gestational maternal hypothyroxinemia and increased autism risk. *Annals of Neurology*, *74*(5), 733–42. http://doi.org/10.1002/ana.23976

Rosenmund, C., & Westbrook, G. L. (1993). Calcium-induced actin depolymerization reduces NMDA channel activity. *Neuron*, *10*(5), 805–14. Retrieved from http://www.ncbi.nlm.nih.gov/pubmed/7684233

Rossignol, D. A., & Frye, R. E. (2012). Mitochondrial dysfunction in autism spectrum disorders: a systematic review and meta-analysis. *Molecular Psychiatry*, *17*(3), 290–314. http://doi.org/10.1038/mp.2010.136

Rycroft, B. K., & Gibb, A. J. (2004). Regulation of single NMDA receptor channel activity by alpha-actinin and calmodulin in rat hippocampal granule cells. *The Journal of Physiology*, *557*(Pt 3), 795–808. http://doi.org/10.1113/jphysiol.2003.059212

Salimi, A., Nadri, S., Ghollasi, M., Khajeh, K., & Soleimani, M. (2014). Comparison of different protocols for neural differentiation of human induced pluripotent stem cells. *Molecular Biology Reports*, *41*(3), 1713–21. http://doi.org/10.1007/s11033-014-3020-1

Santini, E., Huynh, T. N., MacAskill, A. F., Carter, A. G., Pierre, P., Ruggero, D., … Klann, E. (2013). Exaggerated translation causes synaptic and behavioural aberrations associated with autism. *Nature*, *493*(7432), 411–5. http://doi.org/10.1038/nature11782

Schmeisser, M. J., Ey, E., Wegener, S., Bockmann, J., Stempel, A. V., Kuebler, A., … Boeckers, T. M. (2012). Autistic-like behaviours and hyperactivity in mice lacking ProSAP1/Shank2. *Nature*, *486*(7402), 256–60. http://doi.org/10.1038/nature11015

Schmidt, E. K., Clavarino, G., Ceppi, M., & Pierre, P. (2009a). SUnSET, a nonradioactive method to monitor protein synthesis. *Nature Methods*, *6*(4), 275–7. http://doi.org/10.1038/nmeth.1314

Schmidt, E. K., Clavarino, G., Ceppi, M., & Pierre, P. (2009b). SUnSET, a nonradioactive method to monitor protein synthesis. *Nature Methods*, *6*(4), 275–7. http://doi.org/10.1038/nmeth.1314

Schuetz, G., Rosário, M., Grimm, J., Boeckers, T. M., Gundelfinger, E. D., & Birchmeier, W. (2004). The neuronal scaffold protein Shank3 mediates signaling and biological function of the receptor tyrosine kinase Ret in epithelial cells. *The Journal of Cell Biology*, *167*(5), 945–52. http://doi.org/10.1083/jcb.200404108

Schulkin, J. (2007). Autism and the amygdala: an endocrine hypothesis. *Brain and Cognition*, *65*(1), 87–99. http://doi.org/10.1016/j.bandc.2006.02.009

Schumann, C. M., Hamstra, J., Goodlin-Jones, B. L., Lotspeich, L. J., Kwon, H., Buonocore, M. H., … Amaral, D. G. (2004). The amygdala is enlarged in children but not adolescents with autism; the hippocampus is enlarged at all ages. *The Journal of Neuroscience : The Official Journal of the Society for Neuroscience*, *24*(28), 6392–401. http://doi.org/10.1523/JNEUROSCI.1297-04.2004

Sengupta, S., Peterson, T. R., & Sabatini, D. M. (2010). Regulation of the mTOR complex 1 pathway by nutrients, growth factors, and stress. *Molecular Cell*, *40*(2), 310–22. http://doi.org/10.1016/j.molcel.2010.09.026

Shao, K., Koch, C., Gupta, M. K., Lin, Q., Lenz, M., Laufs, S., … Wagner, W. (2013). Induced pluripotent mesenchymal stromal cell clones retain donor-derived differences in DNA methylation profiles. *Molecular Therapy : The Journal of the American Society of Gene Therapy*, *21*(1), 240–50. http://doi.org/10.1038/mt.2012.207

Shcheglovitov, A., Shcheglovitova, O., Yazawa, M., Portmann, T., Shu, R., Sebastiano, V., … Dolmetsch, R. E. (2013a). SHANK3 and IGF1 restore synaptic deficits in neurons from 22q13 deletion syndrome patients. *Nature*, *503*(7475), 267–71. http://doi.org/10.1038/nature12618

Shcheglovitov, A., Shcheglovitova, O., Yazawa, M., Portmann, T., Shu, R., Sebastiano, V., … Dolmetsch, R. E. (2013b). SHANK3 and IGF1 restore synaptic deficits in neurons from 22q13 deletion syndrome patients. *Nature*, *503*(7475), 267–71. http://doi.org/10.1038/nature12618

Sheng, M., & Kim, E. (2000). The Shank family of scaffold proteins. *Journal of Cell Science*, *113 (Pt 1*, 1851–6. Retrieved from http://www.ncbi.nlm.nih.gov/pubmed/10806096

Shepherd, G. M. G. (2013). Corticostriatal connectivity and its role in disease. *Nature Reviews. Neuroscience*, *14*(4), 278–91. http://doi.org/10.1038/nrn3469

Sheridan, S. D., Theriault, K. M., Reis, S. A., Zhou, F., Madison, J. M., Daheron, L., … Haggarty, S. J. (2011). Epigenetic characterization of the FMR1 gene and aberrant neurodevelopment in human induced pluripotent stem cell models of fragile X syndrome. *PloS One*, *6*(10), e26203. http://doi.org/10.1371/journal.pone.0026203

Shi, Y., Kirwan, P., & Livesey, F. J. (2012). Directed differentiation of human pluripotent stem cells to cerebral cortex neurons and neural networks. *Nature Protocols*, *7*(10), 1836–46. http://doi.org/10.1038/nprot.2012.116

Shoji, K., Ohashi, K., Sampei, K., Oikawa, M., & Mizuno, K. (2012). Cytochalasin D acts as an inhibitor of the actin-cofilin interaction. *Biochemical and Biophysical Research Communications*, *424*(1), 52–7. http://doi.org/10.1016/j.bbrc.2012.06.063

Smith, S. M., & Vale, W. W. (2006). The role of the hypothalamic-pituitary-adrenal axis in neuroendocrine responses to stress. *Dialogues in Clinical Neuroscience*, *8*(4), 383–95. Retrieved from http://www.pubmedcentral.nih.gov/articlerender.fcgi?artid=3181830&tool=pmcentrez&rendertype=abstract

Smrt, R. D., Eaves-Egenes, J., Barkho, B. Z., Santistevan, N. J., Zhao, C., Aimone, J. B., … Zhao, X. (2007). Mecp2 deficiency leads to delayed maturation and altered gene expression in hippocampal neurons. *Neurobiology of Disease*, *27*(1), 77–89. http://doi.org/10.1016/j.nbd.2007.04.005

Spratt, E. G., Nicholas, J. S., Brady, K. T., Carpenter, L. A., Hatcher, C. R., Meekins, K. A., … Charles, J. M. (2012). Enhanced cortisol response to stress in children in autism. *Journal of Autism and Developmental Disorders*, *42*(1), 75–81. http://doi.org/10.1007/s10803-011-1214-0

Sterneckert, J. L., Reinhardt, P., & Schöler, H. R. (2014). Investigating human disease using stem cell models. *Nature Reviews. Genetics*, *15*(9), 625–39. http://doi.org/10.1038/nrg3764

Suvrathan, A., Hoeffer, C. A., Wong, H., Klann, E., & Chattarji, S. (2010). Characterization and reversal of synaptic defects in the amygdala in a mouse model of fragile X syndrome. *Proceedings of the National Academy of Sciences of the United States of America*, *107*(25), 11591–6. http://doi.org/10.1073/pnas.1002262107

Swaab, D. F. (2008). Sexual orientation and its basis in brain structure and function. *Proceedings of the National Academy of Sciences of the United States of America*, *105*(30), 10273–4. http://doi.org/10.1073/pnas.0805542105

Takahashi, K., Tanabe, K., Ohnuki, M., Narita, M., Ichisaka, T., Tomoda, K., & Yamanaka, S. (2007). Induction of pluripotent stem cells from adult human fibroblasts by defined factors. *Cell*, *131*(5), 861–72. http://doi.org/10.1016/j.cell.2007.11.019

Takahashi, K., & Yamanaka, S. (2006). Induction of pluripotent stem cells from mouse embryonic and adult fibroblast cultures by defined factors. *Cell*, *126*(4), 663–76. http://doi.org/10.1016/j.cell.2006.07.024

Tapia-Arancibia, L., Rage, F., Givalois, L., & Arancibia, S. (2004). Physiology of BDNF: focus on hypothalamic function. *Frontiers in Neuroendocrinology*, *25*(2), 77–107. http://doi.org/10.1016/j.yfrne.2004.04.001

Tavazoie, S. F., Alvarez, V. A., Ridenour, D. A., Kwiatkowski, D. J., & Sabatini, B. L. (2005). Regulation of neuronal morphology and function by the tumor suppressors Tsc1 and Tsc2. *Nature Neuroscience*, *8*(12), 1727–34. http://doi.org/10.1038/nn1566

Tavosanis, G. (2012). Dendritic structural plasticity. *Developmental Neurobiology*, *72*(1), 73–86. http://doi.org/10.1002/dneu.20951

Tornero, D., Wattananit, S., Grønning Madsen, M., Koch, P., Wood, J., Tatarishvili, J., … Kokaia, Z. (2013). Human induced pluripotent stem cell-derived cortical neurons integrate in stroke-injured cortex and improve functional recovery. *Brain : A Journal of Neurology*, *136*(Pt 12), 3561–77. http://doi.org/10.1093/brain/awt278

Tropea, D., Giacometti, E., Wilson, N. R., Beard, C., McCurry, C., Fu, D. D., … Sur, M. (2009). Partial reversal of Rett Syndrome-like symptoms in MeCP2 mutant mice. *Proceedings of the National Academy of Sciences of the United States of America*, *106*(6), 2029–34. http://doi.org/10.1073/pnas.0812394106

Tsai, P.-S., Moenter, S. M., Postigo, H. R., El Majdoubi, M., Pak, T. R., Gill, J. C., … Weiner, R. I. (2005). Targeted expression of a dominant-negative fibroblast growth factor (FGF) receptor in gonadotropin-releasing hormone (GnRH) neurons reduces FGF responsiveness and the size of GnRH neuronal population. *Molecular Endocrinology (Baltimore, Md.)*, *19*(1), 225–36. http://doi.org/10.1210/me.2004-0330

Tsilioni, I., Dodman, N., Petra, A. I., Taliou, A., Francis, K., Moon-Fanelli, A., … Theoharides, T. C. (2014). Elevated serum neurotensin and CRH levels in children with autistic spectrum disorders and tail-chasing Bull Terriers with a phenotype similar to autism. *Translational Psychiatry*, *4*, e466. http://doi.org/10.1038/tp.2014.106

Tu, J. C., Xiao, B., Naisbitt, S., Yuan, J. P., Petralia, R. S., Brakeman, P., … Worley, P. F. (1999). Coupling of mGluR/Homer and PSD-95 complexes by the Shank family of postsynaptic density proteins. *Neuron*, *23*(3), 583–92. Retrieved from http://www.ncbi.nlm.nih.gov/pubmed/10433269

Uchino, S., Wada, H., Honda, S., Nakamura, Y., Ondo, Y., Uchiyama, T., … Kohsaka, S. (2006). Direct interaction of post-synaptic density-95/Dlg/ZO-1 domain-containing synaptic molecule Shank3 with GluR1 alpha-amino-3-hydroxy-5-methyl-4-isoxazole propionic acid receptor. *Journal of Neurochemistry*, *97*(4), 1203–14. http://doi.org/10.1111/j.1471-4159.2006.03831.x

Uchino, S., & Waga, C. (2013). SHANK3 as an autism spectrum disorder-associated gene. *Brain & Development*, *35*(2), 106–10. http://doi.org/10.1016/j.braindev.2012.05.013

Urbach, A., Bar-Nur, O., Daley, G. Q., & Benvenisty, N. (2010). Differential modeling of fragile X syndrome by human embryonic stem cells and induced pluripotent stem cells. *Cell Stem Cell*, *6*(5), 407–11. http://doi.org/10.1016/j.stem.2010.04.005

Uslaner, J. M., Parmentier-Batteur, S., Flick, R. B., Surles, N. O., Lam, J. S. H., McNaughton, C. H., … Hutson, P. H. Dose-dependent effect of CDPPB, the mGluR5 positive allosteric modulator, on recognition memory is associated

with GluR1 and CREB phosphorylation in the prefrontal cortex and hippocampus. *Neuropharmacology*, *57*(5-6), 531–8. http://doi.org/10.1016/j.neuropharm.2009.07.022

van Kooten, I. A. J., Palmen, S. J. M. C., von Cappeln, P., Steinbusch, H. W. M., Korr, H., Heinsen, H., … Schmitz, C. (2008). Neurons in the fusiform gyrus are fewer and smaller in autism. *Brain : A Journal of Neurology*, *131*(Pt 4), 987–99. http://doi.org/10.1093/brain/awn033

Veenstra-VanderWeele, J., & Cook, E. H. (2004). Molecular genetics of autism spectrum disorder. *Molecular Psychiatry*, *9*(9), 819–32. http://doi.org/10.1038/sj.mp.4001505

Verpelli, C., Dvoretskova, E., Vicidomini, C., Rossi, F., Chiappalone, M., Schoen, M., … Sala, C. (2011a). Importance of Shank3 protein in regulating metabotropic glutamate receptor 5 (mGluR5) expression and signaling at synapses. *The Journal of Biological Chemistry*, *286*(40), 34839–50. http://doi.org/10.1074/jbc.M111.258384

Verpelli, C., Dvoretskova, E., Vicidomini, C., Rossi, F., Chiappalone, M., Schoen, M., … Sala, C. (2011b). Importance of Shank3 protein in regulating metabotropic glutamate receptor 5 (mGluR5) expression and signaling at synapses. *The Journal of Biological Chemistry*, *286*(40), 34839–50. http://doi.org/10.1074/jbc.M111.258384

Verpelli, C., Schmeisser, M. J., Sala, C., & Boeckers, T. M. (2012). Scaffold proteins at the postsynaptic density. *Advances in Experimental Medicine and Biology*, *970*, 29–61. http://doi.org/10.1007/978-3-7091-0932-8_2

Waga, C., Okamoto, N., Ondo, Y., Fukumura-Kato, R., Goto, Y.-I., Kohsaka, S., & Uchino, S. (2011). Novel variants of the SHANK3 gene in Japanese autistic patients with severe delayed speech development. *Psychiatric Genetics*, *21*(4), 208–11. http://doi.org/10.1097/YPG.0b013e328341e069

Wagner, A. R., Luan, Q., Liu, S.-L., & Nolen, B. J. (2013). Dip1 defines a class of Arp2/3 complex activators that function without preformed actin filaments. *Current Biology : CB*, *23*(20), 1990–8. http://doi.org/10.1016/j.cub.2013.08.029

Wang, L., Meece, K., Williams, D. J., Lo, K. A., Zimmer, M., Heinrich, G., … Leibel, R. L. (2015). Differentiation of hypothalamic-like neurons from human pluripotent stem cells. *The Journal of Clinical Investigation*, *125*(2), 796–808. http://doi.org/10.1172/JCI79220

Wang, X., McCoy, P. A., Rodriguiz, R. M., Pan, Y., Je, H. S., Roberts, A. C., … Jiang, Y.-H. (2011). Synaptic dysfunction and abnormal behaviors in mice lacking major isoforms of Shank3. *Human Molecular Genetics*, *20*(15), 3093–108. http://doi.org/10.1093/hmg/ddr212

Wang, Y., Wang, W., Li, D., Li, M., Wang, P., Wen, J., … Yin, Y. (2014). IGF-1 alleviates NMDA-induced excitotoxicity in cultured hippocampal neurons against autophagy via the NR2B/PI3K-AKT-mTOR pathway. *Journal of Cellular Physiology*, *229*(11), 1618–29. http://doi.org/10.1002/jcp.24607

Waterhouse, E. G., An, J. J., Orefice, L. L., Baydyuk, M., Liao, G.-Y., Zheng, K., … Xu, B. (2012). BDNF promotes differentiation and maturation of adult-born neurons through GABAergic transmission. *The Journal of Neuroscience : The Official Journal of the Society for Neuroscience*, *32*(41), 14318–30. http://doi.org/10.1523/JNEUROSCI.0709-12.2012

Wegiel, J., Flory, M., Kuchna, I., Nowicki, K., Ma, S. Y., Imaki, H., … Brown, W. T. (2015). Neuronal nucleus and cytoplasm volume deficit in children with autism and volume increase in adolescents and adults. *Acta Neuropathologica Communications*, *3*, 2. http://doi.org/10.1186/s40478-015-0183-5

Wegiel, J., Kuchna, I., Nowicki, K., Imaki, H., Wegiel, J., Marchi, E., … Wisniewski, T. (2010). The neuropathology of autism: defects of neurogenesis and neuronal migration, and dysplastic changes. *Acta Neuropathologica*, *119*(6), 755–70. http://doi.org/10.1007/s00401-010-0655-4

Welsh, J. P., Ahn, E. S., & Placantonakis, D. G. Is autism due to brain desynchronization? *International Journal of Developmental Neuroscience : The Official Journal of the International Society for Developmental Neuroscience*, *23*(2-3), 253–63. http://doi.org/10.1016/j.ijdevneu.2004.09.002

Whitlock, K. E. (2005). Origin and development of GnRH neurons. *Trends in Endocrinology and Metabolism: TEM*, *16*(4), 145–51. http://doi.org/10.1016/j.tem.2005.03.005

Wierman, M. E., Kiseljak-Vassiliades, K., & Tobet, S. (2011). Gonadotropin-releasing hormone (GnRH) neuron migration: initiation, maintenance and cessation as critical steps to ensure normal reproductive function. *Frontiers in Neuroendocrinology*, *32*(1), 43–52. http://doi.org/10.1016/j.yfrne.2010.07.005

Williams, D. L., & Lindsley, C. W. (2005). Discovery of positive allosteric modulators of metabotropic glutamate receptor subtype 5 (mGluR5). *Current Topics in Medicinal Chemistry*, *5*(9), 825–46. Retrieved from http://www.ncbi.nlm.nih.gov/pubmed/16178729

Wilson, P. G., & Stice, S. S. (2006). Development and differentiation of neural rosettes derived from human embryonic stem cells. *Stem Cell Reviews*, *2*(1), 67–77. http://doi.org/10.1007/s12015-006-0011-1

Winder, S. J., & Ayscough, K. R. (2005). Actin-binding proteins. *Journal of Cell Science*, *118*(Pt 4), 651–4. http://doi.org/10.1242/jcs.01670

Won, H., Lee, H.-R., Gee, H. Y., Mah, W., Kim, J.-I., Lee, J., … Kim, E. (2012). Autistic-like social behaviour in Shank2-mutant mice improved by restoring NMDA receptor function. *Nature*, *486*(7402), 261–5. http://doi.org/10.1038/nature11208

Won, H., Mah, W., & Kim, E. (2013). Autism spectrum disorder causes, mechanisms, and treatments: focus on neuronal synapses. *Frontiers in Molecular Neuroscience*, *6*, 19. http://doi.org/10.3389/fnmol.2013.00019

Wray, S. (2010). From nose to brain: development of gonadotrophin-releasing hormone-1 neurones. *Journal of Neuroendocrinology*, *22*(7), 743–53. http://doi.org/10.1111/j.1365-2826.2010.02034.x

Xi, D., Li, Y.-C., Snyder, M. A., Gao, R. Y., Adelman, A. E., Zhang, W., … Gao, W.-J. (2011). Group II metabotropic glutamate receptor agonist ameliorates MK801-induced dysfunction of NMDA receptors via the Akt/GSK-3β pathway in adult rat prefrontal cortex. *Neuropsychopharmacology : Official Publication of the American College of Neuropsychopharmacology*, *36*(6), 1260–74. http://doi.org/10.1038/npp.2011.12

Yang, M., Bozdagi, O., Scattoni, M. L., Wöhr, M., Roullet, F. I., Katz, A. M., … Crawley, J. N. (2012). Reduced excitatory neurotransmission and mild autism-relevant phenotypes in adolescent Shank3 null mutant mice. *The Journal of Neuroscience : The Official Journal of the Society for Neuroscience*, *32*(19), 6525–41. http://doi.org/10.1523/JNEUROSCI.6107-11.2012

Yao, I., Hata, Y., Hirao, K., Deguchi, M., Ide, N., Takeuchi, M., & Takai, Y. (1999). Synamon, a novel neuronal protein interacting with synapse-associated protein 90/postsynaptic density-95-associated protein. *The Journal of Biological Chemistry*, *274*(39), 27463–6. Retrieved from http://www.ncbi.nlm.nih.gov/pubmed/10488079

Yau, V. M., Lutsky, M., Yoshida, C. K., Lasley, B., Kharrazi, M., Windham, G., … Croen, L. A. (2015). Prenatal and neonatal thyroid stimulating hormone levels and autism spectrum disorders. *Journal of Autism and Developmental Disorders*, *45*(3), 719–30. http://doi.org/10.1007/s10803-014-2227-2

Zheng, J.-J., Yang, X., Zhang, L.-Y., Fei, Q.-J., Pan, C.-S., Ni, W.-H., … Huang, X.-F. (2012). [Sperm DNA damage and sperm-nucleoprotein transition correlate to acrosin activity and seminal parameters]. *Zhonghua Nan Ke Xue = National Journal of Andrology*, *18*(10), 925–9. Retrieved from http://www.ncbi.nlm.nih.gov/pubmed/23297503

Zoghbi, H. Y. (2003). Postnatal neurodevelopmental disorders: meeting at the synapse? *Science (New York, N.Y.)*, *302*(5646), 826–30. http://doi.org/10.1126/science.1089071

Supplementary figures

Table1.0: Taqman probes: Table below describes the taqman probes for the *SHANK3* gene and their sequence.

Taqman Probe	Chromosome Position	Cytoband	Amplicon Length	Sequence
Probe int2	Chr.22:51114281	22q13.33b	98	TGTGTGCAGTGTGGGCTGTGTGCCACA
probe int3	Chr.22:51115993	22q13.33b	110	GGCCTTGGCACTATGGCTGGGCAGA
probe ex5	Chr.22:51117256	22q13.33b	102	GCTAAAGGTGCTGAAGAATGGTGGT
probe int13	Chr.22:51137625	22q13.33b	105	TGAGAAAAGAGCGTTTTTCCAAAGT
probe ACR	Chr22:51174223	22q13.33b	81	ACAGCATGAAGAAGGTCAGACAAAG

Table 2.0: Taqman Assay values: Table below describes the values obtained for each probe for control gDNA, SHANK3 patient 1 and 2. The probe value between 1.5 to 2 is considered as both copies of *SHANK3* are being expressed, while values less than 1.5 is considered as deletion as only one copy of *SHANK3* is being expressed. For both patients, it is evident that after probe exon 5, there is only one copy of *SHANK3* being expressed the other is deleted.

Taqman Probe	Average CNV value for control	Average CNV value for SHANK patient 1	Average CNV value for SHANK3 patient 2
Probe intron 2	1.91	1.74	1.6
Probe intron 3	2.04	2.12	2.38
Probe exon5	2.05	1.02	0.9
Probe intron 13	1.98	1.31	0.495
Probe ACR	2.05	1.41	0.9775

The RABL2 gene could not be assessed via TaqMan assay as this region is highly GC rich (about 80%). For this I used, qPCR RABL2 primer, which gave the mean CNV value of 2.08 for SHANK3 patient 1 and 1.44 for SHANK3 patient 2. This suggested that SHANK3 patient 1 has a heterozygous deletion in SHANK3 from exon 4 onwards to ACR while SHANK3 patient 2 has a heterozygous deletion in SHANK3 that stretches from exon4 to RABL2. RABL2 forward primer sequence: ACGCTCTTTGATCTGCCTTC and reverse primer CCCTGGAGTTTTGGTTTGTC.

Human *SHANK3* ORF sequence that was sent Genewiz for synthesis.

Please note: The green highlighted bit is the Myc sequence

XbaIATGGAA CAA AAA CTC ATC TCA GAA GAG GAT CTGgacggccccggggccagcgccgtggtcgtgcgcgtcggcat
cccggacctgcagcagacgaagtgcctgcgcctggacccggccgcgcccgtgtgggccgccaagcagcgcgtgctctgcgccctcaaccacagcc
tccaggacgcgctcaactatgggcttttccagccgccctcccggggccgcgccggcaagttcctggatgaggagcggctcctgcaggagtacccgccc
aacctggacacgcccctgccctacctggagtttcgatacaagcggcgagtttatgcccagaacctcatcgatgataagcagtttgcaaagcttcacaca
aaggcgaacctgaagaagttcatggactacgtccagctgcatagcacggacaaggtggcacgcctgttggacaaggggctggaccccaacttccat
gaccctgactcaggagagtgccccctgagcctcgcagcccagctggacaacgccacggacctgctaaaggtgctgaagaatggtggtgcccacctg
gacttccgcactcgcgatgggctcactgccgtgcactgtgccacacgccagcggaatgcggcagcactgacgaccctgctggacctgggggcttcac
ctgactacaaggacagccgcggcttgacacccctctaccacagcgccctgggggggtggggatgccctctgctgtgagctgcttctccacgaccacgctc
agctggggatcaccgacgagaatggctggcaggagatccaccaggcctgccgctttgggcacgtgcagcatctggagcacctgctgttctatggggca
gacatgggggcccagaacgcctcggggaacacagccctgcacatctgtgccctctacaaccaggagagctgtgctcgtgtcctgctcttccgtggagct
aacagggatgtccgcaactacaacagccagacagccttccaggtggccatcatcgcagggaactttgagcttgcagaggttatcaagacccacaaag
actcggatgttgtaccattcagggaaacccccagctatgcgaagcggcggcgactggctggccccagtggcttggcatcccctcggcctctgcagcgct
cagccagcgatatcaacctgaaggggaggcacagccagcagcttctcctggaccctcgctgagaagcctcccccaccagctgctgctccagcggct
gcaagaggagaaagatcgtgaccgggatgccgaccaggagagcaacatcagtggccctttagcaggcagggccggccaaagcaagatcagccc
gagcgggcccggcggccccggccccgcgcccggccccggccccgcgccccctgcgccccccgcaccgccgccccggggcccgaagcggaaac
tttacagcgccgtccccggccgcaagttcatcgccgtgaaggcgcacagcccgcagggtgaaggcgagatcccgctgcaccgcggcgaggccgtg
aaggtgctcagcattggggagggcggtttctgggagggaaccgtgaaaggccgcacgggctggttcccggccgactgcgtggaggaagtgcagatg
aggcagcatgacacacggcctgaaacgcgggaggaccggacgaagcggctctttcggcactacacagtgggctcctacgacagcctcacctcaca
cagcgattatgtcattgatgacaaagtggctgtcctgcagaaacgggaccacgagggctttggttttgtgctccggggagccaaagcagagacccccat
cgaggagttcacgcccacgccagccttcccggcgctgcagtatctcgagtcggtggacgtggagggtgtggcctggagggccgggctgcgcacggg
agacttcctcatcgaggtgaacggggtgaacgtggtgaaggtcggacacaagcaggtggtggctctgattcgccagggtggcaaccgcctcgtcatga
aggttgtgtctgtgacaaggaagccagaagaggacggggctcggcgcagagccccaccgccccccaagagggcccccagcaccacactgaccct
gcgctccaagtccatgacagctgagctcgaggaacttgcctccattcggagaagaaaaggggagaagctggacgagatgctggcagccgccgcag
agccaacgctgcggccagacatcgcagacgcagactccagagccgccaccgtcaaacagaggcccaccagtcggaggatcacacccgccgag
attagctcattgtttgaacgccagggcctcccaggcccagagaagctgccgggctccttgcggaaggggattccacggaccaagtctgtaggggagg
acgagaagctggcgtccctgctggaagggcgcttcccgcggagcacctcgatgcaagacccggtgcgcgagggtcgcggcatcccgcccccgccg
cagaccgcgccgcctcccccgcccgcgccctactacttcgactcggggccgcccccggccttctcgccgccgcccccgccgggccgcgcctacgac
acggtgcgctccagcttcaagcccggcctggaggcgcgcctgggcgcgggcgctgccggcctgtacgagccgggcgcggccctcggcccgctgcc
gtatcccgagcggcagaagcgcgcgcgctccatgatcatcctgcaggactcggcgcccgagtcgggcgacgcccctcgacccccgcccgcggcca
ccccgcccgagcgacccaagcgccggccgcggccgcccggccccgacagcccctacgccaacctgggcgccttcagcgccagcctcttcgctccg
tccaagccgcagcgccgcaagagccccctggtgaagcagctgcaggtggaggacgcgcaggagcgcgcggccctggccgtgggcagccccggt
cccggcggcggcagcttcgcccgcgagccctccccgacccaccgcggtccgcgcccgggtggcctcgactacggcgcgggcgatggcccggggct
cgcgttcggcggcccgggcccggccaaggaccggcggctggaggagcggcgccgctccactgtgttcctgtccgtgggggccatcgagggcagcg
cccccggcgcggatctgccatccctacagccctcccgctccatcgacgagcgcctcctggggaccggccccaccgccggccgcgacctgctgctgcc
ctccccggtgtctgccctgaagccgttggtcagcggcccgagcctggggccctcgggttccaccttcatccacccactcaccggcaaaccccctggaccc
cagctcacccctggcccttgccctggctgcccgagagcgagctctggcctcccaggcgccctcccggtcccccacacccgtgcacagtcccgacgcc
gaccgccccggacccctgtttgtggatgtacaggcccgggacccagagcgagggtccctggcttccccggctttctccccacggagcccagcctggatt
cctgtgcctgctcgcagggaggcagagaaggtcccccgggaggagcggaagtcacccgaggacaagaagtccatgatcctcagcgtcctggacac
atccctgcagcggccagctggcctcatcgttgtgcacgccaccagcaacgggcaggagcccagcaggctgggggggccgaagaggagcgcccg
ggcaccccggagttggccccggcccccatgcagtcagcggctgtggcagagcccctgcccagccccgggcccagccccctggtggcaccccggc
agacgccgggccaggccagggcagctcagaggaagagccagagctggtgtttgctgtgaacctgccacctgcccagctgtcgtccagcgatgagga
gaccagggaggagctggcccgaattgggttggtgccacccccctgaagagtttgccaacggggtcctgctggccaccccactcgctggcccgggcccc
tcgcccaccacggtgcccagcccggcctcagggaagcccagcagtgagccacccccctgcccctgagtctgcagccgactctggggtggaggaggct
gacacacgcagctccagcgacccccacctggagaccacaagcaccatctccacggtgtccagcatgtccaccttgagctcggagagcggggaactc
actgacacccacacctccttcgctgacggacacacttttctactcgagaagccaccagtgcctcccaagcccaagctcaagtccccgctggggaaggg
gccggtgaccttcagggacccgctgctgaagcagtcctcggacagcgagctcatggcccagcagcaccacgccgcctctgccgggctggcctctgcc
gccgggcctgcccgccctcgctacctcttccagagaaggtccaagctatggggggacccgtggagagccgggggctccctgggcctgaagacgac
aaaccaactgtgatcagtgagctcagctcccgcctgcagcagctgaacaaggacacgcgttccctgggggaggaaccagttggtggcctgggcagc
ctgctggaccctgccaagaagtcgcccatcgcagcagctcggctcttcagcagcctcggtgagctgagctccatttcagcgcagcgcagccccgggg
gcccgggcggcggggcctcgtactcggtgaggcccagtggccgctaccccgtggcgagacgcgccccgagcccggtgaagcccgcgtcgctgga
gcgggtggaggggctgggggcgggcgcgggggcgcagggcggcccttcggcctcacgccccccaccatcctcaagtcgtccagcctctccatccc
gcacgagcccaaggaggtgcgcttcgtggtgcgcagcgtgagcgcgcgcagtcgctccccctcgccgtcgccgctgccctcgcccgcgtccggcccc
ggccccggcgcccccggcccacgccgacccttccagcagaagccgctgcagctctggagcaagttcgacgtgggcgactggctggagagcatcca
cctaggcgagcaccgcgaccgcttcgaggaccatgagatagaaggcgcgcacctacccgcgcttaccaaggacgacttcgtggagctgggcgtcac
gcgcgtgggccaccgcatgaacatcgagcgcgcgctcaggcagctggacggcagctgaEcoRI

Human *SHANK3* ORF without exon 18 highlighted in blue, that was sent Genewiz for synthesis.

Please take out the highlighted blue region (24 bp)

XbaATGGAA CAA AAA CTC ATC TCA GAA GAG GAT CTGgacggccccggggccagcgccgtggtcgtgcgcgtcggcat
cccggacctgcagcagacgaagtgcctgcgcctggacccggccgcgcccgtgtgggccgccaagcagcgcgtgctctgcgccctcaaccacagcc
tccaggacgcgctcaactatgggcttttccagccgccctcccggggccgcgccggcaagttcctggatgaggagcggctcctgcaggagtacccgccc
aacctggacacgcccctgccctacctggagtttcgatacaagcggcgagtttatgcccagaacctcatcgatgataagcagtttgcaaagcttcacaca
aaggcgaacctgaagaagttcatggactacgtccagctgcatagcacggacaaggtggcacgcctgttggacaaggggctggaccccaacttccat
gaccctgactcaggagagtgccccctgagcctcgcagcccagctggacaacgccacggacctgctaaaggtgctgaagaatggtggtgcccacctg
gacttccgcactcgcgatgggctcactgccgtgcactgtgccacacgccagcggaatgcggcagcactgacgaccctgctggacctgggggcttcac
ctgactacaaggacagccgcggcttgacacccctctaccacagcgccctgggggggtggggatgccctctgctgtgagctgcttctccacgaccacgctc
agctggggatcaccgacgagaatggctggcaggagatccaccaggcctgccgctttgggcacgtgcagcatctggagcacctgctgttctatggggca
gacatgggggcccagaacgcctcggggaacacagccctgcacatctgtgccctctacaaccaggagagctgtgctcgtgtcctgctcttccgtggagct
aacagggatgtccgcaactacaacagccagacagccttccaggtggccatcatcgcagggaactttgagcttgcagaggttatcaagacccacaaag
actcggatgttgtaccattcagggaaacccccagctatgcgaagcggcggcgactggctggccccagtggcttggcatcccctcggcctctgcagcgct
cagccagcgatatcaacctgaaggggaggcacagccagcagcttctcctggaccctcgctgagaagcctcccccaccagctgctgctccagcggct
gcaagaggagaaagatcgtgaccgggatgccgaccaggagagcaacatcagtggccctttagcaggcagggccggccaaagcaagatcagccc
gagcgggcccggcggccccggccccgcgcccggccccggccccgcgccccctgcgccccccgcaccgccgccccggggcccgaagcggaaac
tttacagcgccgtccccggccgcaagttcatcgccgtgaaggcgcacagcccgcagggtgaaggcgagatcccgctgcaccgcggcgaggccgtg
aaggtgctcagcattggggagggcggtttctgggagggaaccgtgaaaggccgcacgggctggttcccggccgactgcgtggaggaagtgcagatg
aggcagcatgacacacggcctgaaacgcgggaggaccggacgaagcggctctttcggcactacacagtgggctcctacgacagcctcacctcaca
cagcgattatgtcattgatgacaaagtggctgtcctgcagaaacgggaccacgagggctttggttttgtgctccggggagccaaagcagagacccccat
cgaggagttcacgcccacgccagccttcccggcgctgcagtatctcgagtcggtggacgtggagggtgtggcctggagggccgggctgcgcacggg
agacttcctcatcgaggtgaacggggtgaacgtggtgaaggtcggacacaagcaggtggtggctctgattcgccagggtggcaaccgcctcgtcatga
aggttgtgtctgtgacaaggaagccagaagaggacggggctcggcgcagagccccaccgccccccaagagggcccccagcaccacactgaccct
gcgctccaagtccatgacagctgagctcgaggaacttgcctccattcggagaagaaaaggggagaagctggacgagatgctggcagccgccgcag
agccaacgctgcggccagacatcgcagacgcagactccagagccgccaccgtcaaacagaggcccaccagtcggaggatcacacccgccgag
attagctcattgtttgaacgccagggcctcccaggcccagagaagctgccgggctccttgcggaaggggattccacggaccaagtctgtaggggagg
acgagaagctggcgtccctgctggaagggcgcttcccgcggagcacctcgatgcaagacccggtgcgcgagggtcgcggcatcccgcccccgccg
cagaccgcgccgcctcccccgcccgcgccctactacttcgactcggggccgcccccggccttctcgccgccgcccccgccgggccgcgcctacgac
acggtgcgctccagcttcaagcccggcctggaggcgcgcctgggcgcgggcgctgccggcctgtacgagccgggcgcggccctcggcccgctgcc
gtatcccgagcggcagaagcgcgcgcgctccatgatcatcctgcaggactcggcgcccgagtcgggcgacgcccctcgacccccgcccgcggcca
ccccgcccgagcgacccaagcgccggccgcggccgcccggccccgacagcccctacgccaacctgggcgccttcagcgccagcctcttcgctccg
tccaagccgcagcgccgcaagagccccctggtgaagcagctgcaggtggaggacgcgcaggagcgcgcggccctggccgtgggcagccccggt
cccggcggcggcagcttcgcccgcgagccctccccgacccaccgcggtccgcgcccgggtggcctcgactacggcgcgggcgatggcccggggct
cgcgttcggcggcccgggcccggccaaggaccggcggctggaggagcggcgccgctccactgtgttcctgtccgtgggggccatcgagggcagcg
cccccggcgcggatctgccatccctacagccctcccgctccatcgacgagcgcctcctggggaccggccccaccgccggccgcgacctgctgctgcc
ctccccggtgtctgccctgaagccgttggtcagcggcccgagcctggggccctcgggttccaccttcatccacccactcaccggcaaaacccctggaccc
cagctcacccctggcccttgccctggctgcccgagagcgagctctggcctcccaggcgccctcccggtccccacacccgtgcacagtcccgacgcc
gaccgccccggacccctgtttgtggatgtacaggcccgggacccagagcgagggtccctggcttccccggctttctccccacggagcccagcctggatt
cctgtgcctgctcgcagggaggcagagaaggtcccccgggaggagcggaagtcacccgaggacaagaagtccatgatcctcagcgtcctggacac
atccctgcagcggccagctggcctcatcgttgtgcacgccaccagcaacgggcaggagcccagcaggctgggggggccgcgaagaggagcgcccg
ggcaccccggagttggccccggcccccatgcagtcagcggctgtggcagagcccctgcccagccccgggcccagcccccctggtggcaccccggc
agacgccgggccaggccagggcagctcagaggaagagccagagctggtgtttgctgtgaacctgccacctgcccagctgtcgtccagcgatgagga
gaccagggaggagctggcccgaattgggttggtgccacccccctgaagagtttgccaacggggtcctgctggccaccccactcgctggcccgggcccc
tcgcccaccacggtgcccagcccggcctcagggaagcccagcagtgagccacccccctgcccctgagtctgcagccgactctggggtggaggaggct
gacacacgcagctccagcgacccccacctggagaccacaagcaccatctccacggtgtccagcatgtccaccttgagctcggagagcggggaactc
actgacacccacacctccttcgctgacggacacacttttctactcgagaagccaccagtgcctcccaagcccaagctcaagtccccgctggggaaggg
gccggtgaccttcagggacccgctgctgaagcagtcctcggacagcgagctcatggcccagcagcaccacgccgcctctgccgggctggcctctgcc
gccgggcctgcccgccctcgctacctcttccagagaaggtccaagctatggggggaccccgtggagagccgggggctccctgggcctgaagacgac
aaaccaactgtgatcagtgagctcagctcccgcctgcagcagctgaacaaggacacgcgttccctgggggaggaaccagttggtggcctgggcagc
ctgctggaccctgccaagaagtcgcccatcgcagcagctcggctcttcagcagcctcggtgagctgagctccatttcagcgcagcgcagccccgggg
gcccgggcggcggggcctcgtactcggtgaggcccagtggccgctaccccgtggcgagacgcgccccgagcccggtgaagcccgcgtcgctgga
gcgggtggaggggctgggggcgggcgcgggggcgcagggcggcccttcggcctcacgccccccaccatcctcaagtcgtccagcctctccatccc
gcacgagcccaaggaggtgcgcttcgtggtgcgcagcgtgagcgcgcgcagtcgctccccctcgccgtcgccgctgccctcgcccgcgtccggcccc
ggccccggcgcccccggcccacgccgacccttccagcagaagccgctgcagctctggagcaagttcgacgtgggcgactggctggagagcatcca

cctaggcgagcaccgcgaccgcttcgaggaccatgagatagaaggcgcgcacctacccgcgcttaccaaggacgacttcgtggagctgggcgtcac
gcgcgtgggccaccgcatgaacatcgagcgcgcgctcaggcagctggacggcagctgaEcoRI.

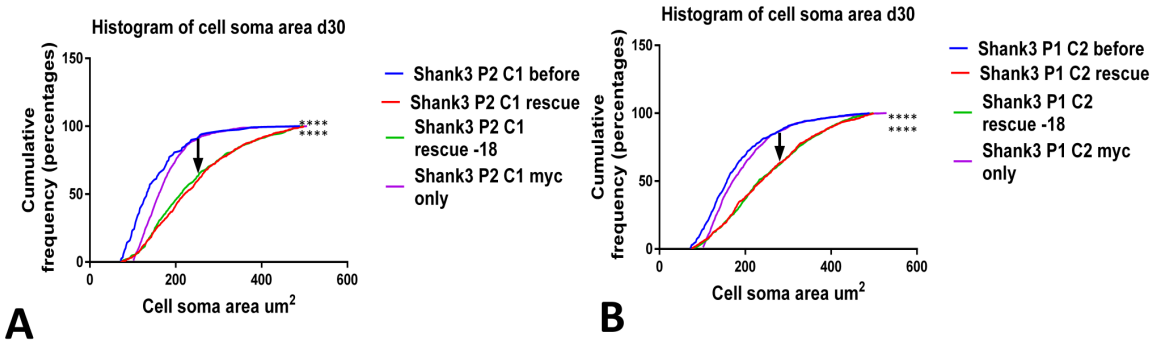

Figure 1.0: ***SHANK3*** **rescue compared to Myc only: A**. In this I compared the cell soma area after the overexpression of the SHANK3 (SHANK3 P2 C1 rescue and SHANK3 P2 C1 rescue-18) to SHANK3 P2 C1 myc only. Dunn's Multiple comparison test revealed SHANK3 P2 C1 myc only vs. SHANK3 P2 C1 rescue ****p<0.0001, similarly Dunn's Multiple comparison test revealed SHANK3 P2 C1 myc only vs. SHANK3 P2 C1 rescue-18 ****p<0.0001.
B. In this I compared the cell soma area after the overexpression of the SHANK3 (SHANK3 P1 C2 rescue and SHANK3 P1 C2 rescue-18) to SHANK3 P1 C2 myc only. Dunn's Multiple comparison test revealed SHANK3 P1 C2 myc only vs. SHANK3 P1 C2 rescue ****p<0.0001, similarly Dunn's Multiple comparison test revealed SHANK3 P1 C2 myc only vs. SHANK3 P1 C2 rescue-18 ****p<0.0001. The purpose of this experiment was to show that it is the SHANK3 gene that causes the rescue of morphogenetic phenotype and the only myc tag did not influence rescue effect.